JULY-SEPTEMBER 2016 VOL. 8 № 3 (30)

ISSN 2075-8251

ActaNaturae

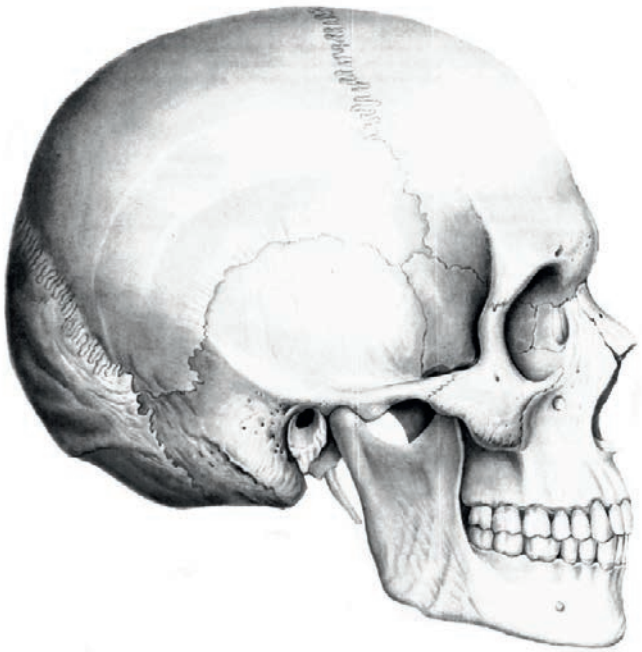

Epigenetics of Ancient DNA

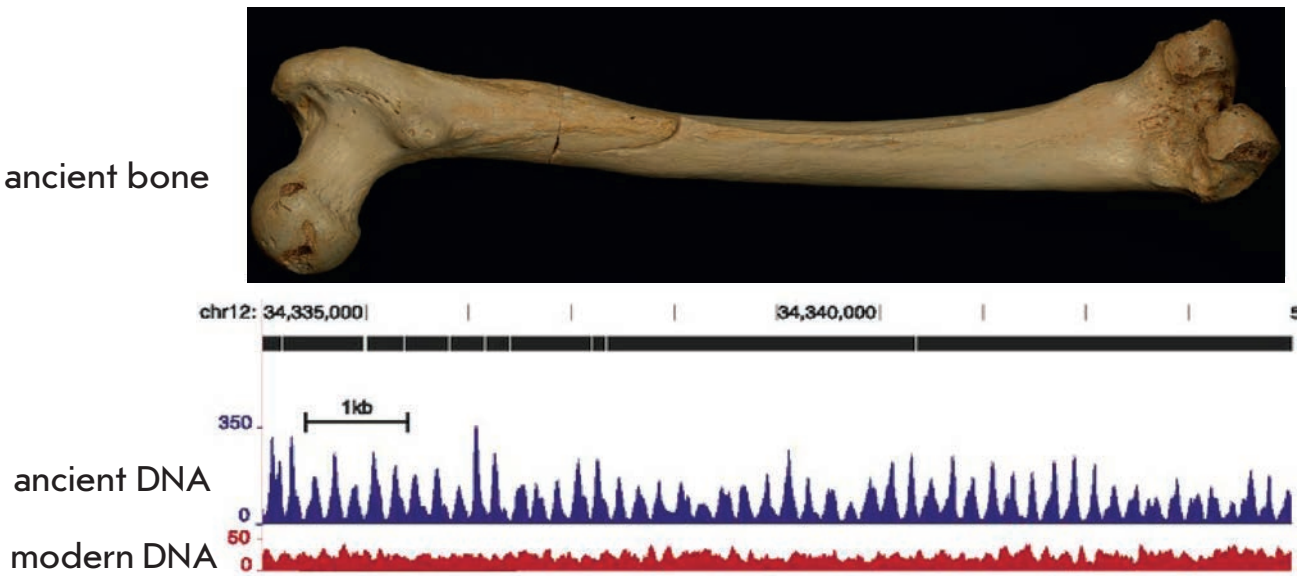

PLACE WHERE NEW DRUGS ARE BORN

CHEMRAR HI-TECH CENTER

CHEMRAR Hi-Tech Center is a unique pharma and biotech cluster built in Russian Federation by highly innovative life science R&D organizations, discovering, developing and commercializing novel drugs for partners in Russia and worldwide.

We see **our mission** in bringing novel therapies for unmet needs in treating CNS, oncology, cardiovascular, metabolic and infection diseases through using novel post genomic technology platforms.

CHEMRAR`s companies offer a broad range of services and flexible partnering models in the following areas:

Streamlined drug discovery preclinical and clinical development;

Partnering for innovative drug combinations;

Formulation, nano-based delivery technologies for improved pharmacokinetics and efficacy;

Co-partnering of innovative molecules from target to market.

CHEMRAR`s companies invite financial and development partners for collaboration on pharmaceutical market in Russia!

www.chemrar.ru Phone: +7 (495) 225-1192 Fax: +7 (495) 626-9780

Letter from the Editors

Dear readers of ActaNaturae,

We are delighted to bring you the 30th issue of the journal.

We continue to develop steadily. In 2015, our impact factor rose to 1.77, making *Acta Naturae* third among Russian research journals in all disciplines. The credit goes to the highly professional work of the editorial staff, the Editorial Board, as well as to the increased quality of the papers published. Gone are the days when the Editorial Board had to put in a lot of effort in attracting well-known authors to submit articles. Today, with the portfolio full, we have an opportunity to select the submitted papers more carefully and strictly.

In the near future we intend to launch the "electronic editorial board" system, which will hopefully make communication between authors and the editorial staff, peer reviewers, and the Editorial Board more mobile, will allow one to check manuscript status, to look through the comments of peer reviewers, and to edit one's personal data provided upon initial registration.

We are looking forward to receiving new interesting manuscripts to publish with great pleasure!

See you in our next issue! ●

The Editorial Board

INNOVATION RUSSIA

Discussion club

We create a dialogue between all socially active groups of people: students, scientists, lecturers, businessmen, managers, innovators, investors, designers, art critics, architects, photographs.

Learn more at WWW.STRF.RU

Everyone with something to say and ideas to share is welcome to visit our events

Tel.: +7 (495) 930-87-07, 930-88-50
E-mail: seminar@strf.ru

Ex Vivo Expansion of Hematopoietic Stem and Progenitor Cells from Umbilical Cord Blood

E.V. Sotnezova, E.R. Andreeva, A.I. Grigoriev, L.B. Buravkova

Transplantation of umbilical cord blood cells is widely used in clinical practice. However, the limited number of hematopoietic stem cells and prolonged time of recovery after the transplantation are significant limitations for the use of the cord blood. The goal of the present review is to analyze the recent methodological approaches to increase the effectiveness of using umbilical cord blood-derived hematopoietic stem cells.

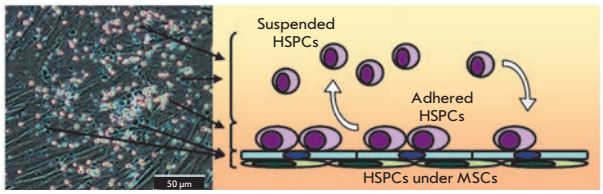

Cultivation of cord blood mononuclear cells on mesenchymal stromal cells as a feeder layer.

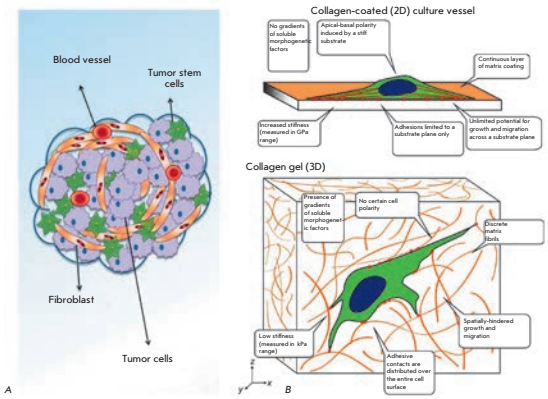

Structure of a malignant tumor and the changes taking place during 2D and 3D cultivation of cells *in vitro*

Bioreactor-Based Tumor Tissue Engineering

A. E. Guller, P. N. Grebenyuk, A. B. Shekhter, A. V. Zvyagin, S. M. Deyev

Tumor tissue engineering is a new method of three-dimensional (3D) simulation of malignant neoplasms whose main goal is to provide the maximally realistic reproduction and long-term maintenance of the simulated tumor properties in vitro to study cancer biology and to develop new methods for diagnosis and treatment of neoplasms. The review focuses on the problem of bioreactor-based tissue-engineering simulation of malignant tumors.

Cleavage of Human Embryos: Options and Diversity

Yu. K. Doronin, I. V. Senechkin, L. V. Hilkevich, M. A. Kurcer

The time-lapse imaging data of preimplantation human embryo development were used to estimate the different forms of embryo cleavage relative to embryo progress (blastocyst formation). These data on the early development of human embryos obtained using noninvasive methods complement and extend our understanding of the embryogenesis of eutherian mammals and may be applied in the practice of reproductive technologies.

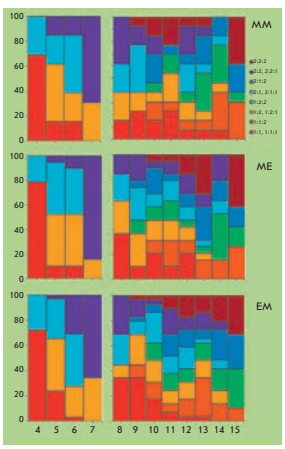

Distribution of blastomere cleavage periods for 4-cell and 8-cell embryos.

ActaNaturae
JULY–SEPTEMBER 2016 VOL. 8 № 3 (30)

Founders
Ministry of Education and
Science of the Russian Federation,
Lomonosov Moscow State University,
Park Media Ltd

Address: 119234 Moscow, Russia, Leninskiye Gory, Nauchny
Park MGU, vlad.1, stroeniye 75G.
Phone/Fax: +7 (495) 727 38 60
E-mail: vera.knorre@gmail.com, actanaturae@gmail.com

Номер подписан в печать 26 мая 2016 г.
Тираж 200 экз. Цена свободная.
Отпечатано в типографии «МИГ ПРИНТ»

Indexed in Pubmed, Web of Science, Scopus, and RISC

CONTENTS

RESEARCH ARTICLES

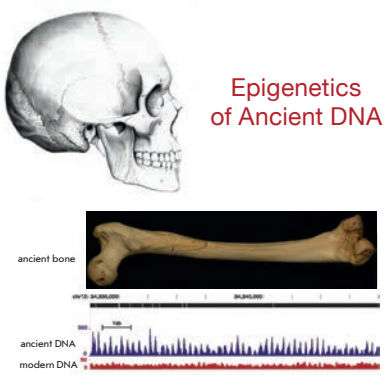

IMAGE ON THE COVER PAGE
(see the article by Zhenilo *et al.*)

Ex Vivo Expansion of Hematopoietic Stem and Progenitor Cells from Umbilical Cord Blood

E.V. Sotnezova, E.R. Andreeva, A.I. Grigoriev, L.B. Buravkova*
Institute of Biomedical Problems of the Russian Academy of Sciences, Khoroshovskoye shosse 76A, Moscow, 123007, Russia
*E-mail: buravkova@imbp.ru
Received February 10, 2016; in final form, March 30, 2016

ABSTRACT **Transplantation of umbilical cord blood cells is currently widely used in modern cell therapy. However, the limited number of hematopoietic stem and progenitor cells (HSPCs) and prolonged time of recovery after the transplantation are significant limitations in the use of cord blood. *Ex vivo* expansion with various cytokine combinations is one of the most common approaches for increasing the number of HSPCs from one cord blood unit. In addition, there are protocols that enable *ex vivo* amplification of cord blood cells based on native hematopoietic microenvironmental cues, including stromal components and the tissue-relevant oxygen level. The newest techniques for *ex vivo* expansion of HSPCs are based on data from the elucidation of the molecular mechanisms governing the hematopoietic niche function. Application of these methods has provided an improvement of several important clinical outcomes. Alternative methods of cord blood transplantation enhancement based on optimization of HPSC homing and engraftment in patient tissues have also been successful. The goal of the present review is to analyze recent methodological approaches to cord blood HSPC *ex vivo* amplification.**
KEYWORDS **cord blood, hematopoietic stem cells, *ex vivo* expansion.**
ABBREVIATIONS **UCB, umbilical cord blood, HSPC, hematopoietic stem and progenitor cells, MSC, mesenchymal stromal cells, CFU, colony-forming units, G-CSF, granulocyte-colony stimulating factor, GM-CSF, granulocyte-macrophage colony-stimulating factor, IL-2, IL-3, IL-4 etc., interleukin 2, 3, 4 etc., TGF-β, transforming growth factor beta, dmPGE2, 16,16 dimethyl prostaglandin E2, SDF-1, stromal cell-derived factor-1, CXCR4, CXC chemokine receptor type 4, C3a, complement fragment 3a.**

INTRODUCTION

At the end of the last century, umbilical cord blood (UCB) attracted the interest of researchers and physicians in the field of bone marrow transplantation due to its successful use as an alternative source of hematopoietic cells. Currently, UCB is used for more than just hematological transplantations. The list of diseases and pathologies which can be treated with UCB is expanding every year. It should be noted that UCB contains blood cells of different commitment, including mature blood elements and hematopoietic stem and progenitor cells (HSPCs), as well as other cell types: undifferentiated somatic stem cells [1–5], multipotent mesenchymal stromal cells (MSCs) [6–9], and endothelial progenitor cells [10].

As a hematopoietic tissue transplant, cord blood has the following undisputable advantages: a non-invasive method of collection, availability, and safety for a donor and lower incidence and severity of "graft-versus-host" reactions compared to the bone marrow or mobilized peripheral blood [11–13]. However, due to a low content of HSPCs, UCB also has some disadvantages associated with the slow recovery of hematopoiesis and immunity. UCB substantially differs from that of bone marrow or mobilized peripheral blood in quantity, composition, and properties of hematopoietic cells. In contrast to bone marrow HSPCs, UCB HSPCs are outside of the cell cycle, but they have a pronounced and rather fast proliferative response to growth factors stimulation [14–17]. The ability of UCB HSPCs to expand *ex vivo* in response to stimulation became the basis for the development of different approaches towards increase of the HSPC number in UCB transplants.

There are two main strategies to enrich the HSPC number in a UCB mononuclear fraction: the first one is based on the expansion of committed hematopoietic progenitors and the other one, on increasing the number of cells with a high proliferative potential, HSPCs [18]. In the first case, the use of committed cells reduces the duration of hematopoietic recovery after transplantation, while the second one eliminates the need for an additional unit of UCB. For example,

successful long-term recovery of hematopoiesis after bone marrow aplasia with *ex vivo* expanded committed progenitors requires the administration of an additional unit of UCB which has not been subjected to any manipulations and contains HSPCs. However, if the *ex vivo* expansion provides cells that are capable of long-term support of the hematopoiesis (long-term repopulating cells), then further manipulations will produce both undifferentiated and committed cells, which can guarantee short-term and long-term recovery of hematopoiesis after the transplantation. This approach does not require the administration of an additional unit of UCB. It is worth noting that in addition to the approaches described above, there are other strategies to improve the efficiency of UCB application that are not aimed at expansion, but focus on enabling effective homing and engraftment of the transplanted cells [19–25].

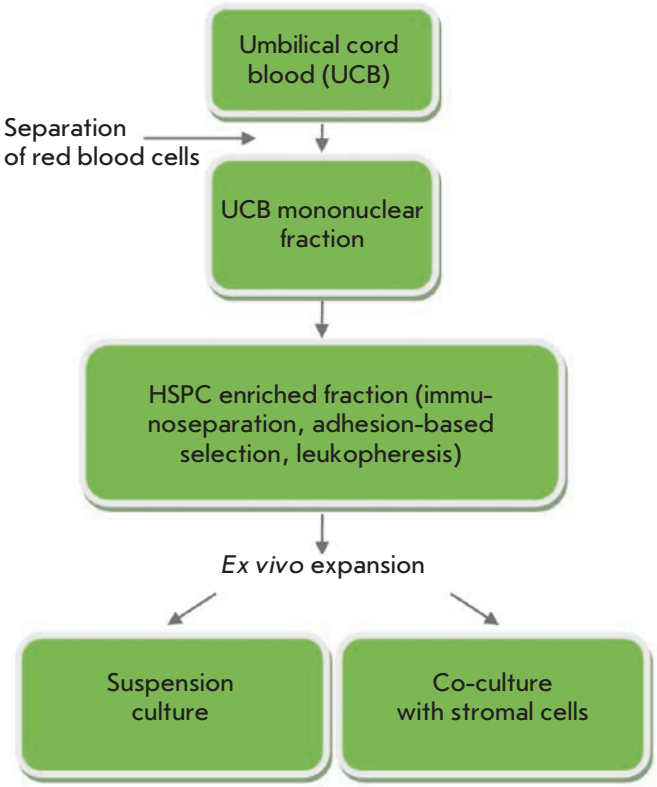

Fig. 1. Methodological approaches for *ex vivo* expansion of cord blood cells

BASIC APPROACHES TO *EX VIVO* EXPANSION OF UMBILICAL CORD BLOOD HSPCs

The development of effective and controlled approaches to generating a large number of HSPCs focuses primarily on the selection of growth media components and methods for the isolation of undifferentiated cells. However, most of the existing models for culturing HSPCs from UCB underestimate the importance of the local microenvironment: interactions with stromal elements, paracrine regulation, and oxygen concentration (*Fig. 1*).

Use of enriched fractions of UCB

The choosing of an approach to the expansion of umbilical cord blood cells starts with the choice between the use of an unfractionated hematopoietic tissue sample and conducting a selection. The separation of HSPCs is performed using magnetic or fluorescent-labeled monoclonal antibodies against specific antigens. It is possible to use either a positive (isolation of certain types of cells from heterogeneous initial material) or negative (unwanted cells are removed from the suspension) selection. It has been shown that the use of a fraction enriched in hematopoietic cells leads to better outcomes of expansion *in vitro* [26].

CD34 and CD133 are the most common markers for a positive selection of hematopoietic stem cells, but their use excludes from the expansion cells that are negative for these antigens, but possess stem cells properties [27]. The presence of certain surface markers is not indicative of the physiological features of a cell, such as its capacity for self-renewal, proliferation, or differentiation. In addition, the expression of a phenotype may be unstable. For example, Summers et al. have shown that a population of $CD34^-Lin^-$ umbilical cord blood cells generates $CD34^+$-HSPCs in co-culture with murine bone marrow stromal cells [28]. This approach has other disadvantages, as well: it requires a large number of initial cells and some hematopoietic cells are lost during the isolation [29]. A decision to forgo prior immune separation prevents potential cellular damage during numerous laboratory manipulations (centrifugation, resuspension, etc) and changes in the functional state of the cells provoked by the binding of antibodies to surface molecules [30].

Some studies have applied unfractionated UCB in HSPC expansion [31–33]. There are also approaches in which one portion of a cord blood unit is administered to a recipient without any treatment, while the other portion is used for expansion with prior enrichment ($CD34^+$ or $CD133^+$ selection). In this approach, the graft retains its immunological potential, which improves its engraftment and immunological restoration [34, 35].

Soluble components of culturing systems

Fetal calf serum (FCS), which contains a natural cocktail of growth factors, adhesion mediators, minerals,

lipids and hormones, is the standard component for cultivation of most human cell types, including HSPCs. However, there is no consensus on the possibility of using cells after FCS-supported expansion in clinical settings. The disadvantages of a serum include difficulties in standardization of its composition, potential viral contamination, and high risk of immunization of a recipient with foreign proteins [36, 37]. Therefore, some researchers reject FCS in favor of cytokine cocktails [26, 38]. Nevertheless, it should be taken into account that the serum contains some minor components whose exact activity has not yet been identified and, therefore, may not be fully compensated for in serum-free media.

Numerous soluble factors that affect the proliferation and differentiation of HSPCs have been identified to date. Their various combinations define the timing and degree of expansion of the cultured cells. Both peripheral blood cells and UCB cells synthesize cytokines. In particular, UCB T-cells, NK-cells, and macrophages produce a granulocyte colony-stimulating factor (G-CSF), a granulocyte-macrophage colony-stimulating factor (GM-CSF), a macrophage colony-stimulating factor, interleukins 2, 3 and 4 (IL-2 -3, -4), transforming the growth factor (TGF-β), and interferon-γ [39–41]. However, the amount of the mediator synthesized, its biological activity, and the number of producing cells are considerably lower in UCB than in peripheral blood.

Despite the abundance of recombinant cytokines that are used for the expansion of primitive hematopoietic progenitors, no optimal combination has yet been approved for use in clinical practice. The most commonly used factors are the stem cell factor (SCF), IL-3 and -6, G-CSF, thrombopoietin (TPO), and Flt-3 ligand [42, 43].

It should be noted that in addition to the set of factors, their concentration and the sequence of their use are also important. For example, cultivation of HSPCs during the first three days using SCF, IL-3, Flt-3, TPO, in 4% fetal calf serum, followed by transfer into a medium with 20% fetal calf serum and macrophage colony stimulating factor, Flt-3, IL-3, and SCF promotes the expansion of $CD34^+$ cells [43]. Growth factors SCF, Flt-3, IL-11, IL-3, IL-6, GM-CSF are responsible for cell proliferation, whereas the macrophage-colony-stimulating factor, G-CSF, erythropoietin (EPO), and TPO are responsible for cell differentiation and maturation. SCF, IL-3, and IL-6 act in the G0/G1 phase of the cell cycle and collectively induce mitosis [44].

Other combinations of cytokines are also used for the expansion of hematopoietic cells. Haylock et al. showed that expansion with a combination of IL-lβ, IL-3, IL-6, G-CSF, GM-CSF, and SCF is more effective than without one of these six cytokines [45].

It should be noted that there are factors whose presence in the culture medium reduces the expansion of hematopoietic cells. It has been shown that IL-8, platelet factor-4, protein induced by IFN-γ, and monocyte chemotactic factor-1 downregulate *in vitro* proliferation of colony-forming units of granulocytes, erythrocytes, monocytes and megakaryocytes (CFU-GEMM), granulocytes and monocytes (CFU-GM), and burst-forming units of red blood cells (BFU-RBC), stimulated by growth factors [46, 47]. Also, macrophage inflammatory protein-α inhibits the proliferation of murine stem cells, corresponding to CFU-S 12 (colony forming units of the spleen, which give rise to granulocytic, monocytic, erythroid, megakaryocytic and lymphoid colonies on Day 12 after the transplantation into irradiated animals) and earlier CFU-Bl cells (cells forming blast cell colonies in the culture) in mice in an *ex vivo* system [48].

Culture systems that contain only soluble factors deprive hematopoietic cells of the supporting influence of the microenvironment: cell interactions with non-hematopoietic cells, components of the tissue matrix, and paracrine mediators. On the other hand, the addition of exogenous cytokines into stroma-based co-cultures where feeder cells produce SCF and IL-6, as well as many other paracrine factors, may promote the maintenance of hematopoietic progenitors, but this is not strictly mandatory.

MODELING A SPECIFIC MICROENVIRONMENT FOR *EX VIVO* EXPANSION OF UCB HSPCS

It should be mentioned that early studies of adult hematopoietic stem cells have been associated with modeling of their natural microenvironment [49, 50]. For example, the initial attempts to cultivate hematopoietic cells in suspension cultures demonstrated a rapid decline of hematopoiesis and replacement of hematopoietic cells with macrophages. The use of a culturing system comprising the bone marrow cell layer, however, yielded a culture containing hematopoietic progenitors possessing the properties of intact bone marrow hematopoietic stem cells [49]. Further studies were focused on the development of various modifications and improvement of the cultivation system.

Co-cultivation with stromal cells

Co-culturing with stromal feeder cells is a more physiological alternative to the application of recombinant cytokines, which had been used since the beginning of bone marrow hematopoietic cell studies [49]. Researchers are actively looking for new cell lines that support *in vitro* expansion of HSPCs during co-cultivation [51]. Co-culturing of hematopoietic progenitors with different types of cells which exhibit feeder properties

towards them is not only useful for the expansion of undifferentiated precursors for their subsequent clinical use, but also allows one to elucidate the relationship between the cells within the hematopoietic niche.

The traditional and most rational approach to the expansion of HSPC *in vitro* is to use mesenchymal stromal cells as a feeder layer [52–59]. Besides the feeder properties, MSCs have high proliferative activity and are more accessible than other types of human feeder cells (such as ductal epithelial cells or splenocytes) [60]. It has been shown that in Dexter-cultures bone marrow stromal cells can support hematopoiesis *in vitro* for more than 6 months [49]. Some researchers use MSCs after differentiation into osteoblasts, thus creating a semblance of an endosteal niche [61].

MSCs and more differentiated stromal cells secrete various cytokines [62–64]. Almost all data on cytokine production by human MSCs are collected *in vitro*; therefore, it is impossible to state with any degree of confidence how each cytokine is involved in paracrine regulation *in vivo*. Nevertheless, it has been shown that MSCs produce large amounts of cytokines that support resting or self-renewed HSPCs, in particular SCF, a leukemia cell inhibitory factor, stromal cell-derived factor 1 (SDF-1), oncostatin M, morphogenetic bone protein-4 , Flt-3 ligand, and TGF-β, IL-1, -6, -7, -8, -11, -12, -14, -15 [62, 63]. Furthermore, when IL-1α is added to the culture medium, MSCs can produce growth factors, such as GM-CSF and G-CSF, which affect more mature hematopoietic precursors, indicating mutual regulation of hematopoietic cells and MSCs [65–67].

Stromal precursors from different sources are applied in *in vitro* modeling of bone marrow niche conditions [52, 54, 68]. MSCs from the bone marrow are the most commonly used, and, therefore, they are well characterized as feeder cells. MSCs have also been derived from the walls of blood vessels, the synovial membrane, placenta, umbilical cord blood, and the subendothelial layer of the umbilical vein. MSCs from different sources differ in the expression of some markers, their ability to proliferate and differentiate, but in general their characteristics are similar [69–72]. MSCs from the stromal-vascular fraction of human adipose tissue have been shown to support hematopoiesis *in vitro* [53, 73]. Therefore, they are a good alternative to bone marrow MSCs and represent an easily accessible source of feeder cells for the expansion of UCB HSPCs for widespread clinical use [74].

McNiece *et al.* developed a protocol for culturing HSPCs according to which 14-day expansion includes 7 days of co-cultivation with bone marrow MSCs in the presence of hematopoietic cytokines, followed by 7 days of culturing in the presence of cytokines alone [52]. This technique significantly reduces the neutrophils and platelets recovery time after transplantation of two units of UCB, one of which is enriched with HSPCs using the protocol above. Thus, the use of feeder layers for expansion of UCB HSPCs allows one to exclude exogenous growth factors that reduce the efficiency of cell amplification.

Tissue-related oxygen level

Oxygen concentration is one of the main factors of hematopoietic microenvironment that is involved in the regulation of hematopoietic cell development. The oxygen level in bone marrow varies from 1 to 6%; the hypoxic areas contain resting HSPCs, whereas proliferating HSPCs are located in sites with higher O_2 [75]. Low partial oxygen pressure plays an important role in the maintenance of certain physiological properties of hematopoietic cells, which is important for studies of stromal and hematopoietic cells interactions *in vitro*, and must always be taken into consideration when designing amplification protocols for UCB cells [76, 77].

A lower oxygen level is known to have a significant effect on hematopoietic cells *in vitro*, affecting their colony-forming ability, resistance to radiation, and their potential to restore hematopoiesis in lethally irradiated animals [75, 78]. Additionally, low partial oxygen pressure promotes the viability and proliferation of undifferentiated hematopoietic cells over committed progenitors [78, 79].

Remarkably, a combination of different O_2 concentrations and cytokine sets results in amplification of UCB cells with different properties. For example, Ivanovic *et al.* have shown that the application of 3% oxygen in the presence of SCF, G-CSF, TPO, and IL-3 supports primitive hematopoietic cells capable of restoring hematopoiesis in irradiated animals after transplantation and contributes to the expansion of committed precursors (CFU) [80].

It has also been shown that cultivation of a UCB fraction enriched with $CD133^+$ cells supplemented with the recombinant cytokines SCF, Flt-3, TPO, IL-6, and IL-3 under 5% O_2 results in an almost 27-fold increase in the number of $CD34^+CD38^-$ cells (irrespective of the presence of serum in the medium), which is significantly ($P < 0.01$) higher than in the case of a standard oxygen concentration [81]. Cells amplified in low oxygen condition contained more CFU with a myeloid potential and had a higher ability to restore hematopoiesis after transplantation into irradiated animals. It has been shown that a low oxygen level induces the expression of the *HIF-1α*, *VEGF*, and *ABCG2* genes in hematopoietic cells and activates the expression of CXC chemokine receptor 4 (CXCR4) [82].

Tursky *et al.* cultivated UCB cells at 10% oxygen in a medium supplemented with cytokines (TPO, SCF,

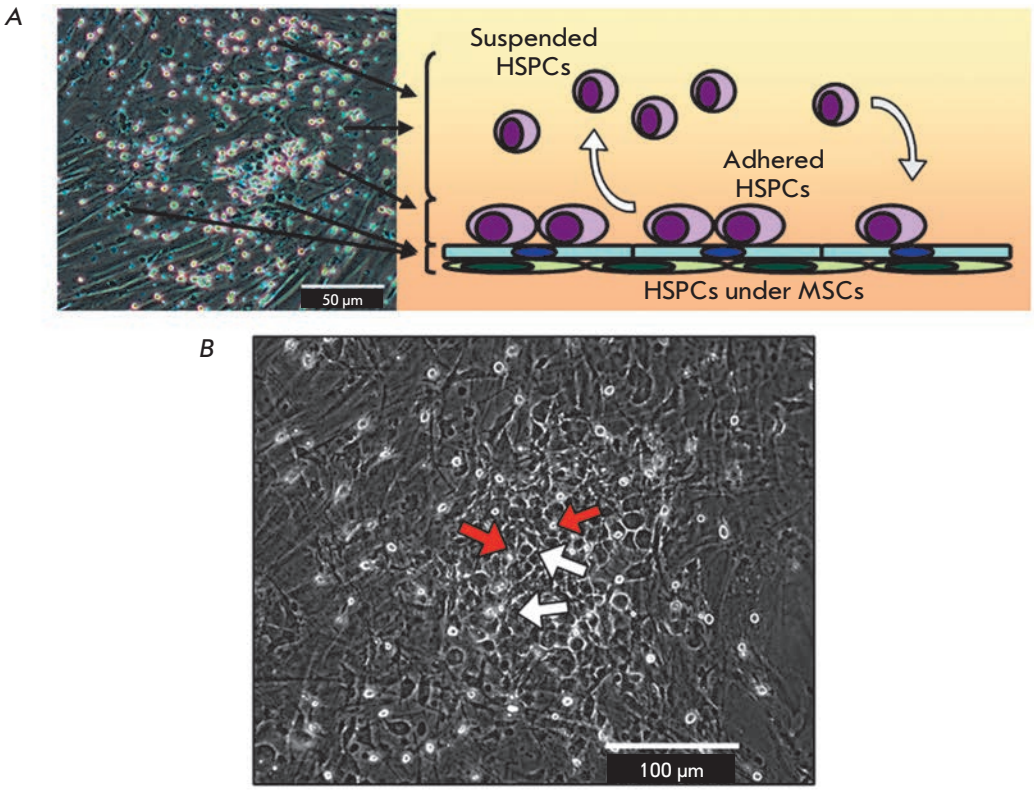

Fig. 2. Cord blood mononuclear cultivation on a MSC feeder layer. A. Representative image of HSPC/MSC co-culture and schematic distribution of HSPCs. B. MSC-associated HSPCs in HSPC/MSC co-culture. HSPCs attached to the MSC surface (white arrows), "cobblestone" area forming cells beneath the MSCs (red arrows).

Flt-3 ligand and IL-6) and obtained a higher HSPC expansion compared with the most common UCB cell culturing protocol (20% oxygen, TPO, SCF, and G- CSF) [42].

One of the important features of hematopoietic cells in occuping certain "niches" when co-cultured with stromal cells is also dependent on the oxygen level. Already in 1977, Dexter *et al.* had described the compartmentalization of hematopoietic cells in such co-cultures: some hematopoietic progenitors were present in the suspension above the feeder layer, some adhered to the stromal surface, and some cells migrated to the substromal space (*Fig. 2A*) [49]. Long-term co-cultivation was accompanied by the formation of sites of HSPC active proliferation and the formation of so-called "cobblestones" areas, which are detected by phase-contrast microscopy and look like dense cell clusters under the MSC layer (*Fig. 2B*) [82].

The spatial organization of hematopoietic cells in a co-culture is comparable to their distribution in bone marrow: based on a state of resting or active proliferation, cells are located in areas with different oxygen levels and nutrients availability. It was assumed that the fraction of cells which adhered to the surface of MSCs was enriched in actively proliferating cells. Compared to other fractions of hematopoietic progenitors in the co-culture, the cells that migrated under the stromal monolayer rarely divided and retained an immature $CD34^+CD38^-$ phenotype [83]. Therefore, the peculiarities of HSPCs distribution in certain compartments based on their proliferative potential can be used for the fractionation of cells according to their ability to adhere and the isolation of populations of cells with certain properties (*Fig. 3*) [73].

According Jing *et al.*, the most "hypoxic" hematopoietic cells were localized under the stromal monolayer when cultured under standard (atmospheric) 20% O_2 [83]. The adhesion of HSPCs to the stromal layer decreased under reduced O_2, but these conditions promoted the migration of the cells under the MSC monolayer. Hypoxia conditions amplified the production of vascular endothelial growth factor A, which apparently enhanced the permeability of the MSCs monolayer. It should be noted that a reduced oxygen concentration affects both hematopoietic and stromal cells and their interaction [83].

Reconstruction of the bone marrow microenvironment *ex vivo* involves generating a tissue-related oxygen level and the application of feeder layers, in particular MSCs, as a cellular component of the microenvironment [76, 77]. However, it should be taken into account that the reduced O_2 in the culture medium affects not only the hematopoietic cells, but also MSCs. *In vitro* studies revealed a decrease in the ostegenic and adipogenic differentiating potential of MSCs under hypoxic conditions [84, 85]. Furthermore, a reduced

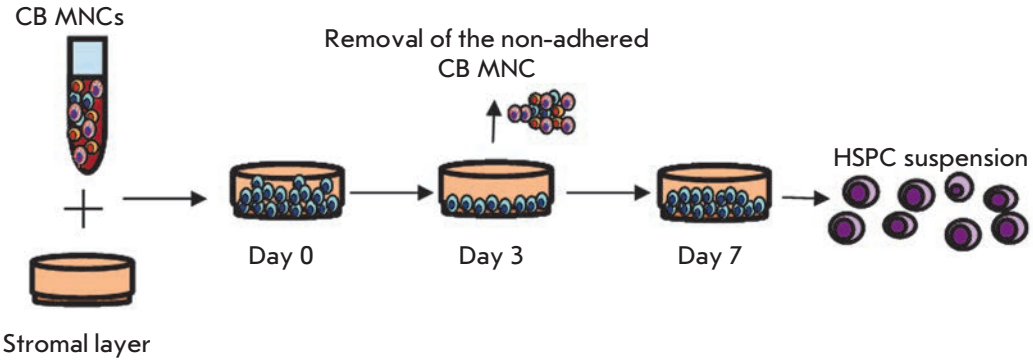

Fig. 3. The experimental design of cord blood mononuclear (CB MNC) expansion on a MSC layer, where the adhered fraction of CB MNCs is able to generate a new cell population enriched with HSPCs (Maslova *et al.*, 2013).

oxygen concentration during cultivation promoted chondrogenic differentiation and an increase in the proliferative activity and the number of fibroblast-colony-forming units [84, 86, 87]. These findings highlight the role of oxygen as an important factor that defines the fate of stromal and hematopoietic cells. It is important to consider the effect of oxygen on the production of biologically active MSC mediators, when these cells are used as a feeder layer for the cultivation of hematopoietic cells. It has been shown that MSC production of such mediators as IL-1β, IL-10, the hepatocyte growth factor, vascular endothelial growth factor, basic fibroblast growth factor, TGF-β, and GM-CSF increases under 4–5% O_2, while that of the tumor necrosis factor α decreases [64, 88].

Koller *et al.* conducted *in vitro* expansion of hematopoietic cord blood cells using an approach based on the effect of a combination of hematopoietic microenvironment factors [89]. The UCB cells were cultured in the presence or absence of recombinant cytokines and an MSC underlayer at 5 or 20% O_2. It was found that the use of IL-3/IL-6 allows one to achieve a more efficient expansion of hematopoietic progenitors than IL-1/IL-3 for more than 8 weeks. This effect was enhanced under reduced O_2. The presence of irradiated stromal cells had no significant effect on the expansion of hematopoietic cells in the presence of cytokines, especially at low oxygen.

The effect on hematopoietic cells may vary depending on the oxygen concentration in the medium. Co-culturing of umbilical cord blood mononuclears and bone marrow MSCs at 2% O_2 promotes a substantially lower production of $CD34^+$ cells (25-fold increase vs. 60-, 64- and 92-fold increase at 5, 21, 10% O_2, respectively, on Day 10). Studies of growth dynamics revealed a higher proliferative rate of the UCB cells cultured at 5, 10, and 21% oxygen than that of those cultured at 2% O_2 [90].

Therefore, to develop effective and controlled approaches for obtaining large quantities of hematopoietic stem and progenitor cells for transplantation, it is necessary to take into account the particular features of the microenvironment of hematopoietic niches, including the tissue-related oxygen level.

MOLECULAR GENETIC APPROACHES TO EXPANSION OF HEMATOPOIETIC STEM AND PROGENITOR CELLS FROM UMBILICAL BLOOD *EX VIVO*

The routine approaches to the expansion of UCB cells are based on data from studies of the effect of cellular and non-cellular hematopoietic microenvironment factors on the HSPC, including the tissue-releated oxygen level, interaction with stromal cells, and paracrine mediators. However, the development of molecular genetic techniques has greatly enhanced our understanding of the mechanisms that mediate the function of hematopoietic niches, thereby allowing us to develop new technological approaches to the amplification of UCB HSPCs.

Notch-mediated expansion

A family of Notch ligands and receptors is involved in numerous processes [91–93]. The Notch 1 receptor is found on $CD34^+$ hematopoietic progenitors [94]. Moreover, activation of Notch signaling contributes to maintenance of the phenotype of the most primitive hematopoietic stem cells *in vitro*. This results in a serum-free system for culturing $CD34^+$ hematopoietic cells that consist of immobilized Delta1 Notch-ligand and early hematopoietic stem cells cytokines (SCF, TPO, Flt-3 ligand, IL-3 and IL-6) [95]. Ambiguous results were obtained for the transplantation of two units of UCB, one of which was enriched in HSPCs using the Notch-system, during a clinical trial. The use of Notch-graft reduced the neutrophils recovery time; however, after 3 months the hematopoiesis in the recipients

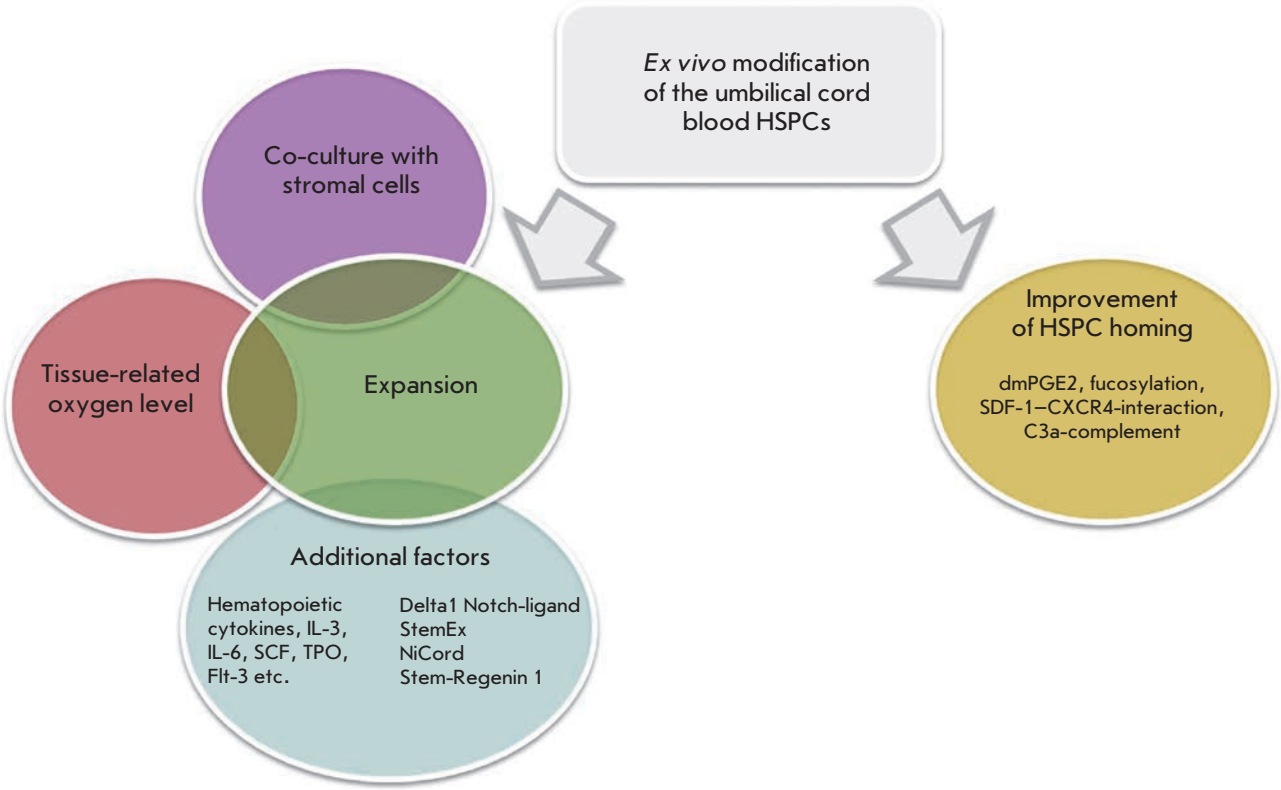

Fig. 4. Current technological approaches to the modification of hematopoietic stem and progenitor cells from umbilical cord blood *ex vivo*

was maintained by the other UCB transplant. The observed effect can be explained by two reasons: the loss of cells providing long-term hematopoietic recovery (long-term repopulating cells) during the cultivation and the immune response of the T-cells of the intact UCB transplant [34, 35].

Expansion in the presence of StemEx (copper chelate)

Copper-deficient patients have a significantly slower granulocytopoiesis and erythropoiesis and their bone marrow biopsy specimens reveal a reduction in the number of mature granulocytes and increase in the number of promyelocytes and myelocytes compared to people without this deficiency [96, 97]. This observation led to a hypothesis that copper deficiency affects the differentiation of myeloid progenitors. Later, a StemEx component of a culture system was developed whose action is based on the effect of low copper concentrations on the differentiation of hematopoietic stem cells *in vitro*. In StemEx, a copper chelator, tetraethylenepentamine interacts with early and late hematopoietic cytokines [98, 99]. The use of the StemEx technology involves the expansion of cells from one unit of the UCB in the presence of StemEx for 21 days. The other portion of the UCB is left intact, and they are administered together with the cells amplified in the presence of the StemEx [100]. This approach has improved several important clinical outcomes compared to intact UCB, indicating the effectiveness of this cultivation system for the amplification of UCB HSPC *ex vivo* [101].

NiCord expansion

The NiCord technology is based on the action of an epigenetic factor, nicotinamide, which slows down the differentiation and increases the functionality of hematopoietic stem and progenitor cells obtained during *ex vivo* expansion. The addition of nicotinamide, together with hematopoietic cytokines, to the culture increases the proportion of $CD34^+CD38^-$ primitive cells and enhances migration towards SDF-1 *in vitro*. In addition, highly efficient engraftment of the amplified cells has been demonstrated in *in vivo* models [102]. NiCord not only increases the number of HSPCs compared with the technologies presented above, but also promotes efficient engraftment of cells. The particular feature of a NiCord graft is that after a 21-day expansion it contains, in addition to a HSPC fraction, a fraction of uncultivated T-cells, which is collected and re-frozen after cryopreservation. Therefore, a NiCord graft retains its immunological potential, which improves engraft-

ment and immunological reconstitution. The results of a clinical application of HSPCs that were amplified according to the NiCord protocol and transplanted together with an additional unit of the UCB indicate an earlier recovery of neutrophils (median of 11 days vs. 25 days, $p = 0.001$) and platelets (30 days versus 41 days, $p = 0.012$) compared to the controls [103]. This study confirms the presence of long-term repopulating cells and short-term repopulating cells in the umbilical cord blood transplant after NiCord expansion.

Expansion in the presence of Stem-Regenin 1

Stem-Regenin 1 is a purine derivative that promotes *ex vivo* expansion of HPSCs [104]. The Stem-Regenin 1 technology uses a fractionated $CD34^+$ population of UCB cells to initiate the cell culture. It has been shown that 3 weeks of expansion in a serum-free medium supplemented with Stem-Regenin 1, TPO, SCF, Flt-3 ligand, and IL-6 results in 1118-fold amplification of $CD34^+$ cells relative to the initial population. The removal of the Stem-Regenin 1 from the cultivation system leads to rapid differentiation, indicating the important role of this component in maintaining an undifferentiated state of the hematopoietic UCB progenitors. The cells obtained with Stem-Regenin 1 are capable of highly efficient engraftment after transplantation into immunocompromised mice, indicating that the presence of hematopoietic progenitors in them provides for early and sustained hematopoietic recovery. This technology has performed well in clinical trials and is actively studied today [105].

STRATEGIES AIMED AT IMPROVING HSPC HOMING

Besides the described-above techniques there are also approaches to improving homing and engraftment of potential UCB stem cells which do not involve prior expansion. They represent an inexpensive and safe alternative to *ex vivo* expansion of HPSCs.

Co-cultivation with E2 prostaglandin

The study of hematopoiesis in *Danio rerio* fish revealed the involvement of dmPGE2 (16,16-dimethyl prostaglandin E2) in the homeostasis of hematopoietic stem cells [22]. It suggested that short *ex vivo* exposure of UCB cells to dmPGE2 would increase the "effective dose" of hematopoietic stem cells without significant toxicity for the patient. It has been shown that a short-term incubation of HSPCs with dmPGE2 increases the number of these cells after transplantation and provides an advantage in serial transplantation with full multilineage bone marrow recovery in mice [106]. Promising results were obtained in the clinical use of dmPGE2, and the method continues to be actively developed [24].

Fucosylation

This approach aims to improve the homing of UCB stem cells in the bone marrow stroma. The technique is based on the fact that hematopoietic UCB stem cells do not migrate to the bone marrow as actively as adult bone marrow cells or mobilized peripheral blood cells. The reduced efficacy of homing in the bone marrow can be attributed partly to the lack of binding to adhesion molecules (P- and E-selectins), which are expressed on endothelial cells in bone marrow vessels [19]. Fucosylation of the selectin ligands expressed on UCB stem cells increases their affinity for P- and E-selectins of the hematopoietic microvasculature bed, which is crucial for enabling HSPC "rolling" [107]. The rather simple fucosylation procedure includes incubating the UCB cells with fucosyl transferase IV and its substrate GDP-fucose for 30 min at room temperature. The increased efficiency of UCB stem cells engraftment has been demonstrated in *in vivo* models for the use of pre-transplantation *ex vivo* fucosylation in immunodeficient mice [25, 108].

CXCR4-SDF-1 interaction

SDF-1 and its receptor CXCR4 also enable HSPC homing and their retention in the bone marrow. CXCR4 is expressed in different cells, including MSCs, endothelial cells, and various hematopoietic cell subpopulations, including HSCPs. SDF-1 is a potent chemoattractant for $CD34^+$ HSPCs, which subsequently migrate to the bone marrow along the SDF-1 gradient after transplantation [109–113]. The optimum expression of CXCR4 in HSPCs and the effective level of SDF-1 in the recipient bone marrow support the engraftment. Dipeptidyl peptidase-4 (DPP4) is a down-regulator of this interaction, since it can cleave the N-terminal dipeptide from SDF-1, thereby reducing its activity and ability to interact with the receptor. Inhibition of this enzyme has resulted in a 2- to 3-fold increase in the homing of human $CD34^+$ and Lin^- cells in transplantation into NOD/SCID/$B2m^{null}$ mice [114]. Furthermore, it is known that dipeptidyl peptidase-4 regulates the function of hematopoietic growth factors. Therefore, inhibition of this enzyme improves not only the homing, but also cell growth mediated by growth factors [115]. The use of drugs that inhibit dipeptidyl peptidase-4 has demonstrated encouraging results for the engraftment of UCB transplants [116]. Further studies are aimed at determining the optimal dosage and timing.

Component of C3a complement

A C3a fragment is a product of the proteolytic cleavage of the complement protein C3. Along with numerous immunoregulatory properties, C3a sensitizes human hematopoietic stem and progenitor cells to homing towards SDF-1 via binding of C3a to the CXCR4 receptor.

C3a, along with DPP4 and hyaluronic acid, fibronectin and fibrinogen, regulates the expression of SDF-1 on HSPCs [117, 118]. Preclinical studies have shown that incubation of hematopoietic stem cells with C3a prior to transplantation to lethally irradiated mice accelerates engraftment [20, 21]. However, the results of clinical application were not as successful, since C3a did not provide any advantages in terms of engraftment [23].

CONCLUSION

Despite numerous studies aimed at optimizing the enrichment of hematopoietic transplants with stem cells, no optimized technology for the amplification of stem cells has been developed to date. The main challenges for researchers include the need for a better understanding of the composition and biological properties of the hematopoietic transplants that are responsible for hematopoietic recovery in a recipient and the development of approaches that enable the amplification of HSPCs.

A comparative analysis of data reveals two trends: the application of stromal feeder layers in systems for amplifying UCB cells or the use of various combinations of hematopoietic cytokines. However, suspension cultures in which the maintenance of hematopoietic precursors occurs only through hematopoietins do not take into account the role of the local microenvironment (interactions with stromal cells and oxygen regulation) even though it has been shown that these factors may be critical for the development of blood cells. The expansion of UCB HSPCs in co-culture is more effective than in a suspension culture. In addition, co-cultivation improves the engraftment of the amplified cells after transplantation. The addition of exogenous cytokines to the co-culturing system further supports the expansion of HSPCs. Thus, it seems appropriate to use *ex vivo* systems, which include both the stromal sublayer, physiological level of oxygen, and the necessary cocktail of cytokines and growth factors, for amplification.

Molecular genetic approaches have proven to be quite successful, as well; they are aimed at both amplification of hematopoietic cells and improvement of the homing of transplanted cells in a recipient's bone marrow (*Fig. 4*). *Ex vivo* systems for the amplification of HSPCs have already been developed and successfully used: however, the search for new effective approaches to UCB cells expansion that are based on modern cellular and molecular biological techniques continues. ●

This work was supported by the Program of the Presidium of RAS "Fundamental Research for the Development of Biomedical Technologies".

REFERENCES

1. Kögler G., Radke T.F., Lefort A., Sensken S., Fischer J., Sorg R.V., Wernet P. // Exp Hematol. 2005. V. 33. № 5. P. 573–583.
2. Kögler G., Sensken S., Airey J.A., Trapp T., Müschen M., Feldhahn N., Liedtke S., Sorg R.V., Fischer J., Rosenbaum C. et al. // J Exp Med. 2004. V. 200. № 2. P. 123–135.
3. Kögler G., Sensken S., Wernet P. // Exp Hematol. 2006. V. 34. № 11. P. 1589–1595.
4. Sensken S., Waclawczyk S., Knaupp A.S., Trapp T., Enczmann J., Wernet P., Kogler G. // Cytotherapy. 2007. V. 9. №4. P. 362–378.
5. Greschat S., Schira J., Küry P., Rosenbaum C., de Souza Silva M.A., Kögler G., Wernet P., Müller H.W. // Stem Cells Dev. 2008. V. 17. № 2. P. 221–232.
6. Musina R.A., Bekchanova E.S., Belyavskii A.V., Grinenko T.S., Sukhikh G.T. // Bull Exp Biol Med. 2007. V. 143. № 1. P. 127–31.
7. Erices A., Conget P., Minguell J. J. // Br J Haematol. 2000. V. 109. № 1. P. 235–242.
8. Bieback K., Kern S., Klüter H., Eichler H. // Stem Cells. 2004. V. 22. №4. P. 625–634.
9. Yang S.E., Ha C.W., Jung M., Jin H.J., Lee M., Song H., Choi S., Oh W., Yang Y.S. // Cytotherapy. 2004. V. 6. № 5. P. 476–486.
10. Yoder M.C., Mead L.E., Prater D., Krier T.R., Mroueh K.N., Li F., Krasich R., Temm C.J., Prchal J.T., Ingram D.A. // Blood. 2007. V. 109. № 5. P. 1801–1809.
11. Cutler C., Antin J.H. // Stem Cells. 2001. V. 19, № 2. P. 108–117.
12. Gluckman E., Rocha V. // Haematologica. 2009. V. 94. № 4. P. 451–454.
13. Semyonova Zh.B., Sushkevich G.N., Karasyeva O.V., Akhadov T.A., Semyonova N.A., Semyonova N.Yu., Sorokina E.G., Fufaeva E.V., Romanov Yu.A., Roshal L.M., et al. // Pediatric Neurosurgery and Neurology. 2011. V. 27. № 1. P. 70–82.
14. Broxmeyer H.E., Hangoc G., Cooper S., Ribeiro R.C., Graves V., Yoder M., Wagner J., Vadhan-Raj S., Benninger L., Rubinstein P., et al. // Proc Natl Acad Sci U S A. 1992. V. 89. № 9. P. 4109–4113.
15. Lu L., Xiao M. Shen R.N., Grigsby S., Broxmeyer H.E. // Blood. 1993. V. 81. № 1. P. 41–48.
16. Moore M.A., Hoskins I. // Blood Cells. 1994. V. 20. № (2-3) P. 468–479; discussion P. 479–481.
17. Movassagh M., Caillot L., Baillou C., Guigon M., Lemoine F.M. // Stem Cells. 1997. V. 15. № 3. P. 214–222.
18. Horwitz M.E., Frassoni F. // Cytotherapy. 2015. V. 17. № 6. P. 730–738.
19. Hidalgo A., Weiss L.A., Frenette P.S. // J Clin Invest. 2002. V. 110. № 4. P. 559–569.
20. Reca R., Mastellos D., Majka M., Marquez L., Ratajczak J., Franchini S., Glodek A., Honczarenko M., Spruce L.A., Janowska-Wieczorek A., et al. // Blood. 2003. V. 101. № 10. P. 3784–3793.
21. Ratajczak J., Reca R., Kucia M., Majka M., Allendorf D.J., Baran J.T., Janowska-Wieczorek A., Wetsel R.A., Ross G.D, Ratajczak M.Z. // Blood. 2004. V. 103. № 6. P. 2071–2078.
22. North TE, Goessling W, Walkley CR, Lengerke C, Kopani

KR, Lord AM, Weber GJ, Bowman TV, Jang IH, Grosser T, et al. // Nature. 2007. V. 447. № 7147. P. 1007–1011.
23. Brunstein C.G., McKenna D.H., DeFor T.E., Sumstad D., Paul P., Weisdorf D.J., Ratajczak M., Laughlin M.J., Wagner J.E. // Biol Blood Marrow Transplant. 2013. V. 19. № 10. P. 1474–1479.
24. Cutler C., Multani P., Robbins D., Kim H.T., Le T., Hoggatt J., Pelus L.M., Desponts C., Chen Y.B., Rezner B., et al. // Blood. 2013. V 122. № 17. P. 3074–3081.
25. Robinson S.N., Thomas M.W., Simmons P.J., Lu J., Yang H., Parmar S., Liu X., Shah N., Martín-Antonio B., Bollard C., Dotti G., et al. // Cytotherapy. 2014. V. 16. № 1. P. 84–89.
26. Briddell R.A., Kern B.P., Zilm K.L., Stoney G.B., McNiece I.K. // J Hematother. 1997. V. 6. № 2. P. 145–150.
27. Ufimtseva A.I., Kanov E.V. // Cell Transplan Tiss Eng. 2012. V. 6. № 4. P. 21–27.
28. Summers Y.J., Heyworth C.M., de Wynter E.A., Chang J., Testa N.G. // Stem Cells. 2001. V. 19. № 6. P. 505–513.
29. Koller M.R., Manchel I., Newsom B.S., Palsson M.A., Palsson B.O. // J Hematother. 1995. V. 4. № 3. P. 159–169.
30. Gilner J.B., Walton W.G., Gush K., Kirby S.L. // Stem Cells. 2007. V. 25. № 2. P. 279–288.
31. de Lima M., McNiece I., Robinson S.N., Munsell M., Eapen M., Horowitz M., Alousi A., Saliba R., McMannis JD, Kaur I, et al. // N Engl J Med. 2012. V. 367. № 24. P. 2305–2315.
32. Mantel C.R., O'Leary H.A., Chitteti B.R., Huang X., Cooper S., Hangoc G., Brustovetsky N., Srour E.F., Lee M.R., Messina-Graham S., et al. // Cell. 2015. V. 161. № 7. P. 1553–1565.
33. Aliyari Z., Khaziri N., Brazvan B., Saayah Melli M., Tayefi Nasrabadi H., Akbarzadeh A., Nozad Charoudeh H. // Artif Cells Nanomed Biotechnol. 2015. P. 1–8.
34. Gutman J.A., Turtle C.J., Manley T.J., Heimfeld S., Bernstein I.D., Riddell S.R., Delaney C. // Blood. 2010. V. 115. № 4. P. 757–765.
35. Moretta A., Andriolo G., Lisini D., Martinetti M., Pasi A., Rebulla P., Soligo D., Giordano R., Lazzari L., Maccario R. // Biol Blood Marrow Transplant. 2012. V. 18. № 7. P. 1108–1118.
36. Spees J.L., Gregory C.A., Singh H., Tucker H.A., Peister A., Lynch P.J., Hsu S.C., Smith J., Prockop D.J. // Mol Ther. 2004. V. 9. № 5. P. 747–756.
37. Sundin M., Ringdén O., Sundberg B., Nava S., Götherström C., Le Blanc K. // Haematologica. 2007. V. 92. № 9. P. 1208–1215.
38. Petevka N.V., Goncharova N.V., Severin I.N., Kosmacheva S.M., Potapnev M.P. // Cell Transplan Tiss. Eng. 2012. V. 7. № 1. P. 40–48.
39. Sano-Martins I.S., Dabrowski Z., Tabarowski Z., Witkowska- Pelc E., Spadacci Morena D.D., Spodaryk K. // Cell Tissue Res. 2002. V. 310. № 1. P. 67–75.
40. Gao L., Chen X., Zhang X., Liu Y., Kong P., Peng X., Liu L., Liu H., Zeng D. // Blood Cells Mol Dis. 2006. V. 36. № 2. P. 322–328.
41. Ławicki S., Mroczko B., Szmitkowski M. // Postepy Hig Med Dosw. 2001. V. 55. № 3. P. 449–465.
42. Tursky M.L., Collier F.M., Ward A.C., Kirkland M.A. // Cytotherapy. 2012. V. 14. № 6. P. 679–685.
43. Hordyjewska A., Popiołek Ł., Horecka A. // Cytotechnology. 2015. V. 67. № 3. P. 387–396.
44. Grskovic B., Ruzicka K., Karimi A., Qujeq D., Müller M.M. // Clin Chim Acta. 2004. V. 343. № 1-2. P. 173–178.
45. Haylock D.N., To L.B., Dowse T.L., Juttner C.A., Simmons P.J. // Blood. 1992. V. 80. № 6. P. 1405–1412.
46. Broxmeyer H.E., Sherry B., Lu L., Cooper S., Oh K.O., Tekamp-Olson P., Kwon B.S., Cerami A. // Blood. 1990. V. 76. № 6. P. 1110–1116.
47. Broxmeyer H.E., Cooper S., Cacalano G., Hague N.L., Bailish E., Moore M.W. // J Exp Med. 1996. V. 184. № 5. P. 1825–1832.
48. Graham G.J., Wright E.G., Hewick R., Wolpe S.D., Wilkie N.M., Donaldson D., Lorimore S., Pragnell I.B. // Nature. 1990. V. 344. № 6265. P. 442–444.
49. Dexter T.M, Allen T.D., Lajtha L.G. // J Cell Physiol. 1977. V. 91. № 3. P. 335–344.
50. Friedenstein A.J., Chailakhyan R.K., Latsinik N.V., Panasyuk A.F., Keiliss-Borok I.V. // Transplantation. 1974. V. 17. № 4. P. 331–340.
51. De Angeli S., Di Liddo R., Buoro S., Toniolo L., Conconi M.T., Belloni A.S., Parnigotto P.P., Nussdorfer G.G. // Int J Mol Med. 2004. V. 13. № 3. P. 363–371.
52. McNiece I., Harrington J., Turney J., Kellner J., Shpall E.J. // Cytotherapy. 2004. V. 6. № 4. P. 311–317.
53. Corre J., Barreau C., Cousin B., Chavoin J.P., Caton D., Fournial G., Penicaud L., Casteilla L., Laharrague P. // J Cell Physiol. 2006. V. 208. № 2. P. 282–288.
54. Jang Y.K., Jung D.H., Jung M.H, Kim D.H., Yoo K.H., Sung K.W., Koo H.H., Oh W., Yang Y.S., Yang S.E. // Ann Hematol. 2006. V. 85. № 4. P. 212–225.
55. Kilroy G.E., Foster S.J., Wu X., Ruiz J., Sherwood S., Heifetz A., Ludlow J.W., Stricker D.M., Potiny S., Green P., et al. // J Cell Physiol. 2007. V. 212. № 3. P. 702–709.
56. Nakao N., Nakayama T., Yahata T., Muguruma Y., Saito S., Miyata Y., Yamamoto K., Naoe T. // Am J Pathol. 2010. V. 177. № 2. P. 547–554.
57. De Toni F., Poglio S., Youcef A.B., Cousin B., Pflumio F., Bourin P. Casteilla L., Laharrague P. // Stem Cells Dev. 2011. V. 20. № 12. P. 2127–2138.
58. Zhambalova A.P., Darevskaya A.N., Kabaeva N.V., Romanov Y.A., Buravkova L.B. // Bull Exp Biol Med. 2009. V. 147. № 4. P. 525–530.
59. Petrova N. V., Svinareva D. A., Nifontova I. N., Momotyuk K. S., Savchenko V. G., Drize N. I. // Bull Exp Biol Med. 2006. V. 142. № 4. P. 527–530.
60. Anisimov S.V. // Tsitologiia. 2012. V. 54. № 4. P. 289–97.
61. Mishima S., Nagai A., Abdullah S., Matsuda C., Taketani T., Kumakura S., Shibata H., Ishikura H., Kim S.U., Masuda J. // Eur J Haematol. 2010. V. 84. № 6. P. 538–546.
62. Haynesworth S.E., Baber M.A., Caplan A.I. // J Cell Physiol. 1996. V. 166. № 3. P. 585–592.
63. Majumdar M.K., Thiede M.A., Mosca J.D., Moorman M., Gerson S.L. // J Cell Physiol. 1998. V. 176. № 1. P. 57–66.
64. Buravkova L.B., Zhambalova A.P., Kabaeva N.V., Romanov Y.A. // Stem cells and regenerative medicine(In Russian). M: Maks Press, 2011. P. 145–161
65. Taichman R.S., Reilly M.J., Verma R.S., Emerson S.G. // Blood. 1997. V. 89. № 4. P. 1165–1172.
66. Ahmed N., Sammons J., Carson R.J., Khokher M.A., Hassan H.T. // Cell Biol Int. 2001. V. 25. № 5. P. 429–435.
67. Petit I., Szyper-Kravitz M., Nagler A., Lahav M., Peled A., Habler L., Ponomaryov T., Taichman R.S., Arenzana-Seisdedos F., Fujii N. et al. // Nat Immunol. 2002. V. 3. № 7. P. 687–694.
68. Kim J.W., Kim S.Y., Park S.Y., Kim Y.M., Kim J.M., Lee M.H., Ryu H.M. // Ann Hematol. 2004. V. 83. № 12. P. 733–738.
69. Tepliashin A.S., Korzhikova S.V., Sharifullina S.Z., Chupikova N.I., Rostovskaia M.S., Savchenkova I.P. // Tsitologiia. 2005. V. 47. № 2. P. 130–135.
70. Paiushina O.V., Domaratskaia E.I., Starostin V.I. // Izv

Akad Nauk Ser Biol. 2006. № 1. P. 6–25.
71. Romanov Y.A., Darevskaya A.N., Kabaeva N.V., Antonova O.A. // Bull Exp Biol Med. 2006. V. 142. № 4. P. 515–520.
72. Shahpazyan N.K., Astrelina T.A., Yakovleva M.V. // Cell Transpl Tiss Eng. 2012. V. 7. № 1. P. 23–33.
73. Maslova E.V., Andreeva E.R., Andrianova I.V., Bobyleva P.I., Romanov Y.A., Kabaeva N.V., Balashova E.E., Ryaskina S.S., Dugina T.N., Buravkova L.B. // Bull Exp Biol Med. 2014. V. 156. № 4. P. 584–589.
74. Gimble J.M., Katz A.J., Bunnell B.A. // Circ Res. 2007. V. 100. № 9. P. 1249–1260.
75. Parmar K., Mauch P., Vergilio J.A., Sackstein R., Down J.D // Proc Natl Acad Sci U S A. 2007. V. 104. № 13. P. 5431–5436.
76. E.V. Sotnezova (Maslova), A.N. Gornostaeva, E.R. Andreeva, Y.A. Romanov, E.E. Balashova, L.B. Buravkova // Cell Tiss Biology. 2015. V. 9. № 5, P. 341–347.
77. Andreeva E.R., Andrianova I.V., Sotnezova E.V., Buravkov S.V., Bobyleva P.I., Romanov Y.A., Buravkova L.B. // PLoS One. 2015. V. 10. № 4. P. e0124939.
78. Cipolleschi M.G., Dello Sbarba P., Olivotto M. // Blood. 1993. V. 82. P. 7. P. 2031–2037.
79. Shima H., Takubo K., Iwasaki H., Yoshihara H., Gomei Y., Hosokawa K., Arai F., Takahashi T., Suda T. // Biochem Biophys Res Commun. 2009. V. 378. № 3. P. 467–472.
80. Ivanovic Z., Hermitte F., Brunet de la Grange P., Dazey B., Belloc F., Lacombe F., Vezon G., Praloran V. // Stem Cells. 2004. V. 22. № 5. P. 716–724.
81. Roy S., Tripathy M., Mathur N., Jain A., Mukhopadhyay A. // Eur J Haematol. 2012. V. 88. № 5. P. 396–405.
82. Ploemacher R.E., van der Sluijs J.P., Voerman J.S., Brons N.H. // Blood. 1989. V. 74. № 8. P. 2755–2763.
83. Jing D., Wobus M., Poitz D.M., Bornhäuser M., Ehninger G., Ordemann R. // Haematologica. 2012. V. 97. № 3. P. 331–339.
84. Buravkova LB, Grinakovskaya OS, Andreeva EP, Zhambalova AP, Kozionova MP. // Cell Tiss Biology. 2009. V. 3 № 1. P. 23–28.
85. Malladi P., Xu Y., Chiou M., Giaccia A.J., Longaker M.T. // Am J Physiol Cell Physiol. 2006. V. 290. № 4. P. 1139–1146.
86. Wang D.W., Fermor B., Gimble J.M., Awad H.A., Guilak F. // J Cell Physiol. 2005. V. 204. № 1. P. 184–191.
87. Xu Y., Malladi P., Chiou M., Bekerman E., Giaccia A.J., Longaker M.T. // Tissue Eng. 2007. V. 13. № 12. P. 2981–2993.
88. Li Z., Wei H., Deng L., Cong X., Chen X. // FEBS J. 2010. V. 277. № 18. P. 3688–3698.
89. Koller M.R., Bender J.G., Papoutsakis E.T., Miller W.M. // Blood. 1992. V. 80. № 2. P. 403–411.
90. Andrade P.Z., de Soure A.M., Dos Santos F., Paiva A., Cabral J.M., da Silva C.L. // J Tissue Eng Regen Med. 2015. V. 9. № 10. P. 1172–1181.
91. Andersson E.R., Sandberg R., Lendahl U. // Development. 2011. V. 138. № 17. P. 3593–3612.
92. Sethi N., Kang Y. // Br J Cancer. 2011. V. 105. № 12. P. 1805–1810.
93. Rumyantsev S.A., Osipova E.Y., Ipatov S.E., Shamanskaya T.V., Mayorova O.A., Rumyantsev A.G. // Oncohematology. 2011. V. 6. № 1. P. 64–75.
94. Milner L.A., Kopan R., Martin D.I., Bernstein I.D. // Blood. 1994. V. 83. № 8. P. 2057–2062.
95. Delaney C., Varnum-Finney B., Aoyama K., Brashem-Stein C., Bernstein I.D. // Blood. 2005. V. 106. № 8. P. 2693–2699.
96. Zidar B.L., Shadduck R.K., Zeigler Z., Winkelstein A. // Am J Hematol. 1977. V. 3. P. 177–185.
97. Percival S.S. // Nutr Rev. 1995. V. 53. № 3. P. 59–66.
98. Peled T., Landau E., Mandel J., Glukhman E., Goudsmid N.R., Nagler A., Fibach E. // Exp Hematol. 2004. V. 32. № 6. P. 547–555.
99. Peled T., Mandel J., Goudsmid R.N., Landor C., Hasson N., Harati D., Austin M., Hasson A., Fibach E., Shpall E.J., Nagler A. // Cytotherapy. 2004. V. 6. № 4. P. 344–355.
100. de Lima M., McMannis J., Gee A., Komanduri K., Couriel D., Andersson B.S., Hosing C., Khouri I., Jones R., Champlin R., et al // Bone Marrow Transplant. 2008. V. 41. № 9. P. 771–778.
101. Montesinos P., Peled T., Landau E., Rosenheimer N., Mandel J., Hasson N., Olesinski E., Glukhman E., Snyder D.A., Cohen E.G., et al. // Blood. 2013. V. 122. № 21. P. 295.
102. Peled T., Shoham H., Aschengrau D., Yackoubov D., Frei G., Rosenheimer G.N., Lerrer B., Cohen H.Y., Nagler A., Fibach E., et al. // Exp Hematol. 2012. V. 40. № 4. P. 342–355.
103. Horwitz M.E., Chao N.J., Rizzieri D.A., Long G.D., Sullivan K.M., Gasparetto C., Chute J.P., Morris A., McDonald C., Waters-Pick B. et al. // J Clin Invest. 2014. V. 124. № 7. P. 3121–3128.
104. Boitano A.E., Wang J., Romeo R., Bouchez L.C., Parker A.E., Sutton S.E., Walker J.R., Flaveny C.A., Perdew G.H., Denison M.S., Schultz P.G., Cooke M.P. // Science. 2010. V. 329. № 5997. P. 1345–1348.
105. Wagner W., Wein F., Roderburg C., Saffrich R., Faber A., Krause U., Schubert M., Benes V., Eckstein V., Maul H. et al. // Exp Hematol. 2007. V. 35. № 2. P. 314–325.
106. Hoggatt J., Singh P., Sampath J., Pelus L.M. // Blood. 2009. V. 113. № 22. P. 5444–5455.
107. Robinson S.N., Simmons P.J., Thomas M.W., Brouard N., Javni J.A., Trilok S., Shim J.S., Yang H., Steiner D., Decker W.K. et al. // Exp Hematol. 2012. V. 40. № 6. P. 445–456.
108. Xia L., McDaniel J.M., Yago T., Doeden A., McEver R.P. // Blood. 2004. V. 104. № 10. P. 3091–3096.
109. Tashiro K., Tada H., Heilker R., Shirozu M., Nakano T., Honjo T. // Science. 1993. V. 261. № 5121. P. 600–603.
110. Kim C.H., Broxmeyer H.E. // Blood. 1998. V. 91. № 1. P. 100–110.
111. Aiuti A., Webb I.J., Bleul C., Springer T., Gutierrez-Ramos J.C. // J Exp Med. 1997. V. 185. № 1. P. 111–120.
112. Bleul C.C., Fuhlbrigge R.C., Casasnovas J.M., Aiuti A., Springer T.A. // J Exp Med. 1996. V. 184. № 3. P. 101–109.
113. Peled A., Petit I., Kollet O., Magid M., Ponomaryov T., Byk T., Nagler A., Ben-Hur H., Many A., Shultz L. et al. // Science. 1999. V. 283. № 5403.P. 845–848.
114. Christopherson K.W. 2nd, Paganessi L.A., Napier S., Porecha N.K. // Stem Cells Dev. 2007. V. 16. № 3. P. 355–360.
115. Broxmeyer H.E., Hoggatt J., O'Leary H.A., Mantel C., Chitteti B.R., Cooper S., Messina-Graham S., Hangoc G., Farag S., Rohrabaugh S.L. et al. // Nat Med. 2012. V. 18. № 12. P. 1786–1796.
116. Farag S.S., Srivastava S., Messina-Graham S., Schwartz J., Robertson M.J., Abonour R., Cornetta K., Wood L., Secrest A., Strother R.M. et al. // Stem Cells Dev. 2013. V. 22. № 7. P. 1007–1015.
117. Avigdor A., Goichberg P., Shivtiel S., Dar A., Peled A., Samira S., Kollet O., Hershkoviz R., Alon R., Hardan I. et al // Blood. 2004. V. 103. № 8. P. 2981–2989.
118. Wysoczynski M., Reca R., Ratajczak J., Kucia M., Shirvaikar N., Honczarenko M., Mills M., Wanzeck J., Janowska-Wieczorek A., Ratajczak M.Z. // Blood. 2005. V. 105. № 1. P. 40–48.

Molecular and Cellular Mechanisms of Antitumor Immune Response Activation by Dendritic Cells

O. V. Markov*, N. L. Mironova†, V. V. Vlasov, M. A. Zenkova
Institute of Chemical Biology and Fundamental Medicine, Lavrentieva Ave., 8, Novosibirsk, 630090, Russia
E-mails: *markov_oleg@list.ru; †mironova@niboch.nsc.ru
Received December 03, 2015; in final form, April 29, 2016

ABSTRACT **Dendritic cells (DCs) play a crucial role in the initiation and regulation of the antitumor immune response. Already , DC-based antitumor vaccines have been thoroughly explored both in animal tumor models and in clinical trials. DC-based vaccines are commonly produced from DC progenitors isolated from peripheral blood or bone marrow by culturing in the presence of cytokines, followed by loading the DCs with tumor-specific antigens, such as DNA, RNA, viral vectors, or a tumor cell lysate. However, the efficacy of DC-based vaccines remains low. Undoubtedly, a deeper understanding of the molecular mechanisms by which DCs function would allow us to enhance the antitumor efficacy of DC-based vaccines in clinical applications. This review describes the origin and major subsets of mouse and human DCs, as well as the differences between them. The cellular mechanisms of presentation and cross-presentation of exogenous antigens by DCs to T cells are described. We discuss intracellular antigen processing in DCs, cross-dressing, and the acquisition of the antigen cross-presentation function. A particular section in the review describes the mechanisms of tumor escape from immune surveillance through the suppression of DCs functions.**
KEYWORDS **dendritic cells, subsets, antigen presentation and cross-presentation, proteasome, tumor immunosuppression.**
ABBREVIATIONS **Ag – antigen; APC – antigen-presenting cell; pDC – plasmacytoid dendritic cell; pre-DC – DC precursor; TCR – T cell receptor; Treg – regulatory T cell; CMP – common myeloid progenitor; HLA – human leukocyte antigen; MDP – macrophage-dendritic cell progenitor; MDSC – myeloid-derived suppressor cell; NK – natural killer; TAM – tumor-associated macrophage; Th – T helper cell; TLR – toll-like receptor; ^{low} – low expression level; ^{mid} – middle expression level; ^{high} – high expression level.**

INTRODUCTION

Today, methods based on the activation of the immune system are of particular importance in cancer therapy. Dendritic-cell- (DC)-based vaccines capable of triggering and maintaining a tumor-specific T and B cell immune response stand out among various approaches [1]. DCs are professional antigen-presenting cells (APCs) the main function of which is to capture foreign antigens and process and present them on the cell surface in complexes with major histocompatibility complex (MHC) class I and II molecules to naive T cells. This interaction results in the maturation and activation of tumor-specific cytotoxic T lymphocytes (CTLs) capable of migrating to tumor sites, identifying tumor cells, and destroying them. In addition, the interaction triggers a response by type 1 and 2 T helper cells (Ths), which stimulates the T and B cell arms of the antitumor immune response. Additional stimulation by DC-secreted cytokines promotes the proliferation of tumor-specific CTL clones. The challenge today is to develop DC-based vaccines for the effective treatment of cancers and overcoming tumor-induced immunodeficient conditions.

The tumor microenvironment is known to suppress the immune system, which enables that tumor to escape immune surveillance. The tumor and its microenvironment produce various chemokines and cytokines that inhibit the maturation of APCs and T cells, which finally leads to the suppression of the functional activity of the T cell arm of antitumor immunity. Immunosuppression caused by the action of substances secreted by the tumor environment leads to the failure of standard treatments for malignant tumors. Therefore, the development of antitumor therapies based on the activation of the immune system is topical today. DC-based vaccines are considered as one of the most effec-

tive ways to overcome immunodeficiency on the basis of body resources.

This review describes the origin of DCs, their subsets, the molecular and cellular mechanisms of DC-based antitumor immune response activation, and the resistance of the tumor and its environment to the ability of dendritic cells to suppress tumor growth.

BASICS OF DC FUNCTIONING: THE RELATIONSHIP TO INNATE AND ADAPTIVE IMMUNITY

The main task of the DCs present in all body tissues is to recognize exogenous or endogenous pathogenic antigens (Ags) and transmit the received information to adaptive immunity cells (naive T cells) through the presentation of Ags in a complex with the MHC molecules on the DC surface.

DCs are key cells that interconnect ancient low-specific innate immunity and evolutionarily new, highly specific adaptive immunity. DCs originate from bone marrow progenitors that a are common to monocytes, macrophages, and granulocytes – the main cellular factors of innate immunity. DCs share the common properties of these cells; in particular, the ability of phagocytosis, i.e. to uptake solids (cells, apoptotic bodies, proteins, etc). Indeed, almost all innate immune cells, except eosinophils and natural killers (NKs), use phagocytosis as one of the important mechanisms for the destruction of targets (bacteria and foreign or self, infected or tumor cells) [2]. DCs use phagocytosis, along with pinocytosis and receptor-mediated endocytosis, to uptake Ags for subsequent processing and presentation.

Innate immune cells have a nonspecific mechanism of target recognition using receptors that identify not single molecules (Ag epitopes), as the T cells of adaptive immunity, but groups of molecules, reporting on the foreignness or aggressiveness of their carriers [3]. For example, the surface of most innate immune cells bears lectins that recognize the terminal sugar residues of proteoglycans. The cell surface of DCs also possesses a large amount of C lectins, in particular mannose receptors (CD206) that bind terminal mannose residues [4]. Mannose receptors are also widely expressed by macrophages.

Another property common to DCs and innate immune cells, namely phagocytes (monocytes and macrophages), is the DCs ability to present Ags in complexes with MHC molecules to lymphocytes. However, DCs, which are professional APCs, stimulate T cells 10–100 times more effectively than other APCs (monocytes, macrophages, B cells) [5–7]. Only DCs are able to cross-present Ags most effectively; i.e. to present exogenous Ags in complexes with MHC class I molecules to $CD8^+$ T cells, triggering an Ag-specific response by CTLs [8]. In addition, only DCs can present Ags to the naive T cells in lymphoid organs [9].

Another cellular factor of innate immunity is NKs that have a lymphocytic origin but differ from adaptive immune lymphocytes by a more primitive recognition mechanism and the only way of destroying target cells through perforin-dependent cytolysis involving perforin and granzyme [3]. DCs were shown to closely interact with NKs, stimulate NK proliferation and cytokine production, and also increase NK cytotoxicity. Activated NKs, in turn, play an important role in the elimination of immature tolerogenic DCs. On the other hand, NKs can induce DC maturation and affect the polarization of T cell responses. After recognizing a target, NKs secrete the tumor necrosis factor α (TNF-α) and interferon-γ (IFN-γ) that promote DC maturation and polarization of the T helper type 1 response (Th1 response). Furthermore, these cytokines enhance cross-presentation of Ags by dendritic cells to T cells. Thus, the relationship between DCs and NKs is of great importance in developing an effective tumor-specific adaptive immune response [10].

To generate an antigen-specific adaptive immune response, immature DCs leave the bone marrow and migrate with the blood flow to peripheral tissues. There, DCs uptake foreign or self Ags, process, and expose Ags on the cell surface in complexes with MHC class I and II molecules. At the same time, DCs in peripheral tissues are affected by pathogenic agents and/or inflammatory cytokines, which leads to DC maturation. Mature Ag-loaded DCs migrate via afferent lymphatic vessels to the lymph nodes, where they interact with naive $CD4^+$ and $CD8^+$ T cells [11, 12] (*Fig. 1*).

Upon interaction with DCs, naive T cells can differentiate into antigen-specific effector T cells with different functions. For example, $CD4^+$ T cells can become type 1, 2, and 17 T helper cells, as well as regulatory T cells (Treg). Their main functions are to stimulate cytotoxic T cells, activate the B cells producing antibodies under their control, regulate the autoimmune and pro-inflammatory responses, and suppress the functions of other lymphocytes, respectively. Naive $CD8^+$ T cells differentiate into CTLs that can specifically recognize and destroy tumor cells [13]. Therefore, DCs can, both directly and indirectly, specifically trigger, program, and regulate the T and B cell antitumor immune responses.

The origin and subsets of DCs

DCs are a heterogeneous cell population originating from a dedicated hematopoietic lineage of bone marrow progenitors [14]. There are several DC subsets differing in origin, phenotype, localization, migration pathways, functions, and, as a result, impact on in-

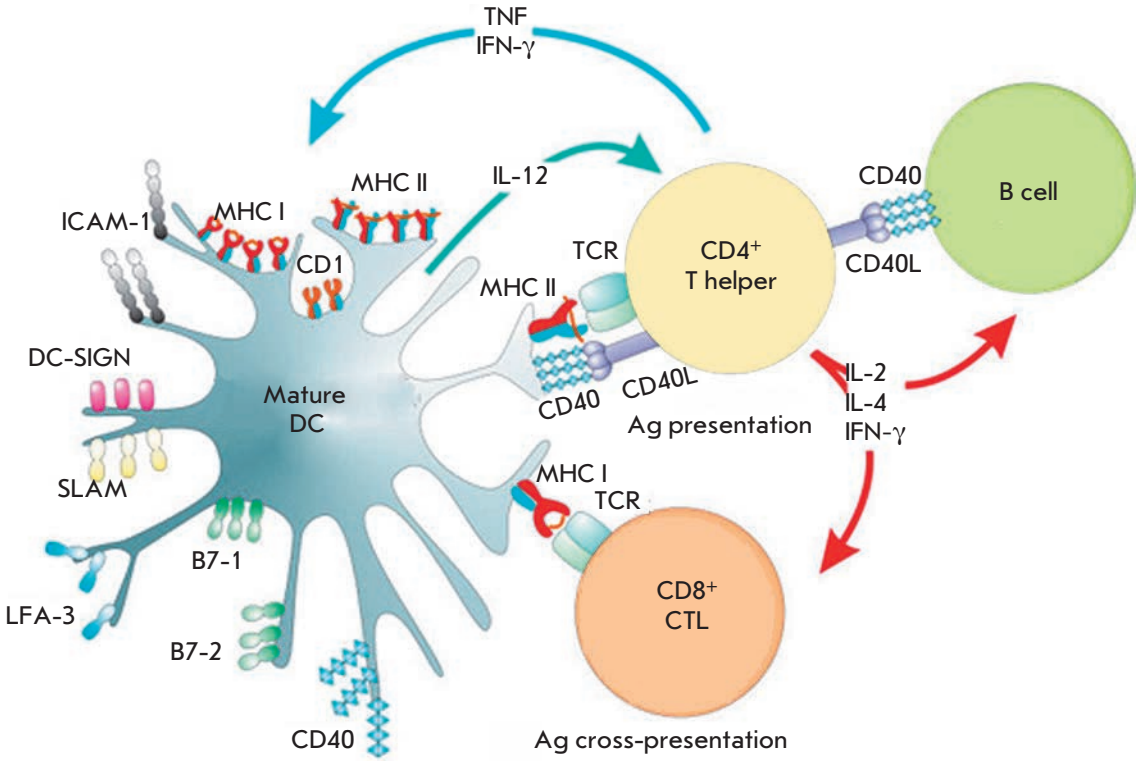

Fig. 1. Interaction between DCs and $CD4^+$ and $CD8^+$ T cells [12].

nate and adaptive immunity [15]. These subsets can be grouped into two main groups: conventional DCs (cDCs) and plasmacytoid DCs (pDCs).

DC precursors (pre-DCs)

Pre-DCs are believed to originate from bone marrow precursors that lose, as they mature, the potential to develop into other cell types. This process is called commitment. The earliest committed pre-DCs are clonogenic common myeloid progenitors (CMPs), found in both mice and humans [16] (*Fig. 2*), that give rise to erythrocytes, granulocytes, megakaryocytes, monocytes, macrophages, DCs, and pDCs [17, 18].

Precursors of cDCs (pre-cDCs) with a $Lin^-CD11c^+MHC\ II^+$ phenotype leave the bone marrow and travel with the blood to lymphoid organs, where they differentiate into lymphoid tissue-resident $CD8^+$ and $CD11b^+$ cDCs. They also occur in non-lymphoid organs, such as the liver, kidneys, lungs, and intestines, where they give rise to $CD103^+$ and $CD11b^+$ cDCs [19, 20]. Therefore, pre-cDCs are immediate cDC progenitors that permanently migrate from the bone marrow to the periphery to differentiate into the cDCs of peripheral tissues and resident DCs of lymphoid organs.

Langerhans cells are different from other DC subsets, because they self-renew independently of the bone marrow and differentiate from the precursors that entered the skin before birth [21]. However, these cells can develop from blood monocytes under inflammatory conditions, when the Langerhans cell population is very depleted [22].

DC subsets

Plasmacytoid DCs. pDCs are a small DC subset (0.3–0.5% of human peripheral blood cells or mouse lymphoid organ cells) that share a similar origin with, but a different life cycle than, conventional DCs. pDCs accumulate mainly in the blood and lymphoid organs and migrate to the lymph nodes via the bloodstream [14]. A low expression level of MHC class II and co-stimulatory molecules was detected in pDCs. The $CD11c^{low}CD11b^-CD45R/B220^+$ phenotype is typical of mouse cDCs [23, 24], and the $Lin^-CD11c^-CD123(IL\text{-}3\ R\alpha)^+$ phenotype is typical of human cDCs [25]. Most pDCs develop from common bone marrow preDCs (CDPs) with both a dendritic cell and lymphoid potential [26].

pDCs are called cells that produce type I interferons (IFN-α/β), because they secrete large amounts of IFN-α/β upon interaction between pathogenic nucleic acids and the Toll-like receptors (TLR3, TLR7, TLR8, and/or TLR9) expressed in pDCs [27–29]. In this case, a protective immune response is induced because IFNs-α/β enhance the cross-presenting ability of conventional DCs and activate immune cells, such as B and T cells and NK cells. Therefore, activated pDCs

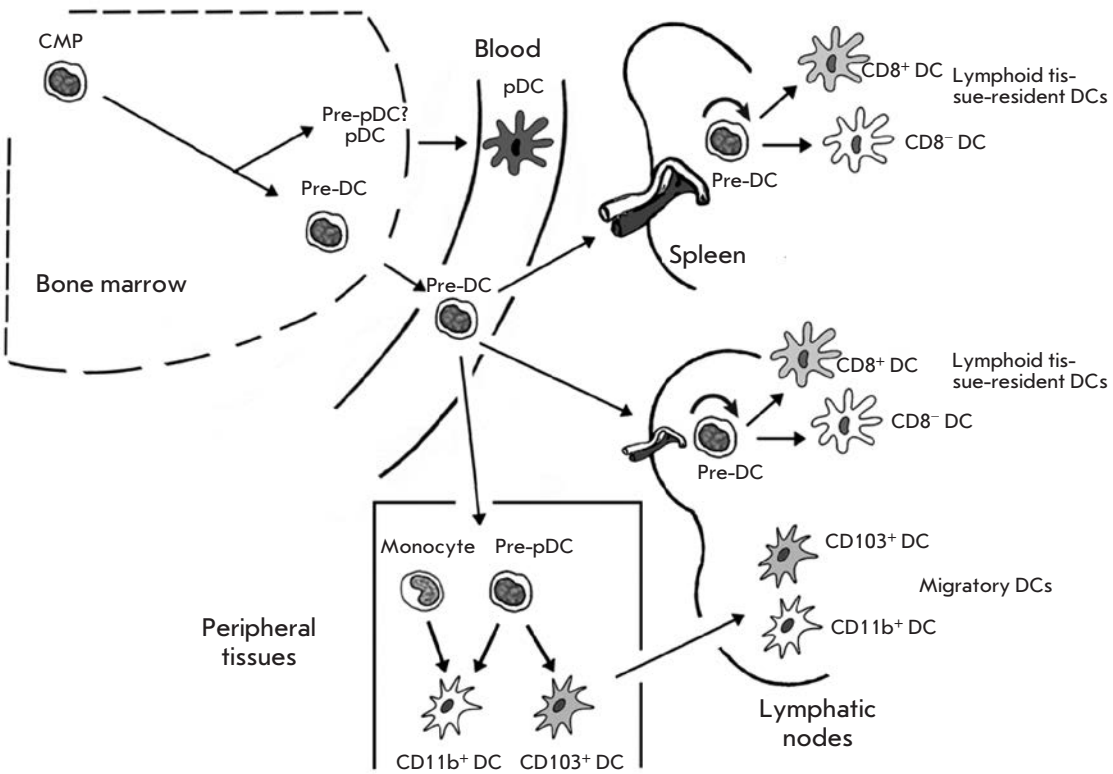

Fig. 2. DC progenitors [16].

play an important role in innate and the adaptive immune responses [30].

Normally, mouse pDCs are localized in the lymphoid organs and blood, as well as in the liver, lungs, and skin. In humans, pDCs are found not only in the liver and blood, but also in lymphoid organs. They can migrate from the lymphoid organs through the bloodstream to the T cell zones of secondary lymphoid tissues and to the splenic marginal zone. In pathological conditions, pDCs leave the bone marrow, organs, or bloodstream and infiltrate inflamed tissues, where they interact with alarm signals (foreign Ags, pathogenic agents, etc.) and release large amounts of type I interferons [31].

Conventional DCs. Conventional DCs (cDCs) include all DCs, except plasmacytoid DCs. They can be found in most lymphoid and non-lymphoid tissues. cDCs can find damaged tissues, capture foreign or self Ags, and process and very efficiently present antigens to T cells. Therefore, cDCs can induce immunity in any foreign Ags entering tissues and trigger tolerance to self Ags.

cDCs constitutively express the hematopoietic markers CD45, MHC II, Flt3, and CD11c and lack the lineage-specific markers of T and B cells, natural killers, granulocytes, and erythrocytes [14]. According to their localization, conventional DCs can be classified into migratory non-lymphoid cDCs and lymphoid tissue-resident cDCs that never leave lymphoid organs.

Mouse conventional DCs. In non-lymphoid tissue, cDCs account for 1–5% of the cells, depending on a particular organ, and consist of two subsets: $CD103^+CD11b^-$ and $CD11b^+$ cDCs (*Fig. 3*). $CD103^+CD11b^-$ cDCs reside in most connective tissues. These are the main APCs that can more effectively, compared to other DC subsets, cross-present Ags to naïve T cells [32] (*Fig. 3*). Both non-lymphoid tissue and lymphoid tissue-resident $CD11b^+$ cDCs play the major role in the presentation of Ags with MHC class II molecules [33] (*Fig. 3*).

The third cDC subset, Langerhans cells, is presented in the epidermal skin layer. They account for 2–4% of the total amount of epidermal cells [34] and are characterized by MHC $II^{low}CD11c^{mid}CD207^{high}$. Langerhans cells can trigger an antiviral $CD8^+$ T cell response against various viral pathogens, except cytolytic viruses, such as herpes simplex and vaccinia viruses, because they possess the ability to induce the apoptosis of DCs, including Langerhans cells [35].

Resident cDCs of lymphoid organs consist mainly of two subsets: $CD8^+$ and $CD11b^+$ cDCs [36] (*Fig. 3*). $CD8\alpha^+$ DCs account for 20–40% of the cDCs of the spleen and lymph nodes. $CD11b^+$ DCs prevail among lymphoid-resident cDC populations in all lymphoid

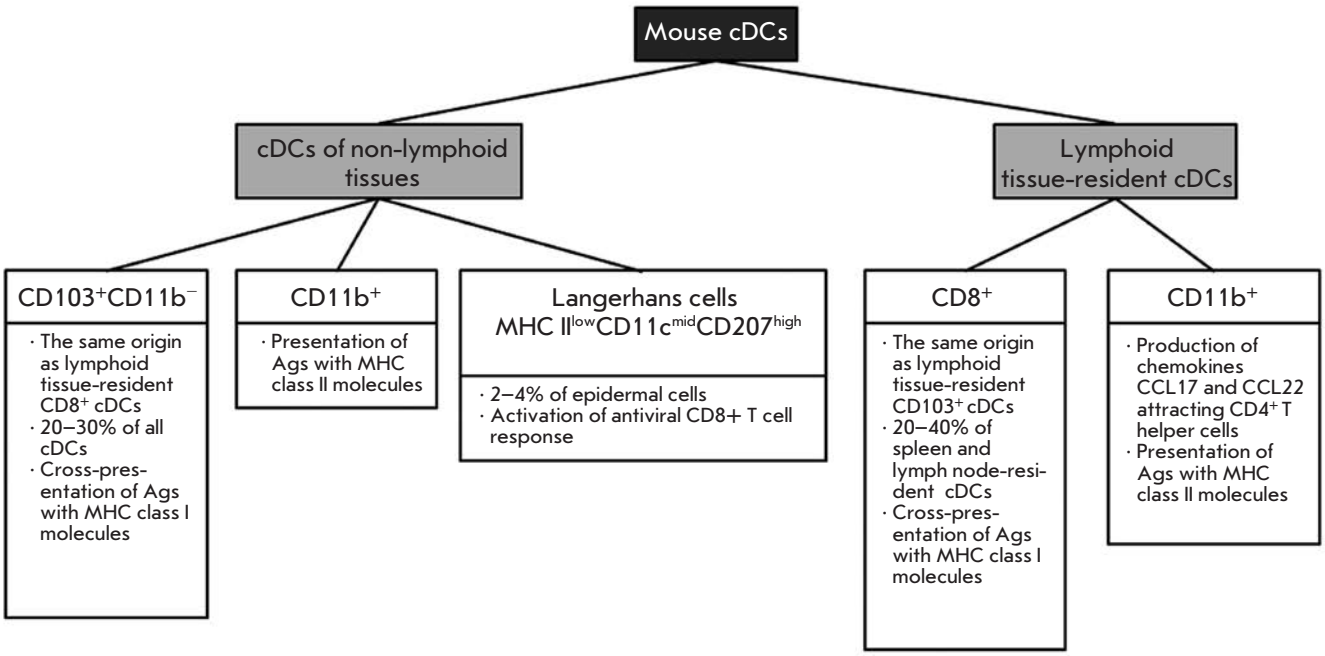

Fig. 3. Subsets of mouse conventional DCs.

tissues, except the thymus. These cells produce high levels of $CD4^+$ T cell attractant chemokines CCL17 and CCL22 [14].

Human conventional DCs. The main difference between human and mouse cDCs is associated with the spectrum of surface markers. Human cDCs are divided into non-lymphoid tissue, blood, and lymphoid tissue-resident cDCs (*Fig. 4*). Human blood cDCs have the $Lin^-MHC\ II^+CD11c^+$ phenotype and are present in two subsets expressing non-overlapping markers: CD1c (BDCA1) or CD141 (BDCA3). The dominant peripheral blood DC subset is represented by $CD1c^+$ cells, while $CD141^+$ DCs form a minute population [14] (*Fig. 4*).

Non-lymphoid tissue cDCs include $CD1a^+CD14^-$ DCs, $CD1a^-CD14^+$ DCs [37], and a separate $CD141^{+}$-$Flt3^{high}$ DC subset originating from peripheral blood $CD141^+$ DCs [38]. Non-lymphoid tissue cDCs also include Langerhans cells expressing the markers CD45, MHC II, epithelial cell adhesion molecules (EpCAMs), langerin CD207, and CD1a [14] (*Fig. 4*).

Lymphoid tissue-resident cDCs consist of $CD1c^+$ and $CD141^+$ cDC subsets similar to blood DCs [38]. Lymph node cells also include $MHC\ II^{high}CD11c^{mid}EpCAM^+CD1a^+$, $EpCAM^-CD1a^+$, and $CD206^+$ cells that are classified as migratory Langerhans cells, migratory dermal $CD1a^+$ DCs, and dermal $CD14^+$ DCs, respectively [39] (*Fig. 4*). Most human thymus cDCs have the $CD11c^+CD11b^-CD45RO^{low}$ phenotype and lack the myeloid markers presented on $CD141^+$ DCs.

FUNCTIONS OF DCS

MHC class II antigen presentation by DCs

Professional APCs (DCs, macrophages, and B cells) are characterized first of all by a high expression level of MHC class II molecules on the cell surface. Virtually all DC subsets are able to uptake exogenous Ags, process and present them in complexes with MHC class II molecules to $CD4^+$ T cells, and trigger T helper immune responses of different types. For effective activation of a T helper response, DCs require, in addition to $MHC\ II^-Ag$ complexes, the presence of co-stimulatory and adhesion molecules (CD80, CD86, CD40, etc.) on the cell surface, as well as the synthesis of cytokines, such as IL-12, IFN-γ (Th1 response), IL-4 (Th2 response), or IL-23 (Th17 response) [40] (*Fig. 1, 5*).

Figure 5 depicts the presentation of exogenous Ags by DCs with MHC class II molecules. The MHC class II molecule is a heterodimer composed of two homogeneous peptides, the α- and β-chains, that are assembled in the endoplasmic reticulum (ER) and are attached to the invariant chain (Ii) (*Fig. 5*). MHC II/Ii complexes are transported to late endosomes, called MHC II compartments (MIIC). The transport is regulated by two dileucine motifs which are located on the cytoplasmic

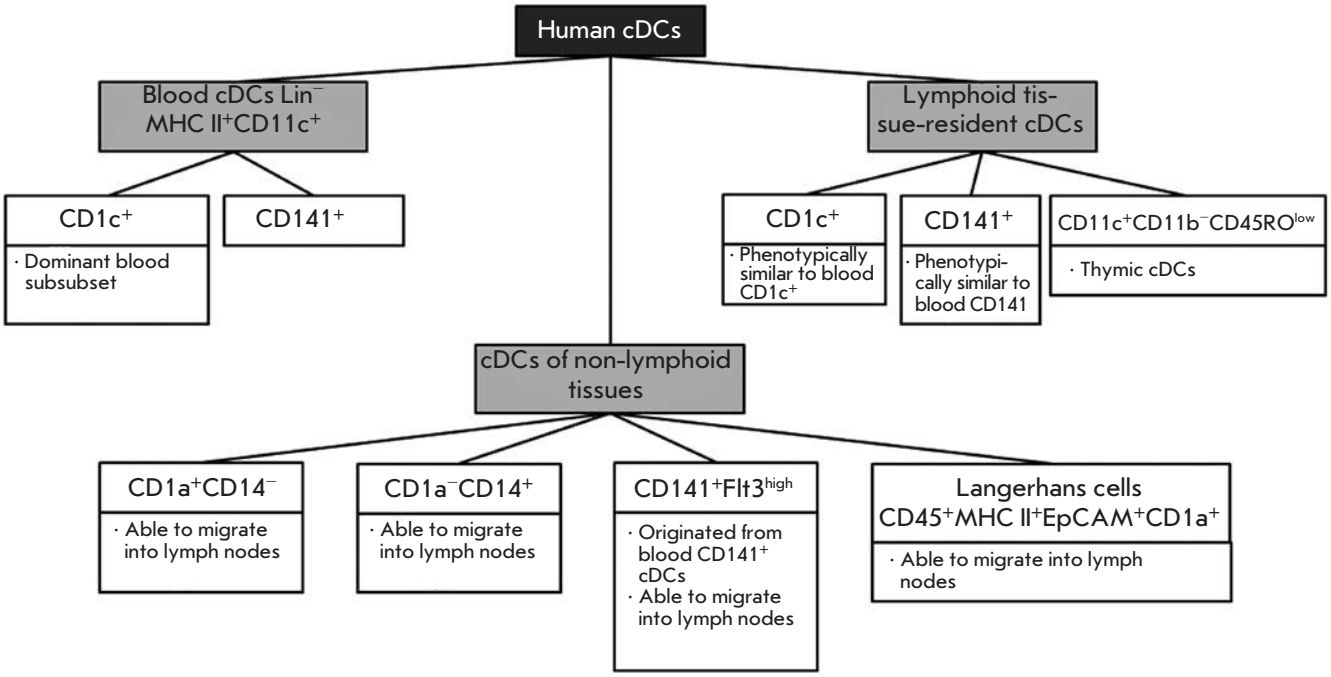

Fig. 4. Subsets of human conventional DCs.

terminus of the invariant chain and are recognized by the sorting adaptors AP1 (a *trans*-Golgi network adaptor) and AP2 (a plasma membrane adaptor). The AP2-dependent endocytic endocytic transport pathway of MHC class II molecules from the plasma membrane to MIIC prevails in immature DCs, whereas the AP1-dependent transport from the *trans*-Golgi network is typical of mature DCs [41].

In MIIC, the invariant chain is cleaved from the MHC class II molecule by proteases cathepsin S and L, with the class II-associated Ii peptide (CLIP) remaining in the MHC class II peptide-binding groove. MHC class II molecules need a chaperone protein, H2-DM in mice or HLA-DM in humans, to exchange CLIP for a high-affinity antigenic peptide. To present Ags with MHC class II molecules, DCs use the vacuolar Ag processing pathway, where captured proteins are cleaved into peptides by lysosomal proteases.

The resulting MHC II/peptide complexes are transported in vesicles to the plasma membrane via fast microtubule transport involving motor proteins dynein (inward transport) and kinesin (outward transport), as well as via slow transport with actomyosin motor proteins.

The efficiency of Ag presentation with MHC class II molecules is inversely related to (i) the susceptibility of protein Ags to degradation and (ii) the concentration and activity of proteolytic enzymes in late endosomes. DCs differ from other phagocytic cells (e.g., macrophages) by a significantly lower expression level of lysosomal proteases and a reduced level of proteolytic activity. This is related to the high pH level of endosomal compartments, which is due to the low activity of V-ATPase and increased activity of NADPH-oxidase 2 [42].

MHC class I Ag cross-presentation

Cross-presentation is the presentation of exogenous Ags with MHC class I molecules, which is necessary to trigger a cytotoxic $CD8^+$ T cell response (*Fig. 6*). DCs are unique APCs, because only they can cross-present Ags to naive $CD8^+$ T cells [8]. This ability is essential for immune surveillance and enables the immune system to identify the tumors and viruses not infecting DCs. It should be noted that not all DC subsets have the ability of effective cross-presentation. In mice, the most effective DCs are migratory $CD103^+CD11b^-$ and lymphoid tissue-resident $CD8^+CD11b^-$ DCs [32]; in humans – $CD141^+$ DCs [14].

MHC class I molecules are expressed by all nuclear cells. The main function of MHC class I molecules in cells is the presentation of endogenous AGs to the immune system to send a signal that this is not a foreign cell, but the organism's cell. The MHC class I molecule is a heterodimeric protein consisting of a polymorphic heavy chain and a light chain called β2-microglobulin. The heavy chain polymorphism provides a variety of peptide-binding sites in MHC class I molecules, which

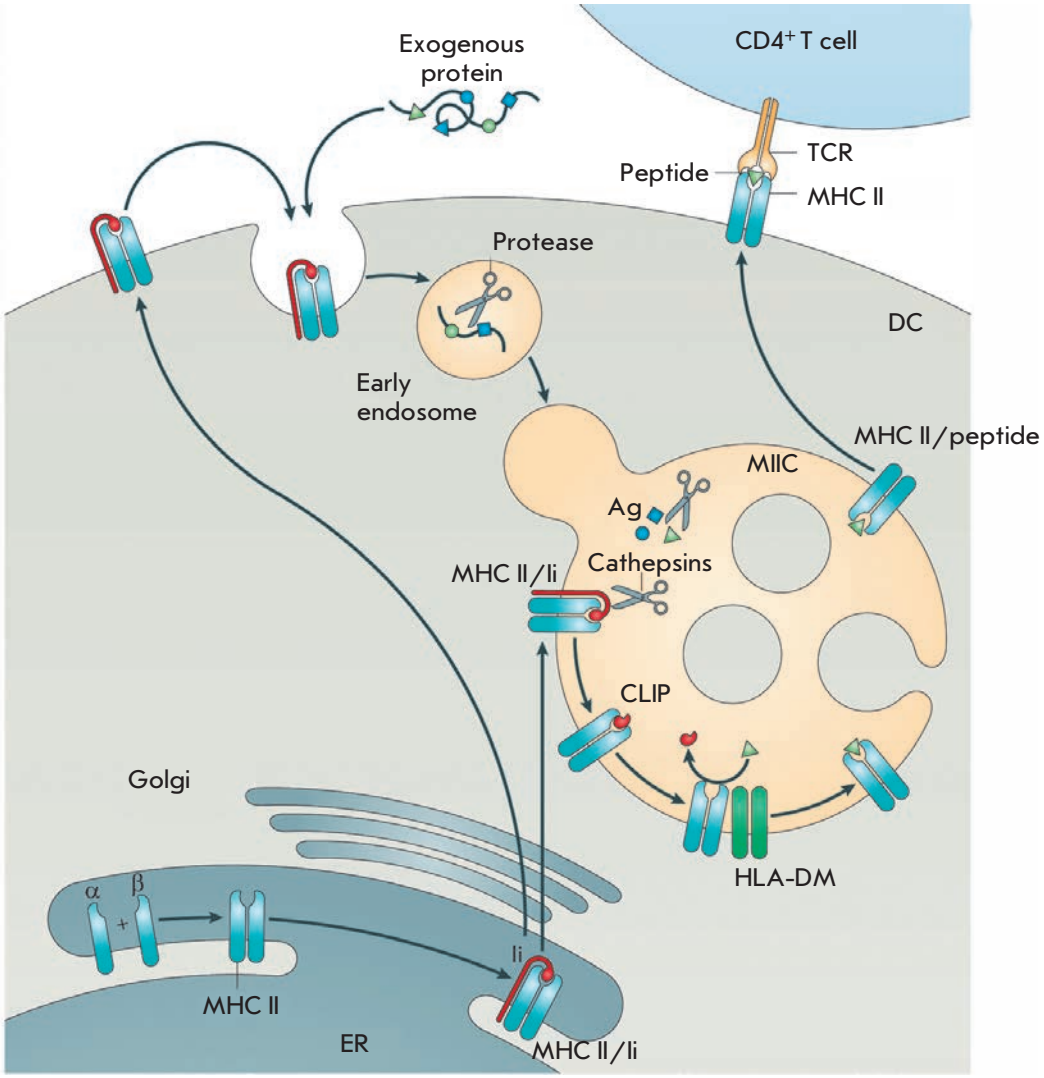

Fig. 5. Presentation of exogenous antigens by DCs with MHC class II molecules [41].

enables MHC class I molecules to recognize unique antigenic peptides due to the differences in the anchor residues to which peptides dock [41].

MHC class I molecules accumulate in the ER and stay there due to the interaction with chaperone proteins, such as calnexin, calreticulin, ERp57, PDI, and tapasin, before binding peptides. MHC I heterodimers are unstable and readily dissociate under physiological conditions in the absence of a suitable peptide.

Processed antigenic peptides for cross-presentation are transferred by TAP proteins to MHC class I molecules in the ER. The peptide-binding site of MHC class I molecules accommodates 8 to 10 residue peptides, depending on the MHC haplotype. Peptides bind to the anchor sequences of MHC class I molecules mainly via N- and C-terminal amino acid residues, as well as via the side chains of some intramolecular residues [43]. Binding of a peptide to a MHC class I molecule leads to the stabilization of the interaction between MHC class I heavy and light chains and the release of chaperones. After this, the fully assembled MHC class I/peptide complex can leave the ER for presentation on the cell surface. This mechanism prevents the transport of "empty" MHC class I molecules to the plasma membrane to interact there with exogenous Ags. Peptides and MHC class I molecules that are not bound to the ER are returned to the cytosol for degradation [44].

Ag processing and MHC class I complex formation

There are two major mechanisms of Ag processing during cross-presentation: vacuolar and cytosolic. They can act either separately or simultaneously, depending on the type of cross-presented Ag.

Vacuolar Ag processing pathway. In the vacuolar Ag processing pathway, the cross-presented Ags are processed and bind to MHC class I molecules inside endosomes/phagosomes. One of the mechanisms suggests the involvement of the chaperone CD74 in the transport of newly synthesized MHC class I molecules from the ER to the endocytic compartments of DCs [45]. In the phagosome, Ag processing for cross-presentation involves cysteine protease cathepsin S [46]. In addition, the synthesis of cross-presented peptides during the cytosolic Ag processing pathway involves insulin-regulated aminopeptidase IRAP that is similar to the aminopeptidases ERAP1 and ERAP2 of the ER [47, 48].

Cytosolic Ag processing pathway. The cytosolic pathway plays a major role in the processing of Ags in DCs [46]. It was demonstrated that blockage of the vacuolar Ag processing pathway weakly inhibits cross-presentation and is even capable of strengthening it, while inhibitors of the proteasome and protein transport to the Golgi complex (lactacystin and brefeldin A, respectively) completely suppress the DC ability to cross-present Ags to $CD8^+$ T cells [49].

In the cytosolic pathway, Ags are transported from phagosomes to the cytosol, where they are processed by proteasomal proteolysis, like endogenous Ags, for cross-presentation. The mechanism of Ag transport from endosomes to the cytosol is not completely understood. The mechanism is supposed to involve the ER-associated degradation machinery (ERAD machinery), in particular its constituent proteins SEC61 and p97 [50]. Translocation of DC-captured Ags by mannose receptors is controlled by ubiquitination of cytosolic mannose receptor sites. The protein p97, which is an ATP-ase, is attracted to the endosome/phagosome membrane through the interaction with polyubiquitinated mannose receptors [51]. An alternative mechanism of the endosome-to-cytosol translocation of Ags may include simple endosomal membrane destabilization by reactive oxygen species that are efficiently produced in the endocytic compartments of DCs [52].

Ags translocated to the cytosol undergo proteasomal processing that involves both conventional proteasomes and immunoproteasomes [53, 54]. Antigenic peptides generated by the proteasome and/or immunoproteasome are transported by TAP proteins into the ER lumen, where the peptides are hydrolyzed by terminal aminopeptidase ERAP1 into peptides of a suitable length for loading onto MHC class I molecules and subsequent cross-presenting to $CD8^+$ T cells.

Cross-dressing by DCs

Apart from direct presentation and cross-presentation of exogenous Ags, there is an additional mechanism of Ag presentation, called cross-dressing, when DCs acquire MHC I/ antigen peptide complexes from dead tumor cells. Cross-dressing is mediated by secreted exosomes and trogocytosis that is a process by which cells exchange by cell membrane and membrane protein fragments. This enables DCs to present directly captured Ags without further processing. Unlike Ag cross-presentation involving the activation of $CD8^+$ CTLs against DC-processed peptides, cross-dressing promotes activation of $CD8^+$ T cells specific to peptides generated by the tumor cell, which may enhance the antigen specificity of the antitumor immune response. Cross-dressing can involve $CD8\alpha^+/CD103^+$ DCs, activated and naive $CD8^+$ T cells, and $CD8^+$ memory T cells [55–57].

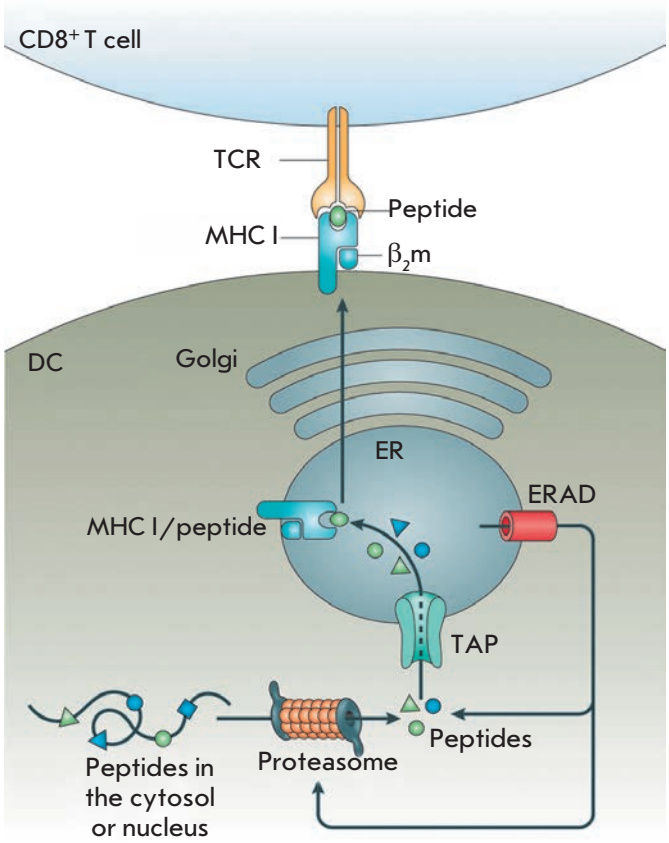

Fig. 6. Cross-presentation of exogenous antigens by DCs with MHC class I molecules [41].

Induction of DC cross-presentation function

The cross-presentation function is acquired at the last stage of DC maturation, upon stimulation by microbial products, e.g. TLR-ligands, or cytokines, e.g. the granulocyte macrophage colony-stimulating factor (GM-CSF). Therefore, effective cross-presentation is typical of peripheral DC subsets during inflammation and infection.

$CD8^+CD103^-$ DCs isolated from a normal mouse spleen proved ineffective in the cross-presentation of Ags with MHC class I molecules in a medium lacking TLR ligands and cytokines, but they effectively presented Ags with MHC class II molecules [58]. Additional activation factors were required to induce cross-presentation, which indicates that this property of $CD8^+$ DCs may be regulated.

TLR ligands not only activate the maturation of $CD8^+$ DCs, but also promote an increase in the level of co-stimulatory and adhesion molecules on the DC surface and can also affect the processing of Ags by $CD8^+$ DCs and enhance the cross-presentation of Ags [58].

In addition to microbial products, such as TLR ligands, the cross-presentation function in early progenitors of $CD8^+$ DCs can be induced by GM-CSF. Normally, GM-CSF is produced at a low level, but its production is dramatically increased in infection or inflammation. GM-CSF-based induction of the cross-presentation function of DCs is not accompanied by an increase in the expression of standard DC activation markers (MHC II, CD80, CD86, or CD40), but the expression of CD103, a key marker of migratory DCs, is increased.

The mechanism of cross-presentation induction in $CD8^+$ DCs under the influence of these factors is not quite clear; apparently, it may involve the strengthening of DC proteasome activity, induction of TAP protein transport to early endosomes, or enhancement of Ag transport from early endosomes to the cytosol [58].

In the normal state, cross-presentation in the absence of "danger signals" is an important mechanism for the induction and maintenance of tolerance to self Ags. For example, thymic $CD8^+$ DCs have the ability of cross-presentation in normal conditions and participate in the destruction of developing autoreactive T cells [58].

Presentation of lipid antigens by DCs with CD1 molecules

Presentation of lipid Ags with CD1 molecules is a T cell stimulation pathway independent of MHC class I and class II molecules. CD1 proteins are structurally similar to MHC class I molecules, because they are heterodimers consisting of a CD1 heavy chain non-covalently bound to β2-microglobulin. Human DCs express five CD1 proteins: CD1a, CD1b, CD1c, CD1d, and CD1e, whereas mouse DCs express only one CD1d protein. The structure and function of these proteins have some differences, but their common main function is to present lipid antigens to T cells [59].

CD1a, CD1b, CD1c, and possibly CD1d are involved in the presentation of microbial lipid and lipopeptide antigens, such as mycolic acid, phosphatidylinositol mannoside, lipoarabinomannan, didehydroxy mycobactin, etc., to T cells. In addition, CD1d and, in some cases, CD1a, CD1b, and CD1c are able to present self lipid antigens. T cells recognize CD1-antigen complexes with T cell receptors (TCRs) that do not differ structurally from the TCRs interacting with MHC-antigen complexes. CD1-restricted TCRs that recognize foreign antigens are able to distinguish even small changes in the structure of a hydrophilic group of the lipid antigen [59].

The resulting T cells are involved in immune responses against bacterial (*Mycobacterium tuberculosis*, *Pseudomonas aeruginosa*, *Borrelia burgdorferi*, etc.), parasitic (*Leishmania major*, *Trypanosoma cruzi*, *Trypanosoma gondii*, etc.), viral (herpes simplex virus type 1 and 2, coxsackie virus b3, hepatitis B virus, etc.), and fungal (*Cryptococcus neoformans*) infections [59].

Tumor escape from immune surveillance through the suppression of DC functions

Many types of tumors are known to contain functionally abnormal DCs [60–62]. Furthermore, direct suppression of the proliferation and differentiation of T cells by a tumor or its environment or suppression of DC differentiation are considered to be an important mechanism of tumor escape from the immune system. In this part of the review, we describe the adverse effects of a tumor and its environment on the functional activity of DCs, leading to a suppression of the specific activation of effector $CD4^+$ and $CD8^+$ T cells.

Tumor stroma

An important component that ensures tumor resistance to the immune system is the tumor stroma. The stroma consists of fibroblasts, endothelial cells, and components of the extracellular matrix and inflammatory infiltrate. The latter is localized in the tumor stroma and consists of, in particular, myeloid-derived suppressor cells (MDSCs) and tumor-associated macrophages (TAMs) [63, 64]. Stromal cells produce a variety of factors, including cytokines, chemokines, growth factors, hormones, prostaglandins, lactic acid salts, and gangliosides, promoting the suppression of a DC-mediated response of effector $CD4^+$ and $CD8^+$ T cells and induction of Treg cells [65, 66]. In addition, direct chemical or enzymatic interactions between leukocytic products and clones of tumor-specific T cells have been reported, e.g. nitrotyrosination of T cell receptors and CD8 molecules, which led to the attenuation of antitumor T cell functions [67].

Mechanisms of suppression of DC functions by tumor

There are several mechanisms by which a tumor suppresses or even switches off DC functions. First, the tu-

mor can prevent the penetration (infiltration) of DCs and pre-DCs into the tumor tissue. However, according to some reports, most tumors are infiltrated with even a higher number of DCs than normal tissues [68, 69]. This is due to the fact that tumor cells can produce chemokines, e.g. MIP-3α, that are "selectively chemotaxic" for immature DCs expressing the CCR6 receptor for MIP-3α [69].

Second, a tumor can suppress the maturation of infiltrating immature DCs, which may lead to the development of T cell tolerance. In fact, increased expression of co-stimulatory molecules by macrophages and DCs was found in the leukocytic infiltrate of certain tumors, but the ability of these DCs to present Ags was significantly reduced [61, 70].

Third, phagocytosis and processing of soluble tumor Ags in DCs can be suppressed or completely blocked. For example, a reduced efficiency of Ag uptake was observed in DCs derived from kidney cancer patients [68]. Inhibition of DC phagocytosis is often associated with secretion of the vascular endothelial growth factor (VEGF), which is one of the most important immunosuppressive cytokines produced by a tumor [71]. Several studies have demonstrated a relationship between an elevated VEGF level in the serum of cancer patients and the number and functionality of circulating DCs [72, 73]. Blockage of VEGF was found to increase Ag uptake and the migratory ability of tumor-specific DCs [71].

Fourth, DC migratory activity can be reduced, which is considered as another mechanism by which a tumor escapes the immune response [66]. Indeed, cytokines and growth factors such as IL-10, TGF-β, and VEGF [61] are overexpressed in tumor tissue just as the chemoattractant factors MIP-3α/CCL20 are [69]. On the other hand, tumor tissue contains factors such as gangliosides that inhibit DC migration. Both mechanisms can regulate the recruitment and migration of DCs into the tumor environment.

Fifth, the suppression of DC functions and tumor progression are affected by the inflammation that often accompanies malignancies [74]. Inflammatory mediators can be produced by both tumor cells and tumor stromal cells comprising various leukocyte subsets, in particular myeloid-derived suppressor cells [63] and tumor-associated macrophages [64]. Inflammatory mediators can cause leucopenia and affect angiogenesis and tumor cell survival, motility, and chemotaxis [75].

Overexpression of the STAT3 protein by tumor cells affects the expression of several immunosuppressive cytokines, including IL-10 and TGF-β, suppresses the Th1 response, reduces the expression of co-stimulatory molecules and MHC class II molecules, and activates TGF-β expression in DCs. Tumor progression also correlates with the accumulation of the immature DCs that induce Treg proliferation in tumor-infiltrated lymph nodes.

Sixth, the role of the tumor-secreted exosomes that mediate a variety of effects on immune competent cells, in particular on DCs, has been demonstrated [76, 77]. Exosomes of tumor cells are capable of suppressing the immune system through several mechanisms, including a reduction in the amount of DCs and suppression of their functions, attenuation of the proliferation and cytotoxicity of natural killer cells and T cells, and an increase in the amount of immunosuppressive cells (MDSC and Treg) [76, 77].

By affecting DCs, tumor exosomes facilitate an increase in STAT3 phosphorylation and IL-6 expression and, therefore, reduce both the activity and the number of DCs by inhibiting the differentiation of $CD14^+$ monocytes into immature DCs. Furthermore, $CD14^+$ cells in this case differentiate into $HLA\text{-}DR^{-/low}$ cells that synthesize the TGF-β that inhibits T cell functions [76].

The role of the tumor environment in the suppression of DC functions

Cytokines and growth factors associated with tumor progression. The macrophage colony-stimulating factor (M-CSF) and IL-6 are important factors that are involved in the differentiation of monocytes [78, 79] and suppress the differentiation of DCs [80] by increasing the expression of M-CSF receptors in parallel with a reduction of the amount of GM-CSF α-receptors in pre-DCs. Similar phenomena are also characteristic of the IL-10 produced by tumor cells [81, 82]. *In vitro*, IL-10 inhibits the differentiation, maturation, and functional activity of DCs [83–85], switching the differentiation to mature macrophages [86].

Another growth factor secreted by various tumors under hypoxic conditions is VEGF. The VEGF level both in serum and in tumor tissue correlates with tumor progression [87, 88]. VEGF was shown to inhibit *in vitro* the development of DCs from $CD34^+$ progenitors [89]. Furthermore, VEGF-exposed DCs reduced the production of IL-12, as well as the ability to stimulate allogeneic T cells [90]. VEGF inhibits the development of DCs, increasing the amount of immature myeloid cells [91].

The effect of tumor-associated hypoxia on DC functions. The tumor microenvironment is characterized by a low oxygen level (hypoxia) caused by reduced blood circulation in the tumor tissue [92]. Tumor hypoxia is associated with tumor progression, resistance to radio- and chemotherapy [93], and macrophage phenotype

changes [94, 95]. Under hypoxic conditions, DCs have a normal expression level of surface markers and cytokines, but the migration activity of DCs is inhibited [96, 97]. The physiological response to hypoxia is caused by the action of the hypoxia-induced factor (HIF) induced in the cell under hypoxic conditions [98, 99]. HIF targets include the genes encoding VEGF-A, glucose transporter 1 (Glut-1), and lactate dehydrogenase (LDH) [100]. A lactate dehydrogenase isoform, LDH-5, that transforms lactic acid into pyruvate at the lowest rate among enzymes of this type is not only overexpressed in various tumors, but is also associated with the aggressive phenotype of tumor cells [101]. A high expression of this isoenzyme leads to the accumulation of lactic acid in the tumor cells and microenvironment.

The effect of an altered metabolism of tumor cells on DC functions. The metabolism of tumor cells is well known to differ from that of normal cells. Tumor cells produce energy primarily through very active glycolysis, with subsequent formation of lactic acid, rather than through slow glycolysis and pyruvate oxidation in mitochondria using oxygen as in most normal cells. This phenomenon, called "aerobic glycolysis" or the "Warburg effect" (first described by Otto Warburg), leads to increased lactic acid production [102].

Tumors with a high level of lactic acid have an elevated lactate dehydrogenase level compared to that in normal tissue [103]; furthermore, the isoenzyme LDH-5 was detected in some tumors [101, 104]. A similar overexpression in non-small cell lung cancer or bowel adenocarcinoma is associated with an unfavorable prognosis [101, 104]. In 60–75% of colorectal cancer cases, high LDH-5 expression is strongly correlated with high expression of VEGF-R2 (KDR/Flk-1) [105]. Lactic acid is an important factor affecting DCs, which can facilitate tumor escape from the immune response.

Lactic acid has both negative and positive effects on the development of the T cell immune response [106, 107]. The sodium salt of lactic acid and glucose metabolites suppress the phenotypic and functional maturation of DCs, which correlates with the suppression of NF-κB activation [108]. Lactic acid induces changes in the expression of Ags in human monocyte-derived DCs and a decrease in the secretory capacity of DCs [109]. Lactic acid can also directly inhibit $CD8^+$ T cells [110]. Extracellular acidosis leads to an accumulation of lactic acid in the tumor tissue. Several studies have described the adverse effects of acidic pHs on the functions of T cells and NK cells [111–113]. However, some researchers have noted an improved uptake of Ags by mouse DCs in acidosis and an increased efficiency of induction of specific CTLs [114].

Apart from lactic acid, other tumor cell metabolites can affect DC functions. The synthesis of arachidonic acid metabolites (prostanoids), including prostaglandin and thromboxane, is catalyzed by cyclooxygenases 1 and 2 (COX-1/2) [115]. The cyclooxygenase expression is altered in many tumors, e.g. colon, breast, lung, and ovarian cancers and melanoma [116–118]. COX-2 expression was found in tumor cells and tumor stroma cells [115]. In addition to a direct effect on tumor growth, apoptosis, cell-cell interactions, and angiogenesis, prostanoids suppress the antitumor immune response [118], in particular by inhibiting the differentiation and functions of DCs. For example, C. Sombroek *et al.* found an inhibitory effect of prostanoids and IL-6 on DC differentiation from $CD34^+$ precursors and monocytes [119].

Gangliosides are tumor-cell-produced lipid derivatives that suppress the antitumor immune response [120–122] by inhibiting the differentiation of hematopoietic cells [120]. Some tumor types (neuroblastoma, retinoblastoma, melanoma, liver cancer, and colon cancer) and lymphomas are characterized by an anomalous ganglioside composition [123, 124], which may be associated with hypoxia [125]. Gangliosides impair the maturation and migration activity of Langerhans cells [126] and inhibit the differentiation, maturation, and functions of DCs [127].

CONCLUSION

Knowledge about the origin and functions of dendritic cells, which has been accumulated over the past decade, has enabled the development of tumor immunology principles based on the involvement of body immune cells in fighting malignant diseases. However, many tumor types are associated with the suppression of the dendritic cells that are the most important immune system element that activates a specific antitumor response. This tumor escape of immune surveillance leads to a weakening of the components of both innate immunity (macrophages) and specific immunity (T cell elements). In this regard, it is evident that the development of DC-based antitumor vaccines should focus on the following issues: DC activation/maturation; the type of a tumor-specific antigen used to load dendritic cells; additional constructs encoding co-stimulatory molecules, to increase the efficiency of tumor antigen presentation; and methods of antigen delivery to dendritic cells which provide the highest level of processing and presentation of the antigen in complexes with MHC class I and class II molecules. Solving these problems will help develop protocols for the production of DC-based vaccines for an effective treatment of patients with various tumors. ●

REFERENCES

1. Palucka K., Ueno H., Fay J., Banchereau J. // J. Intern. Med. 2011. V. 269. P. 64–73.
2. Greenberg S., Grinstein S. // Curr. Opin. Immunol. 2002. V. 14. P. 136–145.
3. Yarilin A.A. The basics of immunology. M.: Medicine, 1999. P. 608.
4. Figdor C.G., van Kooyk Y., Adema G.J. // Nat. Rev. Immunol. 2002. V. 2. P. 77–84.
5. Fong L., Engleman E.G. // Annu. Rev. Immunol. 2000. V. 18. P. 245–273.
6. Massard G., Tongio M.M., Wihlm J.M., Morand J. // Ann. Thorac. Surgeon. 1996. V. 61. P. 252–258.
7. Nussenzweig M.C., Steinman R.M., Gutchinov B., Cohn Z.A. // J. Exp. Med. 1980. V. 152. P. 1070–1084.
8. Jung S., Unutmaz D., Wong P., Sano G., De los Santos K., Sparwasser T., Wu S., Vuthoori S., Ko K., Zavala F., et al. // Immunity. 2002. V. 17. P. 211–220.
9. Heath W.R., Belz G.T., Behrens G.M., Smith C.M., Forehan S.P., Parish I.A., Davey G.M., Wilson N.S., Carbone F.R., Villadangos J.A. // Immunol. Rev. 2004. V. 199. P. 9–26.
10. Bonaccorsi I., Pezzino G., Morandi B., Ferlazzo G. // Immunol. Lett. 2013. V. 155. P. 6–10.
11. Banchereau J., Briere F., Caux C., Davoust J., Lebecque S., Liu Y.J., Pulendran B., Palucka K. // Annu. Rev. Immunol. 2000. V. 18. P. 767–811.
12. Gogolák P., Réthi B., Hajas G., Rajnavölgyi E. // J. Mol. Recognit. 2003. V. 16. P. 299–317.
13. Palucka K., Banchereau J. // Nat. Rev. Cancer. 2012. V. 12. P. 265–277.
14. Merad M., Sathe P., Helft J., Miller J., Mortha A. // Annu. Rev. Immunol. 2013. V. 31. P. 563–604.
15. Ueno H., Schmitt N., Klechevsky E., Pedroza-Gonzalez A., Matsui T., Zurawski G., Oh S., Fay J., Pascual V., Banchereau J., et al. // Immunol. Rev. 2010. V. 234. P. 199–212.
16. Helft J., Ginhoux F., Bogunovic M., Merad M. // Immunol. Rev. 2010. V. 234. P. 55–75.
17. Manz M.G., Traver D., Akashi K., Merad M., Miyamoto T., Engleman E.G., Weissman I.L. // Ann. N. Y. Acad. Sci. 2001. V. 938. P. 167–174.
18. Traver D., Akashi K., Manz M., Merad M., Miyamoto T., Engleman E.G., Weissman I.L. // Science. 2000. V. 290. P. 2152–2154.
19. Diao J., Winter E., Cantin C., Chen W., Xu L., Kelvin D., Phillips J., Cattral M.S. // J. Immunol. 2006. V. 176. P. 7196–7206.
20. Ginhoux F., Liu K., Helft J., Bogunovic M., Greter M., Hashimoto D., Price J., Yin N., Bromberg J., Lira S.A., Stanley E.R., Nussenzweig M., Merad M. // J. Exp. Med. 2009. V. 206. P. 3115–3130.
21. Chorro L., Sarde A., Li M., Woollard K.J., Chambon P., Malissen B., Kissenpfennig A., Barbaroux J.B., Groves R., Geissmann F. // J. Exp. Med. 2009. V. 206. P. 3089–3100.
22. Ginhoux F., Tacke F., Angeli V., Bogunovic M., Loubeau M., Dai X.M., Stanley E.R., Randolph G.J., Merad M. // Nat. Immunol. 2006. V. 7. P. 265–273.
23. O'Keeffe M., Hochrein H., Vremec D., Caminschi I., Miller J.L., Anders E.M., Wu L., Lahoud M.H., Henri S., Scott B., etal. // J. Exp. Med. 2002. V. 196. P. 1207–1319.
24. Nakano H., Yanagita M., Gunn M.D. // J. Exp. Med. 2001. V. 194. P. 1171–1178.
25. Shortman K., Liu Y.J. // Nat. Rev. Immunol. 2002. V. 2. P. 151–161.
26. Reizis B., Bunin A., Ghosh H.S., Lewis K.L., Sisirak V. // Annu. Rev. Immunol. 2011. V. 29. P. 163–183.
27. Van Lint S., Renmans D., Broos K., Dewitte H., Lentacker I., Heirman C., Breckpot K., Thielemans K. // Expert Rev. Vaccines. 2015. V. 14. P. 235–251.
28. Hanabuchi S., Liu Y.-J. // Immunity. 2011. V. 35. P. 851–853.
29. Takagi H., Fukaya T., Eizumi K., Sato Y., Sato K., Shibazaki A., Otsuka H., Hijikata A., Watanabe T., Ohara O., et al. // Immunity. 2011. V. 35. P. 958–971.
30. Tel J., de Vries I.J. // Immunotherapy. 2012. V. 4. P. 979–982.
31. Pinto A., Rega A., Crother T.R., Sorrentino R. // Oncoimmunology. 2012. V. 1. P. 726–734.
32. Joffre O.P., Segura E., Savina A., Amigorena S // Nat. Rev. Immunol. 2012. V. 12. P. 557–569.
33. Dudziak D., Kamphorst A.O., Heidkamp G.F., Buchholz V.R., Trumpfheller C., Yamazaki S., Cheong C., Liu K., Lee H.W., Park C.G., et al. // Science. 2007. V. 315. P. 107–111.
34. Valladeau J., Saeland S. // Semin. Immunol. 2005. V. 17. P. 273–283.
35. Merad M., Ginhoux F., Collin M. // Nat. Rev. Immunol. 2008. V. 8. P. 935–947.
36. Vremec D., Zorbas M., Scollay R., Saunders D.J., Ardavin C.F., Wu L., Shortman K. // J. Exp. Med. 1992. V. 176. P. 47–58.
37. Nestle F.O., Zheng X.G., Thompson C.B., Turka L.A., Nickoloff B.J. // J. Immunol. 1993. V. 151. P. 6535–6545.
38. Haniffa M., Shin A., Bigley V., McGovern N., Teo P., See P., Wasan P.S., Wang X.N., Malinarich F., Malleret B., et al. // Immunity. 2012. V. 37. P. 60–73.
39. Segura E., Valladeau-Guilemond J., Donnadieu M.H., Sastre-Garau X., Soumelis V., Amigorena S. // J. Exp. Med. 2012. V. 209. P. 653–660.
40. Cintolo J.A., Datta J., Mathew S.J., Czerniecki B.J. // Future Oncol. 2012. V. 8. P. 1273–1299.
41. Neefjes J., Jongsma M.L., Paul P., Bakke O. // Nat. Rev. Immunol. 2011. V. 11. P. 823–836.
42. Delamarre L., Pack M., Chang H., Mellman I., Trombetta E.S. // Science. 2005. V. 307. P. 1630–1634.
43. Rock K.L., Goldberg A.L. // Annu. Rev. Immunol. 1999. V. 17. P. 739–779.
44. Koopmann J.O., Albring J., Hüter E., Bulbuc N., Spee P., Neefjes J., Hämmerling G.J., Momburg F. // Immunity. 2000. V. 13. P. 117–127.
45. Basha G., Omilusik K., Chavez-Steenbock A., Reinicke A.T., Lack N., Choi K.B., Jefferies W.A. // Nat. Immunol. 2012. V. 13. P. 237–245.
46. Rock K.L., Farfan-Arribas D.J., Shen L. // J. Immunol. 2010. V. 184. P. 9–15.
47. Weimershaus M., Maschalidi S., Sepulveda F., Manoury B., van Endert P., Saveanu L. // J. Immunol. 2012. V. 188. P. 1840–1846.
48. Saveanu L., Carroll O., Weimershaus M., Guermonprez P., Firat E., Lindo V., Greer F., Davoust J., Kratzer R., Keller S.R., et al. // Science. 2009. V. 325. P. 213–217.
49. Kovacsovics-Bankowski M., Rock K.L. // Science. 1995. V. 267. P. 243–246.
50. Ackerman A.L., Giodini A., Cresswell P. // Immunity. 2006. V. 25. P. 607–617.
51. Zehner M., Chasan A.I., Schuette V., Embgenbroich M., Quast T., Kolanus W., Burgdorf S. // Proc. Natl. Acad. Sci. USA. 2011. V. 108. P. 9933–9938.
52. Boya P., Kroemer G. // Oncogene. 2008. V. 27. P. 6434–6451.

53. Chapatte L., Ayyoub M., Morel S., Peitrequin A.L., Lévy N., Servis C., van den Eynde B.J., Valmori D., Lévy F. // Cancer Res. 2006. V. 66. P. 5461–5468.
54. Angeles A., Fung G., Luo H. // Front. Biosci. 2012. V. 17. P. 1904–1916.
55. Yewdell J.W., Dolan, B.P. // Nature. 2011. V. 471. P. 581–582.
56. Dolan B.P., Gibbs K.D.Jr., Ostrand-Rosenberg S. // J. Immunol. 2006. V. 177. P. 6018–6024.
57. Li L., Kim S., Herndon J.M., Goedegebuure P., Belt B.A., Satpathy A.T., Fleming T.P., Hansen T.H., Murphy K.M., Gillanders W.E. // Proc. Natl. Acad. Sci. USA. 2012. V. 109. P. 12716–12721.
58. Dresch C., Leverrier Y., Marvel J., Shortman K. // Trends Immunol. 2012. V. 33. P. 381–388.
59. Brigl M., Brenner M.B. // Annu. Rev. Immunol. 2004. V. 22. P. 817–890.
60. Pinzon-Charry A., Maxwell T., Lopez J.A. // Immunol. Cell. Biol. 2005. V. 83. P. 451–461.
61. Shurin M.R., Shurin G.V., Lokshin A., Yurkovetsky Z.R., Gutkin D.W., Chatta G., Zhong H., Han B., Ferris R.L. // Cancer Metastasis Rev. 2006. V. 25. P. 333–356.
62. Kusmartsev S., Gabrilovich D.I. // Cancer Metastasis Rev. 2006 V. 25. P. 323–331.
63. Marigo I., Dolcetti L., Sefarini P., Zanovello P., Bronte V. // Immunol. Rev. 2008. V. 222. P. 162–179.
64. Sica A., Bronte V. // J. Clin. Invest. 2007. V. 117. P. 1155–1166.
65. Töpfer K., Kempe S., Müller N., Schmitz M., Bachmann M., Cartellieri M., Schackert G., Temme A. // J. Biomed. Biotechnol. 2011. V. 2011. P. 918471.
66. Benencia F., Sprague L., McGinty J., Pate M., Muccioli M. // J. Biomed. Biotechnol. 2012. V. 2012. P. 425476.
67. Nagaraj S., Gabrilovich D.I. // Cancer Res. 2008. V. 6. P. 82561–82563.
68. Thurnher M., Radmayr C., Ramoner R., Ebner S., Böck G., Klocker H., Romani N., Bartsch G. // Int. J. Cancer. 1996 V. 68. P. 1–7.
69. Bell D., Chomarat P., Broyles D., Netto G., Harb G.M., Lebecque S., Valladeau J., Davoust J., Palucka K.A., Banchereau J. // J. Exp. Med. 1999. V. 190. P. 1417–1426.
70. Chaux P., Moutet M., Faivre J., Martin F., Martin M. // Lab. Invest. 1996. V. 74. P. 975–983.
71. Ishida T., Oyama T., Carbone D.P., Gabrilovich D.I. // J. Immunol. 1998. V. 161. P. 4842–4852.
72. Almand B., Resser J.R., Lindman B., Nadaf S., Clark J.I., Kwon E.D., Carbone D.P., Gabrilovich D.I. // Clin. Cancer Res. 2000. V. 6. P. 1755–1766.
73. Lissoni P., Malugani F., Bonfanti A., Bucovec R., Secondino S., Brivio F., Ferrari-Bravo A., Ferrante R., Vigoré L., Rovelli F., et al. // J. Biol. Regul. Homeost. Agents. 2001. V. 15. P. 140–144.
74. Mantovani A., Pierotti M.A. // Cancer Lett. 2008. V. 267. P. 180–181.
75. Borello M.G., Degl`innocenti D., Pierotti M.A. // Cancer Lett. 2008. V. 267. P. 262–270.
76. Zhang H.G., Grizzle W.E. // Am. J. Pathol. 2014. V. 184. P. 28–41.
77. Kharaziha P., Ceder S., Li Q., Panaretakis T. // Biochim. Biophys. Acta. 2012. V. 1826. P. 103–111.
78. Stanley E.R., Berg K.L., Einstein D.B., Lee P.S., Pixley F.J., Wang Y., Yeung Y.G. // Mol. Reprod. Dev. 1997. V. 46. P. 4–10.
79. Jansen J.H., Kluin-Nelemans J.C., Van Damme J., Wientjens G.J., Willemze R., Fibbe W.E. // J. Exp. Med. 1992. V. 175. P. 1151–1154.
80. Menetrier-Caux C., Montmain G., Dieu M.C., Bain C., Favrot M.C., Caux C., Blay J.Y. // Blood. 1998. V. 92. P. 4778–4791.
81. Smith D.R., Kunkel S.L., Burdick M.D., Wilke C.A., Orringer M.B., Whyte R.I., Strieter R.M. // Am. J. Pathol. 1994. V. 145. P. 18–25.
82. Krüger-Krasagakes S., Krasagakis K., Garbe C., Schmitt E., Huls C., Blankenstein T., Diamantstein T. // Br. J. Cancer. 1994. V. 70. P. 1182–1185.
83. Steinbrink K., Wölfl M., Jonuleit H., Knop J., Enk A.H. // J. Immunol. 1997. V. 159. P. 4772–4780
84. Buelens C., Verhasselt V., De Groote D., Thielemans K., Goldman M., Willems F. // Eur. J. Immunol. 1997. V. 27. P. 756–762.
85. Enk A.H., Angeloni V.L., Udey V.C., Katz S.I. // J. Immunol. 1993. V. 151. P. 2390–2398.
86. Allavena P., Piemonti L., Longoni D., Bernasconi S., Stoppacciaro A., Ruco L., Mantovani A. // Eur. J. Immunol. 1998. V. 28. P. 359–369.
87. Yamamoto Y., Toi M., Kondo S., Matsumoto T., Suzuki H., Kitamura M., Tsuruta K., Taniguchi T., Okamoto A., Mori T., et al. // Clin. Cancer. Res. 1996. V. 2. P. 821–826.
88. Toi M., Matsumoto T., Bando H. // Lancet Oncol. 2001. V. 2. P. 667–673.
89. Gabrilovich D.I., Chen H.L., Girgis K.R., Cunningam H.T., Meny G.M., Nadaf S., Kavanaugh D., Carbone D.P. // Nat. Med. 1996. V. 2. P. 1096–1103.
90. Takahashi A., Kono K., Ichihara F., Sugai H., Fujii H., Matsumoto Y. // Cancer Immunol. Immunother. 2004. V. 53. P. 543–550.
91. Gabrilovich D.I., Ishida T., Oyama T., Ran S., Kravtsov V., Nadaf S., Carbone D.P. // Blood. 1998. V. 92. P. 4150–4166.
92. Groebe K., Vapuel P. // Int. J. Radiat. Oncol. Biol. Phys. 1998. V. 15. P. 691–697.
93. Teicher B.A. // Cancer Metastasis Rev. 1994. V. 13. P. 139–168.
94. Turner L., Scotton C., Negus R., Balkwill F. // Eur. J. Immunol. 1999. V. 29. P. 2280–2287.
95. Lewis J.S., Lee J.A., Underwood J.C., Harris A.L., Lewis C.E. // J. Leukoc. Biol. 1999. V. 66. P. 889–900.
96. Zhao W., Darmanin S., Fu Q., Chen J., Cui H., Wang J., Okada F., Hamada J., Hattori Y., Kondo T., et al. // Eur. J. Immunol. 2005. V. 35. P. 3468–3477.
97. Qu X., Yang M.X., Kong B.H., Qi L., Lam Q.L., Yan S., Li P., Zhang M., Lu L. // Immunol. Cell. Biol. 2005. V. 83. P. 668–673.
98. Semenza G.L., Wang G.L. // Mol. Cell. Biol. 1992. V. 12. P. 5447–5454.
99. Semenza G.L. // Curr. Opin. Genet. Dev. 1998. V. 8. P. 588–594.
100. Wenger R.H., Stiehl D.P., Camenisch G. // Sci. STKE. 2005. V. 2005. P. re12.
101. Koukourakis M.I., Giatromanolaki A., Simopoulos C., Polychronidis A., Sivridis E. // Clin. Exp. Metastasis. 2005. V. 22. P. 25–30.
102. Warburg O. // Munch. Med. Wochenschr. 1961. V. 103. P. 2504–2506.
103. Walenta S., Schroeder T., Mueller-Klieser W. // Cyrr. Med. Chem. 2004. V. 11. P. 2195–2204.
104. Koukourakis M.I., Giatromanolaki A., Sivridis E., Bougioukas G., Didilis V., Gatter K.C., Harris A.L.; Tumour and Angiogenesis Research Group. // Br. J. Cancer. 2003. V. 89. P. 877–885.
105. Koukourakis M.I., Giatromanolaki A., Sivridis E., Gatter K.C., Harris A.L. // J. Clin. Oncol. 2006. V. 24. P. 4301–4308.

106. Droge W., Roth S., Altmann A., Mihm S. // Cell Immunol. 1987. V. 108. P. 405–416.
107. Roth S., Gmunder H., Droge W. // Cell Immunol. 1991. V. 136. P. 95–104.
108. Puig-Kroger A., Muniz-Pello O., Selgas R., Criado G., Bajo M.A., Sanchez-Tomero J.A., Alvarez V., del Peso G., Sánchez-Mateos P., Holmes C., et al. // J. Lekoc. Biol. 2003. V. 73. P. 482–492.
109. Gottfried E., Kunz-Schughart L.A., Ebner S., Mueller-Kliesser W., Hoves S., Andreesen R., Mackensen A., Kreutz M. // Blood. 2006. V. 107. P. 2013–2021.
110. Fischer K., Hoffmann P., Voelkl S., Meidenbauer N., Ammer J., Edinger M., Gottfried E., Schwarz S., Rothe G., Hoves S., et al. // Blood. 2007. V. 109. P. 2812–2819.
111. Loeffler D.A., Juneau P.L., Heppner G.H. // Int. J. Cancer. 1991. V. 48. P. 895–899.
112. Fischer B., Muller B., Fischer K.G., Baur N., Kreutz W. // Clin. Immunol. 2000. V. 96. P. 252–263.
113. Muller B., Fischer B., Kreutz W. // Immunology. 2000. V. 99. P. 375–384.
114. Vermeulen M., Giordano M., Trevani A.S., Sedlik C., Gamberale R., Fernandes-Calotti P., Salamone G., Raiden S., Sanjurjo J., Geffner J.R. // J. Immunol. 2004. V. 172. P. 3196–3204.
115. Gately S., Li W.W. // Semin. Oncol. 2004. V. 31. P. 2–11.
116. Denkert C., Kobel M., Berger S., Siegert A., Leclere A., Trefzer U., Hauptmann S. // Cancer Res. 2001. V. 61. P. 303–308.
117. Denkert C., Kobel M., Pest S., Koch I., Berger S., Schwabe M., Siegert A., Reles A., et al. // Am. J. Pathol. 2002. V. 160. P. 893–903.
118. Tsuji S., Tsuji M., Kawano S., Hori M. // J. Exp. Clin. Cancer Res. 2001. V. 20. P. 117–129.
119. Sombroek C.C., Stam A.G., Masterson A.J., Lougheed S.M., Schakel M.J., Meijer C.J., Pinedo H.M., van den Eertwegh A.J., Scheper R.J., de Gruijl T.D. // J. Immunol. 2002. V. 168. P. 4333–4343.
120. Sietsma H., Nijhof W., Donje B., Vellenga E., Kamps W.A., Kok J.W. // Cancer Res. 1998. V. 58. P. 4840–4844.
121. Ladisch S., Wu Z.L., Feig S., Ulsh L., Schwartz E., Floutsis G., Wiley F., Lenarsky C., Seeger R. // Int. J. Cancer. 1987. V. 39. P. 73–76.
122. Biswas K., Richmond A., Rayman P., Biswas S., Thornton M., Sa G., Das T., Zhang R., Chahlavi A., Tannenbaum C.S., et al. // Cancer Res. 2006. V. 66. P. 6816–6825.
123. Birkle S., Zheng G., Gao L., Yu R.K., Aurby J. // Biochimie. 2003. V. 85. P. 455–463.
124. Tourkova I.L., Shurin G.V., Chatta G.S., Perez L., Finke J., Whiteside T.L., Ferrone S., Shurin M.R. // J. Immunol. 2005. V. 175. P. 3045–3052.
125. Yin J., Hashimoto A., Izawa M., Miyazaki K., Chen G.Y., Takematsu H., Kozutsumi Y., Suzuki A., Furuhata K., Cheng F.L., et al. // Cancer Res. 2006. V. 66. P. 2937–2945.
126. Bennaceur K., Popa I., Portoukalian J., Berthier-Vergnes O., Peuget-Navarro J. // Int. Immunol. 2006. V. 18. P. 879–886.
127. Shurin G.V., Shurin M.R., Bykovskaya S., Shogan J., Lotze M.T., Barksdale Jr., E.M. // Cancer Res. 2001. V. 61. P. 363–369.

Stem Cells in the Treatment of Insulin-Dependent Diabetes Mellitus

M. A. Borisov[1,3], O. S. Petrakova[1,2], I. G. Gvazava[1,3], E. N. Kalistratova[2], A. V. Vasiliev[2,3]
[1]Pirogov Russian National Research Medical University, Ostrovitianov str. 1, Moscow, 117997, Russia
[2]Lomonosov Moscow State University, Faculty of Biology, Leninskie Gory 1, bld. 12, Moscow, 119991, Russia
[3]Koltsov Institute of Developmental Biology, Russian Academy of Sciences, Vavilova str. 26, Moscow, 119334, Russia
*E-mail: PetrakovaOl@yandex.ru
Received October 10, 2015; in final form, March 11, 2016

ABSTRACT **Diabetes affects over 350 million people worldwide, with the figure projected to rise to nearly 500 million over the next 20 years, according to the World Health Organization. Insulin-dependent diabetes mellitus (type 1 diabetes) is an endocrine disorder caused by an autoimmune reaction that destroys insulin-producing β-cells in the pancreas, which leads to insulin deficiency. Administration of exogenous insulin remains at the moment the treatment mainstay. This approach helps to regulate blood glucose levels and significantly increases the life expectancy of patients. However, type 1 diabetes is accompanied by long-term complications associated with the systemic nature of the disease and metabolic abnormalities having a profound impact on health. Of greater impact would be a therapeutic approach which would overcome these limitations by better control of blood glucose levels and prevention of acute and chronic complications. The current efforts in the field of regenerative medicine are aimed at finding such an approach. In this review, we discuss the time-honored technique of donor islets of Langerhans transplantation. We also focus on the use of pluripotent stem and committed cells and cellular reprogramming. The molecular mechanisms of pancreatic differentiation are highlighted. Much attention is devoted to the methods of grafts delivery and to the materials used during its creation.**
KEYWORDS **cellular therapy, diabetes, differentiation, gene expression, pancreas**
ABBREVIATIONS **iPS cells – induced pluripotent stem cells, ECM – extracellular matrix; MSCs – mesenchymal stem cells, iL – islets of Langerhans, the PSCs – pluripotent stem cells, E – embryonic development, ES cells – embryonic stem cells.**

MOLECULAR MECHANISMS OF PANCREATIC DIFFERENTIATION

To gain insights into the pancreatic differentiation of cells *in vitro*, the primary stages of pancreatic organogenesis need to be clarified. Numerous studies in mouse models have greatly advanced our understanding of developmental mechanisms and delineated the stages of organ formation (*Table*).

The pancreas plays a crucial metabolic role by producing various hormones and enzymes. The pancreas contains exocrine and endocrine cells. The exocrine compartment consists of acinar cells that produce digestive enzymes, such as amylases, lipases, proteases, and nucleases. These enzymes are released into ducts which form the branching duct system lined with epithelial cells [1]. The endocrine pancreas is composed of cell clusters called islets of Langerhans (iL). Each pancreatic islet is composed of α, β, δ, ε and PP cells that produce glucagon, insulin, somatostatin, ghrelin, and pancreatic polypeptide, respectively.

The pancreas is of endodermal origin. Following formation, the endoderm differentiates into the embryonic gut tube that undergoes regional specification in response to molecular contexts. The pancreas develops as dorsal and ventral buds from the foregut between the duodenum and the stomach [2, 3]. The dorsal bud receives signals from the notochord and dorsal aorta [4], whereas the ventral bud receives signals from the overlying cardiac mesenchyme and the lateral plate mesoderm [5].

However, fibroblast growth factors (FGFs) and bone morphogenetic proteins (BMPs) exposed to endodermal explants can redirect the fate of pancreatic cells to hepatic lineage. On the other hand, downregulation of the p300-dependent histone acetylation associated with gene expression reverses the hepatic phenotype [8]. On embryonic day E11.5, the mouse ventral and dorsal buds increase in size and merge into a single organ [9]. Along with this fusion, proliferation of pancreatic epithelial cells is mainly guided by the growth factors of

Progression of human pancreas development *in vivo* [6, 7]

Stage	Stem cell	Endoderm	Embryonic gut	Pancreatic endoderm	Precursor cell	β-cells
Embryonic day	6	14	21–28	30–33	45+	55+
Markers	$Oct4^+$ $Sox2^+$	$Sox17^+$ $Foxa2^+$ $EpCAM^+$ $Sox7^-$ $Pdgfra^-$	$Sox17^+$ $Foxa2^+$	$Pdx1^+$ $Nkx6.1^+$ $Ptf1a^+$ $Ki67^+$ $Sox9^+$ $Sox17^-$	$Ngn3^+$ $Pdx1^+$ $Nkx6.1^+$ $Ptf1a^-$	Ins^+ $Nkx6.1^+$ $Mafa^+$ Gcg^- $Sox9^-$

mesenchymal cells (E12.5 in the mouse) [10]. Further proliferation promotes branching of epithelial ducts. In parallel with these processes, precursor endocrine cells detach from the epithelium and finally associate into iL. At E16.5, monohormonal insulin-positive and acinar cells arise [11]. The adult human pancreas contains 1 mln iL [12]. During the endocrine differentiation, the islet progenitor cells co-express various hormones, eventually maturing into monohormonal cells [13, 14]. In a mouse model, it was shown that glucagon-secreting cells are the first endocrine cells to occur, being detectable as early as E9.5 [15, 16]. This is followed by the formation of cells co-expressing insulin and glucagon, whereas first insulin-secreting β-cells and glucagon-secreting α-cells are observed from day 14. By E18, somatostatin-producing δ-cells and pancreatic polypeptide-producing PP cells can be detected in the islets [14, 15].

All endocrine cells originate from Pdx1-positive pancreatic progenitors. During pancreas development, Pdx1 is expressed in endocrine and exocrine progenitor cells; however, to the end of specification, Pdx1 expression is restricted to β- and δ-cells [16]. The endocrine cell fate determination is regulated by the transcription factor Ngn3. Its inhibition at E11.5 dramatically suppresses endocrine differentiation [17].

The use of genetic tools has improved our understanding of the transcription factors functions in the generation of different types of pancreatic endocrine cells. These factors include such markers as Sox9, Pdx1, Ngn3, Ia-1, Pax4, Arx, Nkx2.2, Nkx6.1, Nkx6.2, Pax6, and Mafa.

Sox9 is expressed in $Pdx1^+$ epithelial cells from E9. At E14.5, Sox9 expression is restricted to uncommitted cells with low Pdx1 expression and not observed in hormone-secreting cells. In postnatal mice, Sox9 localizes in centroacinar cells and certain ductal epithelial cells [19]. There is evidence that Sox9 acts as a marker of pancreatic progenitor cells: its expression remains unaltered in *Ngn3*- and *Nkx6.1*-knockout mice. Transgenic mice with pancreatic precursor cells artificially maintained in the progenitor state demonstrate abnormally constant levels of Sox9 expression. Sox9 and the proendocrine transcription factor Ngn3 are co-expressed on embryonic day 15.5; however, they are not detected in Nkx2.2- and Isl1-positive cells found in mature iL. Deletion of Sox9 in $Pdx1^+$ progenitor cells reduces the number of endocrine cells with premature cell differentiation into glucagon- and Isl1-expressing cells. Thus, Sox9 is a marker of progenitor cells and its activity is required to maintain them in a proliferative state and prevent their premature differentiation [20, 21].

Both Sox9 and Pdx1 are co-expressed at E8.5 in the dorsal and ventral endoderm beneath the stomach and duodenum. Later, Pdx1 expression is confined to β-cells, regulating glucose-dependent insulin secretion [22–24]. There are studies that suggest that mature pancreatic cells derive from $Pdx1^+$ progenitor cells [25]. This agrees with the pancreatic agenesis in Pdx1-deficient mice [26]. Pdx1 inactivation at different stages of development and in mature β-cells revealed its necessity for the establishment and maintenance of the phenotype of β-cells [27, 28]. Furthermore, Gannon *et al* [29] demonstrated that down-regulation of Pdx1 in β-cells at late stages of embryonic development leads to a decrease in the proliferative capacity of insulin-secreting cells, along with an increased proliferative activity in glucagon-producing cells. These findings support the view that Pdx1 plays an essential role in the specification and differentiation of β-cells, as well as in maintaining the pool of endocrine cells at late stages of embryonic development [29].

In contrast to Pdx1, Ngn3 affects only the differentiation of endocrine tissue. It can be detected from E8.5 with peak expression at E15.5, resulting in a low expression level in mature endocrine tissue. Ngn3 is crucial for all enteroendocrine and endocrine lineage specification [25, 30, 31]. Ngn3 inactivation in mature $Pdx1^+$ cells impairs the functions of iL [32], whereas its upregulation induces endocrine cell differentiation [33, 34]. Ectopic Ngn3 expression in $Pdx1^+$ cells prematurely converts cells into endocrine lineage, which only produces glucagon [35, 36]. Villasenor *et al* [37] report that developmental Ngn3 expression occurs in two distinct temporal waves that are consistent with the "first" and

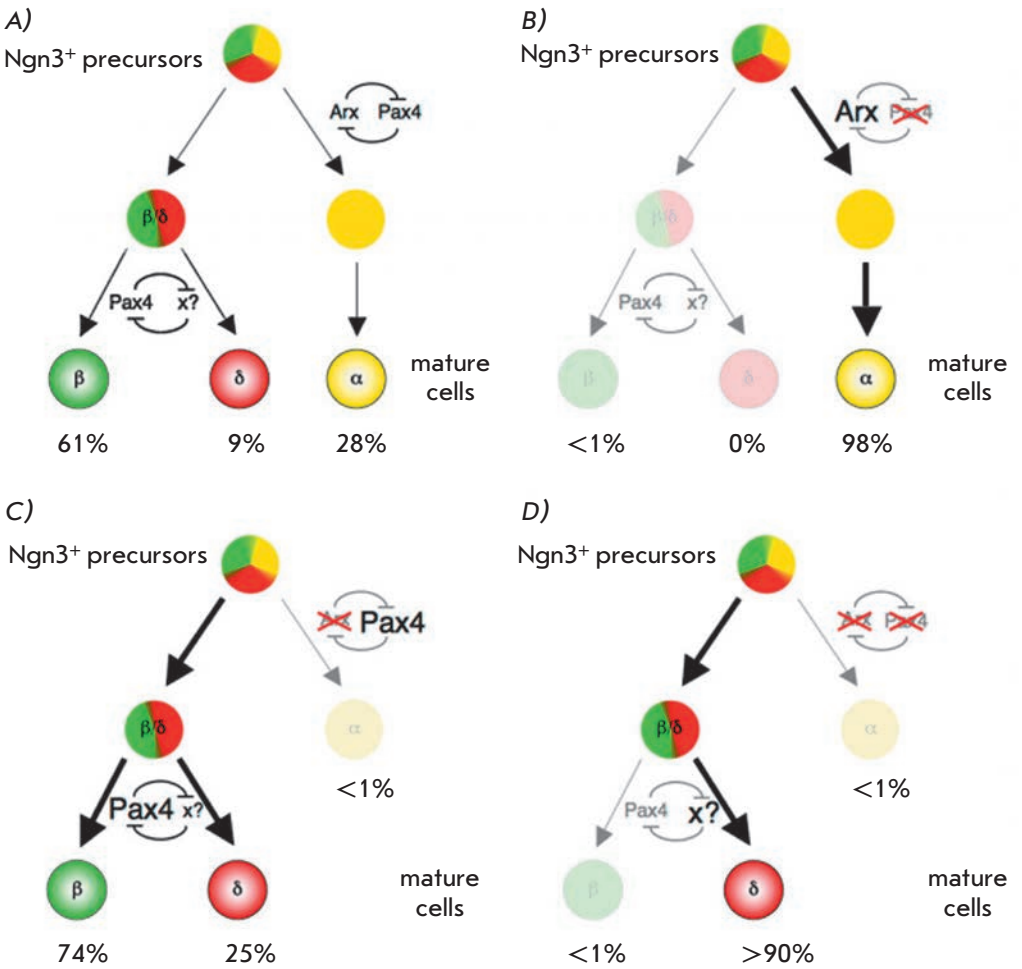

Fig. 1. Schematic representation of endocrine cell fate specification during pancreatic development. A) An uncommitted endocrine progenitor cell can become an α-cell or transform into a second progenitor cell with the β- or δ-cell lineage fates expressing Arx and Pax4. B) A change in the cell fate decision is caused by the lack of Pax4; C) A change in the cell fate decision is caused by the lack of Arx; D) A change in the cell fate decision is caused by the lack of Pax4 and Arx [By 18]

"second" transitions previously described by Pictet *et al* [38], giving rise to early- and late-forming endocrine cells with different developmental potentials [37, 38]. A study by Johansson *et al* [39] showed that early Ngn3$^+$ cells differentiate into α-cells. Activation of Ngn3 at late stages induces the lineage commitments of β- and PP-cells after embryonic day 11.5 and δ-cells after embryonic day 14.5, whereas the emergence of α-cells progressively decreased [39].

The transcription factor Ia-1 is a target of Ngn3 and participates in endocrine cell differentiation. In the case of Ia-1 mutations, endocrine cells are observed but most of them do not secrete hormones [40]. Unlike Ngn3, ectopic expression of Ia-1 in ductal cells is insufficient to induce endocrine differentiation. However, co-expression of Ngn3 and Ia-1 significantly improves endocrine induction efficiency as compared to Ngn3 alone expression [41].

Arx and Pax4 play crucial roles in the specification of endocrine cells subtypes. Arx acts as a differentiation promoter of α- and PP-cells, while Pax4 specifies the β- and δ-lineages (*Fig. 1*). Pax4 deficiency fails to promote the differentiation of β- and δ- progenitors into their programmed pathways, leading to an increase in the population of α-cells [42]. On the other hand, Arx loss leads to an increase in β- and δ-cells, with the disappearance of α-populations [43]. Closer analysis showed that the Arx and Pax4 factors act as antagonists. Simultaneous Pax4 and Arx knockout leads to the disappearance of β- and α-cell populations with an increase in δ-cells concomitantly with no changes in the number of PP-cells [44]. The authors conclude that Pax4 is not necessary for the fate of β-/δ-cell determination but inhibits α-cells differentiation by Arx suppression.

At early stages of embryonic development, Nkx2.2 is important for the specification of the β-cells. However, in mature iL, Nkx2.2 appears as a α-, β- and PP-cells marker. Nkx2.2-deficient mice display a loss of α-cells as well as a reduced number of β- and PP-cells, whereas the number of δ-cells remains unaltered [45, 46].

Another marker of pancreatic epithelial cells, Nkx6.1, is observed as early as E9.5. It is first detected in Ngn3$^+$ endocrine progenitors, followed by mature β-cells, in which it regulates insulin secretion [47, 48].

Nkx6.1-knockout mice mostly lack mature β-cells despite the normal development of other islet cell types [47]. Nkx6.2, a paralog of Nkx6.1, shares expression patterns with Nkx6.1, but it is not observed in mature β-cells [49, 50]. Nkx6.2-knockout mice exhibit a wild-type phenotype, whereas Nkx6.1/Nkx6.2 double-mutant mice show phenotypic alterations characteristic of a Nkx6.1 mutant phenotype, concomitantly with a striking decline in glucagon-producing cells. Based on these findings, the authors suggest a broader role for Nkx-factors in α-cell specification [49].

Another member of the Pax family, Pax6, is critical for the differentiation of islet cells. Pax6 is expressed in all endocrine hormone-producing cells. Pax6 guides the differentiation of the four islet cell types and iL development, as evidenced by Pax6 loss in mice [51, 52].

Members of the Maf gene family (Mafa, Mafb and cMaf) control the terminal differentiation of β- and α-cells. Mafa binds to the promoter in the insulin gene and acts as a strong transactivator of insulin gene expression [53–55]. Mafa gene expression is induced at E13.5 and confined to just insulin$^+$ cells during embryonic development and after birth [56]. Mice lacking Mafa have diabetes type 1 with a pronounced decrease in insulin blood levels and perturbed islet organization. Mafa deficiency abrogates glucose-dependent secretion of insulin in isolated insulin$^+$ cells [57]. In addition, ectopic Mafa expression in the endoderm of chicken embryos and in cell cultures of nonpancreatic cells is sufficient to trigger insulin production [58].

Overall, the description of the key genes' roles in the specification of different endocrine cells unveils the complexity of their regulation mechanisms. The objectives for the next few years are *in vitro* and *in vivo* studies of insulin-producing β-cells genesis for the optimization of *in vitro* cell differentiation programs.

TRANSPLANTATION OF DONOR ISLETS OF LANGERHANS

Transplantation of a pancreas is a promising therapy for patients with diabetes [59]. However, this approach contains procedural risks for the recipient and leads to the need for lifelong immunosuppression.

Transplantation of allogeneic isolated islet cells allows one to avoide abdominal surgery. In 1983, human iL were transplanted to rats with experimentally induced diabetes [60]. The first allogenic iL transplantation into a Type I diabetic patient was reported in 1990 [61]. However, the efficiency of this approach remained extremely poor until 2000. It is likely that this was due to the limited techniques of islet isolation available at the time, low islet yield, and severe immunosupression. Shapiro *et al* [62] developed the Edmonton protocol that reduced the alloimmune response and improved the survival rate of transplanted islets [62–64]. Owing to this protocol, the need for exogenous insulin was eliminated following islet transplantation. Moreover, Shamoon *et al* [65] reported that in patients receiving therapy glycosylated hemoglobin HbA1c reached a normal level. The Edmonton protocol employs an enzymatic dissociation of islet cells. Islets are infused intraportally by portal vein catheterization, after which the cells become trapped in the venous sinuses of the recipient, have access to oxygen supply, and initiate glucose-dependent insulin secretion. The important step in this procedure is a combination of immunosuppressive agents. Following infusion, the recipient receives daclizumab to prevent initial rejection. The use of another immunosuppressive component, sirolimus, allows one to avoid corticosteroid use, which shows toxicity to islet cells. The third agent, tacrolimus, is administered at small doses to minimize the side-effects it has on the islet mass. Current immunosuppressive therapies are successful at reducing graft rejection rates and prolonging islet survival up to 5 years [66–68]. However, the risks of long-term immunosuppression, as well as profound shortage of donor material, hinder the wide-scale application of this procedure.

The similarity of human and porcine insulin [69, 70] and successful use of porcine insulin in diabetic patients before the recombinant human insulin was first produced [71] allowed researchers to consider porcine islet cells as material for transplantation. Encapsulation procedures have been created to ameliorate rejection responses. A recent study from Living Cell Technologies showed that encapsulated porcine islets are safe and potent without the need for immunosuppressive agents when used in diabetes type 1 patients (http://www.lctglobal.com). Neither inflammation nor subsequent fibrosis, nor increase in glycosylated hemoglobin levels, was observed following a progressive reduction in daily insulin doses [72–74].

There are a number of studies that have achieved a positive outcome with encapsulated human islets [73, 75–78]. However, despite the absence or reduced need for immunomodulation, the limited availability of donors remains the major limiting factor.

Encapsulation materials may include water-soluble (alginate hydrogels) and water-insoluble polymers [79]. Although alginates are water-soluble, they remain intact over several years [78, 80–84]. Creating double-layered capsules contributes to decreased membrane porosity and enhances membrane durability and better immunoisolation. For protection against immune destruction, membranes can be coated with poly-L-lysine and polyornithine in prejudice of mechanical stability and durability [79, 85, 86].

Alternative sites for grafting have remained the focus of numerous studies. To attenuate early graft

loss and to yield an insulin delivery environment, implanted islets need to be vascularized for appropriate oxygen and nutrient supply. Unfortunately, current research efforts have not been very successful with an ideal site for encapsulated islet transplants due to their sizes. Appropriate for the transplantation of a non-encapsulated pancreatic islet, grafts sites (such as the liver and spleen) are space-limited to accommodate a large capsule volume (diameter ranges from 600 μm). Common laparoscopic techniques allow one to implant a capsule into the abdominal cavity. However, abdominal mesothelial cells trigger a severe immune response indirectly through macrophages and directly by producing TNF-α, IL-1β, and IL -10, and other cytokines [87]. Better outcomes were observed both with encapsulated and non-encapsulated islets when implanted beneath the renal capsule or subcutaneously [88]. These sites yielded a mild cytotoxic response, concomitantly with high islet survival rates and graft function [89].

THE USE OF PLURIPOTENT STEM CELLS

Pluripotent stem cells (PSCs) can become any cell of the three germ layers, which opens up the possibility to obtain insulin-secreting cells for diabetes treatment. There are two types of pluripotent cells: embryonic pluripotent stem cells (ES), derived from the inner blastocyst mass, and induced pluripotent stem cells (iPS), derived by reprogramming somatic cells into pluripotent ones. Thomson *et al* [90] were the first to report on culturing ES cells, thus marking the era of somatic cell reprogramming [91]. The differentiation potential, proliferative capacity, morphology, and gene expression profiles are similar between ES and iPS cells, which allow one to use iPS cells without the ethical restrictions associated with embryo destruction [92, 93]. Autologous human iPS cells are not cleared by immune system post-transplantation; however, there are risks associated with the rejection of implanted insulin-producing cells by the same autoimmune mechanism that leads to the emergence of diabetes.

Both ES and iPS cells can undergo differentiation *in vitro* into insulin-secreting cells [94–98]. Differentiation of PSCs into insulin-producing cells normally follows a well-defined developmental program, consisting of several stages. The first stage is endoderm formation. ES cells express multiple endoderm markers such as Sox17, Foxa2, Cxcr4; however, Sox7 is not observed [95, 96, 99–102]. Differentiation of ES and iPS cells is triggered by Nodal and Wnt signaling [95, 99, 103, 104]. The Nodal pathway is activated by activin A, a member of the TGF-β family, at a concentration of 50–100 ng/ml [105, 106]. The proportion of differentiated cells can be increased by combining activin A and certain inhibitors (wortmannin, CHIR99021 [107], sodium butyrate [96]) and activators of the Wnt-signaling pathway, such as CHIR9902 [108]. In addition, the efficacy of differentiation improves following exposure to IDE1 and IDE2 [109]. There is evidence that endodermal cells could give rise to both pancreatic and hepatic lineages. Subsequent differentiation of pancreatic cells *in vitro* requires treatment with TGF-β and BMP4 antagonists such as SU5402 and Noggin, which suppress hepatic differentiation [101].

The second stage of pancreatic differentiation is the exposure to dorsomorphine or its homolog 1 that induces the lineage commitment of $Pdx1^+$ progenitors [96, 99, 109]. The mechanisms by which the cultured cells eventually become mature insulin-producing cells remain to be elucidated. There have been attempts to trigger differentiation *in vitro* with nicotinamide, insulin-like growth factor 1, and hepatocyte growth factor [96, 101, 103]. Further differentiation of $Pdx1^+$ cells was induced with indolactam V and enhanced by retinoic acid [108]. There is evidence suggesting that the ability of PSCs to differentiate into endocrine cells strongly depends on the cell seeding density [110, 111]. Importantly, cells differentiated *in vitro* tend to produce several hormones and have an immature phenotype insensitive to the glucose level [103, 112, 113]. In this regard, progenitors are implanted to allow for a permissive *in vivo* environment for differentiation [99, 105, 114–117]. Studies in normal [99, 105] and streptozotocin-induced diabetic mice [114] demonstrate that ES cells can differentiate into functional insulin-producing cells. In addition, it is also shown that even encapsulated progenitors can be converted into mature insulin-producing cells capable of insulin secretion in diabetic mice [118].

The breakthrough work of Pagliuca *et al* [119] reports on the development of a cell differentiation protocol to produce functional insulin-secreting cells. Differentiation of human PSCs is conducted for 28–33 days in the presence of a wide set of growth factors and small molecules. The insulin-secreting cells obtained following this protocol show a glucose-responsive phenotype comparable with mature β-cells. These cells package insulin into secretory granules with an ultrastructure similar to that of adult β-cells. These cells were able to normalize the glucose level after transplantation in diabetic mice [119].

It was found that Ucn3, a corticotropin release factor, has a high expression level in β-cells and regulates glucose-dependent insulin secretion [120]. Cells differentiated *in vitro* fail to express Ucn3 [121]. At the same time, the expression levels of Ucn3 in mature and immature β-cells may differ up to 7-fold. Thus, maturation of cells *in vivo* is important to its functionality. This suggests the presence of some specific signals in

the transplantation sites which trigger the differentiation and maturation of β-cells.

DIRECT REPROGRAMMING

Reprogramming protocols developed to produce iPS cells find wide application in biomedical research. Direct reprogramming is based on the use of genetic constructs for the direction of various cell types into the desired cell type without a reversal to pluripotency. Similar to obtaining iPS cells, the direct reprogramming technique entails DNA integration (mainly through viral vectors). In particular, artificially induced Pdx1 gene expression in the liver of diabetic mice has led to the appearance of insulin$^+$ cells near blood vessels. The conversion, however, was incomplete. Therefore, this motivated researchers to search for other genes with a synergistic effect between themselves and with Pdx1. Moreover, the search for cells suitable for programming has begun. Ductal cells show promise. In as early as 1980, Noguch *et al* [122] showed that β-cells can be derived from ductal cells. Pdx1 expression in human ductal cells activates insulin production [122]. An intraperitoneal infection of recombinant Pdx1 into streptozotocin-induced diabetic mice induced amelioration of hyperglycemia [123]. Ductal cells of adult mice transduced with an adenoviral vector carrying the Pdx1, Pax4, Ngn3, and NeuroD genes start insulin secretion [124].

According to recent research, pancreatic acinar tissue of mice can be reprogrammed through artificially induced gene expression: acinar cells first undergo differentiation into ductal cells, followed by conversion into islet cells [125]. The large number of acinar cells in the pancreas makes them an ideal model for β-cell generation studies. Acinar cells readily differentiate into insulin-producing cells when cultured *in vitro* in the presence of a low serum content supplemented with the epidermal growth factor and nicotinamide. The expression levels of glucagon, somatostatin, and pancreatic polypeptide also increase [126]. Under certain culture conditions, human acinar cells can change into duct-like structures. Dexamethasone supplementation induces an acinar-to-ductal transition, but, unfortunately, they do not differentiate into insulin-producing cells [127]. It is shown that hyperglycemia elevates the infiltration of acinar tissue by T-cells and induces differentiation of acinar cells into either β-cells or duct-like structures that can eventually become β-cells [128]. Desai *et al* reported on acianar-islet transdifferentiation in dexamethasone-treated rat pancreas [129]. Recent research suggests that acinar cells of mice can be reprogrammed by inducing expression of the Pdx1, Ngn3, and Mafa genes. The experimental mice showed a decrease in blood glucose levels, though full recovery was not observed. It is likely that the implanted cells failed to aggregate, which finally affected the cell communication regulating glucose-stimulated insulin secretion [130–132]. These results were confirmed by *in vitro* studies on a AR42J acinar cell line and then on a human exocrine cells culture [133, 134]. Importantly, Wang *et al* discovered that hyperglycemia in diabetic mice is better corrected in the case of a strong immune response elicited by the adenoviral capsid used as a vector for gene delivering [135].

The primary physiological role for α-cells is glucagon secretion, counteracting insulin by promoting glucose mobilization. The conversion of α-cells into β-cells is induced by an increase in the ectopic expression of Pax4 and Ngn3 [136]. Enforced Pdx1 expression under the Ngn3 promoter can cause α-to-β conversion during the early embryonic period; however, at later stages activation of Pdx1 has no effect on the β-cell allocation [137]. In a recent study, Chung *et al* employed pancreatic duct ligation and observed large numbers of β-cells generated from α-cells within 2 weeks [138]. Notably, the α-to-β conversion seems to occur following deep depletion of pre-existing β-cells [138, 139]. Studies involving partial elimination of β-cells failed to observe this conversion [140].

APPLICATION OF COMMITTED CELS

The use of ES cells is ethically ambiguous, but it has other pitfalls. For example, ES- and iPS-derived transplants may generate teratomas from the residual pool of uncommitted cells. In addition, the need for immunosuppression still exists [141, 142]. Postnatal stem cells can sidestep these limitations [143–146].

Skin-derived precursors represent an available source of progenitors. They were first described by Toma *et al* [147]. They harbor broad differentiation plasticity, giving rise to multiple cell types *in vitro* (glial cells, smooth muscle cells, adipocytes). Bakhtiari *et al* [148] reported an efficient method for cryopreservation of human skin-derived precursors for long-term storage. The skin is now a promising source of autologous cells with a wide differentiation capacity and long-term storage ability [148]. Skin-derived precursors were converted *in vitro* into cells capable of glucose-dependent insulin and C-peptide secretion. The obtained cells expressed markers such as Pdx1, Nkx2.2, Pax4, NeuroD, and Isl1 found in mature β-cells [149].

The most frequently mentioned in the context of regenerative medicine postnatal stem cells are mesenchymal stem cells (MSCs) residing in various tissues [150]. They can be successfully cultured *in vitro* and readily undergo differentiation into osteogenic, adipogenic, and chondrogenic lineages using standard differentiation protocols [151]. Eyelid adipose-derived MSCs

appear to be more suitable for differentiation into insulin-producing cells, since these cells originate from neural crest cells. MSCs from human periodontal ligament are also derived from neural crest cells [152–154]. However, it is currently impossible to bring MSCs close to the phenotype of β-cells under *in vitro* conditions. MSCs from umbilical cord blood offer more flexibility. Prabakar *et al* discovered that the properties of these MSCs are similar to those of ES cells, including the differentiation potential towards a pancreatic endocrine phenotype [155]. Another therapeutic option is the infusion of undifferentiated MSCs, resulting in various degrees of regeneration [153, 154, 156, 157]. Such host responses are likely to be due to the immunomodulatory, anti-inflammatory, pro-angiogenic, and trophic functions of MSCs. A more pronounced immunomodulatory effect has been described for hematopoietic stem cells that were successfully used to reset the immune system in diabetes [158, 159]. Multipotent stem cells derived from umbilical cord blood seem to be involved in the instruction of the immune system. When loaded into a circulatory device pre-seeded with umbilical-cord-blood-derived MSCs of healthy individuals, lymphocytes of type 1 diabetic patients seem to receive instructions and acquire the ability to ameliorate type 1 diabetic symptoms [160, 161].

There exists a hypothesis that an injury to the pancreas activates facultative progenitors to increase the population of β-cells. It was shown that ductal progenitors of mice can give rise to β-cells [161]. In addition, in a cohort study of chronic pancreatitis and asymptomatic fibrosis patients Gianani *et al* found that the pancreas of all patients analyzed had neogenic cells aggregated into islet-ductal structures, which appeared to be an association of the endocrine compartment with the ductal system [162]. Streptozotocin-induced diabetic mice have two types of β-cell progenitors expressing Glut2 and Pdx1/somatostatin. These cells are likely to be of ductal origin [163, 164]. Studies dedicated to investigating embryonic pancreas *in vitro* demonstrated that insulin-producing cells can originate from ductal epithelial cells. Porcine ductal cells harvested during the neonatal period can be enforced to express insulin and markers of endocrine precursors [165]. Following 3- to 4-wk incubation, human ductal cells form 3D structures which express insulin and other islets hormones. This means that they are in a state of differentiation. Moreover, insulin release in these cells is glucose-dependent [161]. Pdx1 can dramatically accelerate *in vitro* differentiation of ductal epithelial cells towards an insulin-producing phenotype [166]. In streptozotocin-induced diabetic mice, it was determined that ductal cells express insulin in the early stages of inflammation, followed by termination of production [167]. This finding suggests induction of β-cell regeneration by an early-stage inflammatory response in type 1 diabetes. It is likely that new β-cells are highly prone to apoptosis. TNF-α expression induced in β-cells of mice leads to insulit rather than diabetes. This is accompanied by the development of intraislet ducts with β-cell placement, which could imply a regenerative process [168]. Similarly, transgenic mice expressing IFN-γ showed resistance to streptozotocin treatment. The transgenic mice exhibited regeneration of pancreatic duct cells and iL neogenesis [169]. Expression of Pdx1 and Msx2 in the duct cells of these mice suggests a connection between the expressed markers and ductal cells differentiation in this model [170]. In individuals with autoimmune chronic pancreatitis, T-cell mediated β-cell destruction promotes β-cell regeneration from ductal cells [171]. Type 1 diabetes patients demonstrate generation of insulin-producing $Pdx1^+$ duct cells following a combined transplantation of the pancreas and a kidney.

The hyperglycemia in alloxan-induced diabetic mice can be reversed through EGF and CNTF treatment due to the generation of insulin-producing cells [172]. To elucidate the origin of the newly formed insulin-expressing cells, the authors utilized the Cre/LoxP system to track the acinar and ductal cells. It was discovered that a total of 40% of newly formed insulin-expressing cells originated from acinar cells, whereas other cell types contributed only 4%. This allows one to suggest the existence of transdifferentiation in mammalian pancreas.

There are a number of studies that are searching for non-pancreatic sources of cells which can secrete insulin. One of the promising sites is large salivary glands. Egéa *et al* identified preproinsulin I and II mRNA expression in adult rat submandibular glands [173]. Insulin in the parotid gland of rats has been found using the immunohistochemistry method [174]. It was shown that the submandibular salivary glands perform a compensatory function in diabetic mice [175]. After transplantation of the submandibular gland under the renal capsule, streptozotocin-induced diabetic mice restored normoglycemia [176]. Human and animal (mouse, rat, swine) submandibular gland cells are readily amenable for culture *in vitro* [177–179]. Under 3D culture conditions, they acquire the capacity of glucagon, albumin, or insulin expression [177, 178]. Human submandibular gland cells acquire the ability to produce C-peptide in a glucose-dependent manner in a spheroid culture system in the presence of nicotinamide [179]. Rat submandibular gland cells expressing α6β1/c-Kit maintained the morphology, proliferative capacity, and multipotency typical of stem cells for over 92 passages. The presence of activin A, exendine-4, and retinoic acid in the medium induces the expression of pancreatic

markers in these cells, such as Pdx1, insulin, pancreatic polypeptide, and Ngn3 [180].

THE USE OF BIOMATERIALS FOR THE CONSTRUCTION OF THREE-DIMENSIONAL SCAFFOLDS

It is widely known that three-dimensional culture systems can provide different advantages, compared to standard two-dimensional cultures. Cells are kept in conditions much closer to native: so, cell-cell and cell-medium interactions are promoted, and differentiation is accelerated [181]. These systems closely mimic the natural environment found *in vivo*. This stays true for pancreatic cells cultivation *in vitro* and their *in vivo* delivery.

Studies have shown that seeding cells onto a porous scaffold increases their viability and enhances the functionality of isolated iL *in vitro,* thus improving transplant outcomes. For example, rat islet cells showed an almost two-fold increase in viability and produced 4-fold more insulin when cultured on a porous polyglycolic acid scaffold as compared to 2D culturing [182]. In yet another study, a porous scaffold of poly(lactic-co-glycolic acid) (PLGA) prepared by electrospinning with type I collagen-loaded pores was used. RINm5F cells were cultured on it, and insulin secretion was enhanced by 2-fold [183].

Another advantage of porous scaffolds is the opportunity to co-culture different cell types that allows one to mimic *in vivo* cell interactions. Murine islet cells co-cultured with human umbilical cord endothelial cells and human prepuce fibroblasts on a PLLA\PGLA scaffold improved the survival of islet cells by up to 75%. Furthermore, the addition of fibroblasts and epithelial cells promoted the expression of Gcg, Pdx1, Nkx6.1, and Glut2 markers. The insulin secretion increased by 1.5 fold [184].

Scaffolds obviously offer a 3D structure for cell culturing; however, the fundamental role of a native extracellular matrix (ECM) on a cell's state is increasingly being recognized. It provides not only mechanical support, but also affects cell adhesion, molecular contents, cell-to-cell interactions, and growth factors binding. Importantly, the rigidity and flexibility of ECM considerably contributes to differentiation, proliferation, viability, cell polarity, and migration [185].

The most fully characterized ECM components are laminins, a family consisting of 15–20 glycoproteins [186], each of which independently enhances insulin secretion [187]. Laminins interact with cells by binding integrins – transmembrane proteins responsible for cell adhesion and transduction of external signals to the cytoskeleton [188]. The 3D-structure of native ECM determines the topographic pattern of endocrine cells that affects secretory activity [189]. Furthermore, such components as collagens, glycoproteins, and glycosaminoglycans can independently suppress the β-cell apoptosis triggered by the loss of cell anchorage [189–195]. It was discovered that ECM components can enhance insulin secretion even in the absence of glucose [196]. ECM also has the ability to bind, store, and regulate the activity of growth factors, such as TGF-β1, which mediates the development, functioning, and regeneration of islets in the pancreas [197, 198].

Attempts are made during the development of materials for artificial 3D-scaffolds to modify their surface by coating it with molecules derived from native ECM. However, to date ECM decellularization treatment is believed to be the most promising (*Fig. 2*) [200–204]. Current approaches enable the elimination of cellular material, DNA, and surface antigens, retaining the intact structure [205]. Recent experiments have allowed researchers to obtain a porcine pancreatic extracellular matrix with preserved ECM components, including different types of collagen, elastin, fibronectin, and laminin. [206]. A decellularized membrane serves as a matrix for cell rehabitation of the organ. To date, there have been successful recellularizations of ECMs of such organs as liver [207], lungs [208], bladder [209], and mammary gland [210]. This provides hope for a positive result in the case of the pancreas as well.

CHALLENGES AND OPPORTUNITIES

Current treatments for patients with type I diabetes are limited and do not eliminate long-term complications. Progress is evident in all lines of research connected with efforts to revive the insulin-producing function of the pancreas. Standard transplantation approaches are hampered by the shortage of donors and the risks associated with the need for immunosuppression. Those risks could be overcome by encapsulation technologies. However, there are unresolved issues in this case as well, such as poor islet longevity and a size/cell count ratio of encapsulated islet mass sufficient to provide normoglycemia without burdening the patient with discomfort. The ability of such cell types as MSCs and hematopoietic cells to address host immune responses can be very useful in preventing neogenic β-cells from repeated autoimmune ablation.

The choice of stem cells is a critical step. ES and iPS cells can differentiate towards pancreatic progenitors and/or insulin-producing cells. The use of allogenic ES cells, however, still requires immunosuppressive therapy or encapsulation. Autologous iPS cells are very costly on an individual basis and require complicated differentiation protocols. In addition, the probability of graft rejection is high due to the autoimmune response that initially leads to type 1 diabetes. The tumorigenic

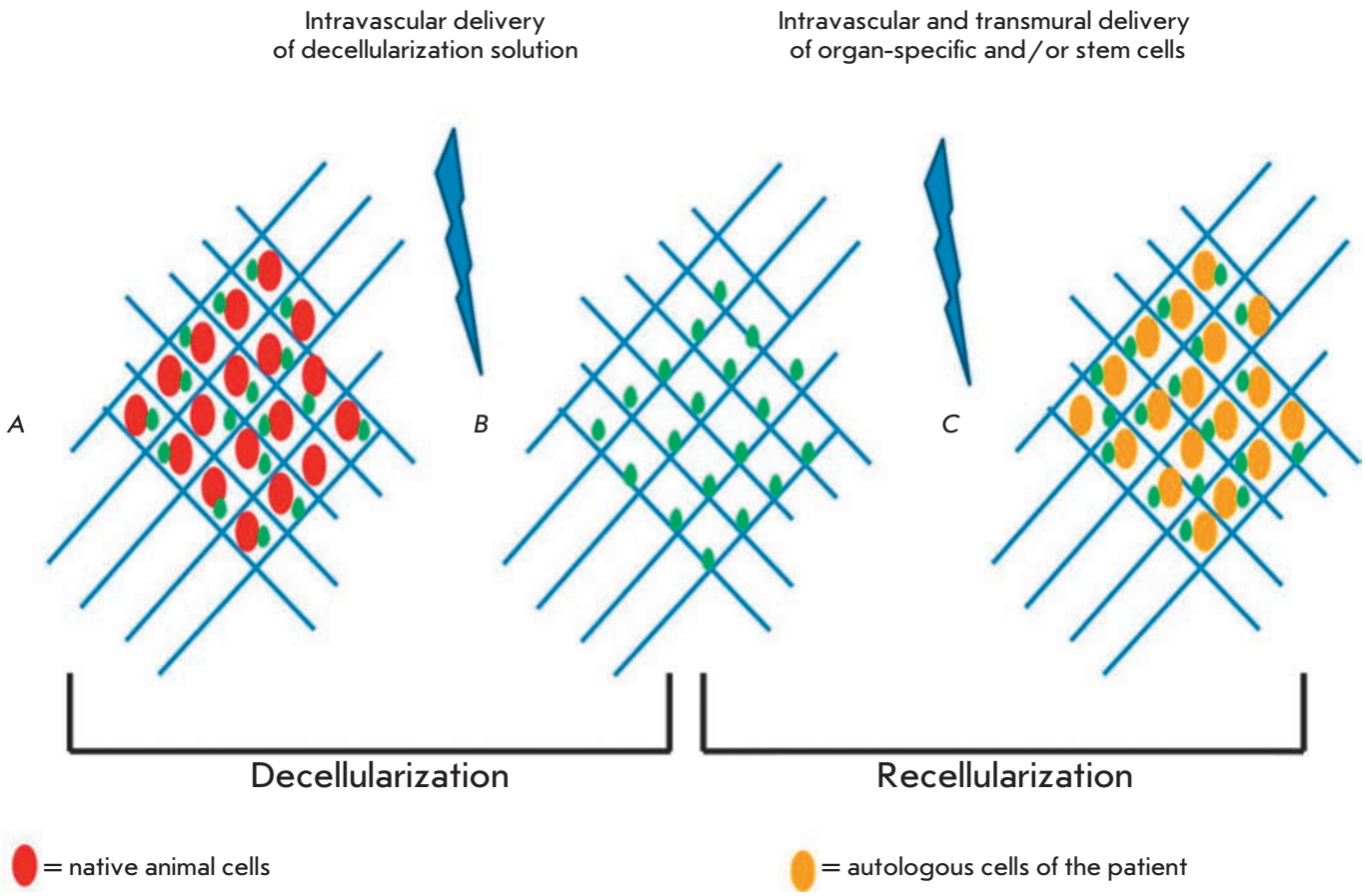

Fig. 2. Schematic overview of decellularization-recellularization technology. A) The intact organ contains cellular components (red ellipses) and ECM (blue network), as well as growth factors (green dots); B) An acellular organ scaffold after complete removal of cellular elements; C) The organ scaffold after recellularization with autologous cells (yellow ellipses) [By 199]

potential of residual undifferentiated PSCs in the implant also remains to be resolved.

Briefly, an ideal theoretical therapeutic approach would include a combined treatment: differentiated towards a pancreatic progenitor phenotype autologous iPS cells are cultured in 3D conditions in the presence of ECM components and autologous MSCs. Another possible way may be to reset the immune system with hematopoietic stem cells and to obtain new insulin-producing cells by direct reprogramming. Studies assessing the feasibility of this approach are underway to perform a thorough analysis of the potential risks associated with the biological safety and tumorigenic activity of the cells being used.

Direct reprogramming appears to be a promising method. However, data on the used protocols and the safety of this approach for obtaining insulin-producing cells is insufficient. Thus, it cannot yet proceed to the practical level.

A large number of studies have proved the positive effect of three-dimensional cell culture systems. In addition, the possibility to co-culture cells allows one to obtain a transplant which is as close to the native organ as possible. The use of decellularized ECM has shown promise; however, *in vivo* studies are in need for an understanding of the effects of the aforementioned structures on an organism.

Attempts to bring committed cells closer to the phenotype of β-cells *in vitro* have so far been unsuccessful. Overall, the current challenge in cell biology is to identify an available and accessible source of cells that are able to differentiate effectively into glucose-responsive insulin-producing cells. ●

This work was supported by The Russian Scientific Foundation grant № 14-50-00029.

REFERENCES

1. Githens S., Schexnayder J.A., Moses R.L., Denning G.M., Smith J.J., Frazier M.L. // *In vitro* Cell. Dev. Biol. Anim. 1994. V. 30A. P. 622–635.
2. Lammert E., Cleaver O., Melton D. // Science. 2001. V. 294. P. 564–567.
3. Field H.A., Dong P.D.S., Beis D., Stainier D.Y. // Dev. Biol. 2003. V. 261. P. 197–208.
4. Hebrok M., Kim S.K., Melton D.A. // Genes Dev. 1998. V. 12. P. 1705–1713.
5. Kumar M., Jordan N., Melton D., Grapin-Botton A. // Dev. Biol. 2003. V. 259. P. 109–122.
6. Riedel M.J., Asadi A., Wang R., Ao Z., Warnock G.L., Kieffer T.J. // Diabetologia. 2012. V. 55. № 2. P. 372–381.
7. Jennings R.E., Berry A.A., Kirkwood-Wilson R., Roberts N.A., Hearn T., Salisbury R.J., Blaylock J., Piper Hanley K., Hanley N.A. // Diabetes. 2013. V. 62. № 10. P. 3514–3522.
8. Pan F.C., Wright C. // Dev. Dyn. 2011. V. 240. P. 530–565.
9. Villasenor A., Chong D.C., Henkemeyer M., Cleaver O. // Development. 2010. V. 137. P. 4295–4305.
10. Bhushan A., Itoh N., Kato S., Thiery J.P., Czernichow P., Bellusci S., Scharfmann R. // Development. 2001. V. 128. P. 5109–5117.
11. Landsman L., Nijagal A., Whitchurch T.J., VanderLaan R.L., Zimmer W.E., MacKenzie T.C., Hebrok M. // PLoS Biol. 2011. V. 9. e1001143.
12. McClenaghan N.H. // Exp. Physiol. 2007. V. 92. № 3. P. 481–496.
13. Peck A.B., Cornelius J.G., Schatz D., Ramiya V.K. // J. Hepato-Biliary-Pancreatic Surgery. 2002. V. 9. № 6. P. 704–709.
14. Teitelman G., Alpert S., Polak J.M., Martinez A., Hanahan D. // Development. 1993. V. 118. № 4. P. 1031–1039.
15. Herrera P.L., Huarte J., Sanvito F., Meda P., Orci L., Vassalli J.D. // Development. 1991. V. 113. № 4. P. 1257–1265.
16. Shao S., Fang Z., Yu X., Zhang M. // Bioch. Biophys. Res. Commun. 2009. V. 384. № 4. P. 401–404.
17. Prasadan K., Tulachan S., Guo P., Shiota C., Shah S., Gittes G. // Biochem. Biophys. Res. Commun. 2010. V. 396. № 4. P. 1036–1041.
18. Kordowich S., Mansouri A., Collombat P. // Mol. Cell Endocrinol. 2010. V. 323. № 1. P. 62–69.
19. Seymour P.A., Freude K.K., Tran M.N., Mayes E.E., Jense J., Kis R., Schere G., Sande M. // Proc. Natl. Acad. Sci. USA. 2007. V. 104. № 6. P. 1865–1870.
20. Seymour P.A., Freude K.K., Dubois C.L., Shih H.P., Patel N.A., Sander M. // Dev. Biol. 2008. V. 323. № 1. P. 19–30.
21. Lynn F.C., Smith S.B., Wilson M.E., Yang K.Y., Nekrep N., German M.S. // Proc. Natl. Acad. Sci. USA. 2007. V. 104. № 25. P. 10500–10505.
22. Ohlsson H., Karlsson K., Edlund T. // EMBO J. 1993. V. 12. P. 4251–4259.
23. Stoffers D.A., Heller R.S., Miller C.P., Habener J.F. // Endocrinology. 1999. V. 140. P. 5374–5381.
24. Guz Y., Montminy M.R., Stein R., Leonard J., Gamer L.W., Wright C.V., Teitelman G. // Development. 1995. V. 121. P. 11–18.
25. Gu G., Brown J.R., Melton D.A. // Mech. Dev. 2003. V. 120. P. 35–43.
26. Offield M.F., Jetton T.L., Labosky P.A., Ray M., Stein R.W., Magnuson M.A., Hogan B.L., Wright C.V. // Development. 1996. V. 122. P. 983–995.
27. Ahlgren U., Jonsson J., Jonsson L., Simu K., Edlund H. // Genes Dev. 1998. V. 12. P. 1763–1768.
28. Holland A.M., Gonez L.J., Naselli G., Macdonald R.J., Harrison L.C. // Diabetes. 2005. V. 54. P. 2586–2595.
29. Gannon M., Ables E.T., Crawford L., Lowe D., Offield M.F., Magnuson M.A., Wright C.V. // Dev. Biol. 2008. V. 314. P. 406–417.
30. Gradwohl G., Dierich A., Lemeur M., Guillemot F. // Proc. Natl. Acad. Sci. USA. 2000. V. 97. P. 1607–1611.
31. Jenny M., Uhl C., Roche C., Duluc I., Guillermin V., Guillemot F., Jensen J., Kedinger M., Gradwohl G. // EMBO J. 2002. V. 21. P. 6338–6347.
32. Wang S., Jensen J.N., Seymour P.A., Hsu W., Dor Y., Sander M., Magnuson M.A., Serup P., Gu G. // Proc. Natl. Acad. Sci. USA. 2009. V. 106. № 24. P. 9715–9720.
33. Schwitzgebel V.M., Scheel D.W., Conners J.R., Kalamaras J., Lee J.E., Anderson D.J., Sussel L., Johnson J.D., German M.S. // Development. 2000. V. 127. P. 3533–3542.
34. Heremans Y., van De Casteele M., In't Veld P., Gradwohl G., Serup P., Madsen O., Pipeleers D., Heimberg H. // J. Cell. Biol. 2002. V. 159. P. 303–312.
35. Apelqvist A., Li H., Sommer L., Beatus P., Anderson D.J., Honjo T., Hrabe De Angelis M., Lendahl U., Edlund H. // Nature. 1999. V. 400. P. 877–881.
36. Grapin-Botton A., Majithia A.R., Melton D.A. // Genes Dev. 2001. V. 15. P. 444–454.
37. Villasenor A., Chong D.C., Cleaver O. // Dev. Dyn. 2008. V. 237. P. 3270–3279.
38. Pictet R.L., Clark W.R., Williams R.H., Rutter W.J. // Dev. Biol. 1972. V. 29. P. 436–467.
39. Johansson K.A., Dursun U., Jordan N., Gu G., Beermann F., Gradwohl G., Grapin-Botton A. // Dev. Cell. 2007. V. 12. P. 457–465.
40. Gierl M.S., Karoulias N., Wende H., Strehle M., Birchmeier C. // Genes Dev. 2006. V. 20. P. 2465–2478.
41. Mellitzer G., Bonne S., Luco R.F., van De Casteele M., Lenne-Samuel N., Collombat P., Mansouri A., Lee J., Lan M., Pipeleers D., *et al.* // EMBO J. 2006. V. 25. P. 1344–1352.
42. Sosa-Pineda B., Chowdhury K., Torres M., Oliver G., Gruss P. // Nature. 1997. V. 386. P. 399–402.
43. Collombat P., Mansouri A., Hecksher-Sorensen J., Serup P., Krull J., Gradwohl G., Gruss P. // Genes Dev. 2003. V. 17. P. 2591–2603.
44. Collombat P., Hecksher-Sorensen J., Broccoli V., Krull J., Ponte I., Mundiger T., Smith J., Gruss P., Serup P., Mansouri A. // Development. 2005. V. 132. P. 2969–2980.
45. Prado C.L., Pugh-Bernard A.E., Elghazi L., Sosa-Pineda B., Sussel L. // Proc. Natl. Acad. Sci. USA. 2004. V. 101. P. 2924–2929.
46. Sussel L., Kalamaras J., Hartigan-O'connor D.J., Meneses J.J., Pedersen R.A., Rubenstein J.L., German M.S. // Development. 1998. V. 125. P. 2213–2221.
47. Sander M., Sussel L., Conners J., Scheel D., Kalamaras J., Dela Cruz F., Schwitzgebel V., Hayes-Jordan A., German M. // Development. 2000. V. 127. P. 5533–5540.
48. Oster A., Jensen J., Edlund H., Larsson L.I. // J. Histochem. Cytochem. 1998. V. 46. P. 717–721.
49. Henseleit K.D., Nelson S.B., Kuhlbrodt K., Hennings J.C., Ericson J., Sander M. // Development. 2005. V. 132. P. 3139–3149.
50. Pedersen J.K., Nelson S.B., Jorgensen M.C., Henseleit K.D., Fujitani Y., Wright C.V., Sander M., Serup P. // Dev. Biol. 2005. V. 288. P. 487–501.
51. St-Onge L., Sosa-Pineda B., Chowdhury K., Mansouri A., Gruss P. // Nature. 1997. V. 387. P. 406–409.
52. Sander M., Neubüser A., Kalamaras J., Ee H.C., Mar-

tin G.R., German M.S. // Genes Dev. 1997. V. 11. № 13. P. 1662–1673.
53. Zhao L., Guo M., Matsuoka T.A., Hagman D.K., Parazzoli S.D., Poitout V., Stein R. // J. Biol. Chem. 2005. V. 280. P. 11887–11894.
54. Matsuoka T.A., Zhao L., Artner I., Jarrett H.W., Friedman D., Means A., Stein R. // Cell. Biol. 2003. V. 23. P. 6049–6062.
55. Aramata S., Han S.I., Yasuda K., Kataoka K. // Biochim. Biophys. Acta. 2005. V. 1730. P. 41–46.
56. Matsuoka T.A., Artner I., Henderson E., Means A., Sander M., Stein R. // Proc. Natl. Acad. Sci. USA. 2004. V. 101. P. 2930–2933.
57. Zhang C., Moriguchi T., Kajihara M., Esaki R., Harada A., Shimohata H., Oishi H., Hamada M., Morito N., Hasegawa K., *et al.* // Mol. Cell. Biol. 2005. V. 25. P. 4969–4976.
58. Artner I., Hang Y., Guo M., Gu G., Stein R. // J. Endocrinol. 2008. V. 198. P. 271–279.
59. Frank A., Deng S., Huang X., Velidedeoglu E., Bae Y.S., Liu C., Abt P., Stephenson R., Mohiuddin M., Thambipillai T., *et al.* // Ann. Surg. 2004. V. 240. № 4. P. 631–640.
60. Blumkin V.N., Skaletskiy N.N., Popov V.L., Shalnev B.I., Danilov M.I // Bulletin of Experimental Biology and Medicine. 1983. № 5. P. 89–91.
61. Scharp D.W., Lacy P.E., Santiago J.V., McCullough C.S., Weide L.G., Falqui L., Marchetti P., Gingerich R.L., Jaffe A.S., Cryer P.E. // Diabetes. 1990. V. 39. № 4. P. 515–518.
62. Shapiro A.M., Ricordi C., Hering B.J., Auchincloss H., Lindblad R., Robertson R.P., Secchi A., Brendel M.D., Berney T., Brennan D.C. // N. Engl. J. Med. 2006. V. 355. № 13. P. 1318–1330.
63. Ryan E.A., Lakey J.R., Rajotte R.V., Korbutt G.S., Kin T., Imes S., Rabinovitch A., Elliott J.F., Bigam D., Kneteman N.M., *et al.* // Diabetes. 2001. V. 50. № 4. P. 710–719.
64. Dedov I.I., Balabolkin M.I., Klebanova E.M. // Diabetes. 2004. № 2. P. 34–41.
65. Shamoon H., Duffy H., Fleischer N., Engel S., Saenger P., Strelzyn M., Litwak M., Wylie-Rosett J., Farkash A., Geiger D., *et al.* // N. Engl. J. Med. 1993. V. 329. № 14. P. 977–986.
66. Bellin M.D., Barton F.B., Heitman A., Harmon J.V., Kandaswamy R., Balamurugan A.N., Sutherland D.E., Alejandro R., Hering B.J. // Am. J. Transplant. 2012. V. 12. № 6. P. 1576–1583.
67. Shapiro A.M. // Curr. Diab. Rep. 2011. V. 11. № 5. P. 345–354.
68. Calafiore R., Basta G. // Adv. Drug. Deliv. Rev. 2013. № 4. P. 67–68:84–92.
69. O'Connell P.J., Cowan P.J., Hawthorne W.J., Yi S., Lew A.M. // Curr. Diab. Rep. 2013. V. 13. № 5. P. 687–694.
70. Graham M.L., Schuurman H.J. // Xenotransplantation. 2013. V. 20. № 1. P. 5–17.
71. Burman K.D., Cunningham E.J., Klachko D.M., Burns T.W. // Mol. Med. 1973. V. 70. № 6. P. 363–366.
72. Skinner S.J.M., Tan P.L.J., Garkavenko O., Muzina M., Escobar L., Elliott R.B. // InTech. 2011. V. 11. P. 391–408.
73. Elliott R.B., Escobar L., Tan P.L., Muzina M., Zwain S., Buchanan C. // Xenotransplantation. 2007. V. 14. № 2. P. 157–161.
74. Elliott R.B., Technologies L.C. // Curr. Opin. Organ Transplant. 2011. V. 16. № 2. P. 195–200.
75. Soon-Shiong P. // Drug Deliv. Rev. 1999. V. 35. P. 259–270.
76. Tuch B.E., Keogh G.W., Williams L.J., Wu W., Foster J.L., Vaithilingam V., Philips R. // Diabetes Care. 2009. V. 32. P. 1887–1889.
77. Basta G., Montanucci P., Luca G., Boselli C., Noya G., Barbaro B., Qi M., Kinzer K.P., Oberholzer J., Calafiore R. // Diabetes Care. 2011. V. 34. P. 2406–2409.
78. Strautz R.L. // Diabetologia. 1970. V. 6. P. 306–312.
79. De Vos P., Hamel A.F., Tatarkiewicz K. // Diabetologia. 2002. V. 45. P. 159–173.
80. Soon-Shiong P., Heintz R.E., Merideth N., Yao Q.X., Yao Z., Zheng T., Murphy M., Moloney M.K., Schmehl M., Harris M., *et al.* // Lancet. 1994. V. 343. P. 950–951.
81. De Vos P., De Haan B., van Schilfgaarde R. // Biomaterials. 1997. V. 18. P. 273–278.
82. De Vos P., De Haan B.J., Wolters G.H., Strubbe J.H., van Schilfgaarde R. // Diabetologia. 1997. V. 40. P. 262–270.
83. De Vos P., van Straaten J.F., Nieuwenhuizen A.G., de Groot M., Ploeg R.J., De Haan B.J., van Schilfgaarde R. // Diabetes. 1999. V. 48. P. 1381–1388.
84. Duvivier-Kali V.F., Omer A., Parent R.J., O'Neil J.J., Weir G.C. // Diabetes. 2001. V. 50. P. 1698–1705.
85. Strand B.L., Ryan T.L., In't Veld P., Kulseng B., Rokstad A.M., Skjak-Brek G., Espevik T. // Cell Transplant. 2001. V. 10. P. 263–275.
86. King A., Sandler S., Andersson A. // J. Biomed. Mater. Res. 2001. V. 57. P. 374–383.
87. Yao V., McCauley R., Cooper D., Platell C., Hall J.C. // Surg. Infect. 2004. V. 5. P. 229–236.
88. Dufrane D., Steenberghe M.Y., Goebbels R.M., Saliez A., Guiot Y., Gianello P. // Biomaterials. 2006. V. 27. P. 3201–3208.
89. Vériter S., Mergen J., Goebbels R.M., Aouassar N., Grégoire C., Jordan B., Levêque P., Gallez B., Gianello P., Dufrane D. // Tissue Eng. Part A. 2010. V. 16. P. 1503–1513.
90. Thomson J.A., Marshall V.S. // Curr. Top. Dev. Biol. 1998. V. 38. P. 133–165.
91. Takahashi K., Yamanaka S. // Cell. 2006. V. 126. № 4. P. 663–676.
92. Yu J., Vodyanik M.A., Smuga-Otto K., Antosiewicz-Bourget J., Frane J.L., Tian S., Nie J., Jonsdottir G.A., Ruotti V., Stewart R., *et al.* // Science. 2007. V. 318. P. 1917–1920.
93. Rao M., Condic M.L. // Stem Cells Dev. 2008. V. 17. P. 1–10.
94. Maehr R., Chen S., Snitow M., Ludwig T., Yagasaki L., Goland R., Leibel R.L., Melton D.A. // Proc. Natl. Acad. Sci. USA. 2009. V. 106. P. 15768–15773.
95. Zhang D., Jiang W., Liu M., Sui X., Yin X., Chen S., Shi Y., Deng H. // Cell Res. 2009. V. 19. P. 429–438.
96. Jiang J., Au M., Lu K., Eshpeter A., Korbutt G., Fisk G., Majumdar A.S. // Stem Cells. 2007. V. 25. P. 1940–1953.
97. Chen S., Borowiak M., Fox J.L., Maehr R., Osafune K., Davidow L., Lam K., Peng L.F., Schreiber S.L., Rubin L.L., *et al.* // Nat. Chem. Biol. 2009. V. 5. P. 258–265.
98. Tateishi K., He J., Taranova O., Liang G., D'Alessio A.C., Zhang Y. // J. Biol. Chem. 2008. V. 283. P. 31601–31607.
99. Kroon E., Martinson L.A., Kadoya K., Bang A.G., Kelly O.G., Eliazer S., Young H., Richardson M., Smart N.G., Cunningham J., *et al.* // Nat. Biotechnol. 2008. V. 26. P. 443–452.
100. D'Amour K.A., Agulnick A.D., Eliazer S., Kelly O.G., Kroon E., Baetge E.E. // Nat. Biotechnol. 2005. V. 23. P. 1534–1541.
101. Mfopou J.K., Chen B., Mateizel I., Sermon K., Bouwens L. // Gastroenterology. 2010. V. 138. P. 2233–2245.
102. Johannesson M., Ståhlberg A., Ameri J., Sand F.W., Norrman K., Semb H. // PLoS One. 2009. V. 4. № 3. e4794.
103. D'Amour K.A., Bang A.G., Eliazer S., Kelly O.G., Agulnick A.D., Smart N.G., Moorman M.A., Kroon E., Carpenter M.K., Baetge E.E. // Nat. Biotechnol. 2006. V. 24. P. 1392–1401.
104. McLean A.B., D'Amour K.A., Jones K.L., Krishnamoorthy M., Kulik M.J., Reynolds D.M., Sheppard A.M., Liu H.,

Xu Y., Baetge E.E., *et al.* // Stem Cells. 2007. V. 25. P. 29–38.
105. Shim J.H., Kim S.E., Woo D.H., Kim S.K., Oh C.H., McKay R., Kim J.H. // Diabetologia. 2007. V. 50. P. 1228–1238.
106. Kubo A., Shinozaki K., Shannon J.M., Kouskoff V., Kennedy M., Woo S., Fehling H.J., Keller G. // Development. 2004. V. 131. P. 1651–1662.
107. Takeuchi H., Nakatsuji N., Suemori H. // Sci. Rep. 2014. V. 4. P. 4488.
108. Kunisada Y., Tsubooka-Yamazoe N., Shoji M., Hosoya M. // Stem Cell Res. 2012. V. 8. P. 274–284.
109. Borowiak M., Maehr R., Chen S., Chen A.E., Tang W., Fox J.L., Schreiber S.L., Melton D.A. // Cell Stem Cell. 2009. V. 4. P. 348–358.
110. Bose B., Shenoy S.P., Konda S., Wangikar P. // Cell Biol. Internat. 2012. V. 36. P. 1013–1020.
111. Gage B.K., Webber T.D., Kieffer T.J. // PLoS One. 2013. V. 8. e82076.
112. Basford C.L., Prentice K.J., Hardy A.B., Sarangi F., Micallef S.J., Li X., Guo Q., Elefanty A.G., Stanley E.G., Keller G., *et al.* // Diabetologia. 2012. V. 55. P. 358–371.
113. Micallef S.J., Li X., Schiesser J.V., Hirst C.E., Yu Q.C., Lim S.M., Nostro M.C., Elliott D.A., Sarangi F., Harrison L.C., *et al.* // Diabetologia. 2012. V. 55. P. 694–706.
114. Rezania A., Bruin J.E., Riedel M.J., Mojibian M., Asadi A., Xu J., Gauvin R., Narayan K., Karanu F., O'Neil J.J., *et al.* // Diabetes. 2012. V. 61. P. 2016–2029.
115. Rezania A., Bruin J.E., Xu J., Narayan K., Fox J.K., O'Neil J.J., Kieffer T.J. // Stem Cells. 2013. V. 31. P. 2432–2442.
116. Schulz T.C., Young H.Y., Agulnick A.D., Babin M.J., Baetge E.E., Bang A.G., Bhoumik A., Cepa I., Cesario R.M., Haakmeester C., *et al.* // PLoS One. 2012. V. 7. e37004.
117. Kirk K., Hao E., Lahmy R., Itkin-Ansari P. // Stem Cell Res. 2014. V. 12. P. 807–814.
118. Bruin J.E., Rezania A., Xu J., Narayan K., Fox J.K., O'Neil J.J., Kieffer T.J. // Diabetologia. 2013. V. 56. P. 1987–1998.
119. Pagliuca F.W., Millman J.R., Gürtler M., Segel M., Van Dervort A., Ryu J.H., Peterson Q.P., Greiner D., Melton D.A. // Cell. 2014. V. 159. № 2. P. 428–439.
120. Xie R., Everett L.J., Lim H.W., Patel N.A., Schug J., Kroon E., Kelly O.G., Wang A., D'Amour K.A., Robins A.J., *et al.* // Stem Cell. 2013. V. 12. P. 224–237.
121. Blum B., Hrvatin S.S., Schuetz C., Bonal C., Rezania A., Melton D.A. // Nat. Biotechnol. 2012. V. 30. P. 261–264.
122. Noguchi H., Kaneto H., Weir G.C., Bonner-Weir S. // Diabetes. 2003. V. 52. P. 1732–1737.
123. Koya V., Lu S., Sun Y.P., Purich D.L., Atkinson M.A., Li S.W., Yang L.J. // Diabetes. 2008. V. 57. № 3. P. 757–769.
124. Noguchi H., Xu G., Matsumoto S., Kaneto H., Kobayashi N., Bonner-Weir S., Hayashi S. // Cell Transplant. 2006. V. 15. № 10. P. 929–938.
125. Kopinke D., Murtaugh L.C. // BMC Dev. Biol. 2010. V. 10. № 38. doi: 10.1186/1471-213X-10-38.
126. Okuno M., Minami K., Okumachi A., Miyawaki K., Yokoi N., Toyokuni S., Seino S. // Am. J. Physiol. Endocrinol. Metab. 2007. V. 292. P. 158–165.
127. Lardon J., Huyens N., Rooman I., Bouwens L. // Virchows Arch. 2004. V. 444. P. 61–65.
128. Lipsett M., Finegood D.T. // Diabetes. 2002. V. 51. P. 1834–1841.
129. Desai B.M., Oliver-Krasinski J., De Leon D.D., Farzad C., Hong N., Leach S.D., Stoffers D.A. // J. Clin. Invest. 2007. V. 117. P. 971–977.
130. Zhou Q., Brown J., Kanarek A., Rajagopal J., Melton D.A. // Nature. 2008. V. 455. № 7213. P. 627–632.
131. Cabrera O., Berman D.M., Kenyon N.S., Ricordi C., Berggren P.O., Caicedo A. // Proc. Natl. Acad. Sci. USA. 2006. V. 103. № 7. P. 334–339.
132. Konstantinova I., Nikolova G., Ohara-Imaizumi M., Meda P., Kucera T., Zarbalis K., Wurst W., Nagamatsu S., Lammert E. // Cell. 2007. V. 129. № 2. P. 359–370.
133. Zhang T., Saunee N.A., Breslin M.B., Song K., Lan M.S. // J. Cell Physiol. 2012. V. 227. № 6. P. 2470–2479.
134. Lima M.J., Muir K.R., Docherty H.M., Drummond R., McGowan N.W., Forbes S., Heremans Y., Houbracken I., Ross J.A., Forbes S.J., *et al.* // Diabetes. 2013. V. 62. № 8. P. 2821–2833.
135. Wang A.Y., Ehrhardt A., Xu H., Kay M.A. // Mol. Ther. 2007. V. 15. № 2. P. 255–263.
136. Collombat P., Xu X., Ravassard P., Sosa-Pineda B., Dussaud S., Billestrup N., Madsen O.D., Serup P., Heimberg H., Mansouri A. // Cell. 2009. V. 138. P. 449–462.
137. Yang Y.P., Thorel F., Boyer D.F., Herrera P.L., Wright C.V. // Genes Dev. 2011. V. 25. P. 1680–1685.
138. Chung C.H., Hao E., Piran R., Keinan E., Levine F. // Stem Cells. 2010. V. 28. P. 1630–1638.
139. Thorel F., Nepote V., Avril I., Kohno K., Desgraz R., Chera S., Herrera P.L. // Nature. 2010. V. 464. P. 1149–1154.
140. Nir T., Melton D.A., Dor Y. // J. Clin. Invest. 2007. V. 117. P. 2553–2561.
141. Fujikawa T., Oh S.-H., Pi L., Hatch H.M., Shupe T., Petersen B.E. // Am. J. Pathol. 2005. V. 166. P. 1781–1791.
142. Enseñat-Waser R., Santana A., Vicente-Salar N., Cigudosa J.C., Roche E., Soria B., Reig J.A. // *In vitro* Cell Dev. Biol. Anim. 2006. V. 42. P. 115–123.
143. Fernandes K.J., McKenzie I.A., Mill P., Smith K.M., Akhavan M., Barnabé- Heider F., Biernaskie J., Junek A., Kobayashi N.R., Toma J.G. // Nat. Cell Biol. 2004. V. 6. P. 1082–1093.
144. Toma J.G., McKenzie I.A., Bagli D., Miller F.D. // Stem Cells. 2005. V. 23. P. 727–737.
145. Bi D., Chen F.G., Zhang W.J., Zhou G.D., Cui L., Liu W., Cao Y. // BMC Cell Biol. 2010. V. 11. P. 46.
146. Kim B., Yoon B.S., Moon J.-H., Kim J., Jun E.K., Lee J.H., Kim J.S., Baik C.S., Kim A., Whang K.Y. // Exp. Mol. Med. 2012. V. 44. P. 26–35.
147. Toma J.G., Akhavan M., Fernandes K.J., Barnabé-Heider F., Sadikot A., Kaplan D.R., Miller F.D. // Nat. Cell Biol. 2001. V. 3. P. 778–784.
148. Bakhtiari M., Mansouri K., Sadeghi Y., Mostafaie A. // Cell Prolif. 2012. V. 45. P. 148–157.
149. Mehrabi M., Mansouri K., Hosseinkhani S., Yarani R., Yari K., Bakhtiari M., Mostafaie A. // *In vitro* Cell Dev. Biol. Anim. 2015. V. 51. № 6. P. 595–603.
150. Da Silva M.L., Chagastelles P.C., Nardi N.B. // J. Cell Sci. 2006. V. 119. № 11. P. 2204–2213.
151. Trounson A // BMC Med. 2009. V. 7. P. 29.
152. Kang H.M., Kim J., Park S., Kim J., Kim H., Kim K.S., Lee E.J., Seo S.I., Kang S.G., Lee J.E., *et al.* // Stem Cells. 2009. V. 27. № 8. P. 1999–2008.
153. Le Douarin N.M., Creuzet S., Couly G., Dupin E. // Development. 2004. V. 131. № 19. P. 4637–4650.
154. Huang C.Y., Peláez D., Domínguez-Bendala J., Garcia-Godoy F., Cheung H.S. // Regen. Med. 2009. V. 4. № 6. P. 809–821.
155. Prabakar K.R., Domínguez-Bendala J., Molano R.D.., Pileggi A., Villate S., Ricordi C., Inverardi L. // Cell Transplant. 2012. V. 21. № 6. P. 1321–1339.
156. Wu Y., Chen L., Scott P.G., Tredget E.E. // Stem Cells. 2007. V. 25. № 10. P. 2648–2659.

157. Ball S.G., Shuttleworth C.A., Kielty C.M. // J. Cell. Mol. Med. 2007. V. 11. № 5. P. 1012–1030.
158. Ferber S., Halkin A., Cohen H., Ber I., Einav Y., Goldberg I., Barshack I., Seijffers R., Kopolovic J., Kaiser N., Karasik A. // Nat. Med. 2000. V. 6. № 5. P. 568–572.
159. Horb M.E., Shen C.N., Tosh D., Slack J.M. // Curr. Biol. 2003. V. 13. № 2. P. 105–115.
160. Li W.C., Horb M.E., Tosh D., Slack J.M. // Mech. Dev. 2005. V. 122. № 6. P. 835–847.
161. Bonner-Weir S., Li W.C., Ouziel-Yahalom L., Guo L., Weir G.C., Sharma A. // Diabetes. 2010. V. 59. P. 2340–2348.
162. Gianani R., Putnam A., Still T., Yu L., Miao D., Gill R.G., Beilke J., Supon P., Valentine A., Iveson A., *et al.* // J. Clin. Endocrinol. Metab. 2006. V. 91. P. 1855–1861.
163. Dor Y., Melton D.A. // Cell. 2008. V. 132. P. 183–184.
164. Li Y., Peng M., Gong G. // Exp. Ther. Med. 2014. V. 7. P. 131–136.
165. Basta G., Racanicchi L., Mancuso F., Guido L., Luca G., Macchiarulo G., Brunetti P., Calafiore R. // Transplant. Proc. 2004. V. 36. P. 2857–2863.
166. Liu T., Wang C.Y., Yu F., Gou S.M., Wu H.S., Xiong J.X., Zhou F. // World J. Gastroenterol. 2007. V. 13. P. 5232–5237.
167. Anastasi E., Ponte E., Gradini R., Bulotta A., Sale P., Tiberti C., Okamoto H., Dotta F., Di Mario U. // Eur. J. Endocrinol. 1999. V. 141. P. 644–652.
168. Higuchi Y., Herrera P., Muniesa P., Huarte J., Belin D., Ohashi P., Aichele P., Orci L., Vassalli J.D., Vassalli P. // J. Exp. Med. 1992. V. 176. P. 1719–1731.
169. Gu D., Arnush M., Sawyer S.P., Sarvetnick N. // Am. J. Physiol. 1995. V. 269. P. 1089–1094.
170. Kritzik M.R., Jones E., Chen Z., Krakowski M., Krahl T., Good A., Wright C., Fox H., Sarvetnick N. // J. Endocrinol. 1999. V. 163. P. 523–530.
171. Tanaka S., Kobayashi T., Nakanishi K., Okubo M., Murase T., Hashimoto M., Watanabe G., Matsushita H., Endo Y., Yoshizaki H., *et al.* // Diabetes Care. 2001. V. 24. P. 1661–1667.
172. Baeyens L., Lemper M., Leuckx G., De Groef S., Bonfanti P., Stangé G., Shemer R., Nord C., Scheel D.W., Pan F.C., *et al.* // Nat. Biotechnol. 2014. V. 32. № 1. P. 76–83.
173. Egéa J.C., Hirtz C., Gross R., Lajoix A.D., Traskawka E., Ribes G., de Périère D.D. // Eur. J. Oral. Sci. 2000. V. 108. № 4. P. 292–296.
174. Smith P.H., Patel D.G. // Diabetes. 1984. V. 33. № 7. P. 661–666.
175. Shubnikova E.A., Pogodina L.S. // Ontogenez. 2000. V. 31. № 6. P. 476–480.
176. Gvazava I.G., Vasiliev A.V., Balan O.V., Terskikh V.V. // Tsitologiia. 2011. V. 53. № 2. P. 129–134.
177. Okumura K., Nakamura K., Hisatomi Y., Nagano K., Tanaka Y., Terada K., Sugiyama T., Umeyama K., Matsumoto K., Yamamoto T., *et al.* // Hepatology. 2003. V. 38. P. 104–113.
178. Hisatomi Y., Okumura K., Nakamura K., Matsumoto S., Satoh A., Nagano K., Yamamoto T., Endo F. // Hepatology. 2004. V. 39. № 3. P. 667–675.
179. Sato A., Okumura K., Matsumoto S., Hattori K., Hattori S., Shinohara M., Endo F. // Cloning Stem Cells. 2007. V. 9. № 2. P. 191–205.
180. Baek H., Noh Y.H., Lee J.H., Yeon S.I., Jeong J., Kwon H. // J. Tissue Eng. Regen. Med. 2014. V. 8. № 9. P. 717–727.
181. Vacanti J.P., Langer R. // Lancet. 1999. V. 354. P. 32–34.
182. Chun S., Huang Y., Xie W.J., Hou Y., Huang R.P., Song Y.M., Liu X.M., Zheng W., Shi Y., Song C.F. // Transplant. Proc. 2008. V. 40. P. 1658.
183. Kawazoe N., Tateishi T. // J. Bioact. Compat. Polym. 2009. V. 24. P. 25.
184. Kaufman-Francis K., Koffler J., Weinberg N., Dor Y., Levenberg S. // PLoS One. 2012. V. 7. e40741.
185. Hynes R.O. // Science. 2009. V. 326. № 5957. P. 1216–1219.
186. Otonkoski T., Banerjee M., Korsgren O., Thornell L.E., Virtanen I. // Diabetes Obes. Metab. 2008. V. 10. № 4. P. 119–127.
187. Edamura K., Nasu K., Iwami Y., Ogawa H., Sasaki N., Ohgawara H. // Cell Transplant. 2003. V. 12. № 4. P. 439–446.
188. Stendahl J.C., Kaufman D.B., Stupp S.I. // Cell Transplant. 2009. V. 18. № 1. P. 1–12.
189. Montesano R., Mouron P., Amherdt M., Orci L. // J. Cell Biol. 1983. V. 97. № 3. P. 935–939.
190. Weber L.M., Hayda K.N., Anseth K.S. // Tissue Eng. Part A. 2008. V. 14. № 12. P. 1959–1968.
191. Wang R.N., Rosenberg L. // J. Endocrinol. 1999. V. 163. № 2. P. 181–190.
192. Rosenberg L., Wang R., Paraskevas S., Maysinger D. // Surgery. 1999. V. 126. № 2. P. 393–398.
193. Meda P., Hooghe-Peters E.L., Orci L. // Diabetes. 1980. V. 29. № 6. P. 497–500.
194. Rabinovitch A., Russell T., Mintz D.H. // Diabetes. 1979. V. 28. № 12. P. 1108–1113.
195. Thivolet C.H., Chatelain P., Nicoloso H., Durand A., Bertrand J. // Exp. Cell Res. 1985. V. 159. № 2. P. 313–322.
196. Lucas-Clerc C., Massart C., Campion J.P., Launois B., Nicol M. // Mol. Cell Endocrinol. 1993. V. 94. № 1. P. 9–20.
197. Han B., Qi S., Hu B., Luo H., Wu J. // J. Immunol. 2011. V. 186. № 10. P. 5833–5844.
198. Crisera C.A., Maldonado T.S., Kadison A.S., Li M., Alkasab S.L., Longaker M.T., Gittes G.K. // Differentiation. 2000. V. 65. № 5. P. 255–259.
199. Salvatori M., Katari R., Patel T., Peloso A., Mugweru J., Owusu K., Orlando G. // J. Diabetes Sci. Technol. 2014. V. 8. № 1. P. 159–169.
200. Song J.J., Ott H.C. // Trends Mol. Med. 2011. V. 17. № 8. P. 424–432.
201. Orlando G., Baptista P., Birchall M., De Coppi P., Farney A., Guimaraes-Souza N.K., Opara E., Rogers J., Seliktar D., Shapira-Schweitzer K., *et al.* // Transpl. Int. 2011. V. 24. № 3. P. 223–232.
202. Orlando G., Wood K.J., Stratta R.J., Yoo J.J., Atala A., Soker S. // Transplantation. 2011. V. 91. № 12. P. 1310–1317.
203. Orlando G., Wood K.J., De Coppi P., Baptista P.M., Binder K.W., Bitar K.N., Breuer C., Burnett L., Christ G., Farney A., *et al.* // Ann. Surg. 2012. V. 255. № 5. P. 867–880.
204. Badylak S.F., Weiss D.J., Caplan A., Macchiarini P. // Lancet. 2012. V. 379. № 9819. P. 943–952.
205. Gilbert T.W., Sellaro T.L., Badylak S.F. // Biomaterials. 2006. V. 27. № 19. P. 3675–3683.
206. Mirmalek-Sani S.H., Orlando G., McQuilling J.P., Pareta R., Mack D.L., Salvatori M., Farney A.C., Stratta R.J., Atala A., Opara E.C., *et al.* // Biomaterials. 2013. V. 34. № 22. P. 5488–5495.
207. Baptista P.M., Siddiqui M.M., Lozier G., Rodriguez S.R., Atala A., Soker S. // Hepatology. 2011. V. 53. № 2. P. 604–617.
208. Song J.J., Kim S.S., Liu Z., Madsen J.C., Mathisen D.J., Vacanti J.P., Ott H.C. // Ann. Thorac. Surg. 2011. V. 92. № 3. P. 998–1006.
209. Loai Y., Yeger H., Coz C., Antoon R., Islam S.S., Moore K., Farhat W.A. // J. Biomed. Mater Res. A. 2010. V. 94. № 4. P. 1205–1215.
210. Wicha M.S., Lowrie G., Kohn E., Bagavandoss P., Mahn T. // Proc. Natl. Acad. Sci. USA. 1982. V. 79. № 10. P. 3213–3217.

Bioreactor-Based Tumor Tissue Engineering

A. E. Guller[1–4*✉], P. N. Grebenyuk[5✉], A. B. Shekhter[3], A. V. Zvyagin[1-4], S. M. Deyev[4,6,7]
[1]Macquarie University, Sydney, 2109, New South Wales, Australia
[2]ARC Centre of Excellence for Nanoscale BioPhotonics, Macquarie University, Sydney 2109, New South Wales, Australia
[3]Sechenov First Moscow State Medical University, Institute for Regenerative Medicine, 8, Trubetskaya Str., Moscow, 119992, Russia
[4]Lobachevsky Nizhniy Novgorod State University, 23, Gagarina Ave., Nizhniy Novgorod, 603950, Russia
[5]Inetex LTD, 10, Plaut Str., Rehovot, 76706, Israel
[6]Institute of Bioorganic Chemistry, 16/10, Miklukho-Maklaya Str., Moscow, 117871, Russia
[7]National Research Tomsk Polytechnic University, 30, Lenina Ave., Tomsk, 634050, Russia
*E-mail: anna.guller@mq.edu.au
✉Authors, who contributed equally to this work
Received June 09, 2016

ABSTRACT **This review focuses on modeling of cancer tumors using tissue engineering technology. Tumor tissue engineering (TTE) is a new method of three-dimensional (3D) simulation of malignant neoplasms. Design and development of complex tissue engineering constructs (TECs) that include cancer cells, cell-bearing scaffolds acting as the extracellular matrix, and other components of the tumor microenvironment is at the core of this approach. Although TECs can be transplanted into laboratory animals, the specific aim of TTE is the most realistic reproduction and long-term maintenance of the simulated tumor properties *in vitro* for cancer biology research and for the development of new methods of diagnosis and treatment of malignant neoplasms. Successful implementation of this challenging idea depends on bioreactor technology, which will enable optimization of culture conditions and control of tumor TECs development. In this review, we analyze the most popular bioreactor types in TTE and the emerging applications.**
KEYWORDS **bioreactors, cancer, models, tissue engineering.**
ABBREVIATIONS **2D – two dimensional/monolayer cell or tissue culture *in vitro*; 3D – three-dimensional; BR – bioreactor; DCL – decellularization; DCL matrix, DCL tissue, DCL organ – decellularized matrix, decellularized tissue, and decellularized organ, respectively; RCL – recellularization; TE – tissue engineering; TEC – tissue engineering construct; TTE – tumor tissue engineering; TETM – tissue-engineered tumor model; SCID – severe combined immunodeficiency mice. Abbreviations used for various types of rotary bioreactors: RWV – rotating-wall vessel (rotating-wall bioreactor); RCCS – rotary cell culture system; HARV – high aspect reactor vessel; STLV – slow turning lateral vessel; RWPV – rotating-wall perfusion vessel; NASA bioreactor – common name of rotary bioreactors developed by NASA, usually RWW, HARV, or STLW.**

INTRODUCTION

An *in vitro* cell or tissue culture is a traditional instrument of research in the field of cancer biology and development of new methods for the prevention, diagnosis, and treatment of this disease. Primary and linear cells of human and animal tumors represent a convenient model for studying the molecular and cellular mechanisms of malignant growth and for evaluating drug effects. However, about 95% of drugs which exhibit significant antitumor effects in experiments in cell cultures and in laboratory animals demonstrate insufficient efficacy or unacceptable toxicity in clinical trials [1]. A possible and likely explanation for this is the poor relevance of existing *in vitro* and *in vivo* cancer models to human tumors that have a dynamic and complex structure and heterogeneous cell composition [1–3].

The most important factors associated with experiments in conventional monolayer cell cultures (2D) include the selection of a specific cell phenotype (adapted for growth on a plastic surface) from an initially very heterogeneous tumor cell population, abnormal cell polarization resulting from limited exposure of the

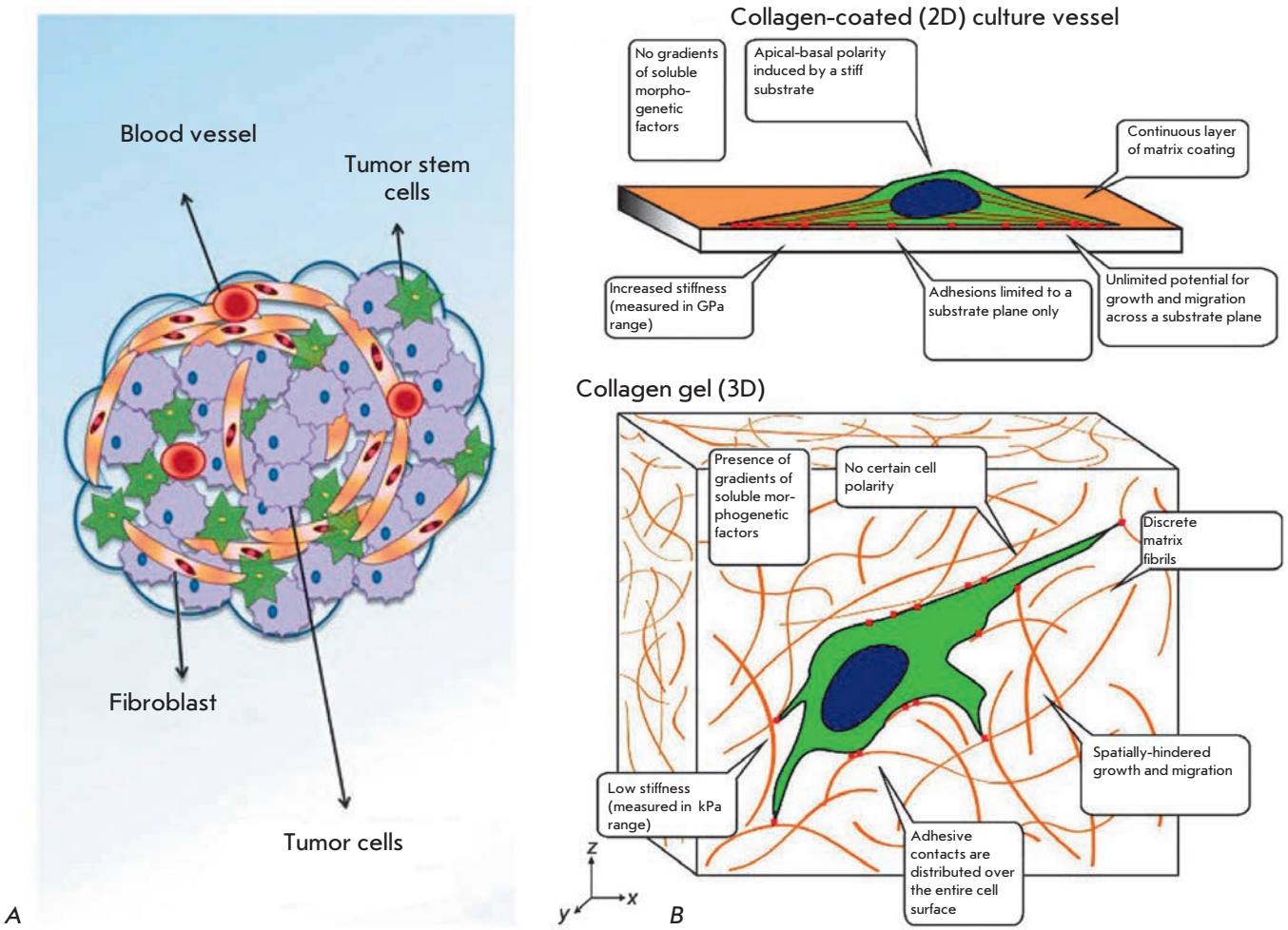

Fig. 1. Malignant tumor structure (*A*) (a schematic view, adapted from [8])) and conditions for traditional 2D-tissue culture *in vitro* (*B*) (adapted from [9]). (*A*) The tumor is a 3D-structure. Due to abnormal local blood circulation and innervation, the tumor possesses multiple metabolic gradients which contribute to the genetic instability of malignant cells. Phenotype selection affects the dynamic responses of a cancer stem cell pool. In addition to the neoplastic cell population, resident cells of the affected organ and cells of the inflammatory infiltrate (including macrophages, lymphocytes, eosinophils, and sometimes plasma cells) are involved in the tumor. The extracellular matrix, blood vessels, and connective tissue inclusions are the second component, known as the stroma of the tumor. The degree of stroma development in malignant tumors varies notably and significantly affects the course of the disease and tumor drug resistance. Also, sites with active growth, necrotic zones, hemorrhages, and purulent pockets can occur within the tumor. (*B*) Changes observed in a 2D culture are induced by the selection of specific cellular phenotypes and abnormal interactions between cells and their micro- and macro-environments.

cell surface to the culture medium, a drastic reduction in the number of cell-cell contacts, and a lack of cell-matrix interactions and metabolic gradients [4–6]. Together, these factors make a 2D-culture inadequate for capturing the critical mechanisms in cancer biology [7], such as the heterogeneity of tumor cell populations, as well as the intensive interaction between the tumor and its microenvironment and the whole organism (*Fig. 1*).

Cancer models in laboratory animals also have some notable disadvantages. For example, in simulations of human tumors in mice by implanting cellular allografts, which is one of the most popular approaches, the histological features of human neoplasms are reproduced inaccurately or not reproduced at all (*Fig. 2A–D*). In addition, the lifespan of laboratory animals is oftentimes shorter than the period of metastases development [8]. Xenografts derived from the tumor tissue of patients

and transplanted into mice with a suppressed immune system (nude, SCID) represent a realistic model of human tumors [10, 11]. These approaches reflect the structure and function of human tumor at the tissue level adequately to some extent (*Fig. 2E, F*), while the host organism plays the same role as that of the culture medium in *in vitro* cultures. At the same time, the physiology of athymic or SCID mice significantly differs from that of humans. The high cost and low reproducibility of these models limit their applications.

Aiming to more accurately reproduce the histological structure of tumors and their physiological properties, technologies of co-culturing of different cell types and three-dimensional (3D) tumor models have been introduced. The latter include multicellular spheroids and cancer cell cultures on matrices of various compositions and structures (gel, fibrous, etc.). One of the most promising approaches is tumor tissue engineering (TTE), which is a new method of 3D-modeling of malignant neoplasms based on the production of complex constructs, including malignant cells, solid porous or fibrous cellular carriers (scaffolds), acting as an extracellular matrix, and other components of the tumor microenvironment. Tissue-engineered tumor models (TETMs) are designed for studying cancer biology and the development of methods for the diagnosis and treatment of malignant tumors. The basic principles of TTE, its advantages and limitations, as well as the implemented models, were discussed in detail in recent reviews [8, 13–19].

As its name suggests, TTE makes use of the tissue engineering (TE) technology of normal tissues in terms of a combination of certain cells and scaffolds with subsequent control of the produced tissue engineering constructs (TECs) [20]. At the same time, TTE is meant for research, unlike TECs of normal tissues, which are used for therapeutic purposes. In general, a tissue engineering model of healthy tissue is a 3D-culture of normal cells on a scaffold, the TEC, that is "assembled" and matures *in vitro* and then is implanted into a patient organism to replace damaged or lost tissues or organs. Then, engraftment of the reconstructed structure occurs to ensure the viability of the structure and its functionality. TECs are often used in regenerative medicine and serve as a temporal functional tissue or organ prostheses that is expected to be bioresorbed up to complete replacement with the organism's own tissues. In contrast, cancer TECs include primarily malignant cells able to survive for a long time outside the body, preserving a structural and functional similarity to the simulated tumors even under *in vitro* conditions. Tumor TECs can also be implanted into laboratory animals, e.g., to study the angiogenic, invasive, and metastatic potential of the engineered tumors. However,

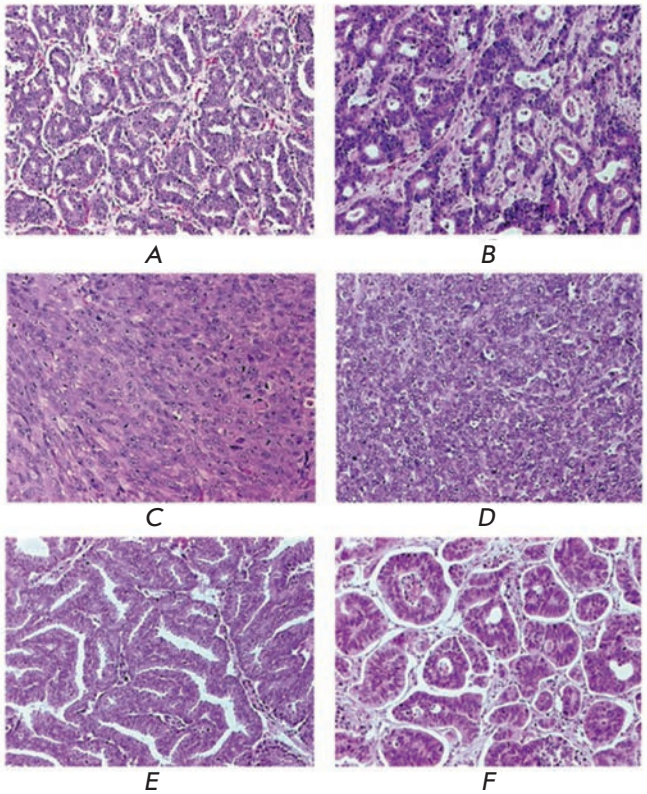

Fig. 2. Comparisons of histological structures of prostate (*A*, *C*, *E*) and colon (*B*, *D*, *F*) cancers observed in primary tumors (*A*, *B*) and the cancers propagated as model systems in mice (*C-F*). Tumors obtained by subcutaneous engraftment of suspensions of linear cells PC-3M (*C*) and Colo205 (*D*) have a homogenous structure with absence of specific glandular elements formed by cancer cells and the lack of a stromal component. Significant alterations of tumor-stroma ratio are also notable in the cases of subcutaneous grafting of surgical biopsy specimens of original human primary tumors (*E*, *F*). Adapted from [12] with changes.

the use of these bioartificial tissues *in vitro* seems to be most attractive for improvement of the reproducibility of the results, development of high-throughput test systems for pharmacological research, and for the replacement of animals in research.

The differences in the growth, differentiation, and metabolism rates between normal and cancer cells obviate a key problem of regenerative medicine: the expansion of the cell population within a TEC (e.g., during controlled differentiation of stem cells). On the other hand, these call for the development of new methods and systems of 3D culture that enable the formation and maintenance of bulky and metabolically active tissue structures outside the body; i.e., in the absence of

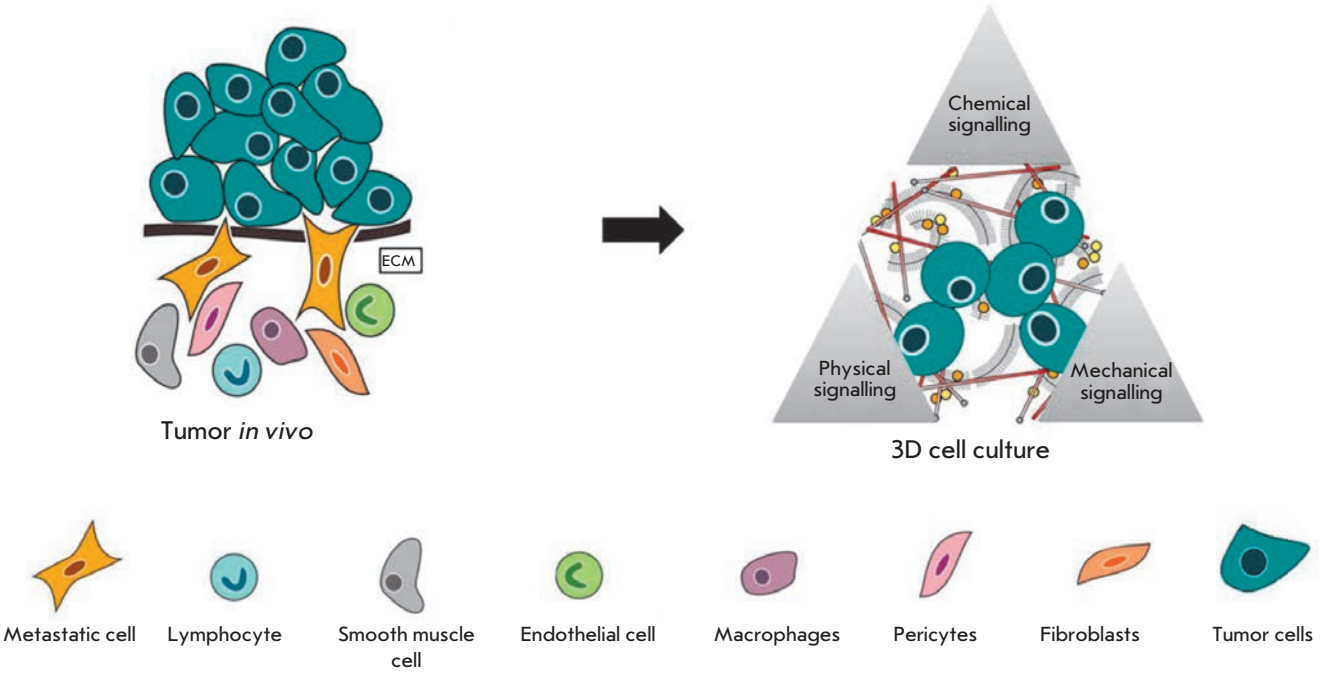

Fig. 3. Principles of formation of tumor TECs. In order to create biomimetic tumor TECs the key components of the original tumor (as cancer cells and a scaffold, representing the extracellular matrix) should be included into the model. In addition, it is very important to reproduce the conditions of tumor growth by the inclusion of physical and chemical signalling factors. Adapted from [23] with changes.

normal homeostatic systems. Similar problems are partially addressed in the modern systems for the temporary storage and maintenance of donor organs.

In tissue engineering, growth and maintenance of TECs occurs in bioreactors (BRs) until implantation [21]. To this aim, purpose-designed systems are needed to automate cell and tissue culturing processes *in vitro* and provide optimal physico-chemical conditions for TEC development. The purpose of this review is to analyze the current state of bioreactor-based tissue engineering modeling of malignant tumors.

TUMOR TEC COMPONENTS

Cells and scaffolds are the main components of TECs (*Fig. 3*). Cells can be presented by one or several types simultaneously (e.g., by fibroblasts and hepatocytes in liver models); however, the tissue specificity of TECs is determined by the most abundant cellular population. In particular, the cellular component of tumor TECs can be formed by both the primary cells isolated from tumor biopsy fragments (from a primary or metastatic foci) or the linear cancer cells obtained by using a special selection and culture procedures. Cells with a varying degree of differentiation and with different metastatic potentials can be selected. In addition to tumor cellular populations, TECs can also include stromal elements (fibroblasts, pericytes and endothelial and smooth muscle cells), the main cells of a resident organ (e.g., hepatocytes in models of liver tumors or osteoblasts and bone marrow cells in the investigation of neoplastic processes in bones), and cells of an inflammatory infiltrate (macrophages, lymphocytes, neutrophils, plasma cells, eosinophils) [22].

Scaffolds represent an important component of TEC. They function as bioactive extracellular matrices serving to provide mechanical support for the cells and promote cellular adhesion and motility (which switches to a number of signaling pathways sensitive to the cytoskeletal organization), provide mechanical and biochemical integration of the construct, stimulate the required differentiation (in TECs of normal tissues), or maintain a specified phenotype and functional activity of the cells. The scaffold architecture ensures the formation of the gradients of signaling molecules and oxygen within TECs and enables the study of the role of cell-matrix interactions in the regulation of carcinogenesis. The convoluted and interdependent effects of mechanical factors, nanotopography, matrix geometry, and cell adhesion are also investigated in the framework of TEC [24].

Scaffolds can be produced using fibrous and porous materials made from synthetic polymers (e.g., polylactate, polycaprolactone, polylactoglycolide) or materials of natural origin (collagen, chitosan, hyaluronic acid) [17], as well as specially treated natural tissues and organs [25, 26]. The major advantage of synthetic scaffolds fabricated by engineering methods (electrospinning, 3D printing, etc.) is a high degree of chemical composition certainty and precise control over spatial organization and mechanical properties, which allows one to study the influence of single signaling factors on tissue morphogenesis. However, such scaffolds do not maintain the necessary adhesion and long-term proliferation of cells, with a few exceptions. Furthermore, they mimic the modeled original tissue poorly, largely remaining a 3D-analogue of conventional plastic culture dishes. Scaffolds made of natural polymers have high biocompatibility, although strict control of their composition, geometry, and biomechanical properties is challenging [17].

An alternative approach involves the processing of natural tissues or organs by removing their cellular elements while preserving the composition and structure of the extracellular matrix. This process is called decellularization (DCL). It results in the production of scaffolds, which are known as decellularized tissues or acellular matrices, tissues, or organs (DCL matrix, DCL tissue, DCL organ, respectively) [26, 27]. Therefore, DCL allows one to prepare scaffolds that reproduce the natural microenvironment of cells in a tissue or organ very closely. Modern DCL methods result not only in scaffolds containing the major extracellular matrix components, such as collagen and elastic fibers, but also templates maintaining the integrity of the basal membranes of blood vessels, which ensures the presence of integrated vascular conduits (decellularized walls of blood vessels of various calibers) that can later be used to perfuse the bioengineered tissue. This feature is of great importance, because the nutrition of the inner regions of TECs is a challenge in tissue engineering and it is critical for TTE.

MAIN OBSTACLES ASSOCIATED WITH "ASSEMBLY" AND CULTURE OF ENGINEERED TUMOR TISSUES THAT REQUIRE THE USE OF BIOREACTORS

Bioreactors (BRs) are closed systems where biological processes occur under strictly controlled conditions [28]. The concept of BRs (as chemostats or fermenters) has been used for growing microbial cultures and obtaining various products of cells for a long time. A typical bioreactor system includes a tank isolated from the environment (flask, vessel, chamber), the actuator components (pumps, motors, etc.), sensors, and, very often, special controllers and software for managing and monitoring the biotechnological process. BRs designed for TE have been used for growing cells and TECs, as well as for exploring the effects of biochemical and biomechanical factors on the development of cells and tissues. There are several key difficulties related to the assembly of tumor TECs and their further *in vitro* culture. An optimal solution for these problems requires the use of bioreactor technologies.

Expansion of cellular populations

A TETM size can vary from a few cubic millimeters to a whole organ of the human or animal body, but the number of necessary cells always largely exceeds the population of a typical monolayer cell culture. Therefore, the first step in the development of a tumor TEC is to expand the number of cells of the required types. This is possible only with the use of a large surface area for their growth. Co-cultivation of several cell types often involves simultaneous expansion of the cells in different conditions. In some cases, the cell populations used to create TECs are prepared as multicellular spheroids requiring special cultivation conditions. Automation and improved control over the cell culture processes afforded by BRs is instrumental in addressing these problems.

Scaffold recellularization

The second step in the development of TECs is recellularization (RCL), which is the colonization of 3D-scaffolds with cells – [29, 30]. The basic technique of a static culture uses dropwise seeding of cells on a scaffold. Then, the cell population spontaneously distributes through the matrix due to gravity and cell migration. However, this method is not effective enough for the preparation of complex tissues and bulky constructs as it does not ensure the uniform distribution of cells throughout the volume of the scaffold and, therefore, does not allow controlled development of the tissue.

Nutrition and metabolism of TECs

The third step is the delivery of the substances which are necessary for the growth and function of cells and removal of metabolic products throughout the TEC. This controlled and optimal mass transfer, in terms of its effect on a tissue, represents the most important goal of bioreactor technologies [28]. In a static culture *in vitro*, this can be achieved by periodical replacement of a culture medium. However, the latter method is suitable only for experiments with cultured objects of small volume, such as cells in a monolayer, a suspension, or thin tissue sections. It is known that the diffusion limit for oxygen in human tissues ranges from 100 μm to 200 μm [31]. As a result, the medium reaches the cells in a TEC only by diffusion in the absence of continuous stirring or pump-

ing. Therefore, the central part of a TEC suffers from insufficient oxygen and nutrients, and removal of metabolic products. This can lead to hypoxia, acidosis, and cell death. Convection fluid flows in dynamic systems improve mass transfer and are preferred. However, agitation of a culture medium can cause damage to the cells and scaffold due to the excessive shear stress [32] associated with the uneven dynamics of the different fluid layers. Therefore, it is important to keep a balance both between the diffusion and convection transport and between the biomechanical properties and metabolic needs of the grown structures. A promising approach to solving the problem of oxygen transport within TECs is using BRs with built-in perfusion systems. Taking into account the complexity of maintenance of TETMs, it is desirable to automate the process of constant supply of a fresh culture medium to the cells and removal of the metabolic products combined. This automation is controlled by real-time monitoring of the biochemical parameters of the culture medium, followed by their feedback-informed tuning.

Control of parameters in a BR culture chamber

Long-term maintenance of sterility is critical for TETM. Since model tissue maturation takes several months, TEC contamination has fatal consequences. In addition, the materials of a BR culture chamber have to be biocompatible and bioinert, with no influence on the tissue being cultured. At the same time, the materials must withstand a humid environment at 37 ˚C and sterilization by autoclaving, radiation, or chemical treatment. A BR chamber made from transparent material enables visual monitoring and use of optical imaging of TECs [21, 33, 34].

Control of the physicochemical parameters of the environment formed in a culture chamber and management of these properties are important both for maintaining TEC viability and for simulating conditions typical for malignant tumors: e.g., acidosis, hypoxia and increased tissue pressure [35, 36]. Regulation of temperature, pH, and the gas composition of the culture chamber environment, introduction/removal of certain signaling molecules, controlled physical impact on the forming tissues (pressure, tension, bending, etc.), a special electromagnetic environment, or electrical stimulation of TECs, etc. [37] are often required.

TYPES OF BIOREACTORS USED IN TTE

Most BRs exert their action on TECs through the culture medium. There are six BR types (*Table 1*): 1) BRs with static cultivation systems, 2) stirring BRs, 3) rotary BRs, 4) hollow-fiber BRs, 5) perfusion BRs, and 6) microfluidic BRs. In addition, there is a special class of BRs that acts on the TECs components directly, by means of mechanical, electromagnetic or other stimuli (they are discussed below in a special section).

STATIC CULTIVATION SYSTEMS IN TTE

Historically, the first types of BRs used in tissue engineering were static cultivation systems. They include conventional Petri dishes, flasks, bottles, and plates in which the growing cells, tissues and culture media were stationary. Culture vessels can be supplemented with porous and fibrous scaffolds and, also, with special mesh inserts with a certain pore size, which enables the study of the effects of the signaling factors with a given size of molecules/carriers, as well as the migration and invasive activity of the cells. Plates with special low-adhesive coatings or "gravitational traps" were used for the development of multicellular spheroids. However, mass transfer in static cultivation systems occurred exclusively due to gravity and diffusion. A significant advantage of static BRs is their commercial availability and ease of use. These systems are especially popular in high-throughput screening of pharmaceutical compositions.

Static BRs have been used to create tissue engineering models of breast, lung, and intestine cancers, Ewing's sarcoma, metastatic prostate cancer, and some other neoplasms (*Table 2*). However, it proved possible to maintain TECs only on membrane-like scaffolds with a thickness of less than 1 mm in the absence of active movement of the culture medium. Cell growth in the thicker matrices occurred predominantly on the scaffold surface. For example, we observed this effect during static cultivation of tumor cells and normal epithelium on 3 - 4 mm sections of a DCL organ (rabbit kidney) [39], as well as during RCL of a tubular acellular vascular matrix [40], and hybrid scaffolds [41], with buccal epithelial cells.

A number of the limitations of static cultivation schemes can be circumvented by using dynamic cultivation systems: i.e. BRs where the culture medium moves controllably.

STIRRING BIOREACTORS

Stirring BRs (spinner-flask bioreactor, spinner vessel, stirred tank) represented a leap in improving the mass transfer between cells and the culture medium. These BRs are usually constructed as a tank vessel with a built-in rotating element, a spinner (long spatula), that forms vortex fluid flows, providing dynamic mixing of the medium and mass-transfer between the medium and tissue or scaffold. Stirring BRs also include systems where the movement of the medium around the scaffolds, tissues, or TECs is realized by the movement of the culture containers themselves. Examples include roller bottles and classical culture vessels placed on

Table 1. Comparative characterization of bioreactors with culture-medium-mediated action on TECs*

BR types	Conditions of use	Mass transfer mechanism	Shear stress	Specialization in relation to objectives of tumor tissue engineering	Disputable questions
Static culture systems (conventional culture vessels: plates, flasks, etc.)	Portion replacement of a culture medium	Diffusion	Very small	Expansion of cellular mass, production of multicellular spheroids	Overcoming the mass transfer limitations (e.g., creation of hybrid systems, such as perfusion plates); automation of the operations
Stirring BRs	Stirring of a culture medium with use of special agitators; shaking or rotating of the culture vessels	Convection (high)	High	DCL of tissues and organs, formation of spheroids, RCL of TECs	A balance between mass transfer and shear stress
Rotary BRs	Stirring of a culture medium by the movement of the culture chamber walls; a reduction in shear stress by creating micro-gravity; oxygenation of a medium through a special membrane	Convection (high)	Low	Production of spheroids and a 3D cell culture on microcarriers	Operating modes (including rotational speed), especially when growing bulky TECs
Hollow-fiber BRs	The flow of a culture medium through artificial porous semipermeable fibers mimicking the blood vessels penetrating TECs, oxygenation of a medium through a special membrane	Convection (medium) and diffusion (high)	Very low	Expansion of the cells with a high metabolic rate	Nondestructive control and extraction of TECs from BRs
Perfusion BRs	The flow of culture medium around or through a TEC, by natural or artificial vascular conduits; medium oxygenation by means of a special device	Diffusion (high) and convection (moderate)	Moderate	DCL of tissues and organs, RCL of dense scaffolds, maintenance of 3D cultures on solid scaffolds, creation of the specific cultivation conditions in accordance with experiment purposes	Optimization of perfusion parameters, RCL uniformity, seeding scaffolds with cells, cell adhesion
Microfluidic BRs	A static culture or strictly laminar flow of a culture medium directly through cell mass or TECs, or interaction of cells with the medium through semipermeable barriers/membranes	Diffusion (high) and convection (moderate)	Adjustable	3D cultures on hydrogel scaffolds, simulation of angiogenesis and invasion of tumor cells, co-cultivation of different cell types, investigation of effects of fluid flow movement through a tissue; growth of spheroids; high-throughput screening of pharmaceuticals	Optimization of microfluidic chip design and biological validity of models

* Adapted from [38] with amendments.

shaking, vortexing, or spinning automatic platforms (shakers). In stirring BRs, cell layers, tissue fragments, scaffolds or TECs are placed either on special needles or directly on the inner surfaces of culture vessels. In this case, the tissues/scaffolds can be completely immersed in the fluid occurring at the liquid-gas phase interface or alternately immersed into the culture medium and the gas phase.

Now, stirring BRs are mainly used to expand the cell mass (much more effectively, in comparison with a monolayer [51]), in particular in the form of cultures on microcarriers and as multicellular spheroids. The

Table 2. Tissue engineered tumor models produced in static bioreactors

Tumor	Scaffold	Cells	Result	Reference
Breast cancer	DCL matrix of human adipose tissue	MCF-7, BT474, SKBR3	Phenotypic similarity to breast cancer biopsy tissues in the 3D culture on the DCL matrix is higher than that in a culture on Matrigel	[42]
	Silk fibroin	MDA-MB-231	Sensitivity to anticancer drugs in the cancer 3D model is reduced compared to that in 2D	[43]
Lung cancer, breast cancer, colorectal cancer, pancreatic cancer, ovarian teratocarcinoma, fibrocystic breast disease	DCL matrix synthesized *in vitro* by mouse embryonic fibroblasts (NIH3T3 line)	NCI-H460; PA-1; PA-1/E6; HCT116; HCT116/p53−; SW620; COLO 205; PANC-1; MCF7; HS 578T; MCF10A	The role and mechanisms of integrin-mediated signalling cascades in cell resistance to the action of antitumor agents (taxol) were studied. Prospects of using the cell-derived DCL scaffolds for drug testing were indicated	[44]
Lung cancer; the metastases of breast cancer, colorectal cancer and esophageal squamous cell carcinoma to the lungs	A DCL matrix of human lung cancer synthesized *in vivo* by lung cancer cells A549 (cell xenograft implanted in mice)	A549; MCF-7; SW-480; KYSE-510	The effect of the methods of DCL , mechanical properties and porosity of a produced matrix on the cell growth rate, cell viability, cell invasion into the matrix, and secretion of growth factors	[45]
Lung cancer metastases to the intestine	A DCL matrix of the porcine intestinal mucosa (in the form of a stretched membrane)	HCC827; A549	The superficial penetration of cells into a scaffold only was demonstrated. The effect of a 3D matrix on proliferation, apoptosis, and invasion compared to a culture in 2D was shown. The protein distribution and cell morphology in a 3D culture were similar to those in real tumors. Different cell sensitivity to gefitinib, depending on the presence of the epithelial growth factor receptor EGFR (not found in a 2D culture). The model was used to show an early stage of invasion	[46]
Ewing's sarcoma	Porous 3D electrospun poly(ε-caprolactone) scaffolds	TC-71	Increased drug resistance of tumor cells on a 3D matrix compared to that in a monolayer culture. Significant differences between 3D and 2D cultures in expression of the insulin-like growth factor 1 (IGFR-1, the target for rapamycin)	[47]
	DCL bone seeded with human mesenchymal stem cells	HTB-10, HTB-166	Cells that lost a specific phenotype in a 2D culture restored their specific gene expression profile on a DCL matrix. Genes that may be the therapeutic targets were identified	[48]
Prostate cancer metastases to bones	A tissue engineered bone: a poly-caprolactone scaffold "wrapped up" with a sheet of osteoblasts	PC3; LNCaP	An elevated level of matrix metalloproteinases and other markers of a metastatic phenotype activation	[49]
		LNCaP (in PEG-gel)	Osteoblasts induce paracrine effects that can promote osteomimicry of tumor cells and modulate expression of androgen-responsive genes in LNCaP cells	[50]

better nutrition of cells enables the production of larger spheroids [52]. Studies of the production of heterospheroids, which are co-cultures of tumor and normal cells, are of particular interest. For example, stirring BRs have been used to prepare hetero spheroids consisting of head and neck squamous carcinoma cells and peripheral blood mononuclear cells [53]. Study of the pharmacological effects of catumaxomab in spheroid models adequately reflects the properties of the micrometastases of these tumors. Spheroids derived from human brain tumor cells (glioma and astrocytoma) were seeded on porous scaffolds made from polylactic acid and cultured in multiwell plates on an orbital shaker under hypoxic conditions [54]. The cells in a 3D-medium were found to acquire increased resistance to pro-apoptotic factors. Also, the hypoxia enhanced the resistance to cytotoxic drugs in monolayer cultures, although the molecular anti-apoptotic mechanisms in 2D- and 3D-cultures were different. A hybrid system "plate-on-a-shaker" was used to detect activation of angiogenic signaling pathways regulation and a decrease in the sensitivity of cells to chemotherapeutic anticancer drugs in 3D cultures placed in a complex scaffold made from poly(lactic-co-glycolic acid) and Matrigel [55]. The use of a stirring BR in an experiment with osteosarcoma cells provided compelling evidence of the advantages of complex TETMs on solid scaffolds (fibrous-bed) over tumor cell cultures on micro-carriers, apparently due to the reduced shear stress effects [56]. TECs composed of osteosarcoma cells and a porous fibrous scaffold proved stable in a culture for more than 1 month. On day 4, the cells stopped dividing but the fraction of apoptotic cells did not exceed 15%.

Stirring BRs are also used for DCL and RCL. DCL of small tissue fragments is usually processed in these BRs. In our recent paper [39], we demonstrated that systems like "flask-on-a-shaker" were feasible for the DCL of whole organs of laboratory animals. The efficiency of stirring BRs for the colonization and feeding of the cells was higher than that of static BRs, but it was still insufficient for TECs due to their relatively large sizes. In addition, the culture medium insufficiently penetrated into the construct; therefore, the cells distributed mainly over the scaffold periphery because of the diffusion limitations. The possibility of increasing the convection component with an increase of the rotation speed of the spinner or the culture vessel itself was limited due to shear-stress-induced tissue damage (> 15 dyne/cm^2) [51, 57].

The potential future applications of stirring BRs in TTE were not fully implemented, although these systems had a number of important advantages. These include adjustability of the culture volume, support of various TE models, availability of hydrodynamic computational models [34], accessibility for a sampling culture medium, and TEC state monitoring.

ROTARY BIOREACTORS

Rotary BRs (rotating-wall bioreactors, NASA bioreactors; RWV; RCCSTM; HARV; STLV; RWPV), originally developed by NASA for experiments in space, are normally cylindrical containers with rotating walls completely filled with a culture medium. Horizontal (RWV) [58] and vertical (HARV) [59] rotary BRs revolve around a horizontal or vertical central axis, respectively, while oxygen is delivered through a stationary axial membrane or a similar membrane at the cylinder base. In these reactors, the culture medium is replaced manually via service openings. In a rotary BR with perfusion (RWPV or STLV), the culture medium circulates in a closed loop and is continuously replaced, which enables automatic maintenance of an optimal level of oxygen, pH, and temperature for many months. A RWPV consists of two cylinders, with the inner cylinder (which also serves as a gas exchange membrane) also able to rotate. The culture medium and the TECs are located in an annular space between the cylinders [60].

In rotary BRs, the scaffolds or TECs move freely in a culture chamber completely filled with the culture medium. The rotation speed of the cylinders (about 15–40 rpm) is adjusted to ensure balance between the gravity and the hydrodynamic resistance acting on the scaffolds/TECs, whereby the scaffolds/TECs are in a permanent state of free fall. The dynamic laminar (instead of turbulent, as in stirring BRs) flow of the culture medium can effectively bypass the diffusion limitations for the delivery of nutrients and removal of waste. Rotary systems provide a more uniform distribution of the cells compared to that in a static culture and better metabolism compared to that in stirring BRs. To compensate for the mass of growing tissue, the rotation speed is gradually increased in order to balance the gravity force and to ensure a suspended state of the TECs.

By using a rotary BR, differences in the effect of the 2D and 3D microenvironments on the expression of hepatocellular carcinoma genes were detected. HepG2 cells in multicellular spheroids, which reached a diameter of 100 μm in 72 h and 1 mm during a prolonged cultivation, exhibited increased expression of metabolic and synthetic genes, whereas activation of the genes encoding proteins of the extracellular matrix and cytoskeleton, as well as cell adhesion molecules, was observed in 2D. In addition, the liver cancer cells in spheroids retained a high activity of cytochrome P450 and produced albumin for a long time, whereas these features quickly degraded in a monolayer culture [61].

Interesting results were obtained in co-cultures of tumor and normal cells using a rotary BR. For example, colon adenocarcinoma cells (HT29 and HT29KM lines) formed spheroids in a monoculture, while in the presence of normal fibroblasts these cells competed with them for an attachment substrate and their growth was initially restricted. Then, the tumor cells began to divide actively and form bulky tissue masses of up to 1.5 cm in size that structurally resembled healthy intestinal crypts. A cell layer directly contacting the microcarrier's surface was formed by young mesenchymal cells. Necrotic changes in these 3D cultures were almost absent [62]. Co-culture of breast cancer cells (UACC-893, BT-20, and MDA-MB-453 lines) with fibroblasts in a rotary BR led to the formation of histoids, which are multicellular spheroids composed of fibroblasts with invading cancer cells [63]. Especially large heterospheroids (up to 1 cm in diameter) were produced in a HARV rotary BR from immortalized normal human skin keratinocytes HaCaT and cells of different melanoma lines (murine B16-F10 and human SKMEL-5) [64]. This biomimetic 3D model of melanoma was exploited to demonstrate a technique of cell transfection with plasmids encoding GFP and IL-15 which provided high reproducibility of the results of gene delivery. A rotary BR was also used to study the interaction among prostate cancer cells, osteocytes, and bone tissue cells in a 3D model [65].

An experiment on the production of spheroids from prostate cancer cells of different maturity using a rotary BR revealed significant differences in the spheroid spatial organization and proliferative activity, depending on the proportion of cell types [66]. According to the authors, this indicates the influence of cell differentiation on the spheroid packing density and, consequently, the efficiency of mass transfer between a cell aggregate and a culture medium.

Potential limitations in the use of rotary BRs are associated with the generation of laminar fluid flow shear stress (in the range of 0.5–2 dynes/cm^2) [67]. The efficiency and safety of rotary BRs can be improved by combining them with reactors operating on other principles [68].

PERFUSION (FLOW) BIOREACTORS

Perfusion bioreactors allow one to perform the most accurate reproduction of the mass transfer processes in a living organism. A typical perfusion BR consists of a pump and an incubation chamber connected by flexible tubes to form a system with an open or closed loop. The pump creates a slight overpressure, providing a permanent liquid medium flow through tissues and scaffolds. Perfusion BRs can be used both for DCL and for RCL. In perfusion DCL, solutions of detergents or other substances promoting deattachment, destruction, and removal of the cells are delivered through natural blood vessels connected to a perfusion contour.

During RCL, a cell suspension is transported through the decellularized vascular conduits of the treated tissue/TEC or through other voids in the scaffold. This provides a more homogeneous distribution of cells in the matrix and better transport of liquids compared to those in stirring and rotary devices [69–72]. As a result, long-term growth and maintenance of larger TECs becomes possible [72, 73]. The survival rate of the cells seeded on the scaffolds perfused by means of these BRs is substantially higher compared to that in a static culture or stirring BR [74]. Regulation of the medium flow rate in BRs enables to control both the shear stress associated with the fluid flow and the local distribution of oxygen across a TEC [75]. At the same time, although perfusion BRs definitely can improve the control of mass transfer, in comparison with the other systems, the problem of non-uniform delivery of the necessary substances has still not been completely resolved. This is especially notable for scaffolds with pores of widely varying sizes and also for tissues with a non-uniform growth rate, which results in insufficient nutrition of some areas and excessive delivery to others [70].

Perfusion BRs are of critical importance to whole-organ tissue engineering – a formation of whole-organ TECs [30, 76] using sequential DCL and RCL processes. These reactors are subjected to particularly strict requirements to ensure control over the parameters of the culture medium/cell suspension flow, sterility, temperature, and the possibility to monitor organ treatment or organ TEC formation [76–80].

Perfusion BRs are actively used for the reconstruction of normal tissues and organs, but their application in the development of TETMs has just started. For example, a colorectal cancer model was demostrated using a commercially available perfusion BR [81]. HT-29 line cells were conventionally cultured in a monolayer or seeded on collagen sponges and maintained in a static 3D culture (as the control samples) or in a perfusion BR. Additional control was provided with tumor xenografts implanted in athymic mice using the same cell line. The cells in the perfusion culture were characterized by a much higher proliferation rate and a much more uniform distribution compared to those in the static bulky culture. The produced TECs were morphologically and phenotypically similar to the tumors developed from the implanted cells. A strong correlation between perfusion 3D cultures and tumor xenografts was also observed in the expression profiles of the genes that regulate apoptosis and the response to hypoxia. Comparison of the effects of 5-fluorouracil and ABT-199, an inhibitor of the anti-apoptotic gene

BCL-2, showed a fundamental difference in the cellular responses both in 2D and in 3D TECs. The same paper described a preparation of TECs on collagen scaffolds using cells of colorectal (SW480 and DLD-1), prostate (PC-3), non-small cell lung (A549), and breast (BT-474) cancers.

A sophisticated TE model of schwannoma (neurofibrosarcoma) was developed by German researchers using a specially designed BR [82]. An isolated porcine intestinal fragment was subjected to alternating perfusion DCL through the mesenteric artery and lumen of the intestine and to the immersion DCL on a shaking platform. The resulting matrix was sterilized by gamma radiation. Then, the DCL matrix of the intestine fragment was cut along the long axis and the resulting membrane was stretched between two metal rings and placed in a perfusion BR chamber. The scaffold was seeded with the primary skin fibroblasts and linear tumor cells of schwannoma S462 (on the apical surface) and microvascular endothelial cells (on the basolateral surface of the intestinal segment). The TEC was incubated in a perfusion culture at a permanent or pulsed flow of the culture medium for about 2 weeks.

Recently, the technologies of perfusion DCL and RCL of organs were used to generate a TE lung cancer model [83]. Different types of linear lung cancer cells (A549, H460, H1299) were seeded by perfusion of the cell suspension on a decellularized whole-organ scaffold prepared from mouse lungs. Then, the whole-organ TECs were perfused with an oxygenated culture medium and maintained *ex vivo* for up to 2 weeks. The authors demonstrated the formation of macroscopic tumor nodes with their own vasculature, the development of typical cell-cell and cell-matrix interactions, and the formation of a typical structure and dynamics of tumor growth similar to those of real fragments of human lung cancer tissue.

HOLLOW-FIBER BIOREACTORS

A hollow-fiber BR is a closed vessel filled with a cell suspension in a culture medium or a scaffold or (potentially) a complex TEC permeable to the medium. This scaffold/TEC contains a bundle of mutually parallel semi-permeable hollow fibers mimicking blood vessels and providing delivery of the nutrients to the cells and the removal of waste. The main advantage of these BRs is their ability to deliver nutrients in the depth of the growing engineered tissues. Hollow-fiber BRs are successfully used in experiments on the culture of very sensitive cell types with a high metabolic demand, such as hepatocytes [84], the attempts to use a similar system to create 3D constructs have not been successful. It turned out that the high densities of the cellular suspensions or solid matrices significantly limit mass transfer and oxygen diffusion in this system. This leads to the death of cells at longer distances from the hollow fibers and to the loss of the structural homogeneity of tissue [85]. To solve this problem, a coaxial BR design based on hollow fibers inserted into each other and forming independent compartments for growing cells was proposed [84, 86]. The coaxial design significantly improved mass transfer. However, another serious drawback of these systems is the inability to avoid damage to the formed tissue during extraction of a TEC from the BR for further use.

Hollow-fiber BRs were used in experimental oncology to expand cell mass, obtain the specific cell products, and monitor the tumor tissue metabolism. For example, T-cells isolated from an inflammatory infiltrate of ovarian cancer biopsies were cultured in a hollow-fiber BR [87]. A commercially available BR was used to produce spheroids from breast cancer cells (MCF-7) and to study the effects of δ-tocopherol concentrations [88]. As a result, a technique based on contrast-enhanced MRI was proposed for monitoring the cell density and oxygen concentration in spheroids [88]. Also, MRI and a hollow-fiber BR were used to determine the mechanism of changes in the apparent diffusion coefficient of water (an important diagnostic sign) in a ischemic brain tissue that was simulated using a 3D culture of rat glioma cells [89, 90].

MICROFLUIDIC BIOREACTORS

Microfluidic platforms (microfluidic chips, microfluidic bioreactors) can be considered as a special kind of perfusion BR scheme for the development and study of biological objects consisting of about 10^2–10^3 cells. By using a multistep technology, a glass substrate is covered with a layer of biocompatible silicone material (polydimethylsiloxane) arranged as microchannels and microcontainers. The advantage of this polymer over polystyrene (conventionally used in cell culture) is a combination of high permeability to oxygen and to other gases with almost complete impermeability to water [91]. In microfluidic BRs, mass transfer to cells that grow in hydrogel-filled microwells or directly on the chip elements occurs by perfusion of a culture medium through the microchannels.

The variability and adaptability of microfluidic systems can help solve very different problems and contribute to the active development of organ(s)-on-a-chip and lab-on-a-chip technologies. An important advantage of these BRs is precise control over the parameters of culture medium flows and optical imaging *in situ* in real time [92]. Microfluidic systems are used to study the cell responses to the action of signaling molecules, as well as the effects of metabolic and physical gradients and the role of interstitial fluid flows in

the metabolism of tissues, including tumors. They also are very useful for precise quantification of the permeability of TECs to drugs and nanoparticles [28, 93–96]. Furthermore, these systems can be used to simulate the kinetics of cell populations, progression of tumors, angiogenesis, invasion and other stages of metastasis [97–103].

BIOREACTORS WITH A DIRECT IMPACT ON A SCAFFOLD/TEC

BRs also can provide a direct controlled action of various physical factors on a scaffold or TEC. For example, a TE object can be exposed to mechanical forces, electrical impulses, or different types of radiation. The most progress has been achieved in the bioreactor technologies associated with biomechanical research.

COMPRESSION BIOREACTORS

Compression BRs are widely used in tissue engineering, especially in the preparation of cartilage structures. These BRs consist of an engine, a system providing linear displacement, and a control mechanism. The stress is usually transmitted to a cell-seeded scaffold through flat rollers [104] and exerts a specific mechanical effect on cells and an increased fluid flow through a TEC. In TTE, compression BRs can be used, in particular, to simulate the mechanisms of bone metastatic niche formation. Currently, almost nothing is known about the response of metastatic cancer tissue to mechanical stress [105]. A study on 3D cultures of breast cancer (MDA-MB-231) and glioblastoma (U87, HGL21) cells in a compression BR demonstrated increased expression of the genes responsible for enzymatic lysis of extracellular matrix proteins, as well as adhesion and migration in response to increased static compression. This corresponded to an increase in the metastatic potential [106].

STRAIN BIOREACTORS

BRs with controlled mechanical strain (strain bioreactors) are structurally similar to compression BRs and differ only in the way the stress to a sample is transmitted. Scaffolds/TECs are secured in such a way that the straining force can be applied to them. For example, they are placed on a rubber membrane that is then deformed [107]. In TTE, a model was recently proposed to study the role of mechanical tension of the extracellular matrix in the induction of an invasion of 3D organoids produced by culturing transformed epithelial cells in collagen gels of different concentrations. A gel incorporating cell aggregates and covalently bound to a polydimethylsiloxane base was placed in a microfluidic chip with a device for straining that part of the culture chamber. A positive correlation between the invasiveness of the cells and the gel stiffness was found; a concentration effect associated with changes in the mean pore size was revealed [108].

HYDROSTATIC PRESSURE BIOREACTORS

In hydrostatic pressure BRs, mechanical compression on the scaffolds or TECs is implemented through a periodic reduction in the culture chamber volume, while the culture medium volume remains constant [109]. These BRs are not extensively used in TTE; however, this direction seems promising only for the modeling of one of the most important physiological features of solid tumors such as the increased interstitial pressure [36].

BIOREACTORS FOR ELECTRICAL STIMULATION OF CELLS AND TISSUES

BRs with electrical stimulation are usually used for the modeling of excitable tissues. According to our data, there has been no mass use of such BRs for the development of cancer 3D models, but there are a few reports on the culturing of tumor cells in hydrogel under weak electric field conditions (at an electric field intensity of 1.1 V/cm and a variable frequency of 150 kHz and 200 kHz) in a hybrid microfluidic chip-based device [110]. The authors observed changes in the morphological characteristics of lung (A549) and breast (MDA-MB-231) linear cancer cells, a decreased proliferation rate of both tumor cell lines, and signs of a reduced metastatic potential of A549 cells. At the same time, the electrical stimuli did not alter the activity of normal human endothelial cells (HUVEC).

COMBINED BIOREACTORS

Numerous BR combinations have been developed that allow one to grow tissues under laboratory conditions that are set maximally close to natural ones. Usually, these combinations include adding various methods of mechanical impact on a tissue to a standard perfusion or rotary BR. For example, combining a strain BR, hydrostatic pressure BR, or compression BR with a perfusion or rotary BR combines the advantages of improved mass transfer by perfusion or rotation and mechanical stimulation of TECs.

CONCLUSION

Bioreactor technologies adapted for biomimetic models of malignant tumors were discussed and critically analyzed in this paper.

Static systems and stirring BRs designed on the basis of conventional culture vessels placed on shakers remain the most commonly used in tumor tissue engineering (TTE). At the same time, a number of important developments are emerging. In particular, microfluidic sys-

tems representing a promising TTE platform. It becomes clear now that the best mimicking of the key properties of cancers calls for a multimodal biological reactor (BR), which represents a hybrid of the existing modalities addressed in this review. A new-generation BR is envisaged as a multipurpose device with automated control over tissue engineering processes and augmented standardization of cultivation conditions. This BR could provide one of the gateways to the elucidation of cancer biology. At the same time, BR-based experiments open conceptual possibilities for testing prospective generations of anticancer agents based on recombinant molecules [111–118], multifunctional nanostructures [119–126], as well as the evaluation of new cell and tissue engineering technologies [25, 39–41, 127, 128] for the reprogramming of cancer cells [129, 130]. ●

The authors are grateful to A.Z. Vinarov, D.V. Butnaru, A.V. Luzin, and A.S. Titov (Sechenov First Moscow State Medical University) for their support in organizing and conducting surgical experiments; E.V. Peteresen and I.A. Kornienko (Moscow Institute of Physics and Technology) for their assistance in the development of the technology of acellular organ specific scaffolds. We would also like to apologize to those researchers whose original work we could not quote directly rather than through the review publication, given the limited volume of this article.

This work was supported by the Russian Science Foundation (grant № 14-24-00106). The author (A.G.) is also grateful to the Macquarie University for providing her an iMQRes research scholarship.

REFERENCES

1. Hickman J.A., Graeser R., de Hoogt R., Vidic S., Brito C., Gutekunst M., van der Kuip H., Consortium I.P. // Biotechnol. J. 2014. V. 9. № 9. P. 1115–1128.
2. Breslin S., O'Driscoll L. // Drug Discov. Today. 2013. V. 18. № 5–6. P. 240–249.
3. Aggarwal B.B., Danda D., Gupta S., Gehlot P. // Biochem. Pharmacol. 2009. V. 78. № 9. P. 1083–1094.
4. Yamada K.M., Cukierman E. // Cell. 2007. V. 130. № 4. P. 601–610.
5. Hutmacher D.W., Loessner D., Rizzi S., Kaplan D.L., Mooney D.J., Clements J.A. // Trends Biotechnol. 2010. V. 28. № 3. P. 125–133.
6. Nosenko M.A., Drutskaya M.S., Moysenovich M.M., Nedospasov S.A. // Acta Naturae. 2016. V. 8. № 2. P. 51–66.
7. Hanahan D., Weinberg R.A. // Cell. 2011. V. 144. № 5. P. 646–674.
8. Ricci C., Moroni L., Danti S. // OA Tissue Engineering. 2013. V. 1. № 1. P. 4. http://dx.doi.org/10.13172/2052-9643-1-1-607.
9. Baker B.M., Chen C.S. // J. Cell Sci. 2012. V. 125. Pt 13. P. 3015–3024.
10. Tentler J.J., Tan A.C., Weekes C.D., Jimeno A., Leong S., Pitts T.M., Arcaroli J.J., Messersmith W.A., Eckhardt S.G. // Nat. Rev. Clin. Oncol. 2012. V. 9. № 6. P. 338–350.
11. Siolas D., Hannon G.J. // Cancer Res. 2013. V. 73. № 17. P. 5315–5319.
12. Weinberg R.A. The biology of cancer. N.Y.: Garland Sci., 2007. 960 p.
13. Hutmacher D.W., Horch R.E., Loessner D., Rizzi S., Sieh S., Reichert J.C., Clements J.A., Beier J.P., Arkudas A., Bleiziffer O. // J. Cell. Mol. Med. 2009. V. 13. № 8a. P. 1417–1427.
14. Burdett E., Kasper F.K., Mikos A.G., Ludwig J.A. // Tissue Eng. Part B Rev. 2010. V. 16. № 3. P. 351–359.
15. Ghajar C.M., Bissell M.J. // Tissue Eng. Part A. 2010. V. 16. № 7. P. 2153–2156.
16. Fong E.L., Santoro M., Farach-Carson M.C., Kasper F.K., Mikos A.G. // Curr. Opin. Chem. Eng. 2014. V. 3. P. 112–117.
17. Gill B.J., West J.L. // J. Biomech. 2014. V. 47. № 9. P. 1969–1978.
18. Xu W., Hu X., Pan W. // Technol. Cancer Res. Treat. 2014. V. 13. № 2. P. 149–159.
19. Seib F.P., Berry J.E., Shiozawa Y., Taichman R.S., Kaplan D.L. // Biomaterials. 2015. V. 51. P. 313–319.
20. Langer R., Vacanti J.P. // Science. 1993. V. 260. № 5110. P. 920–926.
21. Martin I., Wendt D., Heberer M. // Trends Biotechnol. 2004. V. 22. № 2. P. 80–86.
22. Pietras K., Ostman A. // Exp. Cell Res. 2010. V. 316. № 8. P. 1324–1331.
23. Alemany-Ribes M., Semino C.E. // Adv. Drug Deliv. Rev. 2014. V. 79–80. P. 40–49.
24. Nelson C.M., Bissell M.J. // Annu. Rev. Cell Dev. Biol. 2006. V. 22. P. 287–309.
25. Shekhter A.B., Guller A.E., Istranov L.P., Istranova E.V., Butnaru D.V., Vinarov A.Z., Zakharkina O.L., Kurkov A.V., Kantimerov D.F., Antonov E.N., et al. // Archiv Pathol. 2015. V. 77. № 6. P. 29–38.
26. Crapo P.M., Gilbert T.W., Badylak S.F. // Biomaterials. 2011. V. 32. № 12. P. 3233–3243.
27. Gilbert T.W., Sellaro T.L., Badylak S.F. // Biomaterials. 2006. V. 27. № 19. P. 3675–3683.
28. Martin Y., Vermette P. // Biomaterials. 2005. V. 26. № 35. P. 7481–7503.
29. Fu R.H., Wang Y.C., Liu S.P., Shih T.R., Lin H.L., Chen Y.M., Sung J.H., Lu C.H., Wei J.R., Wang Z.W., et al. // Cell Transplant. 2014. V. 23. № 4. P. 621–630.
30. Badylak S.F., Taylor D., Uygun K. // Annu. Rev. Biomed. Eng. 2011. V. 13. P. 27–53.
31. Mehta G., Hsiao A.Y., Ingram M., Luker G.D., Takayama S. // J. Control Release. 2012. V. 164. № 2. P. 192–204.
32. Korossis S., Bolland F., Kearney J., Fisher J., Ingham E. // Topics Tissue Eng. 2005. V. 2. № 8. P. 1–23.
33. Wendt D., Riboldi S.A., Cioffi M., Martin I. // Adv. Biochem. Eng. Biotechnol. 2009. V. 112. P. 1–27.
34. Hansmann J., Groeber F., Kahlig A., Kleinhans C., Walles H. // Biotechnol. J. 2013. V. 8. № 3. P. 298–307.
35. Vaupel P., Kallinowski F., Okunieff P. // Cancer Res. 1989. V. 49. № 23. P. 6449–6465.
36. Jain R.K. // Cancer Res. 1987. V. 47. № 12. P. 3039–3051.
37. Stylianopoulos T., Martin J.D., Chauhan V.P., Jain S.R., Diop-Frimpong B., Bardeesy N., Smith B.L., Ferrone C.R., Hornicek F.J., Boucher Y., et al. // Proc. Natl. Acad. Sci. USA. 2012. V. 109. № 38. P. 15101–15108.
38. Salehi-Nik N., Amoabediny G., Pouran B., Tabesh H., Shokrgozar M.A., Haghighipour N., Khatibi N., Anisi F.,

Mottaghy K., Zandieh-Doulabi B. // Biomed. Res. Int. 2013. V. 2013. P. 762132.
39. Guller A., Trusova I., Petersen E., Shekhter A., Kurkov A., Qian Y., Zvyagin A. // SPIE Micro+Nano Materials, Devices, and Systems. 2015. V. 96684G. doi: 10.1117/12.2202473.
40. Glybochko P.V., Alyaev Yu.G., Nikolenko V.N., Shekhter A.B., Vinarov A.Z., Istranov L.P., Istranova E.V., Aboyants R.K., Lyundup A.V., Guller A.E., et al. // Urologiya. 2014. V. 6. P. 41–46.
41. Glybochko P.V., Alyaev Yu.G., Shekhter A.B., Vinarov A.Z., Istranov L.P, Istranova E.V., Aboyants R.K., Lyundup A.V., Guller A.E., et al. // Urologiya. 2015. V. 6. P. 5–13.
42. Dunne L.W., Huang Z., Meng W., Fan X., Zhang N., Zhang Q., An Z. // Biomaterials. 2014. V. 35. № 18. P. 4940–4949.
43. Talukdar S., Mandal M., Hutmacher D.W., Russell P.J., Soekmadji C., Kundu S.C. // Biomaterials. 2011. V. 32. № 8. P. 2149–2159.
44. Serebriiskii I., Castello-Cros R., Lamb A., Golemis E.A., Cukierman E. // Matrix Biol. 2008. V. 27. № 6. P. 573–585.
45. Lü W.-D., Zhang L., Wu C.-L., Liu Z.-G., Lei G.-Y., Liu J., Gao W., Hu Y.-R. // PLoS One. 2014. V. 9. № 7. P. e103672.
46. Stratmann A.T., Fecher D., Wangorsch G., Göttlich C., Walles T., Walles H., Dandekar T., Dandekar G., Nietzer S.L. // Mol. Oncol. 2014. V. 8. № 2. P. 351–365.
47. Fong E.L., Lamhamedi-Cherradi S.E., Burdett E., Ramamoorthy V., Lazar A.J., Kasper F.K., Farach-Carson M.C., Vishwamitra D., Demicco E.G., Menegaz B.A., et al. // Proc. Natl. Acad. Sci. USA. 2013. V. 110. № 16. P. 6500–6505.
48. Villasante A., Marturano-Kruik A., Vunjak-Novakovic G. // Biomaterials. 2014. V. 35. № 22. P. 5785–5794.
49. Sieh S., Lubik A.A., Clements J.A., Nelson C.C., Hutmacher D.W. // Organogenesis. 2010. V. 6. № 3. P. 181–188.
50. Sieh S., Taubenberger A.V., Lehman M.L., Clements J.A., Nelson C.C., Hutmacher D.W. // Bone. 2014. V. 63. P. 121–131.
51. Tandon N., Marolt D., Cimetta E., Vunjak-Novakovic G. // Biotechnol. Adv. 2013. V. 31. № 7. P. 1020–1031.
52. Sutherland R.M., Sordat B., Bamat J., Gabbert H., Bourrat B., Mueller-Klieser W. // Cancer Res. 1986. V. 46. № 10. P. 5320–5329.
53. Hirschhaeuser F., Leidig T., Rodday B., Lindemann C., Mueller-Klieser W. // J. Biomol. Screen. 2009. V. 14. № 8. P. 980–990.
54. Kim J.W., Ho W.J., Wu B.M. // Anticancer Res. 2011. V. 31. № 10. P. 3237–3245.
55. Fischbach C., Chen R., Matsumoto T., Schmelzle T., Brugge J.S., Polverini P.J., Mooney D.J. // Nat. Methods. 2007. V. 4. № 10. P. 855–860.
56. Chen C., Chen K., Yang S.T. // Biotechnol. Prog. 2003. V. 19. № 5. P. 1574–1582.
57. Sucosky P., Osorio D.F., Brown J.B., Neitzel G.P. // Biotechnol. Bioeng. 2004. V. 85. № 1. P. 34–46.
58. Freshney R.I. Culture of Animal Cells: A Manual of Basic Technique and Specialized Applications, 4th Ed. Hoboken, N.J.: John Wiley & Sons, 2000. 624 p.
59. Portner R., Nagel-Heyer S., Goepfert C., Adamietz P., Meenen N.M. // J. Biosci. Bioeng. 2005. V. 100. № 3. P. 235–245.
60. Schwarz R.P., Wolf D.A., Trinh T.T. Horizontally rotated cell culture system with a coaxial tubular oxygenator. Patent USA US5026650 A, Grant. 1991.
61. Chang T.T., Hughes-Fulford M. // Tissue Eng. Part A. 2009. V. 15. № 3. P. 559–567.
62. Goodwin T.J., Jessup J.M., Wolf D.A. // In Vitro Cell Dev Biol. 1992. V. 28A. № 1. P. 47–60.
63. Kaur P., Ward B., Saha B., Young L., Groshen S., Techy G., Lu Y., Atkinson R., Taylor C. R., Ingram M., et al. // J. Histochem. Cytochem. 2011. V. 59. № 12. P. 1087–1100.
64. Marrero B., Heller R. // Biomaterials. 2012. V. 33. № 10. P. 3036–3046.
65. Wang R., Xu J., Juliette L., Castilleja A., Love J., Sung S.Y., Zhau H.E., Goodwin T.J., Chung L.W. // Semin. Cancer Biol. 2005. V. 15. № 5. P. 353–364.
66. Song H., David O., Clejan S., Giordano C.L., Pappas-Lebeau H., Xu L., O'Connor K.C. // Tissue Eng. 2004. V. 10. № 7–8. P. 1266–1276.
67. Spatz J.M., Wein M.N., Gooi J.H., Qu Y., Garr J.L., Liu S., Barry K.J., Uda Y., Lai F., Dedic C., et al. // J. Biol. Chem. 2015. V. 290. № 27. P. 16744–16758.
68. Song K., Yan X., Zhang Y., Song F., Lim M., Fang M., Shi F., Wang L., Liu T. // Bioprocess Biosyst. Eng. 2015. V. 38. № 8. P. 1527–1540.
69. Goldstein A.S., Juarez T.M., Helmke C.D., Gustin M.C., Mikos A.G. // Biomaterials. 2001. V. 22. № 11. P. 1279–1288.
70. Yu X., Botchwey E.A., Levine E.M., Pollack S.R., Laurencin C.T. // Proc. Natl. Acad. Sci. USA. 2004. V. 101. № 31. P. 11203–11208.
71. Nasredinov A.S., Anisimov S.V., Vavilov V.N., Puzanov M.V., Kurapeev D.I. // Tsitologiya. 2014. V. 56. № 12. P. 926–932.
72. Wendt D., Stroebel S., Jakob M., John G., Martin I. // Biorheology. 2006. V. 43. № 3–4. P. 481–488.
73. Wendt D., Marsano A., Jakob M., Heberer M., Martin I. // Biotechnol. Bioeng. 2003. V. 84. № 2. P. 205–214.
74. Barash Y., Dvir T., Tandeitnik P., Ruvinov E., Guterman H., Cohen S. // Tissue Eng. Part C Methods. 2010. V. 16. № 6. P. 1417–1426.
75. Cioffi M., Kuffer J., Strobel S., Dubini G., Martin I., Wendt D. // J. Biomech. 2008. V. 41. № 14. P. 2918–2925.
76. Ott H.C., Matthiesen T.S., Goh S.K., Black L.D., Kren S.M., Netoff T.I., Taylor D.A. // Nat. Medicine. 2008. V. 14. № 2. P. 213–221.
77. Soto-Gutierrez A., Zhang L., Medberry C., Fukumitsu K., Faulk D., Jiang H., Reing J., Gramignoli R., Komori J., Ross M., et al. // Tissue Eng. Part C Methods. 2011. V. 17. № 6. P. 677–686.
78. Bijonowski B.M., Miller W.M., Wertheim J.A. // Curr. Opin. Chem. Eng. 2013. V. 2. № 1. P. 32–40.
79. Price A.P., England K.A., Matson A.M., Blazar B.R., Panoskaltsis-Mortari A. // Tissue Eng Part A. 2010. V. 16. № 8. P. 2581–2591.
80. Panoskaltsis-Mortari A. // Curr. Transplant. Rep. 2015. V. 2. № 1. P. 90–97.
81. Hirt C., Papadimitropoulos A., Muraro M.G., Mele V., Panopoulos E., Cremonesi E., Ivanek R., Schultz-Thater E., Droeser R.A., Mengus C., et al. // Biomaterials. 2015. V. 62. P. 138–146.
82. Moll C., Reboredo J., Schwarz T., Appelt A., Schurlein S., Walles H., Nietzer S. // J. Vis. Exp. 2013. № 78. doi: 10.3791/50460.
83. Mishra D.K., Thrall M.J., Baird B.N., Ott H.C., Blackmon S.H., Kurie J.M., Kim M.P. // Ann. Thorac. Surg. 2012. V. 93. № 4. P. 1075–1081.
84. Jasmund I., Bader A. // Adv. Biochem. Eng. Biotechnol. 2002. V. 74. P. 99–109.
85. Birla R. // Introduction to Tissue Engineering. Hoboken, N.J.: John Wiley & Sons, Inc., 2014. P. 193–236.
86. Piret J.M., Cooney C.L. // Biotechnol. Bioeng. 1991. V. 37. № 1. P. 80–92.
87. Freedman R.S., Ioannides C.G., Mathioudakis G., Platsoucas C.D. // Am. J. Obstet. Gynecol. 1992. V. 167. № 5. P. 1470–1478.

88. Bartusik D., Tomanek B., Siluk D., Kaliszan R., Fallone G. // Anal. Biochem. 2009. V. 387. № 2. P. 315–317.
89. Trouard T.P., Harkins K.D., Divijak J.L., Gillies R.J., Galons J.P. // Magn. Reson. Med. 2008. V. 60. № 2. P. 258–264.
90. Harkins K.D., Galons J.P., Divijak J.L., Trouard T.P. // Magn. Reson. Med. 2011. V. 66. № 3. P. 859–867.
91. Berthier E., Young E.W., Beebe D. // Lab. Chip. 2012. V. 12. № 7. P. 1224–1237.
92. Lee J., Kohl N., Shanbhang S., Parekkadan B. // Technology (Singap World Sci). 2015. V. 3. № 4. P. 179–188.
93. Ng C.P., Pun S.H. // Biotechnol. Bioeng. 2008. V. 99. № 6. P. 1490–1501.
94. Elliott N.T., Yuan F. // Biotechnol. Bioeng. 2012. V. 109. № 5. P. 1326–1335.
95. Albanese A., Lam A.K., Sykes E.A., Rocheleau J.V., Chan W.C.W. // Nature Comm. 2013. T. 4. P. 2718. doi: 10.1038/ncomms3718.
96. Buchanan C., Rylander M.N. // Biotechnol. Bioeng. 2013. V. 110. № 8. P. 2063–2072.
97. Ma H., Xu H., Qin J. // Biomicrofluidics. 2013. V. 7. № 1. P. 11501. doi: 10.1063/1.4774070.
98. Song H.H., Park K.M., Gerecht S. // Adv. Drug. Deliv. Rev. 2014. V. 79–80. P. 19–29. doi: 10.1016/j.addr.2014.06.002.
99. Kim S., Lee H., Chung M., Jeon N.L., Kim S., Lee H., Chung M., Jeon N.L. // Lab. Chip. 2013. V. 13. № 8. P. 1489–1500.
100. Sung K.E., Beebe D.J. // Adv. Drug Deliv. Rev. 2014. V. 79–80. P. 68–78. doi: 10.1016/j.addr.2014.07.002.
101. Haessler U., Teo J.C., Foretay D., Renaud P., Swartz M.A. // Integr. Biol. (Camb.). 2012. V. 4. № 4. P. 401–409.
102. Bersini S., Jeon J.S., Dubini G., Arrigoni C., Chung S., Charest J.L., Moretti M., Kamm R. D. // Biomaterials. 2014. V. 35. № 8. P. 2454–2461.
103. Huang C.P., Lu J., Seon H., Lee A.P., Flanagan L.A., Kim H.Y., Putnam A.J., Jeon N.L. // Lab. Chip. 2009. V. 9. № 12. P. 1740–1748.
104. Thorpe S.D., Buckley C.T., Vinardell T., O'Brien F.J., Campbell V.A., Kelly D.J. // Biochem. Biophys. Res. Comm. 2008. V. 377. № 2. P. 458–462.
105. Lynch M.E., Brooks D., Mohanan S., Lee M.J., Polamraju P., Dent K., Bonassar L.J., van der Meulen M.C., Fischbach C. // J. Bone Miner. Res. 2013. V. 28. № 11. P. 2357–2367.
106. Demou Z.N. // Ann. Biomed. Eng. 2010. V. 38. № 11. P. 3509–3520.
107. Garvin J., Qi J., Maloney M., Banes A.J. // Tissue Eng. 2003. T. 9. № 5. P. 967–979.
108. Cassereau L., Miroshnikova Y.A., Ou G., Lakins J., Weaver V.M. // J. Biotechnol. 2015. V. 193. P. 66–69.
109. Darling E.M., Athanasiou K.A. // Ann. Biomed. Eng. 2003. V. 31. № 9. P. 1114–1124.
110. Pavesi A., Adriani G., Tay A., Warkiani M. E., Yeap W. H., Wong S. C., Kamm R. D. // Sci Rep. 2016. V. 6. P. 26584. DOI: 10.1038/srep26584.
111. Deyev S.M., Lebedenko E.N., Petrovskaya L.E., Dolgikh D.A., Gabibov A.G., Kirpichnikov M.P. // Russ. Chem. Rev. 2015. V. 84. № 1. P. 1–26.
112. Mironova K.E., Proshkina G.M., Ryabova A.V., Stremovskiy O.A., Lukyanov S.A., Petrov R.V., Deyev S.M. // Theranostics. 2013. V. 3. № 11. P. 831–840.
113. Deyev S.M., Lebedenko E.N. // Acta Naturae. 2009. V. 1. № 1. P. 32–50.
114. Stepanov A.V., Belogurov A.A., Jr., Ponomarenko N.A., Stremovskiy O.A., Kozlov L.V., Bichucher A.M., Dmitriev S.E., Smirnov I.V., Shamborant O.G., Balabashin D.S., et al. // PLoS One. 2011. V. 6. № 6. P. e20991.
115. Zdobnova T., Sokolova E., Stremovskiy O., Karpenko D., Telford W., Turchin I., Balalaeva I., Deyev S. // Oncotarget. 2015. V. 6. № 31. P. 30919–30928.
116. Proshkina G.M., Shilova O.N., Ryabova A.V., Stremovskiy O.A., Deyev S.M. // Biochimie. 2015. V. 118. P. 116–122.
117. Lebedenko E., Balandin T., Edelweiss E., Georgiev O., Moiseeva E., Petrov R., Deyev S. // Dokl. Biochem. Biophys. 2007. V. 414. № 1. P. 120–123.
118. Glinka E.M., Edelweiss E.F., Sapozhnikov A.M., Deyev S.M. // Gene. 2006. V. 366. № 1. P. 97–103.
119. Liang L., Care A., Zhang R., Lu Y., Packer N.H., Sunna A., Qian Y., Zvyagin A.V. // ACS Appl. Mater. Interfaces. 2016. V. 8. № 19. P. 11945–11953.
120. Razali W.A., Sreenivasan V.K., Goldys E.M., Zvyagin A.V. // Langmuir. 2014. V. 30. № 50. P. 15091–15101.
121. Nikitin M.P., Shipunova V.O., Deyev S.M., Nikitin P.I. // Nat. Nanotechnol. 2014. V. 9. № 9. P. 716–722.
122. Grebenik E.A., Nadort A., Generalova A.N., Nechaev A.V., Sreenivasan V.K., Khaydukov E.V., Semchishen V.A., Popov A.P., Sokolov V.I., Akhmanov A.S., et al. // J. Biomed. Opt. 2013. V. 18. № 7. P. 76004. doi: 10.1117/1.JBO.18.7.076004.
123. Generalova A.N., Sizova S.V., Zdobnova T.A., Zarifullina M.M., Artemyev M.V., Baranov A.V., Oleinikov V.A., Zubov V.P., Deyev S.M. // Nanomedicine (Lond.). 2011. V. 6. № 2. P. 195–209.
124. Generalova A.N., Kochneva I.K., Khaydukov E.V., Semchishen V.A., Guller A.E., Nechaev A.V., Shekhter A.B., Zubov V.P., Zvyagin A.V., Deyev S.M. // Nanoscale. 2015. V. 7. № 5. P. 1709–1717.
125. Balalaeva I.V., Zdobnova T.A., Krutova I.V., Brilkina A.A., Lebedenko E.N., Deyev S.M. // J. Biophotonics. 2012. V. 5. № 11–12. P. 860–867.
126. Nadort A., Liang L., Grebenik E., Guller A., Lu Y., Qian Y., Goldys E., Zvyagin A. // SPIE Micro+Nano Materials, Devices, and Systems. 2015. V. 96683Y. doi:10.1117/12.2202449.
127. Petersen E.V., Trusova I.A., Zurina I.M., Kosheleva N.V., Gorkun A.A., Guller A.E., Pulin A.A., Saburina I.N., Repin V.S., Shekhter A.B. // Plastic Surgery and Cosmetology. 2012. V.3. P. 353–364.
128. Shekhter A.B., Rudenko T.G., Istranov L.P., Guller A.E., Borodulin R.R., Vanin A.F. // Eur. J. Pharm. Sci. 2015. V. 78. P. 8–18.
129. Trosko J.E. // Anat. Rec. (Hoboken). 2014. V. 297. № 1. P. 161–173.
130. Ingber D.E. // Semin. Cancer Biol. 2008. V. 18. № 5. P. 356–364.

Hyaluronic Acid in Vascular and Immune Homeostasis during Normal Pregnancy and Preeclampsia

M. M. Ziganshina[1*], S. V. Pavlovich[1], N. V. Bovin[2], G. T. Sukhikh[1]
[1]Federal State Budget Institution "Research Center for Obstetrics, Gynecology and Perinatology" of the Ministry of Healthcare of the Russian Federation, Oparin str. 4, 117997, Russia, Moscow
[2]Shemyakin-Ovchinnikov Institute of Bioorganic Chemistry, Russian Academy of Sciences, Miklukho-Maklaya str. 16/10, 117997, Russia, Moscow
*E-mail: mmz@mail.ru
Received December 10, 2015; in final form, April 26, 2016

ABSTRACT **Preeclampsia (PE) is a multisystem pathologic state that clinically manifests itself after the 20th week of pregnancy. It is characterized by high maternal and perinatal morbidity and mortality. According to modern concepts, the impairment of trophoblast invasion into maternal spiral arteries, leading to the development of ischemia in placenta, is considered to be the major pathogenetic factor of PE development. Ischemic lesions initiate the development of a systemic inflammatory response (SIR) and endothelial dysfunction, which is the main cause of the multiple organ failure in PE. Some data has appear indicating the importance of a glycans-forming endothelial glycocalyx and extracellular matrix (ECM) for placenta morphogenesis, as well as their role in the regulation of vascular permeability and vascular tone in hypertension disorders and, in particular, PE. Since intact glycocalyx and ECM are considered to be the major factors that maintain the physiological vascular tone and adequate intercellular interactions, their value in PE pathogenesis is underestimated. This review is focused on hyaluronic acid (HA) as the key glycan providing the organization and stabilization of the ECM and glycocalyx, its distribution in tissues in the case of presence or absence of placental pathology, as well as on the regulatory function of hyaluronic acids of various molecular weights in different physiological and pathophysiological processes. The summarized data will provide a better understanding of the PE pathogenesis, with the main focus on glycopathology.**
KEYWORDS **preeclampsia, hyaluronic acid, glycocalyx, intercellular matrix, glycopathology**
ABBREVIATIONS **PE – preeclampsia; ECM – extracellular matrix; HA – hyaluronic acid; SIR – systemic inflammatory response; FPS – fetoplacental system; HMW-HA – high molecular weight hyaluronic acid; LMW-HA – low molecular weight hyaluronic acid; O-HA – oligomeric hyaluronic acid; MMP-1 – matrix metalloproteinase-1; MMP-2 – matrix metalloproteinase-2**

INTRODUCTION

The main factor that determines the successful course of a pregnancy is the formation of a complete fetoplacental system (FPS) that meets the needs of the developing fetus and regulates the hemodynamic load on the mother's cardiovascular system. The key moment of FPS formation is the transformation of the uterine spiral arteries into uteroplacental vessels that are formed as a result of trophoblast invasion into the wall of the mother's spiral arteries. The invasion is accompanied by tissue remodeling, wherein lysis of the elastic muscle components of radial arteries, their replacement by a fibrinoid material, and the formation of broad spiral cavities adapted to an increasing blood flow take place [1, 2]. Adequate FPS formation is achieved thanks to the ability of trophoblast to differentiate into cell populations that exhibit various invasive and locomotor features. The cells of the invasive (extravillous) trophoblast acquire the properties of pseudoneoplastic cells with a high proliferative, invasive and migratory potential, as well as specific expression of surface markers during placentation, which enables FPS formation and promotes the phenomenon of nonrejection [3]. Pathogenesis of PE is associated with impaired cell proliferation and invasion of trophoblast into uterine spiral arteries, morphologically manifested in the development of a small cell invasion and the absence of spiral artery remodeling, which is especially pronounced in early PE (clinical signs appears prior to 34 weeks gestation) [4, 5]. Another factor which is pathogenetically important both for early and late PE (manifestation of clinical symptoms after 34 weeks of gestation) is an ex-

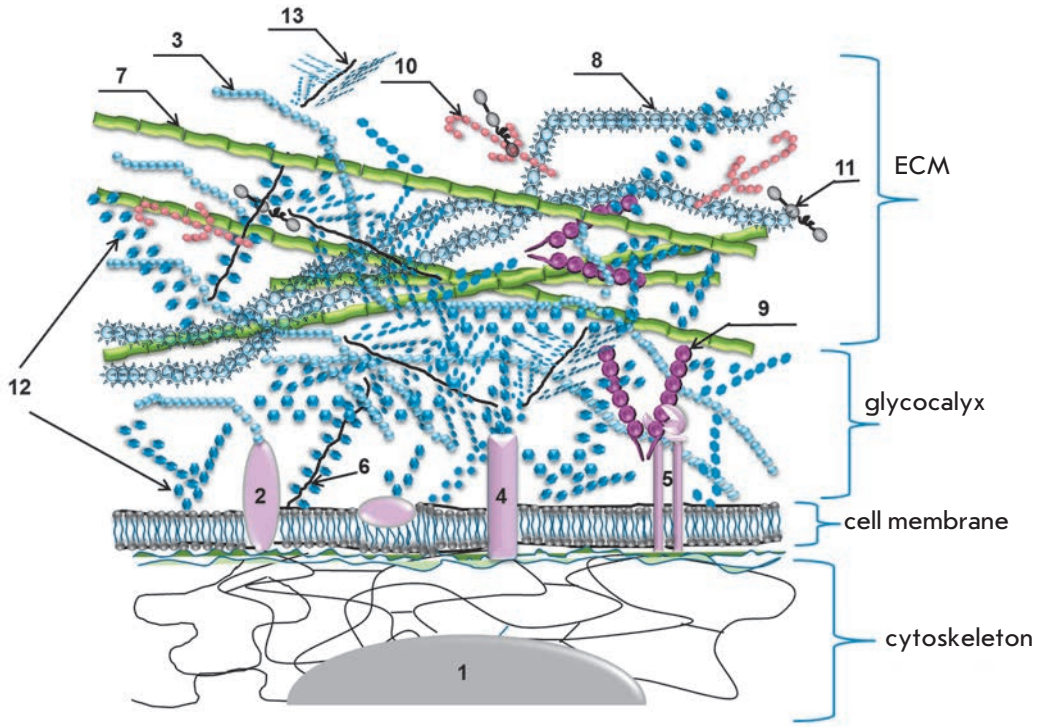

Fig. 1. Composition and structure oftheextracellular matrix (ECM*)
1 – nucleus; 2 – hyaladherin; 3 – hyaluronic acid (HA); 4 – glycoprotein; 5 – integrin; 6 – syndecan; 7 – elastane; 8 – collagen; 9 – fibronectin; 10 – laminin; 11 – nidogen; 12 – gel-forming polysaccharides; 13 – small soluble proteoglycan. *ECM – extracellular complex of glycosaminoglycans and (glyco)-proteins both bound to the membrane and integrated into the complex due to carbohydrate-protein and carbohydrate-carbohydrate interactions. ECM has a cellular construction, forms a framework for the cells and the basis for the connective tissue. ECM provides mechanical support for the cells in tissue, intercellular contacts, and cell transport and migration. The border between ECM and glycocalyx for cells in tissue is rather conventinal. The carbohydrate layer adjacent to plasmolemma is considered to be a glycocalyx, whereas the glycosaminoglycan layer located above and including protein molecules is ECM. ECM impairment leads to disorders in tissue organization with changes in organ function.

cessive systemic inflammatory response (SIR), which results in endothelial activation/dysfunction and immune maladaptation [6]. The clinical manifestations of PE (high blood pressure and proteinuria) are due to these factors.

Cell invasion is accomplished through adhesive interactions between cells and ECM and is regulated by endogenous and exogenous factors: gene expression and biomodulators. Trophoblast cells, on the one hand, share some properties with tumor cells, and, on the other hand, their invasion is strictly determined by the terms of gestation and a tolerable depth of invasion. The ability to invade is determined both by the cell properties themselves (their differentiation, synthesis of proteolytic enzymes and cytokines) and the matrix properties: its structure (forms honeycomb frame for the cells) and regulatory function (contains biologically active molecules and functional groups).

The histology and functional properties of ECM are determined by the severity of SIR; its degree is considered as one of the leading factors that determine, on the one hand, the possibility of tissue remodeling (physiological remodeling in normal pregnancy and pathological remodeling in pathologic pregnancy or oncotransformation) and, on the other, the possibility of intercellular communication (exposed glycans and glycoconjugates change under the impact of inflammatory mediators, which manifests itself in the change in cell and organ functions).

Information on the role of ECM and the molecules that form it in PE pathogenesis is rather limited. The current review describes hyaluronic acid (HA), its function as part of the ECM and endothelial glycocalyx, the distribution in placental structures, and the regulatory effect of HA in the processes of invasion and inflammation.

FUNCTIONS OF HYALURONIC ACID AS PART OF THE EXTRACELLULAR MATRIX

The extracellular matrix is formed by fibrillar and structural proteins, proteoglycans, and glycosaminoglycans (*Fig. 1*). One of the main components of ECM

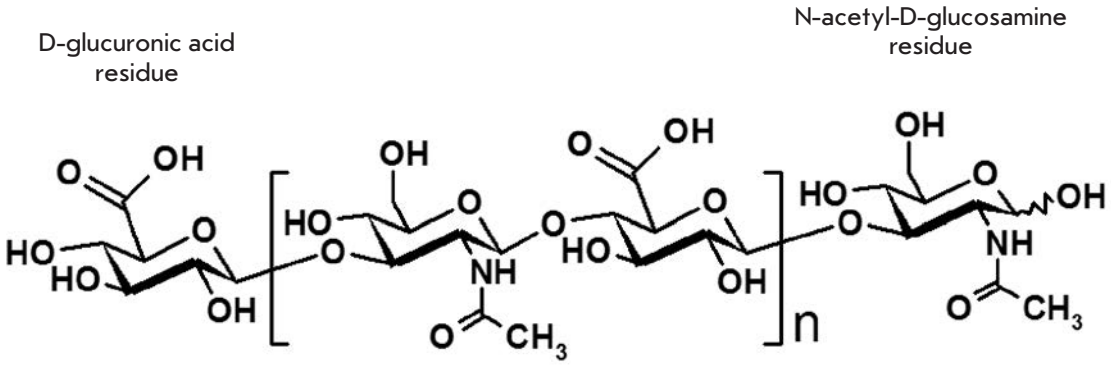

Fig. 2. Chemical structure of hyaluronic acid

Table 1. The biological roles of HA of different molecular weights

HA fractions		
HMW-HA (high molecular weight HA) molecular mass >500 kDa, average mass 10^6–10^7 Da (~2000–25000 disaccharide units) [9, 73, 74]	**LMW-HA (low molecular weight HA)** molecular mass <500 kDa (~1000 disaccharide units or less) [74, 80]	**O-HA (oligomeric HA)** molecular mass 0.75—10 kDa (2 - 20 disaccharide units) [75]
Formation and stabilization of the structure of ECM and glycocalyx; immunologically inert [75, 76]; binds to cell receptors, prevents immune recognition; immunosuppressive action [77]; induction of Foxp3 expression, increases the number of inducible regulatory T-cells [77, 78]; preserves the barrier function of glomerular endothelial barrier [7] HA synthesis suppresses [74]	Functions as a danger signal (danger-associated molecular patterns) [9]; increases permeability of lymphatic capillaries [81], increases vascular permeability [7].	Can regulate various processes both positively and negatively; inhibit endogenous production of hyaluronan [9]
Anti-inflammatory action, inhibition of phagocytosis [77]	Anti-inflammatory action [33]	
Anti-angiogenic effect, prevents transendothelial migration [77]	Pro-angiogenic effect, stimulation of endothelial cell proliferation, adhesion and formation of capillaries [33]	Stimulation/inhibition of angiogenesis, adhesion [9, 80]
Synthesis of immunosuppressive cytokines [77]	Synthesis of pro-inflammatory cytokines [33]	
Stimulates proliferation and inhibits apoptosis of decidual stromal cells in early pregnancy [79]	Stimulates apoptosis of decidual stromal cells in early pregnancy [79]	Stimulation of tumor cell proliferation/apoptosis [74]
Prevents adhesion and invasion of tumor cells [77]	Stimulation of tumor cell invasion and migration, stimulation of extravillous trophoblast cell invasion [82]	

and endothelial glycocalyx of the cell is HA, which belongs to linear, non-sulfated glycosaminoglycans. The structural unit of HA is a repeating disaccharide consisting of D-glucuronic acid and N-acetyl-D-glucosamine (*Fig. 2*): i.e., HA is a regular polysaccharide. HA is presented *in vivo* mainly in high-molecular (native) form (HMW-HA), while low-molecular-weight HA (LMW-HA) is dominated under SIR (*Table 1*) [7]. HA is found in intracellular compartments and also on the cell surface, in the pericellular and extracellular matrix. Significant amounts of HA are contained in tissues with a high proliferative potential and invasive ability [8]. The stabilization of the dimensional structure of ECM is achieved thanks to non-covalent interactions between HA and small proteoglycans, resulting in the formation of a three-dimensional lattice structure surrounding the cells [9], which acts as a filter and the first line of intercellular interactions: adhesion, migration, and subsequent functional activity. The organizing and stabilizing effect of HA, as part of the lattice structure, plays the key role in the physiology of ECM and glycocalyx [10, 11].

FUNCTIONS OF HYALURONIC ACID AS PART OF THE GLYCOCALYX

The endothelial surface layer (ESL) is located on the luminal surface of endothelium and comprises glycocalyx, a complex structure consisting of proteoglycans

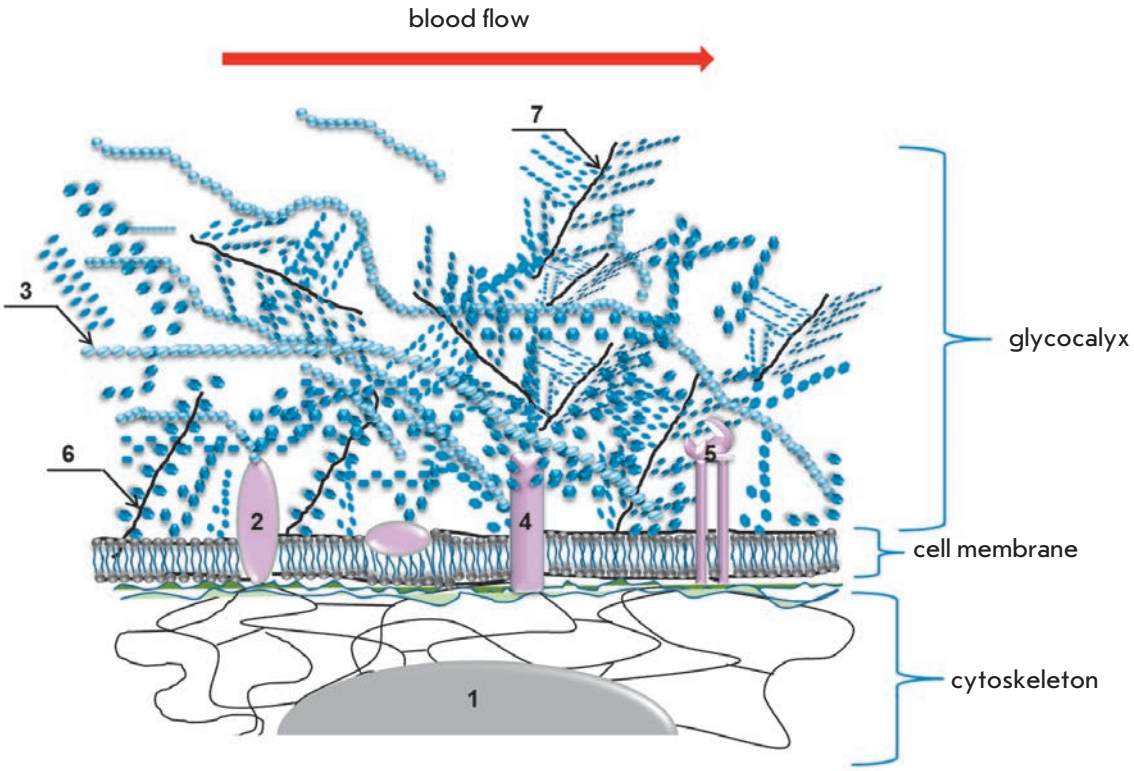

Fig. 3. Composition and structure of endothelial glycocalyx* 1 – nucleus; 2 – hyaladherin; 3 – hyaluronic acid (HA); 4 – glycoprotein; 5 – integrin; 6 – syndecan; 7 – small soluble proteoglycan.
*Glycocalyx is the external cell envelope associated with the plasma membrane that presents a polysaccharide gel. Glycocalyx executes receptor and protective functions, as well as the function of external signal transducer in circulating cells and cells in contact with biological fluids. Glycocalyx shedding leads to changes of cells receptors.

and glycoproteins that are anchored to the membrane and contain many sialic acid and sulfate residues forming the overall negative charge of the surface of endothelial cells (*Fig. 3*). HA is present in the layer which is in constant dynamic interaction with blood and is formed by secreted and circulating molecules (HA, albumin and α1-acid glycoprotein) [12, 13]. Endothelial glycocalyx is thought to play a key role in the regulation of the physiological and pathophysiological processes taking place in the bloodstream: permeability, tone, coagulation, and the inflammation process [14]. Since the loss of control over the regulation of these processes is significant for PE pathogenesis, one can assume that endothelial glycocalyx can be a central target for the application of the factors that destabilize homeostasis (such as placental ischemia and excessive SIR in PE), thereby leading to clinical manifestations of various severities.

According to current concepts, the regulation of the vascular tone involves cell mechanics and the regulation of mechanical stimuli. Mechanical stimuli are external factors that cause the process of mechanotransduction, i.e., changes in gene expression and cell phenotype due to shear stress (tangential blood flow pressure on endothelial cells), vascular tension, hydrostatic blood pressure, and intercellular contacts [15]. The mechanics of endothelial cells include the properties of individual subcellular compartments (glycocalyx, cell membrane, cytoplasm and nucleus), which are regulated by both mechanical stimuli and biologically active molecules [16, 17]. The structures defining the mechanics of endothelial cells are interconnected: the cell cortex located under the plasma membrane is formed by bundles of microfilaments which are in contact with stress fibrils, microtubules, and intermediate filaments; all the components are organized in a network that fills the cytoplasm and is connected to the nucleus (*Fig. 3*) [18]. Therefore, the function of glycocalyx is to convert the biomechanical and biochemical signals going from the bloodstream into endothelial cells [15], and the effectiveness of its performance is determined by the integrity of the endothelial surface layer.

The physiological effect of shear stress on the intact glycocalyx triggers a response from mechanosensitive cellular components, ion channels, caveolae, integrins,

cadherins, growth factor receptors, cytoskeletal structures; and activates the signaling pathways involved in mechanotransduction [19, 20]. The main result of this action is a constant production of endothelial NO synthase (eNO synthase), which regulates the formation of endogenous nitric oxide, a factor that supports the physiological values of the blood pressure in the circulatory system. Under high shear stress values on endothelial cells, which appear with an increasing volume and speed of the blood flow in pregnancy, the functioning glycocalyx provides enhanced eNO synthase activation, thus compensating for the hemodynamic load [21]. Destabilization and desquamation of glycocalyx critically alters the endothelial cell response to mechanical stimuli. Shedding of the glycocalyx layer reduces the mechanosensitivity of endothelial cells, which has a vasoconstrictor effect under increasing blood flow conditions (*Fig. 4*).

A reduction of the glycocalyx layer also manifests itself in a disturbed barrier function of the endothelium, since glycocalyx plays a key role in the regulation of vascular permeability. It has been demonstrated that HA (HMW-HA) binds and inhibits the activity of extracellular serine protease, the enzyme that causes degradation of ECM and glycocalyx [7]. HA fragments of various molecular weights interact with different types of CD44 receptor. HMW-HA negatively regulates vascular permeability by activating the signaling pathways associated with the formation of the cortical layer of actin microfilaments and formation of dense intercellular contacts. LMW-HA positively regulates vascular permeability by inducing the activation of the protease-activated receptor (PAR) of endothelial cells, thus promoting the formation of actin stress fibrils and the disruption of intercellular contacts [22, 23].

An intact glycocalyx is associated with adequate functioning of the glomerular barrier [12]. Enzymatic elimination of HA from the endothelium of glomerular capillaries in mice results in a disturbance of the glomerular filter permeability and the appearance of protein in urine [24].

The integrity of the glycocalyx of tumor cells is assumed to determine their invasive properties, since the shear stress of the interstitial fluid affects cell mechanoreceptors [25, 26]. Experimental modeling of the invasive properties of tumor cells (human kidney carcinoma: cell lines SN12L1 and SN12C with high and low metastatic potential, respectively) in a three-dimensional model of interstitial fluid flow has demonstrated that the impact of hyaluronidase and heparinase on cells blocks the expression of MMP-1 and MMP-2 caused by the pressure of the interstitial fluid, thus reducing the invasive potential of the cells. Glycocalyx degradation, particularly degradation of HA, blocks tumor invasion and negatively regulates the invasive and migratory properties of the cells [27].

Destabilization and shedding of glycocalyx components are promoted by hyperglycemia, endotoxemia, septic shock, oxidized low-density lipoproteins, cytokines, natriuretic peptide, abnormal shear stress, ischemia-reperfusion, as well as by the development of SIR, accompanying, at a certain degree of severity, any pathological process [28, 29]. Shedding/destabilization of the glycocalyx layer due to targeted elimination of HA by hyaluronidases deteriorates the mechanosensitive response of endothelial cells [30].

BIOSYNTHESIS AND METABOLISM OF HYALURONIC ACID

Under physiological conditions, the processes of biosynthesis and degradation of glycocalyx are balanced [28, 31] and are substantiated by the activity of hyaluronan synthases (HAS1, HAS2, HAS3) and hyaluronidases (Hyal1, Hyal2, PH-20/SPAM1) [9, 32–34]. The genes *Hyal3, Hyal4,* and *Hyalp1* share a high degree of homology with the genes encoding hyaluronidases Hyal1, Hyal2, and PH-20, but Hyal3 and Hyal4 do not exhibit hyaluronidase activity, while *Hyalp1* is a pseudogene [35].

Hyaluronan synthases and disruption of hyaluronic acid synthesis

HAS1 synthesizes HA of a wide range of molecular weights (500–2000 kDa). HAS2 synthesizes high molecular weight HA (HMW-HA), while HAS3 is responsible for the production of low-molecular HA (LMW-HA) with a molecular mass less than 500 kDa [33, 34]. The enzymatic activity of HAS2 and HAS3 is higher than that of HAS1 [36].

The activity of human genes of hyaluronan synthases is regulated by the genes *HAS1, HAS2* and *HAS3* localized on different autosomes. Studies of mice embryogenesis have shown that *HAS1* is expressed during gastrulation and early neurulation, *HAS2* is expressed in heart and skeletal structures during the early embryonic period, while *HAS3* expression is limited to teeth germs and hair follicles [34, 37, 38], suggesting different regulatory elements for transcription control. Disrupted expression of *HAS2* during embryogenesis leads to the embryo's death; *HAS2*-null embryos were found to exhibit the defects of endocardial cushion, yolk sac and vasculogenesis, as well as disruption of epithelial-mesenchymal transformation [34, 35, 39, 40]. Deletion of *HAS2* leads to disrupted formation of embryo limbs, including joints [35]. Mice $HAS1^{-/-}$ demonstrate chronic inflammation of joints with damaged articular cartilage; wherein the HA content in the ECM of knockout mice and

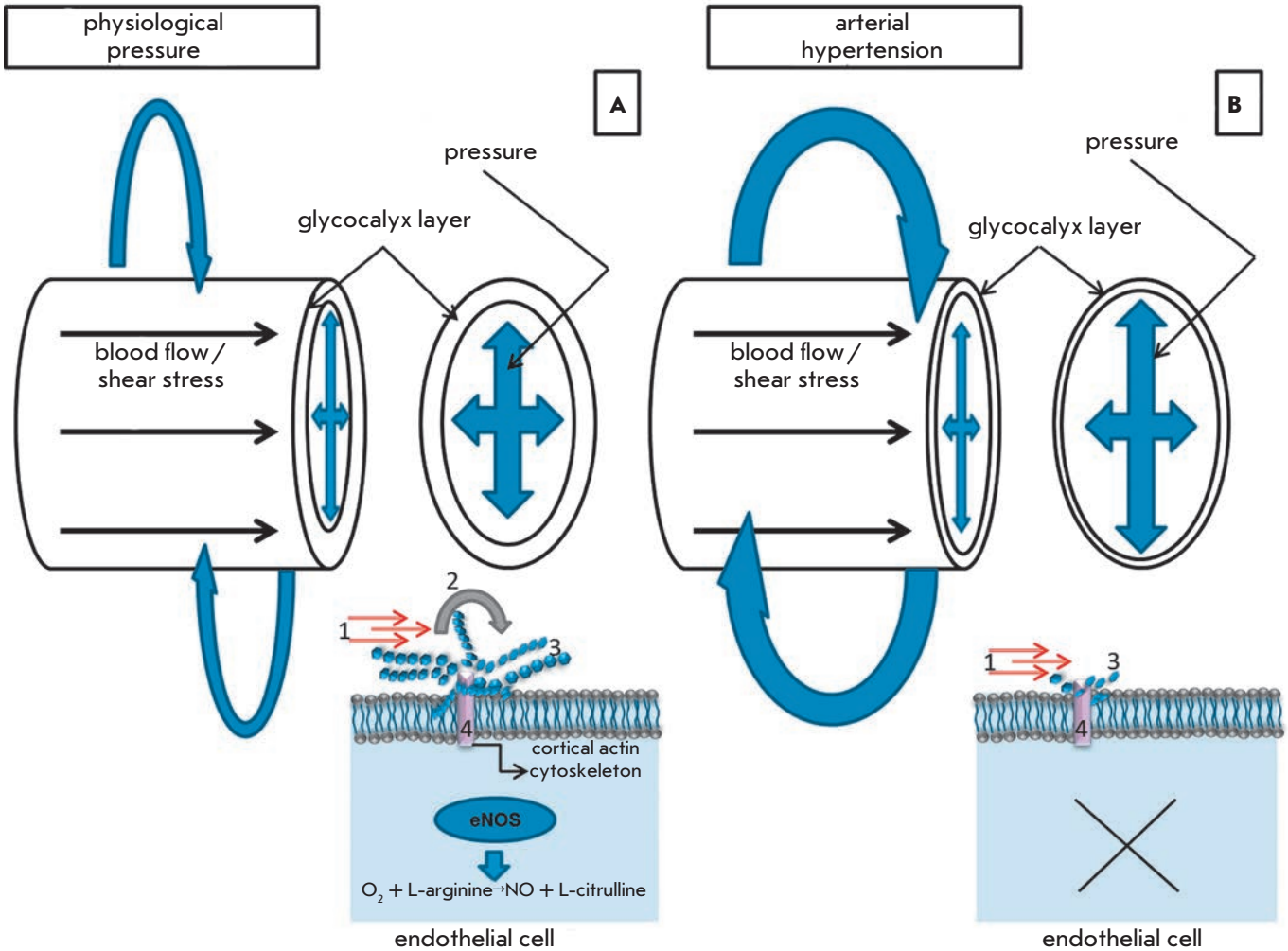

Fig. 4. The role of glycocalyx in the regulation of the vascular tone. *A* – Regulation of the vascular tone in physiological conditions. Physiological (intact) glycocalyx is a conductor-transducer of mechanical signals to endotheliocyte: shear stress (1), acting in parallel with the vascular wall (induces internal tension, which is realized as an activation of the signal systems that regulate the vascular tone and permeability); and blood pressure, acting perpendicularly to the vascular wall and imposing a stretching action on all vessel and ECM components. Glycocalyx assumes the mechanical load in the form of local torque (2), disperses it and transduces the signal through proteoglycan chains (3) to the so-called core (anchored in the membrane) proteins (4). The main result is eNOS activation, synthesis of endogenous NO, which causes a vasodilatory effect and the reorganization of the actin cytoskeleton providing the adaptation of intercellular contacts to the mechanical load [15, 21, 134].
B – Regulation of the vascular tone in arterial hypertension. Shedding or total absence of a glycocalyx layer during pathophysiological processes leads to the mechanical load directly on the apical cell membrane and suppression of endogenous NO production by endothelial cells. As a result, the blood pressure is increased and intercellular contacts are impaired [21, 134].

wild-type mice is identical. *HAS1* is believed to be important for HA metabolism in inflammation [41]. Mice with a knockout of the *HAS1* or *HAS3* gene are viable and fertile. Increased inflammation is observed in double knockout of these genes in mice on a background of a regeneration of skin wound [36]. However, there are reports on brain size reduction and epilepsy seizures in mice with knockout of the *HAS* gene, with epilepsy being most pronounced in mice with knockout of the *HAS3* gene [42]. In mammals, all *HAS* genes are expressed in both embryonic and adult tissues, with the expression of *HAS3* being more pronounced in adult tissues [35]. All *HAS* genes, especially *HAS2*, are overexpressed in carcinogenesis [37].

Increased activity of hyaluronan synthases in Shar-Pei dogs phenotypically manifests itself in skin thick-

ening, skin folds, increased HA skin level, and abnormally high HA blood concentration [43]. The content of HA is also increased in the skin of naked mole rat (*Heterocephalus glaber*), a small burrowing rodent of the African mole-rat family characterized by high life expectancy (about 30 years) and resistance to carcinogenesis. Fibroblasts isolated from the skin of a naked mole rat produce high amounts of HMW-HA. They also demonstrate the presence of an unusual form of HAS2 (Ser to Asn substitution in two conservative parts of the polypeptide chain) and a reduced level of the Hyal2 enzyme responsible for HA degradation [35]. These mammals serve as models for the study of resistance to diseases and aging, in particular (www.naked-mole-rat.org). Noteworthy, a high degree of inbreeding is specific to Shar-Pei dogs and naked mole rats.

In general, the abnormalities of HA biosynthesis have been mostly studied *in vitro* in cells and in animal models. Very limited data suggest a relation between *HAS2* mutation and the development of a ventricular septal defect in Chinese children [44]. It has also been shown that *HAS2* is overexpressed in Down's syndrome [45].

Hyaluronidases and disruption of hyaluronic acid metabolism

Expression of *Hyal1*, *Hyal2*, and *Hyal3* has been detected in somatic tissues; the expression of *SPAM1* – in testicular tissue (SP-20 is required for fertilization); and *Hyal4* – in skeletal muscles and placenta [35, 44, 46–48]. HA degradation can occur both intracellularly in the lysosome and extracellularly. Hyal1 is active in lysosomes, hyaluronidase PH–20 functions on the cell surface as a GPI-anchored protein, and Hyal2 cleaves HA both in lysosomes and the extracellular space [34]. Each hyaluronidase is characterized by a specific localization in different cells and a specific pH range within which they remain active; this leads to the generation of hyaluronic acids of different molecular weights [7].

Rare cases of mucopolysaccharidosis type IX, a genetic disorder of the connective tissue, are associated with the lack of enzymes that degrade HA. Mucopolysaccharidosis type IX biochemically manifests itself in the accumulation of HA in tissues, mainly in the lysosomes of macrophages and rarely in the lysosomes of fibroblasts, as well as by an increase in HA concentration in blood in the absence of the enzyme [35, 49, 50]. Mucopolysaccharidosis type IX clinically manifests itself in craniofacial dysmorphism, growth retardation, swelling, tenderness of the joints and juvenile idiopathic arthritis. The neurological status and intellectual development of patients remains within the normal range [35]. A genetic analysis has revealed homozygosity and mutations in the *Hyal1* gene, but the lack of pronounced anomalies indicates compensation ofthe Hyal1 function by other hyaluronidases [35].

No generalized accumulation of HA has been found in the tissues of *Hyal1*$^{-}$/$^{-}$ mice, although they demonstrate pronounced degenerative changes in the knee joint cartilage. Mice *Hyal2*$^{-}$/$^{-}$ demonstrate skeletal abnormalities, hemolytic anemia, thrombotic microangiopathy, severe cardio-pulmonary failure, and high mortality [51–53]. The consequences of ischemia/reperfusion injury to the kidney in knockout mice proved more severe than in wild-type mice. Knockout mice demonstrated a high level of HA accumulated in the injured kidney, a more pronounced inflammation, and kidney fibrosis [54].

The relation between the expression of HA metabolism genes and the invasive properties of cells, as well as the progression of the disease, remains the most well studied to date. *HAS1* expression has been revealed at low levels in most normal cells, while *HAS2* expression is detected predominantly during embryogenesis. The expression of *HAS1* significantly increases in carcinogenesis, while *HAS2* and *HAS3* are overexpressed in aggressive forms of cancer [37]. Cells expressing *HAS2* exhibit the most aggressive properties. The study of the expression of hyaluronan synthases/hyaluronidases in a panel of human cell lines of breast cancer with different invasive properties has showed that highly invasive cells predominantly express isoforms of HAS2 and Hyal2, while less invasive cells produce HAS3 and Hyal3 [55]. Transfection of human breast adenocarcinoma MCF-7 cells, immortalized human HaCat keratinocytes, and a primary culture of mouse epidermal keratinocytes with *HAS3*-containing conjugates demonstrated that increased HA synthesis causes the formation of numerous microvillus-like cell surface protrusions, which form the sites for cell contact, attachment, and migration [56]. In this regard, expression of the erbB2 (HER-2/neu) receptor in the area of microvilli seems important [57]. It is assumed that HA can play a key role in tumor invasion, since there is a direct relation between overexpression of HA and erbB2, which promotes the activation of the erbB2-dependent signaling pathway and indicates the importance of HA for the manifestation of an invasive cell phenotype [56].

REGULATORY EFFECT OF HA POLYMERS OF VARIOUS SIZES

HA can be found in small quantities in the blood of healthy individuals [28, 31], whereas high levels of HA are found in patients with a chronic kidney disease [58], cardiovascular diseases [59], pulmonary hypertension [60], liver cirrhosis [61, 62], and cancer [63]. There is also evidence of an elevated level of HA in the blood in the PE [64, 65] and HELLP syndromes [66]. The level of an-

Table 2. Characterization of human hyaladherins

Receptor	Expression	Function	Source
CD44 – adhesion molecule, main receptor of HA. Isoforms: CD44s (standard), CD44e (epithelial), CD44v (variable)	Leukocytes, erythrocytes, some epithelial cells, brain cells, decidual stromal cells, Kaschenko-Hofbauer cells, placental tissue; overexpression in tumor cells	Mediates the processes of lymphocyte activation, adhesion, migration (lymphocyte rolling and homing), embryonic development, angiogenesis, placental tissue remodeling in placentogenesis, as well as invasion and growth of tumor cells, inflammation. Stabilization of ECM and glycocalyx, biodegradation of HA, induction of CD4+CD25+ T-regulatory cells	[9, 33, 37, 79, 80, 98–102]
LYVE-1 – partial homolog of CD44, main receptor of HA in lymphatic system	Cells of the lymphatic vessels, endothelium of lymphatic capillaries, sinusoidal endothelial cells of liver and spleen, cerebral cortex neurons, macrophages in normal and tumor tissues, placental macrophages, fetal placental endothelium, syncytiotrophoblast	Regulation of cell motility, biodegradation of HA in the lymphatic system. Regulation of HA metabolism in the fetoplacental system. Regulation of dendritic cell adhesion and migration, lymphangiogenesis. Functional activity is regulated by sialylation/desialylation of the O-glycan chains of the receptor	[11, 103–106]
CD168-RHAMM – extra/intracellular HA-binding receptor	Intracellular localization (cytoplasm, cytoskeleton, mitochondria, nucleus); extracellular localization (transported to the cell surface where it is able to bind to HA and activate different signaling cascades); low expression in normal cells	Cell signaling, migration, locomotion and adhesion, angiogenesis. Regulation of mitosis. Localization on the cell surface correlates with tumor progression	[9, 80, 101, 107–109]
ICAM-1 – intercellular adhesion molecule	Inducible expression on endothelium, monocytes, T- and B-lymphocytes, keratinocytes; expressed in inflammation and tumor processes	Regulation of inflammatory process. Mediates leukocyte or tumor cell contact with endothelium for subsequent transendothelial migration or invasion; contact cell interaction in the immune response. Inhibition of type II collagen catabolism	[110–114]
TSG-6 (TNF-stimulated gene 6)	Inducible secreted peptide expressed by many cells upon activation	Anti-inflammatory action: inhibits neutrophil migration in a model of acute inflammation. Serves as a cofactor for other hyaladherins	[33, 29, 72, 115]
TLR2 and TLR4 (Toll-like receptors)	Dendritic cells, monocytes, lymphocytes	Regulation (stimulation/inhibition) of inflammatory process upon receptor binding	[77, 116]
STABILIN-1/2 (scavenger receptors)	Constitutively expressed by macrophages (M2), sinusoidal endothelial cells; expression is increased in inflammation and carcinogenesis	Biodegradation of HA	[11, 117, 118]
CD38 (bifunctional enzyme – combines activities of adenosine diphosphate-ribosyl cyclase (ADP) and cyclic ADP-ribose hydrolase (cADPR)	During ontogenesis on hematopoietic cells at various stages of differentiation; immune cells, vascular smooth muscle and bronchial cells	An enzyme regulating the concentration of intracellular calcium and energetic homeostasis of the cell	[119–122]
HABP1/C1QBP – HA-binding protein-1/ protein binding c1q subcomonent	Peripheral blood cells, macrophages, monocytic dendritic cells	Cell signaling, regulation of complement system activation	[33, 123]
SHAP – serum HA-associated protein	Circulates in blood	Structurally identical to ITIH2, inter-alpha-trypsin inhibitor heavy chain 2. It forms a complex with HA, acts as a cofactor when binding to other receptors (CD44). The level of SHAP-HA complex is an indicator of degenerative changes in the liver and the absence of the matrix of ovulated oocytes	[33]
ITI – proteoglycans: inter-alpha-trypsin inhibitors	ECM, glycocalyx	Provides integrity and stabilizes the structure of ECM and glycocalyx	[77, 119, 124, 125]
Large aggregated proteoglycans: aggrecan, brevican, neurocan, versican	Matrix proteoglycans are contained mainly: aggrecan – in hyaline cartilages; neurocan and brevican – in brain tissues; versican – in various tissues, endometrial stroma, especially important for endothelial glycocalyx	Provides integrity and stabilizes the structure of ECM and glycocalyx, carcinogenesis	[33, 126]

tibodies to HA and its structural disaccharide are also elevated in PE [67, 68]. The source of HA in the blood in PE remains unknown: HA is assumed to appear in the blood as a result of maternal endothelial dysfunction [69]; placenta can serve as another source of HA [64, 70].

HMW-HA prevails under physiological conditions, while LMW-HA is mostly found in the inflammatory response and tissue damage [71]. The inflammatory response leads to HA degradation and the formation of fragments of different sizes, which have a multidirectional effect on the function of cells, organs, and systems [29]. The interaction of HMW-HA and LMW-HA with cell membrane receptors induces various signaling pathways that positively/negatively regulate the same processes [72]. A characterization of HA of different weights is presented in *Table 1*.

RECEPTORS OF HYALURONIC ACID

The functional properties of HA manifest themselves through interaction with its receptors: hyaluronan-binding proteins, or hyaladherins. Specific interactions of HA regulate intercellular adhesion, cell migration, differentiation, HA clearance, signal transduction to cell, and the inflammatory response [83–85]. The most important HA receptors are: RHAMM, the first of the identified receptors, which was discovered both on the cell surface and inside cells (in the cytoplasm and nucleus) and CD44, the main receptor of cell surface HA [37]. HA-RHAMM interaction plays a key role in the activation of signaling cascades through the PDGF receptor, Ser/Thr-kinase, and MAP-kinase Erk [85, 86]. Activation of the intracellular RHAMM receptor causes a reorganization of the cytoskeleton and regulates cell migration and proliferation [37, 87]. HA-CD44 signals also involve the activation of receptor tyrosine kinases (receptors PDGF-β and ErbB2/Her2), ERM family proteins that provide interaction of the actin cytoskeleton with the cytoplasmic membrane (merlin, ezrin, radixin, and moesin); and the IQGAP1 protein associated with the actin cytoskeleton, the activation of which regulates cell morphology, its motility, adhesion, and cell cycle [34, 37, 88–93]. CD44 is capable of forming a complex with the guanine nucleotide exchange factor Tiam1 [94]. Binding of the complex to HA activates the Rac1-mediated signaling pathway, which also regulates cytoskeleton reorganization [37]. HA metabolism is assumed to be regulated through CD44, since a blocking effect of anti-CD44 antibodies has been shown on endocytosis and HA cleavage *in vitro* [95].

Regulation of HA metabolism is performed by hyaladherins LYVE-1, STABILIN-1, as well as STABILIN-2, the main HA receptor in the liver [34]. Positive regulation of the inflammatory response is observed in the binding of LMW-HA or O-HA with Toll-like receptors (TLR2, TLR4) [33]. Binding with the receptor initiates the MAP-kinase cascade, nuclear translocation of NF-κB, and TNFα production [96]. The function of ECM and glycocalyx structure stabilization is mainly provided by large proteoglycans, ITI-proteoglycans, TSG-6, and SHAP [33, 97]. However, each HA-binding hyaladherin is also involved in the stabilization of supracellular structures. The characteristics of the most studied human hyaladherins are presented in *Table 2*.

HYALURONIC ACID AND ITS RECEPTORS IN PLACENTA

Among placental tissues, HA is found in the stromal structures of the uterus and placenta, as well as in the angiogenic regions of mesometrial decidua basalis [99], mesenchymal villi, and immature intermediate villi of the placenta [101]. Its involvement in endometrial decidualization has been also shown in mice [126]. The study of the distribution of HA and its receptor CD44 in human placental tissue in physiological pregnancy showed that, in the first half of a pregnancy, HA is highly expressed only in the stroma of mesenchymal villi, whose cells proliferate and differentiate rapidly, providing the development of a placental villous tree. In another type of villi, HA was detected only in the fetal vessels and connective tissue adjacent to the trophoblast, as well as in limited stromal areas of the villi adjacent to the cells of extravillous cytotrophoblast and cell colonies. It is assumed that the significant amounts of HA found in mesenchymal and immature intermediate villi are needed in the capacity of substrate through which mesenchymal cell migration and sprouting of blood vessels take place. Villous stromas of all types are homogeneously stained for HA in mature placenta [101].

HA receptors are also expressed in placental tissue. For instance, the expression of CD44 is detected on decidual cells, lymphocytes localized in the decidua basalis, and cellular elements of endometrial stroma during a normal pregnancy [99]. Invasive extravillous trophoblast express CD44 in the first half of a pregnancy. Increased expression of CD44 positively influences the invasive properties of trophoblast in Matrigel, with HMW-HA inhibiting CD44-mediated invasion and LMW-HA, on the contrary, increasing it [82]. R. Zhu *et al.* have shown that expression of HA and HAS2 by trophoblast in a normal pregnancy is higher compared to early abortion, suggesting the involvement of HA in placental morphogenesis. However, an analysis of the influence of HA of various molecular weights on trophoblast invasion in Matrigel has shown that HMW-HA enhances the proliferation and invasive properties of trophoblast, inhibits apoptosis, and activates the PI3K/AKT and MAPK/ERK1/2 signaling pathways in trophoblast, while LMW-HA does not cause these ef-

fects. Blockage of the PI3K/AKT and MAPK/ERK1/2 signals inhibits HA-dependent proliferation and the invasive properties of trophoblast [79]. Similar results have been obtained for decidual stromal cells during early pregnancy: the expression of HA, HAS2, and CD44 was lower in abortion than in a normal pregnancy; HMW-HA positively regulated the proliferation, apoptosis, PI3K/AKT- and MAPK/ERK1/2-mediated signals of decidual stromal cells, which illustrates the role of HA and its receptor in decidualization and placentation early in a pregnancy [127].

In early pregnancy, the CD44 receptor is detected in a limited number of Hofbauer cells of the villous stroma and the endothelial cells of small vessels. Increased expression is observed by the 16th week of gestation: the receptor is detected in the intima of fetal blood vessels and connective tissue adjacent to them; limited staining is noted in the cytotrophoblast islands of the basal plate. By the end of a pregnancy, receptor expression is observed in various types of villi; staining was the most pronounced in stem villi. A change in the regulation of the expression of HA and its receptor in placental tissues at different stages of gestation allowed us to presume an active participation of HA in the early morphogenesis of placenta, as well as the important role of CD44 in tissue remodeling during late pregnancy [128].

The HA receptor LYVE-1 was identified in fetal placental endothelium [104] and syncytiotrophoblast [105]. However, its expression was higher than in the mature placenta by 33–34 weeks of gestation [104]. LYVE-1 is also expressed in the population of placental macrophages with the DC-SIGN+CD163+ phenotype localized in the chorionic villi of mature human placenta [105]. Experimental modeling of peritoneal endometriosis in mice showed that the expression of LYVE-1 by the endothelium of lymphatic vessels is increased only after a pregnancy. This effect was absent in treated non-pregnant animals, indirectly pointing to LYVE-1 involvement in angiogenesis [129]. There are no lymphatic vessels in human endometrium; pregnancy causes a rapid induction of lymphangiogenesis in the decidual membrane of the uterus [130]. It is assumed that LYVE-1 participates in the manifestation of an invasive phenotype of trophoblast in the placenta. However, these assumptions are speculative, since there is evidence of an absence of a receptor on the fetal endothelium and endothelium of lymphatic vessels during decidualization [131, 132].

High levels of HA have been found in the area of fibrin deposits in the villi and intervillous spaces in PE [64, 70]. However, there are reports of an absence of differences in the HA content in placental tissues between a normal pregnancy and PE [133]. It should be noted that the distribution of HA and its receptors in patients with early PE remains poorly studied; this complicates the interpretation of the results, since early development of PE in itself is associated with impaired placental morphogenesis.

CONCLUSION

HA and its receptors are factors that regulate the processes of morphogenesis, epithelial/mesenchymal transformation, tumor metastasis, and tissue remodeling. HA stabilizes endothelial glycocalyx, ensures its integrity and regeneration upon damage; i.e., it maintains vascular homeostasis and provides the barrier function in endothelium. In accordance with the data presented above, one can assume that HA is important during pregnancy, first of all, for placental morphogenesis, and, secondly, for the proper functioning of the regulation of the cardiovascular system, including uteroplacental circulation. Thirdly, since HA regulates the systemic inflammatory response, hyaluronic acids of different molecular weights can have a multidirectional effect on a pregnancy, and even promote pathology. However, despite the proven value of HA in maintaining physiological homeostasis, the role of HA and its receptors in pregnancy remains poorly understood. This applies, primarily, to PE pathogenesis, since the main clinical manifestations of the disease are related to inadequate placentation, excessive systemic inflammatory response, and endothelial dysfunction. The distribution of HA and its receptors in PE, especially in a severe disease, remains poorly studied. To date, the glycocalyx of glomerular and vascular endothelium remains to be studied in cases of a fatal outcome and in an animal model. In addition, the molecular weight of hyaluronic acids in the blood of patients with PE still has to be characterized, and how they affect the disease has not been shown. The study of HA in this context could lead to new discoveries in the pathogenesis of PE. ●

The authors express their deep appreciation and gratitude to employee of the Laboratory of Carbohydrates, M.M. Shemyakin and Yu.A. Ovchinnikov Institute of Bioorganic Chemistry , RAS, I.S. Belyanchikov, and employee of the Department of library and information resources and telemedicine, V.I. Kulakov Research Center for Obstetrics, Gynecology and Perinatology of the Russian Ministry of Health, A.L. Komarovsky, for his help in preparing this manuscript.

This work was performed as part of a state commission on the topic: The study of Molecular Genetic, Proteomic and Mitochondrial Determinants in the Development of Preeclampsia (№ 114040970024). Work of NV Bovin supported by Grant RNF №14-14-00579.

REFERENCES

1. Burton G., Woods A., Jauniaux E., Kindom J. // Placenta. 2009. V. 30. P. 473482.
2. Milovanov A.P. Human fetal development. Moscow.: MDV, 2006. 384 P.
3. Ferretti C., Bruni L., Marie D., Pecking A., Bellet D. // Hum. Reprod. Update. 2007. V. 13. P. 121––141.
4. Benirschke K., Burton G.J. Baergen R.N. Pathology of the human placenta. N.Y.: Springer, 2012. 939 p.
5. Kaufmann P., Black S., Huppertz B. // Biol. Reprod. 2003. V. 69. P. 1–7.
6. Harrison D.G., Guzik T.J., Lob H.E., Madhur M.S., Marvar P.J., Thabet S.R., Vinh A., Weyand C.M. // Hypertension. 2011. V. 57. № 2. P. 132–140.
7. Lennon F.E., Singleton P.A. // Am. J. Cardiovasc. Dis. 2011. V. 1. № 3. P. 200–213.
8. Afratis N., Gialeli C., Nikitovic D., Tsegenidis T., Karousou E., Theocharis A.D., Pavão M.S., Tzanakakis G.N., Karamanos N.K. // FEBS J. 2012. V. 279. № 7. P. 1177–1197.
9. Karbownik M.S., Nowak J.Z. // Pharmacol. Rep. 2013. V. 65. № 5. P. 1056–1074.
10. Heldin P. // Braz. J. Med. Biol. Res. 2003. V. 36. № 8. P. 967–973.
11. Jackson D.G // Immunol. Rev. 2009. V. 230. № 1. P. 216–231.
12. Satchell S. // Nat. Rev. Nephrol. 2013. V. 9. № 12. P. 717–725.
13. Alphonsus C.S., Rodseth R.N. // Anaesthesia. 2014. V. 69. № 7. P. 777–784.
14. Kolářová H., Ambrůzová B., Svihálková Šindlerová L., Klinke A., Kubala L. // Mediators Inflamm. 2014. V. 2014. 17 p. http://dx.doi.org/10.1155/2014/694312
15. Fels J., Jeggle P., Liashkovich I., Peters W., Oberleithner H. // Cell Tissue Res. 2014. V. 355. № 3. P.727–737.
16. Fletcher D.A., Mullins R.D. // Nature. 2010. V. 463. P. 485–492.
17. Herrmann H., Bar H., Kreplak L., Strelkov S.V., Aebi U. // Nat. Rev. Mol. Cell. Biol. 2007. V. 8. P. 562–573.
18. Swift J., Ivanovska I.L., Buxboim A., Harada T., Dingal P.C., Pinter J., Pajerowski J.D., Spinler K.R., Shin J.W., Tewari M., et al. // Science. 2013. V. 341. № 6149. http://www.ncbi.nlm.nih.gov/pmc/articles/PMC3976548/pdf/nihms564861.pdf 1240104
19. Ingber DE. // FASEB J. 2006. V. 20. P. 811–827.
20. Aplin A.E., Howe A., Alahari S.K., Juliano R.L. // Pharmacol. Rev. 1988. V. 50. P. 197–264.
21. Markos F., Ruane O'Hora T., Noble M.I. // Clin. Exp. Pharmacol. Physiol. 2013. V. 40. №8. P. 489–494.
22. Mambetsariev N., Mirzapoiazova T., Mambetsariev B., Sammani S., Lennon F.E., Garcia J.G., Singleton P.A. // Arterioscler. Thromb. Vasc. Biol. 2010. V. 30. P. 483–490.
23. Singleton P.A., Dudek S.M., Ma S.F., Garcia J.G. // J. Biol. Chem. 2006. V. 281. P. 34381–34393.
24. Dane M.J., van den Berg B.M., Avramut M.C., Faas F.G., van der Vlag J., Rops A.L., Ravelli R.B., Koster B.J., van Zonneveld A.J., Vink H., et al. // Am. J. Pathol. 2013. V. 182. № 5. P. 1532–1540.
25. Yung S., Chan T.M. // Int. J. Artif. Organs. 2007. V. 30. № 6. P. 477–483.
26. Wheeler-Jones C.P., Farrar C.E., Pitsillides A.A. // Curr. Opin. Investig. Drugs. 2010. V. 11. № 9. P. 997–1006.
27. Qazi H., Palomino R., Shi Z.D., Munn L.L., Tarbell J.M. // Integr. Biol. 2013. V. 5. № 11. P. 1334–1343.
28. Lipowsky H.H. // Ann. Biomed. Eng. 2012. V. 40. № 4. P. 840–848.
29. Taylor K.R., Gallo R.L. // FASEB J. 2006. V. 20. № 1. P. 9–22.
30. Klinger A.L., Pichette B., Sobolewski P., Eckmann D.M. // Integr. Biol. 2011. V. 3. № 10. P. 1033–1042.
31. Salmon A.H., Ferguson J.K., Burford J.L., Gevorgyan H., Nakano D., Harper S.J., Bates D.O., Peti-Peterdi J. // J. Am. Soc. Nephrol. 2012. V. 23. № 8. P. 1339–1350.
32. Martin-DeLeon P.A. // Mol. Cell. Endocrinol. 2006. V. 250. № 1–2. P. 114–121.
33. Jiang D., Liang J., Noble P.W. // Physiol. Rev. 2011. V. 91. № 1. P. 221–264.
34. Spicer A.P., Tien J.Y. // Birth. Defects. Res. C. Embryo Today. 2004. V. 72. № 1. P. 89–108.
35. Triggs-Raine B., Natowicz M.R. // World J. Biol. Chem. 2015. V. 6. № 3. P. 110–120.
36. Siiskonen H., Oikari S., Pasonen-Seppänen S., Rilla K. // Front. Immunol. 2015. V. 6. P. 43.
37. Heldin P., Basu K., Olofsson B., Porsch H., Kozlova I., Kahata K. // J. Biochem. 2013. V. 154. № 5. P. 395–408.
38. Spicer A.P., McDonald J.A. // J. Biol. Chem. 1998. V. 273. P. 1923–1932.
39. Camenisch T.D., Spicer A.P., Brehm-Gibson T., Biesterfeldt J., Augustine M.L., Calabro A.Jr., Kubalak S., Klewer S.E., McDonald J.A. // J. Clin. Invest. 2000. V. 106. № 3. P. 349–360.
40. McDonald J.A., Camenisch T.D. // Glycoconj. J. 2003. V. 19. P. 331–339.
41. Chan D.D., Xiao W.F., Li J., de la Motte C.A., Sandy J.D., Plaas A. // Osteoarthritis Cartilage. 2015. V. 23. № 11. P. 1879–1889.
42. Arranz A.M., Perkins K.L., Irie F., Lewis D.P., Hrabe J., Xiao F., Itano N., Kimata K., Hrabetova S., Yamaguchi Y. // J. Neurosci. 2014. V. 34. № 18. P. 6164–6176.
43. Ramsden C.A., Bankier A., Brown T.J., Cowen P.S., Frost G.I., McCallum D.D., Studdert V.P., Fraser J.R. // J. Pediatr. 2000. V. 136. № 1. P. 62–68.
44. Zhu X., Deng X., Huang G., Wang J., Yang J., Chen S., Ma X., Wang B. // PLoS One. 2014. V. 9. № 2. P. e87437.
45. Karousou E., Stachtea X., Moretto P., Viola M., Vigetti D., D'Angelo M.L., Raio L., Ghezzi F., Pallotti F., De Luca G., et al. // FEBS J. 2013. V. 280. № 10. P. 2418–2430.
46. Jones M.H., Davey P.M., Aplin H., Affara N.A. // Genomics. 1995. V. 29. P. 796–800.
47. Kim E., Baba D., Kimura M., Yamashita M., Kashiwabara S., Baba T. // Proc. Natl. Acad. Sci. USA. 2005. V. 102. P. 18028–18033.
48. Csoka A.B., Frost G.I., Stern R. // Matrix Biol. 2001. V. 20. № 8. P. 499–508.
49. Natowicz M.R., Short M.P., Wang Y., Dickersin G.R., Gebhardt M.C., Rosenthal D.I., Sims K.B., Rosenberg A.E // N. Engl. J. Med. 1996. V. 335. № 14. P. 1029–1033.
50. Triggs-Raine B., Salo T.J., Zhang H., Wicklow B.A., Natowicz M.R. // Proc. Natl. Acad. Sci. USA. 1999. V. 96. № 11. P. 6296–6300.
51. Jadin L., Wu X., Ding H., Frost G.I., Onclinx C., Triggs-Raine B., Flamion B. // FASEB J. 2008. V. 22. P. 4316–4326.
52. Chowdhury B., Hemming R., Hombach-Klonisch S., Flamion B., Triggs-Raine B. // J. Biol. Chem. 2013. V. 288. P. 520–528.
53. Onclinx C., Dogne S., Jadin L., Andris F., Grandfils C., Jouret F., Mullier F., Flamion B. // Haematologica. 2015.

V. 100. № 8. P. 1023–1030.
54. Colombaro V., Jadot I., Declèves A.E., Voisin V., Giordano .L, Habsch I., Malaisse J., Flamion B., Caron N. // Kidney Int. 2015. V. 88. № 1. P. 61–71.
55. Udabage L., Brownlee G.R., Nilsson S.K., Brown T.J. // Exp. Cell. Res. 2005. V. 310. № 1. P. 205–217.
56. Kultti A., Rilla K., Tiihonen R., Spicer A.P., Tammi R.H., Tammi M.I. // J. Biol. Chem. 2006. V. 281. № 23. P. 15821–15828.
57. Hommelgaard A.M., Lerdrup M., van Deurs B. // Mol. Biol. Cell. 2004. V. 15. № 4. P. 1557–1567.
58. Padberg J.S., Wiesinger A., di Marco G.S., Reuter S., Grabner A., Kentrup D., Lukasz A., Oberleithner H., Pavenstädt H., Brand M., et al. // Atherosclerosis. 2014. V. 234. № 2. P. 335–343.
59. Grundmann S., Fink K., Rabadzhieva L., Bourgeois N., Schwab T., Moser M., Bode C., Busch H.J. // Resuscitation. 2012. V. 83. № 6. P. 715–720.
60. Aytekin M., Comhair S.A., de la Motte C., Bandyopadhyay S.K., Farver C.F., Hascall V.C., Erzurum S.C., Dweik R.A. // Am. J. Physiol. Lung. Cell. Mol. Physiol. 2008. V. 295. № 5. P. 789–799.
61. Nyberg A., Engström-Laurent A., Lööf L. // Hepatology. 1988. V. 8. № 1. P. 142–146.
62. Gressner O.A., Weiskirchen R., Gressner A.M. // J. Cell. Mol. Med. 2007. V. 11. P. 1031–1051.
63. Haserodt S., Aytekin M., Dweik R.A. // Glycobiology. 2011. V. 21. № 2. P. 175–183.
64. Matejevic D., Neudeck H., Graf R., Müller T., Dietl J. // Gynecol. Obstet. Invest. 2001. V. 52. № 4. P. 257–259.
65. Berg S., Engman A., Holmgren S., Lundahl T., Laurent T.C. // Scand. J. Clin. Lab. Invest. 2001. V. 61. P. 131–137.
66. Hofmann-Kiefer K.F., Chappell D., Knabl J., Frank H.G., Martinoff N., Conzen P., Becker B.F., Rehm M. // Reprod. Sci. 2013. V. 20. № 10. P. 1237–1245.
67. Ziganshina M.M., Shilova N.V., Khasbiullina N.R., Navakouski M.E., Nikolaeva M.A., Kan N.E., Vavina O.V., Nikolaeva A.V., Tyutyunnik N.V., Sergunina O.A., et al. // Akusherstvo i Ginekologiya. (Obstetrics and Gynecology) (Rus). 2016. № 3. P. 24–31.
68. Ziganshina M.M., Shilova N.V., Khasbiullina N.R., Navakouski M.E., Nikolaeva M.A., Kan N.E., Vavina O.V., Nikolaeva A.V., Tyutyunnik V.L., Tyutyunnik N.V., Bot I., Sukhikh G.T., Bovin N.V. // Antibodies to hyalyronic acid in preeclampsia. In Glycobiology and Human Diseases / Ed. G. Wiederschain N.Y.: CRC Press, 2016. P. 313–322.
69. Hofmann-Kiefer K.F., Knabl J., Martinoff N., Schiessl B., Conzen P., Rehm M., Becker B.F., Chappell D. // Reprod. Sci. 2013. V. 20. № 3. P. 318–325.
70. Uzun H., Konukoglu D., Albayrak M., Benian A., Madazli R., Aydin S., Gelisgen R., Uludag S. // Hypertens. Pregnancy. 2010. V. 29. № 2. P. 153–162.
71. Noble P.W. // Matrix. Biol. 2002. V. 21. P. 25–29.
72. Vigetti D., Viola M., Karousou E., Deleonibus S., Karamanou K., De Luca G., Passi A. // FEBS J. 2014. V. 281. № 22. P. 4980–4992.
73. Evanko S.P., Tammi M.I., Tammi R.H., Wight T.N. // Adv. Drug. Deliv. Rev. 2007. V. 59. № 13. P. 1351–1365.
74. Stern R., Asari A.A., Sugahara K.N. // Eur. J. Cell. Biol. 2006. V. 85. № 8. P. 699–715.
75. Ibrahim S., Ramamurthi A. // J. Tissue. Eng. Regen. Med. 2008. V. 2. № 1. P. 22—32.
76. Gaudet A.D., Popovich P.G. // Exp. Neurol. 2014. V. 258. P. 24–34.
77. Petrey A.C., de la Motte C.A. // Front. Immunol. 2014. V. 5. Art. 101. P. 1–13. http://www.ncbi.nlm.nih.gov/pmc/articles/PMC3949149/pdf/fimmu-05-00101.pdf
78. Bollyky P.L., Falk B.A., Wu R.P., Buckner J.H., Wight T.N., Nepom G.T. // J. Leukoc. Biol. 2009. V. 86. № 3. P. 567–572.
79. Zhu R., Huang Y.H., Tao Y., Wang S.C., Sun Ch., Piao H.L., Wang X.Q., Du M.R., Li D.J. // Placenta. 2013. V. 34. № 9. P. 784–791.
80. Matou-Nasri S., Gaffney J., Kumar S., Slevin M. // Int. J. Oncol. 2009. V. 35. № 4. P. 761–773.
81. Yu M., He P., Liu Y., He Y., Du Y., Wu M., Zhang G., Yang C., Gao F. // Med. Oncol. 2015. V. 32. Art. 381. P. 1–8.
82. Takahashi H., Takizawa T., Matsubara S., Ohkuchi A., Kuwata T., Usui R., Matsumoto H., Sato Y., Fujiwara H., Okamoto A., Suzuki M., Takizawa T. // Placenta. 2014. V. 35. № 3. P. 163–170.
83. Vigetti D., Karousou E., Viola M., Deleonibus S., De Luca G., Passi A. // Biochim. Biophys. Acta. 2014. V. 1840. № 8. P. 2452–2459.
84. Knudson C.B., Knudson W. // FASEB J. 1993. V. 7. № 13. P. 1233–1241.
85. Hall C.L., Wang C., Lange L.A., Turley E.A. // J. Cell Biol. 1994. V. 126. P. 575–588.
86. Turley E.A., Noble P.W., Bourguignon L.Y. // J. Biol. Chem. 2002. V. 277. P. 4589–4592.
87. Tolg C., Hamilton S.R., Morningstar L., Zhang J., Zhang S., Esguerra K.V., Telmer P. G., Luyt L.G., Harrison R., McCarthy J.B., et al. // J. Biol. Chem. 2010. V. 285. P. 26461–26474.
88. Orian-Rousseau V., Ponta H. // Adv. Cancer Res. 2008. V. 101. P. 63–92.
89. Li L., Heldin. C.H., Heldin P. // J. Biol. Chem. 2006. V. 281. P. 26512–26519.
90. Skandalis S.S., Kozlova I., Engstrom U., Hellman U., Heldin P. // IUBMB Life. 2010. V. 62. P. 833–840.
91. Toole B.P. // Clin. Cancer Res. 2009. V. 15. P. 7462–7468.
92. Toole B.P., Slomiany M.G. // Semin. Cancer Biol. 2008. V. 18. P. 244–250.
93. Ghatak S., Misra S., Toole B.P. // J. Biol. Chem. 2005. V. 280. P. 8875–8883.
94. Bourguignon L.Y., Zhu H., Shao L., Chen Y.W. // J. Biol. Chem. 2000. V. 275. № 3. P. 1829–1838.
95. Culty M., Nguyen H.A., Underhill C.B. // J. Cell. Biol. 1992. V. 116. № 4. P. 1055–1062.
96. Tesar B.M., Jiang D., Liang J., Palmer S.M., Noble P.W., Goldstein D.R. // Am. J. Transplant. 2006. V. 6. P. 2622–2635.
97. Bollyky P.L., Bogdani M., Bollyky J.B., Hull R.L., Wight T.N. // Curr. Diab. Rep. 2012. V. 12. № 5. P. 471–480.
98. Ponta H., Sherman L., Herrlich P.A. // Nat. Rev. Mol. Cell. Biol. 2003. V. 4. № 1. P. 33–45.
99. Goshen R., Ariel I., Shuster S., Hochberg A., Vlodavsky I., de Groot N., Ben-Rafael Z., Stern R. // Mol. Hum. Reprod. 1996. V. 2. № 9. P. 685–691.
100. Marzioni D., Crescimanno C., Zaccheo D., Coppari R., Underhill C.B., Castellucci M. // Eur. J. Histochem. 2001. V. 45. № 2. P. 131–140.
101. Castellucci M., Kosanke G., Verdenelli F., Huppertz B., Kaufmann P. // Hum. Reprod. Update. 2000. V. 6. № 5. P. 485–494.
102. Bollyky P.L., Falk B.A., Wu R.P., Buckner J.H., Wight T.N., Nepom G.T. // J. Leukoc. Biol. 2009. V. 86. № 3. P. 567–572.
103. Banerji S., Ni J., Wang S.X., Clasper S., Su J., Tammi R., Jones M., Jackson D.G. // J. Cell. Biol. 1999. V. 144. № 4. P. 789–801.
104. Gu B., Alexander J.S., Gu Y., Zhang Y., Lewis D.F., Wang

Y. // Lymphat. Res. Biol. 2006. V. 4. № 1. P. 11–17.
105. Böckle B.C., Sölder E., Kind S., Romani N., Sepp N.T. // Placenta. 2008. V. 29. № 2. P. 187–192.
106. Zhang H., Tse J., Hu X., Witte M., Bernas M., Kang J., Tilahun F., Hong Y.K., Qiu M., Chen L. // Invest. Ophthalmol. Vis. Sci. 2010. V. 51. № 12. P. 6157–6161.
107. Gao F., Yang C.X., Mo W., Liu Y.W., He Y.Q. // Clin. Invest. Med. 2008. V. 31. № 3. E. 106–116.
108. Gust K.M., Hofer M.D., Perner S.R., Kim R., Chinnaiyan A.M., Varambally S., Moller P., Rinnab L., Rubin M.A., Greiner J., et al. // Neoplasia. 2009. V. 11. № 9. P. 956–963.
109. Ishigami S., Ueno S., Nishizono Y., Matsumoto M., Kurahara H., Arigami T., Uchikado Y., Setoyama T., Arima H., Yoshiaki K., et al. // BMC Cancer. 2011. V. 11. P. 106.
110. Entwistle J., Hall C.L., Turley E.A. // J. Cell Biochem. 1996. V. 61. № 4. P. 569–577.
111. McCourt P.A.G., Ek B., Forsberg N., Gustafson S. // J. Biol. Chem. 1994. V. 269. P. 30081–30084.
112. Yasuda T. // Inflamm. Res. 2007. V. 56. № 6. P. 246–253.
113. Yasuda T. // J. Pharmacol .Sci. 2012. V. 118. № 1. P. 25–232.
114. Shao Y., Lu G.L., Shen Z.J., He H.C. // World. J. Urol. 2013. V. 31. № 3. P. 535–540.
115. Milner C.M., Day A.J. // J. Cell Sci. 2003. V. 116. № 10. P. 1863–1873.
116. Schaefer L. // J. Biol. Chem. 2014. V. 289. № 51. P. 35237–35245.
117. Kzhyshkowska J., Gratchev A., Goerdt S. // J. Cell. Mol. Med. 2006. V. 10. № 3. P. 635–649.
118. Schledzewski K., Falkowski M., Moldenhauer G., Metharom P., Kzhyshkowska J., Ganss R., Demory A., Falkowska-Hansen B., Kurzen H., Ugurel S., et al. // J. Pathol. 2006. V. 209. № 1. P. 67–77.
119. Hascall V., Esco J.D. // Hyaluronan. In Essentials of Glycobiology / Ed. A. Varki, N.Y.: Cold Spring Harbor Lab. Press, 2009. P. 219–228.
120. Ferrero E., Malavasi F. // J. Leukoc. Biol. 1999. V. 65. № 2. P. 151–161.
121. Brachtl G., Piñón Hofbauer J., Greil R., Hartmann T.N. // Ann. Hematol. 2014. V. 93. № 3. P. 361–374.
122. Solovieva I.A., Sobko E.A., Kraposhin A.Y., Demko I.V., Salmin A.B. // Pulmonology. (Mosc.). 2013. № 5. P. 81–84.
123. Majumdar M., Meenakshi J., Goswami S.K., Datta K. // Biochem. Biophys. Res. Commun. 2002. V. 291. P. 829–837.
124. Bost F., Diarra-Mehrpour M., Martin J.P. // Eur. J. Biochem. 1998. V. 252. № 3. P. 339–346.
125. Suzuki M., Kobayashi H., Tanaka Y., Kanayama N., Terao T. // J. Endocrinol. 2004. V. 183. № 1. P. 29–38.
126. San Martin S., Soto-Suazo M., Zorn T.M. // Braz. J. Med. Biol. Res. 2003. V. 36. № 8. P. 1067–1071.
127. Zhu R., Wang S.C., Sun C., Tao Y., Piao H.L., Wang X.Q., Du M.R., Da-Jin Li // PLoS One. 2013. V. 8. № 9. P. e74812.
128. Marzioni D., Kosanke G., Verdenelli F., Huppertz B., Kaufmann P. // Hum. Reprod. Update. 2000. V. 6. № 5. P. 485–494.
129. Cohen J., Naoura I., Castela M., von N'Guyen T., Oster M., Fontaine R., Chabbert-Buffet N., Darai E., Aractingi S. // Eur. J. Obstet. Gynecol. Reprod. Biol. 2014. V. 183. P. 70–77.
130. Rogers P.A., Donoghue J.F., Girling J.E. // Placenta. 2008. V. 29. S. 48–54.
131. Volchek M., Girling J.E., Lash G.E., Cann L., Kumar B., Robson S.C., Bulmer J.N., Rogers P.A. // Hum. Reprod. 2010. V. 25. № 10. P. 2455–2464.
132. Sölder E., Böckle B.C., Nguyen V.A., Fürhapter C., Obexer P., Erdel M., Stössel H., Romani N., Sepp N.T. // Microvasc. Res. 2012. V. 84. № 1. P. 65–73.
133. Famá E.A., Souza R.S., Melo C.M., Melo Pompei L., Pinhal M.A. // Clin. Chim. Acta. 2014. V. 437. P. 155–160.
134. Maksimenko A.V., Turashev A.D. // J. Atherosclerosis and dyslipidemias. (Rus). 2011. №2. P. 4–17.

Epigenetics of Ancient DNA

S. V. Zhenilo, A.S. Sokolov, E. B. Prokhortchouk*
Institute of Bioengineering, Federal Research Center "Fundamentals of Biotechnology", Russian Academy of Sciences, prospect 60-letiya Oktyabrya, Str. 7/1, Moscow, 117312, Russia
*E-mail: prokhortchouk@gmail.com
Received January 29, 2016; in final form, April 25, 2016

ABSTRACT **Initially, the study of DNA isolated from ancient specimens had been based on the analysis of the primary nucleotide sequence. This approach has allowed researchers to study the evolutionary changes that occur in different populations and determine the influence of the environment on genetic selection. However, the improvement of methodological approaches to genome-wide analysis has opened up new possibilities in the search for the epigenetic mechanisms involved in the regulation of gene expression. It was discovered recently that the methylation status of the regulatory elements of the *HOXD* cluster and *MEIS*1 gene changed during human evolution. Epigenetic changes in these genes played a key role in the evolution of the limbs of modern humans. Recent works have demonstrated that it is possible to determine the transcriptional activity of genes in ancient DNA samples by combining information on DNA methylation and the DNAaseI hypersensitive sequences located at the transcription start sites of genes. In the nearest future, if a preserved fossils brain is found, it will be possible to identify the evolutionary changes in the higher nervous system associated with epigenetic differences.**

KEYWORDS **epigenetics, ancient DNA, DNA methylation**

ABBREVIATIONS **MpG – methylated CpG, PMD – partially methylated domain, DMV – DNA methylation valley, MBD – methyl DNA binding domain**

INTRODUCTION

The study of DNA isolated from archaeological and paleontological specimens provides information about our evolutionary past. Initially, the investigation of ancient DNA had consisted in an analysis of nucleotide sequences. At that stage, researchers encountered a host of difficulties related to the quality of the ancient DNA, its contamination with foreign DNA and others, and these problems were resolved, in particular, by means of improved whole genome sequencing methods. Then, the development of modern sequencing technology has also allowed researchers to analyze the information contained in the epigenetic code. On the one hand, physical characteristics such as susceptibility to a disease, and even some of the psychological characteristics of an individual are determined by genetic factors. On the other hand, it would be a mistake to dismiss the impact of the environment. Gene expression is determined by not only the nucleotide sequence, but also by a number of adaptively regulated processes that lead to changes in the DNA methylation level, histone code, and the spectrum of miRNA. These epigenetic mechanisms are involved in the formation of the chromatin structures required for the regulation of gene expression. With the combination of high-technology sequencing and different methodological approaches, whole genome maps of DNA methylation have been derived in various types of human cells and mice: somatic, stem, germ, cancer, and other types of cells [1].

The central characteristic of any ancient DNA is its degradation and cytosine deamination. Until recently, it was considered impossible to extract information on the transcriptional activity of genes from DNA that had been isolated long after the death of an individual. Nevertheless, in 2010 S. Paabo *et al.* made the first attempts to build methylation maps of ancient DNA, and they demonstrated the potential to determine the *in vivo* patterns of CpG methylation in Neanderthal DNA [2]. Shortly after, by bisulfite allelic sequencing of loci from late Pleistocene bison DNA remains, B. Llamas *et al.* [3] showed that DNA methylation patterns are preserved in ancient DNA.

METHODS USED TO STUDY ANCIENT DNA METHYLATION

Deamination of methylated cytosine residues and their transformation into thymine, which occurs after death, makes it difficult to perform a quantitative analysis of methylated cytosines. Only as recently as 2014 was a method developed that allowed researchers to conduct a genome-wide methylation analysis of ancient DNA [4–6]. During bisulfite sequencing, unmethylated cytosine residues are chemically converted to uracil

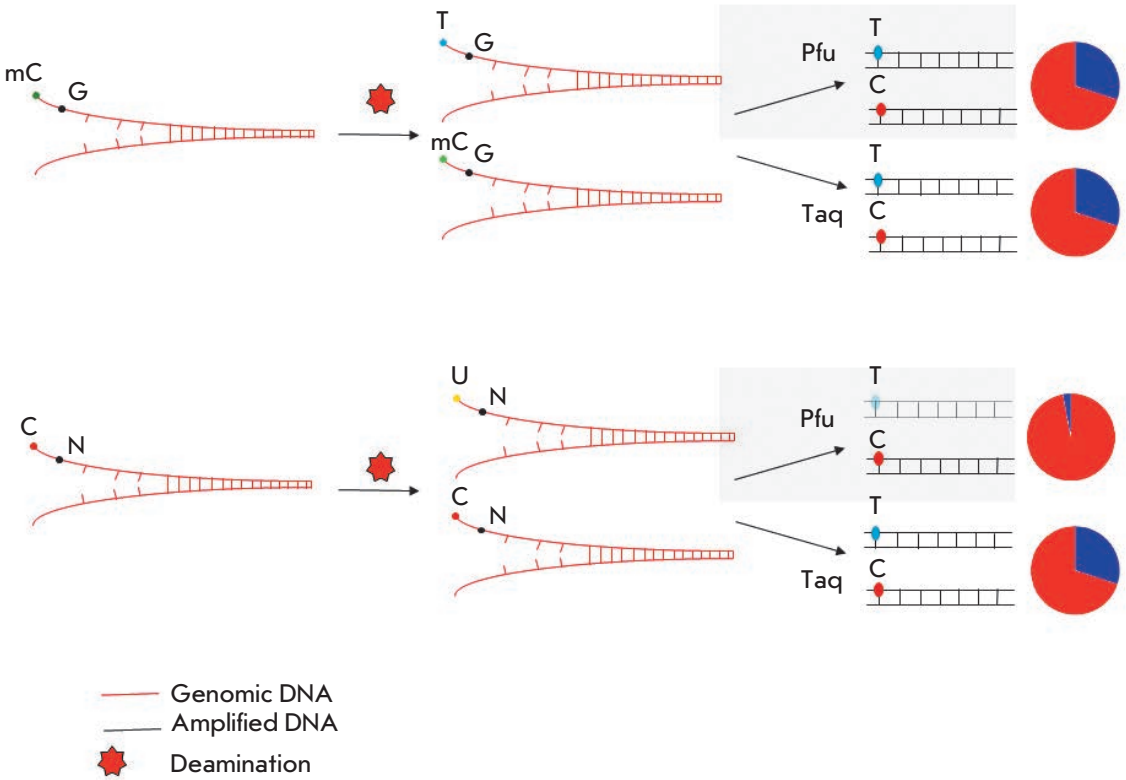

Fig. 1. Scheme of cytosine methylation detection in ancient DNA via substitution rates of C-T relative to the original chain during deamination. Taq polymerase is not sensitive to the presence of uracil, and Pfu polymerase cannot continue the chain synthesis in the presence of uracil. Deamination of methylated cytosines (mC) does not affect the ratio of C-T substitutions detected using Taq- and Pfu-polymerases. Deamination of unmethylated cytosines creates "impassable" uracil for Pfu polymerase. Thus, all the readings starting from T (in the context of genomic CG) in NGS libraries prepared using Pfu polymerase definitely indicate the methylation status of cytosine in ancient DNA.

residues, which are then read by polymerases, such as Taq-polymerase, in the manner of thymines in PCR. In vertebrate cells, mapping of these C-T-mutations is performed at one nucleotide precision. A similar chemical transformation occurs naturally after death, mainly due to the hydrolytic deamination of the cytosines located in single-stranded areas [7]. The use of Taq-polymerase, for example Taq platinum high fidelity (Hifi), which is insensitive to the presence of uracil, leads to an increase in C-T-substitutions relative to the original strand. These substitutions cannot be observed when Pfu-polymerase is used, such as Phusion. Pfu-polymerase is unable to continue the synthesis of a strand in the presence of uracil. 5-methylcytosine is deaminated to thymine, in contrast to unmodified cytosine, and can be successfully amplified by Pfu-polymerase (*Fig. 1*). Thus, an increase in the number of C-T-substitutions in the analysis of ancient DNA allows one to distinguish methylated cytosines from unmethylated cytosines [5]. Deamination is a stochastic process: so, there is always methylated CpG-dinucleotides (MpG) not deaminated with time that are amplifiable as common CpG (*Fig. 1*). However, this method allows one to determine the methylation of not all cytosines, but only the deaminated ones. To identify methylated cytosines with single nucleotide resolution, it is necessary to increase the coverage depth. R. Smith *et al.* [8] demonstrated the possibility of assessing the single CpG-dinucleotide methylation status located in mobile genetic elements LINE-1 in ancient DNA from the skeletal remains of five North Americans ranging in age from approximately 200 to 4,000 years BC. When there is no need to determine MpG at single nucleotide precision, it is sufficient to analyze the number of CpG-TpG-substitutions at the DNA regions of interest. This approach was applied in reconstructing the DNA methylation maps of the Neanderthal, the Denisovan, and the Paleo-Eskimo human genomes [4]. It was demonstrated that

DNA methylation exhibits high conservation over time in bone marrow and in the hair follicle of present-day and ancient humans.

ANALYSIS OF ANCIENT DNA EPIGENOME

In their study of differentially methylated regions, Gokhman D. *et al.* found that the promoters of genes and the sequences of the *HOXD9* and *HOXD10* genes, key regulators of limb development, are methylated in the bone marrow of ancient samples (Neanderthal and the Denisovan humans) and unmethylated in the DNA of present-day humans [4]. In mouse model systems, it was shown that changes in the *HOXD* gene cluster expression, especially the *HOXD9* and *HOXD10* genes, lead to morphological changes [9] which resemble the differences in the limb organization of Neanderthals and modern humans. This fact suggests that epigenetic changes in the *HOXD* gene cluster play a key role in the limb evolution of modern humans. Moreover, a differentially methylated region was found within the *MEIS1* gene encoding a protein that regulates the *HOXD* gene cluster activity [4]. Information on the ancient DNA methylation of large genomic regions via C-T-substitution rates can be used to search for stretches with changes the in methylation level in the bone marrow and hair follicles of our ancestors. Such an analysis will allow us to detect both hypermethylated CpG-islands and also:

1) long (several hundred kbp to several million bp) partially methylated domains (PMD) which do not contain genes and colocalize with lamina-associated domains [10, 11];

2) DNA methylation valleys (DMV) (several kbp), hypomethylated in most tissues containing a large number of developmental genes and regions for transcription factor binding [12, 13], but hypermethylated in colon cancer cells [12];

3) extended regions of low methylation (canyons) (tens of kbp) recently discovered in hematopoietic stem cells [14]; and

4) epigenetic programs of intestinal inflammation that are characterized by hypermethylation of DMV, low CpG density, and active chromatin marks [15].

All of these studies are based on an analysis of the methylation level of genome regions, the length of which varies from several kbp to several million base pairs. Epigenetic analysis of ancient DNA, based on a search for C-T-substitution-rich regions, raises the possibility of assessing the adaptation signals and/or markers of diseases. However, this requires well-preserved tissues (brain, intestine, muscle, blood), which is common for remains found in permafrost, such as the remains of mammoths that lived in the Pleistocene (see below). In 2014, a unique effort was published on

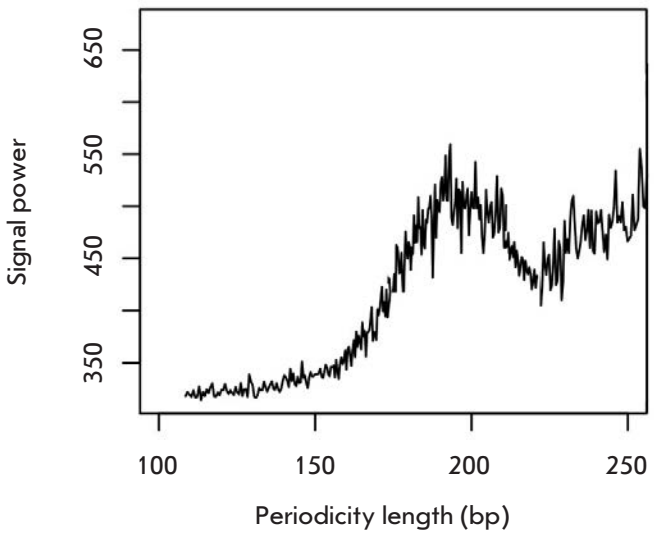

Fig. 2. Graph of the spectral density (power spectral estimation). Analysis of the region around genes transcription starts (+/- 1000 bp), correction with respect to the distribution of background readings in the analysis of the DNA of modern elephants was performed. We used the genome sequencing data of a baby mammoth found in 2009 in the downstream of the Khroma River (Prokhorchuk E.B. et al., unpublished data). The age of the finding exceeds 50,000 years.

an epigenetic map generated from the DNA of one hair follicle that belonged to a Paleo-Eskimo human. It allowed researchers to estimate the age at death of the individual [5]. This was done during a forensic investigation that showed the possibility of determining age based on the methylation level of certain CpG-dinucleotides [16]. Assuming that 6,000 years ago the external environment affected methylation the same way it does today, then based on modern databases one can determine the age of an ancient human. L. Orlando *et al.* showed that the Saqqaq individual (the Paleo-Eskimo era in Greenland) was relatively not young and, probably, about 35–40 years at death [5].

CONTAMINATION CHALLENGE OF ANCIENT DNA

Contamination of material with bacterial DNA is a significant obstacle when working with ancient DNA. It has recently been shown that the epigenetic characteristics of vertebrates (methylation of CpG) can be used for the separation of bacterial and ancient human genomic DNAs [17]. Methylated CpG-dinucleotides are found only in somatic vertebrate cells. Bacterial genome also contains methylated cytosines and adenines, but not in CpG. The MBD protein family contains a methyl-DNA-binding domain (MBD), which binds methylated DNA containing single methylated CpG

[18]. Affinity chromatography using MBD domains is a method routinely used for constructing the methylation maps of the genomes of different organisms. This method allows one to both unravel ancient methylomes and separate the DNA of ancient vertebrates and microorganisms. With the example of the Paleo-Eskimo Saqqaq individual, woolly mammoths (Yuka and Khroma), polar bears, and two equine species it was shown that DNA methylation survives in a variety of tissues, environmental contexts, and over a long temporal range of remains emergence (4,000 to 45,000 years BC). MBD enrichment affinity chromatography allows one to analyze ancient microbiota, as well as potentially pathogenic genomes [17].

TRANSCRIPTIONAL ACTIVITY OF ANCIENT GENES AS INFERRED FROM NUCLEOSOME MAPS

DNA methylation can serve as a marker of gene transcription repression, but the information is insufficient in order to establish whether the gene was expressed or not. To predict the transcriptional activity of a gene, more information is needed, such as histone modification, chromatin structure, and the transcription factors binding to the regulatory regions. The first attempts to work with ancient proteins have been made [19]. The sequencing of ancient DNA revealed an unexpected source of epigenetic information. L. Orlando *et al.* found periodicity in the nucleotide read depth [5]. The authors hypothesized that, instead of being the result of sequence alignment errors or sequencing artifacts, the observed periodicity patterns of the nucleotide read depth could be associated with the protection of DNA by nucleosome binding with a degradation of the linker regions either by DNases that enter the nucleus during cell death or by post-mortem strand breaks. In such a scenario, the observed read depth reflects nucleosome occupancy. Spectral methods of DNA analysis are used to search for hidden periodicities. Thus, in the case of relatively short sequences a Fourier transformation allows one to derive statistical criteria with a self-averaging property [20]. The application of the Fourier transform to the function that correlates the read depth with a coordinate in the genome reveals a strong peak at 180–190 nucleotides, indicating that the periodicity of coverage in sequencing coincides with the periodicity of chromatin organized into nucleosomes (*Fig. 2*). When analyzing the distribution of the 5' read depth, it turned out that the distances of a characteristic length of 100 nucleotides were associated with the periodicity of 10 nucleotides, coinciding with the length of a turn of the DNA helix: the nucleotides facing the nucleosomes will not mark the start of readings, because they are less available to nucleases. In ancient DNA, the positioning of nucleosomes stretching over 4 kbp around the CTCF binding sites was mapped with high precision and the nucleosome location negatively correlated with the DNA methylation levels. Actively transcribed areas can be found by an analysis of the DNase I hypersensitive sites located at the start of transcription [21]. It is assumed that open chromatin state regions are more sensitive to DNase I cleavage during apoptosis or after the death of an organism. Therefore, during full genome sequencing the read depth at the start of active gene transcription will be reduced in comparison with silent genes. Simultaneous consideration of the read depth in the region of a certain transcription start and information on DNase I hypersensitive sites from the ENCODE database opens up a possibility for determining the transcriptional activity of the respective genes.

PROSPECTS

By combining information on DNA methylation and DNase I hypersensitivity sites at transcription start sites we might be able to reconstruct the quantitative expression pattern of genes in ancient samples in the near future. If we are lucky to find a well-preserved fossils of the human brain, that will be a breakthrough in the study of ancient DNA and human evolution. Such a prospect is supported by the recent discovery of a woolly mammoth with well-reserved brain structures [22]. It is assumed that the main differences in the higher nervous activity of ancient and present-day humans will be located at the epigenetic level [23, 24]. ●

REFERENCES

1. Gerstein M.B., Kundaje A., Hariharan M., Landt S.G., Yan K.K., Cheng C., Mu X.J., Khurana E., Rozowsky J., Alexander R., et al. // Nature. 2012. V. 489. P. 91–100.
2. Briggs A.W., Stenzel U., Meyer M., Krause J., Kircher M., Paabo S. // Nucl. Acids Res. 2010. V. 38. P. e87.
3. Llamas B., Holland M.L., Chen K., Cropley J.E., Cooper A., Suter C.M. // PLoS One. 2012. V. 7. P. e30226.
4. Gokhman D., Lavi E., Prufer K., Fraga M.F., Riancho J.A., Kelso J., Paabo S., Meshorer E., Carmel L. // Science. 2014. V. 344. P. 523–527.
5. Pedersen J.S., Valen E., Velazquez A.M., Parker B.J., Rasmussen M., Lindgreen S., Lilje B., Tobin D.J., Kelly T.K., Vang S., et al. // Genome Res. 2014. V. 24. P. 454–466.
6. Smith O., Clapham A.J., Rose P., Liu Y., Wang J., Allaby R.G. // Sci Rep. 2014. V. 4. P. 5559.
7. Hofreiter M., Jaenicke V., Serre D., von Haeseler A., Paabo S. // Nucleic Acids Res. 2001. V. 29. P. 4793–4799.
8. Smith R.W., Monroe C., Bolnick D.A. // PLoS One. 2015. Published online 25 May.
9. Zakany J., Duboule D. // Curr. Opin. Genet. Dev. 2007. V. 17. P. 359–366.

10. Hansen K.D., Timp W., Bravo H.C., Sabunciyan S., Langmead B., McDonald O.G., Wen B., Wu H., Liu Y., Diep D., et al. // Nat. Genet. 2011. V. 43. P. 768–775.
11. Berman B.P., Weisenberger D.J., Aman J.F., Hinoue T., Ramjan Z., Liu Y., Noushmehr H., Lange C.P., van Dijk, C.M., Tollenaar R.A., et al. // Nat. Genet. 2012. V. 44. P. 40–46.
12. Xie W., Schultz M.D., Lister R., Hou Z., Rajagopal N., Ray P., Whitaker J.W., Tian S., Hawkins R.D., Leung D., et al. // Cell. 2013. V. 153. P. 1134–1148.
13. Nakamura R., Tsukahara T., Qu W., Ichikawa K., Otsuka T., Ogoshi K., Saito T.L., Matsushima K., Sugano S., Hashimoto S., et al. // Development. 2014. V. 141. P. 2568–2580.
14. Jeong M., Sun D., Luo M., Huang Y., Challen G.A., Rodriguez B., Zhang X., Chavez L., Wang H., Hannah R., et al. // Nat. Genet. 2014. V. 46. P. 17–23.
15. Abu-Remaileh M., Bender S., Raddatz G., Ansari I., Cohen D., Gutekunst J., Musch T., Linhart H., Breiling A., Pikarsky E., et al. // Cancer Res. 2015. V. 75 (10). P. 2120–2130.
16. Kader F., Ghai M. // Forensic Sci. Int. 2015. V. 249. P. 255–265.
17. Seguin-Orlando A., Gamba C., Sarkissian C.D., Ermini L., Louvel G., Boulygina E., Sokolov A., Nedoluzhko A., Lorenzen E.D., Lopez P., et al. // Sci. Repts. 2015. published online number: 11826.
18. Hendrich B., Bird A. // Mol. Cell Biol. 1998. V. 18. P. 6538–6547.
19. Welker F., Collins M.J., Thomas J.A., Wadsley M., Brace S., Cappellini E., Turvey S.T., Reguero M., Gelfo J.N., Kramarz A., et al. // Nature. 2015. V. 522. P. 81–84.
20. Lobzin V.V., Chechetkin V.R. // Physics-Uspekhi. 2000. V. 43. P. 55–78.
21. Crawford G.E., Holt I.E., Whittle J., Webb B.D., Tai D., Davis S., Margulies E.H., Chen Y., Bernat J.A., Ginsburg D., et al. // Genome Res. 2006. V. 16. P. 123–131.
22. Kharlamova A., Kurtova A., Chernikov V., Protopopov A., Boeskorov G., Plotnikov V., Ushakov V., Maschenko E. // Quaternary International. 2016. P. 86–93.
23. Zeng J., Konopka G., Hunt B.G., Preuss T.M., Geschwind D., Yi S.V. // Am. J. Hum. Genet. 2012. V. 91. P. 455–465.
24. Chopra P., Papale L.A., White A.T., Hatch A., Brown R.M., Garthwaite M.A., Roseboom P.H., Golos T.G., Warren S.T., Alisch R.S. // BMC Genomics. 2014. V. 15. P. 131.

Biosynthesis of poly(3-hydroxybutyrate-co-3-hydroxy-4-methylvalerate) by Strain *Azotobacter chroococcum* 7B

A.P. Bonartsev[1,2,*], G. A. Bonartseva[2], V. L. Myshkina[2], V. V. Voinova[1], T. K. Mahina[2], I. I. Zharkova[1], S. G. Yakovlev[2], A. L. Zernov[1], E. V. Ivanova[1], E. A. Akoulina[2], E. S. Kuznetsova[1], V. A. Zhuikov[2], S. G. Alekseeva[3], V. V. Podgorskii[4], I. V. Bessonov[5], M. N. Kopitsyna[5], A. S. Morozov[5], E. Y. Milanovskiy[6], Z. N. Tyugay[6], G. S. Bykova[6], M. P. Kirpichnikov[1], K. V. Shaitan[1]

[1]Faculty of Biology, M.V.Lomonosov Moscow State University, Leninskie gory, 1-12, Moscow, 119234, Russia

[2]A.N. Bach Institute of Biochemistry, Research Center of Biotechnology of the Russian Academy of Sciences, 33, bld. 2 Leninsky Ave., Moscow, 119071, Russia

[3]JSC «Institute of Plastics», Petrovskiy proezd, 35, Moscow, 111024, Russia

[4]Federal scientific-clinical center of physics-chemical medicine, Federal medical-biological agency, Malaya Pirogovskaya str., 1a, Moscow, 119435, Russia

[5]Bauman Moscow State Technical University, 5, 2-nd Baumanskaya, Moscow, 105005, Russia

[6]Faculty of Soil Science, M.V.Lomonosov Moscow State University, Leninskie gory, 1-12, Moscow, 119234, Russia

*E-mail: ant_bonar@mail.ru

Received October 26, 2015; in final form, June 21, 2016

ABSTRACT **Production of novel polyhydroxyalkanoates (PHAs), biodegradable polymers for biomedical applications, and biomaterials based on them is a promising trend in modern bioengineering. We studied the ability of an effective strain-producer *Azotobacter chroococcum* 7B to synthesize not only poly(3-hydroxybutyrate) homopolymer (PHB) and its main copolymer poly(3-hydroxybutyrate-co-3-hydroxyvalerate) (PHBV), but also a novel copolymer, poly(3-hydroxybutyrate-co-3-hydroxy-4-methylvalerate) (PHB4MV). For the biosynthesis of PHB copolymers, we used carboxylic acids as additional carbon sources and monomer precursors in the chain of synthesized copolymers. The main parameters of these polymers' biosynthesis were determined: strain-producer biomass yield, polymer yield, molecular weight and monomer composition of the synthesized polymers, as well as the morphology of *A. chroococcum* 7B bacterial cells. The physico-chemical properties of the polymers were studied using nuclear magnetic resonance spectroscopy (NMR), differential scanning calorimetry (DSC), contact angle test, and other methods. *In vitro* biocompatibility of the obtained polymers was investigated using stromal cells isolated from the bone marrow of rats with the XTT cell viability test. The synthesis of the novel copolymer PHB4MV and its chemical composition were demonstrated by NMR spectroscopy: the addition of 4-methylvaleric acid to the culture medium resulted in incorporation of 3-hydroxy-4-methylvalerate (3H4MV) monomers into the PHB polymer chain (0.6 mol%). Despite the low molar content of 3H4MV in the obtained copolymer, its physico-chemical properties were significantly different from those of the PHB homopolymer: it has lower crystallinity and a higher contact angle, i.e. the physico-chemical properties of the PHB4MV copolymer containing only 0.6 mol% of 3H4MV corresponded to a PHBV copolymer with a molar content ranging from 2.5% to 7.8%. *In vitro* biocompatibility of the obtained PHB4MV copolymer, measured in the XTT test, was not statistically different from the cell growth of PHB and PHBV polymers, which make its use possible in biomedical research and development.**

KEYWORDS ***Azotobacter chroococcum* 7B; poly(3-hydroxybutyrate); poly(3-hydroxybutyrate-co-3-hydroxy-4-methylvalerate); biosynthesis; crystallinity; biocompatibility; bone marrow stromal cells.**

INTRODUCTION

Intensive development of such biomedical fields as regenerative medicine, bioengineering (including tissue engineering), biopharmaceuticals, and nanobiotechnology has increased demand for the development of new biomaterials, especially biocompatible and biodegradable polymers. A variety of natural and synthetic polymers are used as materials for the manufacture of

medical devices and formulations, including polyhydroxyalkanoates (PHAs), polyanhydrides, polyalkylcyanoacrylates, polyphosphazenes, polyphosphoesters, polyorthoesters, some polysaccharides (chitosan, hyaluronic acid, agarose, dextran, alginates, chondroitin sulfate), and proteins (collagen, fibrin, silk fibroin, spidroin, gelatin) [1–5]. These polymers are used in medical implants in reconstructive surgery [4, 5], tissue engineering [3, 6, 7], for creating new dosage forms in biopharmaceutics [8, 9], new dental materials, and they have other applications [1, 2].

Despite the wide range of polymers used in medicine, the vast majority of them are produced by chemical synthesis or isolated from natural raw materials (algae, higher plants, mushrooms, crustaceans, tissues of domestic animals). Unfortunately, the methods used in the chemical synthesis and isolation of polymers from natural raw materials cannot yield the full range of properties required for biomedical polymers. The obtained polymers require deep, and very expensive, purification, must fulfill very narrow requirements for chemical structure and properties, as well as be biologically safe, etc. Additionally, synthetic polymers and the products of their biodegradation may be toxic, while natural polymers may display pronounced immunogenicity or be contaminated with viruses or prion proteins [10, 11].

Biodegradable poly(3-hydroxyalkanoates), poly(3-hydroxybutyrate) (PHB) and its copolymers (according to the Russian chemical nomenclature of macromolecular compounds and IUPAC [12]), attract particular attention among developed and used biomedical polymers. In contrast to natural polymers (chitosan, alginate, dextran, collagen, etc.) and chemically synthesized polymers, PHAs are produced by biotechnological methods that allow one to achieve a high degree of purity, and to control and specify the physico-chemical properties of the biopolymers within narrow limits during their biosynthesis. PHAs have a set of unique properties: high mechanical strength and thermal plasticity that allows easy processing and obtainment of a wide range of products, ability to form composites with synthetic polymers, inorganic materials, and medicinal products, complete biodegradability to non-toxic products, biocompatibility (including hemocompatibility) with human and animal tissues and organs, and environmental safety. Therefore, PHAs are considered promising for use in medicine [13–16].

PHAs also have a unique nanostructure. As partially crystalline compounds, PHAs can form various supramolecular structures, such as lamellae and spherulites. Such a partially crystalline structure and morphology largely defines the biological properties of PHAs, such as the kinetics of its biodegradation [17, 18].

However, PHAs and other polymeric materials, such as PHB homopolymer, can have certain disadvantages, as well: high hydrophobicity and crystallinity, long-term biodegradation and low plasticity, which in some cases severely limits their use as bioengineered materials in medicine, for example for the manufacture of vessel grafts [19, 20]. Therefore, the development of novel biotechnological methods for obtaining new PHB copolymers for biomedical applications with an optimum combination of the physico-chemical and biological properties of the biomaterials produced from them is considered the most promising trend in modern bioengineering [1, 2, 13–16].

Previously, we had demonstrated that it was possible to biosynthesize different PHB copolymers by the high-performance PHAs strain-producer *Azotobacter chroococcum* 7B using a variety of methodological approaches and had conducted a comprehensive study of the physico-chemical and biological properties of the resulting polymers. This strain is characterized by an ease of culturing and biotechnological process (it requires only the most basic equipment, does not require highly specific culture media, gas feeding, high-precision control of specific parameters, etc.), high productivity (high biomass yield, polymer and dry biomass content in cells up to 80% and above), and high molecular weight of the synthesized polymer (more than 1.5×10^6 Da). These characteristics are extremely important for the biotechnological production of polymers for biomedical applications, since they require technically simple and deep purification, in addition to an assured efficient production [15, 21]. However, these strain-producers have certain limitations in the synthesis of PHB copolymers containing monomers of 3-hydroxycarboxylic acids with a chain length of more than five carbon atoms [22, 23]. The biosynthesis of a new PHB copolymer, poly(3-hydroxybutyrate-co-3-hydroxy-4-methylvalerate), has been demonstrated using such bacterial producers as *Ralstonia eutropha*, *Burkholderia* sp., *Chromobacterium* sp., which can biosynthesize PHAs with short- and long-chain monomers of carboxylic acids [24–27]. However, the chemical structure of the copolymer (its monomer, 3-hydroxy-4-methylvalerate, has a Y-shaped R-group) makes it particularly interesting for the study of its biosynthesis by such bacterial strain-producers as *Azotobacter* sp. due to these restrictions.

The possibility of biosynthesizing new PHB copolymers through such bacterial strain-producers as *Azotobacter* sp. is of great scientific and practical interest. We examined the possibility of biosynthesizing a new PHB copolymer, poly(3-hydroxybutyrate-co-3-hydroxy-4-methylvalerate), by the highly efficient PHA strain-producer *A. chroococcum* 7B, determined

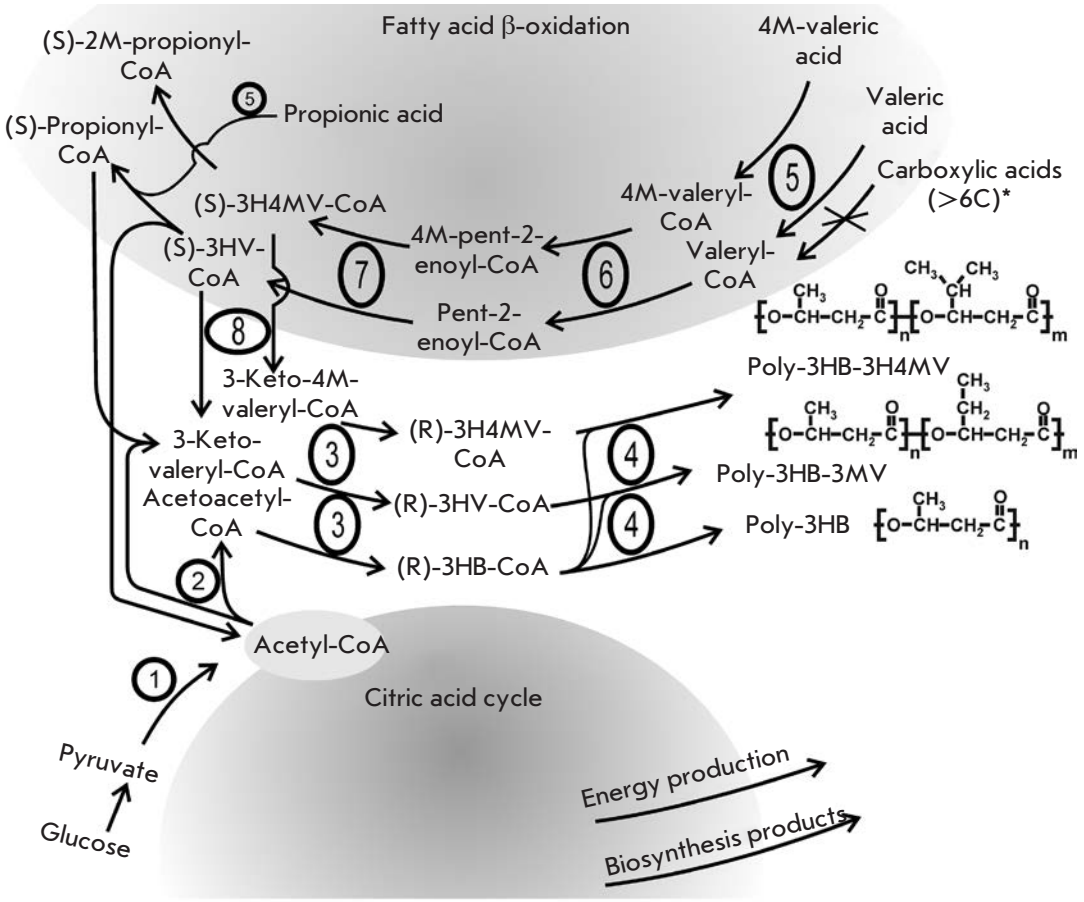

Fig. 1. Scheme of biosynthesis of PHB and its copolymers by *A. chroococcum* 7B. 1 – pyruvate dehydrogenase complex; 2 – β-ketothiolase; 3 – NADPH-dependent acetoacetyl-CoA reductase; 4 – short chain carboxylic acids PHA-polymerase; 5 – acyl-CoA synthase; 6 – acyl-CoA dehydrogenase; 7 – enoyl-CoA hydratase; 8 – NADH-dependent acetoacetyl-CoA reductase. Abbreviations: 4M – 4-methyl-; 2M – 2-methyl-; 3HB – 3-hydroxybutyrate-; 3HV – 3-hydroxyvalerate; 3H4MV – 3-hydroxy-4-methylvalerate; Poly-3HB-3H4MV – poly(3-hydroxybutyrate-co-3-hydroxy-4-methylvalerate); Poly-3HB-3HV – poly(3-hydroxybutyrate-co-3-hydroxyvalerate); poly-3HB – poly(3-hydroxybutyrate).

its physico-chemical properties, as well as its *in vitro* biocompatibility.

MATERIAL AND METHODS

Reagents

Sodium salt of valeric acid or sodium valerate (VA), sodium salt of 4-methylvaleric acid or sodium methylvalerate (4MVA), sodium salt of hexanoic acid or sodium hexanoate (HxA); components of the culture medium: $K_2HPO_4 \cdot 3H_2O$, $MgSO_4 \cdot 7H_2O$, NaCl, $Na_2MoO_4 \cdot 2H_2O$, $CaCO_3$, $FeSO_4 \cdot 7H_2O$, sodium citrate, $CaCl_2$, KH_2PO_4, sucrose, agar, phosphate-buffered saline (PBS). All reagents were purchased from Sigma Aldrich (Germany) and used "as purchased."

Biosynthesis of polymers

Highly efficient PHB strain-producer *A. chroococcum* 7B, non-symbiotic nitrogen-fixing bacteria capable of overproducing the polymer (up to 80% of the cells' dry weight) was used for polymer biosynthesis [28–31]. The strain was isolated from the rhizosphere of wheat (sod-podzolic soil) and maintained in Ashby's medium containing 0.2 g/l $K_2HPO_4 \cdot 3H_2O$, 0.2 g/l $MgSO_4 \cdot 7H_2O$, 0.2 g/l NaCl, 0.006 g/l $Na_2MoO_4 \cdot 2H_2O$, 5.0 g/l $CaCO_3$, 20 g/l of sucrose and 20 g/l agar. All experiments were carried out under laboratory conditions. To achieve high productivity, the culture of *Azotobacter* cells was grown in shake flasks on a microbiological Innova 43 shaker (New Brunswick Scientific, USA) with constant stirring and at 30 ° C in Burk medium under conditions of excess car-

Table 1. The biosynthesis of PHB copolymers by *A. chroococcum* 7B on a sucrose-containing culture medium supplemented with salts of carboxylic acids

Substrate	Time of addition of salts of the carboxylic acid to the culture medium, h	Biomass yield, g/l of the medium	PHA content in biomass, % of dry cells' weight	Molecular weight of PHA, kDa	Content of 3HB/3H4MB in the copolymer, mol. %
Sucrose, 50 mM	-	5.8 ± 0.6	83.4 ± 3.1	1710	0
S + 20 mM PA	12	2.2 ± 0.7*	63.3 ± 3.3*	890	2.9
S + 5 mM VA	12	4.4 ± 0.9*	76.2 ± 3.0*	1290	2.5
S + 20 mM VA	0	3.1 ± 1.3*	67.4 ± 4.6*	1020	7.8
S + 20 mM VA	12	3.5 ± 0.8*	70.5 ± 3.2*	1270	21.3
S + 20 mM 4MVA	0	2.6 ± 1.2*	71.2 ± 4.8*	620	0.04
S + 5 mM 4MVA	12	3.7 ± 0.8*	79.3 ± 3.2*	1390	0.14
S + 10 mM 4MVA	12	3.6 ± 0.9*	78.8 ± 3.4*	1340	0.23
S + 20 mM 4MVA#	12	3.4 ± 0.9*	76.7 ± 3.3*	1300	0.60
S + 35 mM 4MVA	12	2.7 ± 0.8*	71.4 ± 3.5*	1130	0.32
S + 20 mM HxA	12	2.7 ± 0.7*	64.3 ± 3.7*	1020	0

* P <0.05 compared with the "Sucrose" (S) group, n = 8.
# – Experimental data obtained in conditions of PHB4MV copolymer biosynthesis for the given line are shown in *Fig. 2, 4* and in *Tab. 2*.

bon source in a medium containing 0.4 g/l $MgSO_4 \cdot 7H_2O$, 0.01 g/l $FeSO_4 \cdot 7H_2O$, 0.006 g/l $Na_2MoO_4 \cdot 2H_2O$, 0.5 g/l sodium citrate, 0.1 g/l $CaCl_2$, 1.05 g/l $K_2HPO_4 \cdot 3H_2O$, 0.2 g/l KH_2PO_4 and 17 g/l (50 mM) sucrose as the main carbon source. The volume of the medium in the flask was 100 ml, which at high productivity of the *A. chroococcum* 7B strain with sampling at the end of the experiment allows one to analyze the biosynthetic processes and have a sufficient number of samples for statistical processing (each experiment was performed in eight replicates). The salts of carboxylic acids (propionic, valeric, 4-methylvaleric, hexanic) were added to the culture medium as additional carbon sources for the biosynthesis of the PHB copolymers. VA in a concentration of 5 and 20 mM was added to the culture medium immediately and after 12 hours of culturing as a monomer precursor of 3-hydroxyvaleriate within the PHA composition. These concentrations and time points were selected to produce PHBV copolymers with different contents of 3-hydroxyvaleriate in the copolymer chain [28, 29]. 4MVA and HxA were added to the culture medium as potential monomer precursors of 3-hydroxy-4-methylvalerate and 3-hydroxyhexanoate in the composition of the synthesized PHAs at a concentration of 20 mM at 0 hour and concentration of 5, 10, 20 and 35 mM after 12 hours of culturing of the strain-producer. These concentrations of the carboxylic acid were selected by analogy with the other carboxylic acids used for the biosynthesis of new PHB copolymers and according to [24–27, 29]. The strain-producer was cultured for 72 hours. The optical density of the culture medium was monitored by nephelometry. The growth and accumulation of the polymer was also monitored by light microscopy using a Biomed-1 microscope ("Biomed", Russia) with a digital camera. The parameters of the copolymers biosynthesis: the biomass yield (g/l medium) and total polymer content in the cells (% by weight of dry cell weight) (Table 1) were measured according to the previously developed techniques. The process of isolation and purification of the polymer from strain-producer biomass includes chloroform extraction, filtration, precipitation with isopropyl alcohol, purification by multiple cycles of dissolution-precipitation, and drying [28–31].

Study of the chemical composition of the polymer by nuclear magnetic resonance spectroscopy (NMR)

^1H NMR spectra of 1% (w/v) polymer solutions in deuterated chloroform were recorded on a 300 MHz

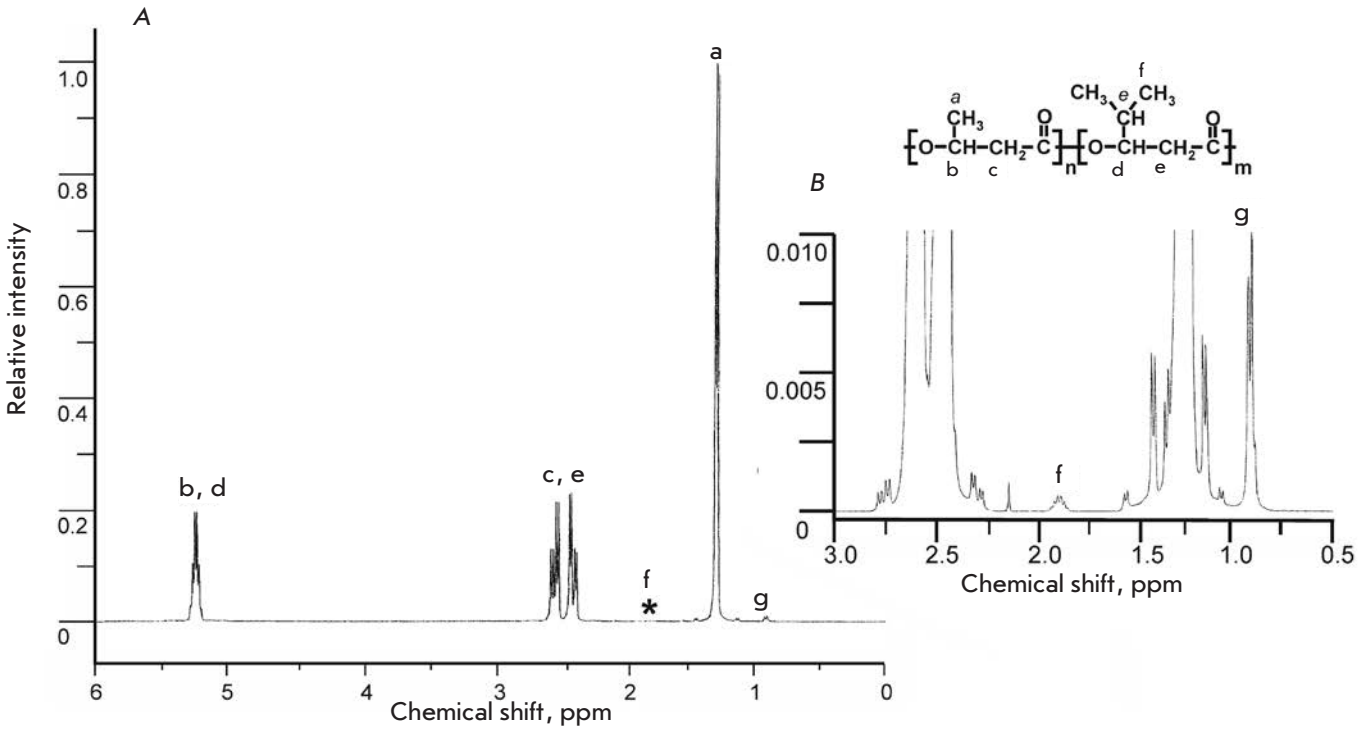

Fig. 2. ^{1}H 500 MHz NMR spectrum of PHB4MV copolymer. A – PHB polymer chain: a – CH_3 (*s*), b – CH (*b*), c – CH_2 (*b*), poly(3-hydroxy-4-methylvalerate) polymer chain: d – CH_2 (*s*), e – CH_3 (*s*), f – CH (*b*), g – CH_2 (*b*), 1 – side groups, 2 – polymer backbone; *an enlarged section of the graph is shown in the inset (*B*)

spectrometer MSL-300 (Bruker, Germany) using the following experimental parameters: temperature 313 K, relaxation delay of 2.5 s, width of the spectral window of 4,000 Hz, and a 500 MHz spectrometer Bruker Avance III with a three-channel TCI Prodigy cryodetector (Bruker, Germany) with the following experimental parameters: temperature of 310 K, relaxation delay of 3.3 s, and width of the spectral window of 10,000 Hz. The chemical shifts (in ppm) were set based on the residual $CDCl_3$ proton signal (7.24 ppm by TMC). The percentage of 3-hydroxyvaleriate content (3HV) in the PHBV copolymer was calculated by the ratio of integrated intensities of the signal of the methyl group of the hydroxyvalerate residue (0.89 ppm) and the sum of signals of the methyl group of the hydroxyvalerate residue (0.89 ppm) and methyl group of the hydroxybutyrate residue (1.27 ppm) [29, 31]. The percentage of 3-hydroxy-4-methylvalerate (3H4MV) content in the PHB4MV copolymer was calculated by the ratio of integrated intensities of the sum of signals of the 4-methyl group (g) (0.90 ppm) and -CH group (f) (1.91 ppm) and the sum of integrated intensities of signals of the 4-methyl group and -CH-group of the 3-hydroxy-4-methylvalerate residue and methyl group of the 3-hydroxybutyrate residue (1.27 ppm) (*Fig. 2*).

Determination of the molecular weight of the polymers

The molecular weights (M_w) of the polymers were determined by gel filtration chromatography (GPC). The data obtained by GPC were correlated with viscometric data [28–31].

Preparation of experimental samples of polymer films

Experimental samples of polymer films with a thickness of 40 μm and diameter of 30 mm were obtained in order to study the physico-chemical properties and *in vitro* growth of cells on polymeric films. The polymers synthesized by bacteria, PHB, PHBV1 (2.5 mol% of 3HV), PHBV2 (7.8 mol% of 3HV) and PHB4MV, whose characteristics are given in Table 2, were used to produce the samples. The polymer films were prepared from a 2% (w/v) solution of the corresponding polymers in chloroform by evaporation of the solvent on a glass substrate. The weight of the films was measured using AL-64 scales (max = 60 g, d = 0.1 mg, Acculab, USA) and was 61 ± 8 mg. The film's thickness as measured by magnetic thickness gauge was 38 ± 6 mm. Prior to working with the cell cultures, the films were sterilized by autoclaving; they were pre-incubated in distilled water at 37 °C in an incubator (EU 1/80 SPU, Russia) for 2 hours [30, 31].

Differential Scanning Calorimetry

The thermophysical characteristics of the polymer films (melting point and crystallization point, melting heat and crystallization heat) were measured by differential scanning calorimetry according to [32, 33]. The temperatures of start and maximum of the melting peak or crystallization were designated as T_m^0, T_m^{peak} and T_c^{peak}, respectively. PHA crystallinity (*Xc*) was calculated according to [33]:

$$X_c = \Delta H_m(PHA)/\Delta H_0\, m(PHB) \times 100\%,$$

where ΔH_0 m(PHB) is the theoretical value of the thermodynamic melting enthalpy, which for 100% crystalline PHB could be 146.6 J/g [34], and ΔH_m(PHA) is the experimental melting enthalpy of the corresponding sample of PHA. Calculations of the degree of crystallinity and melting points of the samples were generated for the data obtained in the second polymers heating cycle; the crystallization temperature is based on the data obtained in the first cooling cycle. The data are presented as mean values of three measurements.

Contact angle measurement

The hydrophilicity of the polymer films' surface was evaluated by measuring the contact angle formed between a water droplet and the polymer film's surface, using a digital inclinometer, Drop Shape Analysis System DSA100 (KRÜSS, GmbH, Germany), according to [30, 31].

Study of the stromal cells growth on polymer films

Stromal cells (BMSCs) were isolated from bone marrow femurs of 3-day-old Wistar rats according to standard procedures [35]. The animals were killed by decapitation, the femurs were removed, epiphyses were cut, and bone marrow was washed out of the diaphysis with a syringe (2 mm, 27G needle). The resulting suspension was incubated in a DMEM medium with type 1 collagenase (1075 U/ml) ("PanEco", Russia) for 1 h at 37 ˚C, centrifuged (10 min, 100 rpm), and the precipitate was precipitated on the culture plastic. The growth medium was changed the next day, and the cells were further cultivated until the formation of a primary monolayer culture.

The cell viability was assessed using the XTT test, an analogue of the widely used MTT test [30, 31, 36]. This test is based on the conversion of uncolored tetrazolium salts into colored formazan compounds by the action of NADPH-dependent oxidoreductases, and it allows one to evaluate the activity of mitochondrial dehydrogenases. We used the XTT set (XTT Cell Proliferation Kit, Biological Industries, Israel).

The aim of our work was not to check the cytotoxicity, but to identify cell proliferation in matrixes: i.e., the biocompatibility of the polymeric films. The cells were maintained in a DMEM medium (Dubecco's Modified Eagle Medium, "PanEco", Russia) with 10% fetal calf serum (Biological Industries, Israel), 100 IU/ml penicillin and 100 μg/ml streptomycin ("PanEco") at 37 ˚C in atmosphere with 5% CO_2. The medium was changed every 3 days. The sterile samples of PHB, PHBV1, and PHB4MV films (sterilization by autoclaving) (n = 6) were placed into the wells of a 96-well plate, and the cell suspension was applied to the top in a concentration of 1,500 cells per sample. The second-passage cells were used, since the proliferation of the first-passage cells was not fully stable, and there were significant differences in the growth of the first-passage cells on polymeric films in repeated experiments. We determined the viability of the cells cultured on the polymer films after 1, 3, 7 days as it was important to assess the dynamics of this parameter. The growth of the cells was stable within this time interval, and the data points allow one to most comprehensively describe the dynamics of BMSCs growth on the films. The culture medium was removed from the wells after the pre-determined time, 100 μl of fresh medium was added into new clean wells, and our samples were transferred therein. This was done in order to take into account only the cells attached to the polymer substrate and to ignore the cells that could detach from the substrate and attach to the polymeric plate. 50 μl of a freshly prepared XTT solution (as described) was added to the wells. After 4 h of incubation at 37 ˚C with gentle rocking, the samples were removed and their optical density was measured on the Zenyth 3100 Microplate Multimode Detector (Anthos Labtec Instruments GmbH, Austria) at 450 nm against 690 nm [30, 31].

Statistical analysis

Statistical processing of the polymers' biosynthetic parameters, their contact angles and *in vitro* biocompatibility in a cell culture was performed using the SPSS/PC+ Statistics™ 12.1 (SPSS) software package. One-way ANOVA was used. The data in the tables and in the figures are presented as mean values and standard error of the mean (M ± SD) at a significance level of $P < 0.05$. The number of measurements (n) is given in the figure captions and footnotes to the tables. The mean values of the polymers' physico-chemical properties calculated from the three measurements are presented.

RESULTS AND DISCUSSION

Biosynthesis of PHB copolymers using additional sources of carbon

The results of the study of PHB copolymers biosynthesis by the strain-producer *A. chroococcum* 7B in

the presence of various additional carbon sources in a culture medium (salts of propionic, valeric, 4-methylvaleric, and hexanoic acids) are shown in *Tab. 1*. The results of the PHBV copolymer biosynthesis study confirm previously obtained data: 3-hydroxyvaleriate monomers are incorporated into the PHBV copolymer chain if valeric and propionic acids are used as additional carbon sources, whereas the presence of a longer chain hexanoic acid does not result in the synthesis of a copolymer. The molar content of 3HV in the synthesized copolymer is directly proportional to the concentration of the VA added to the culture medium. The molecular weight of the PHBV polymer was lower than that of the PHB homopolymer, which is probably due to the inhibitory effect of valerate on the polymer synthesis. If sucrose is the only carbon source in the medium, the strain produces high-molecular PHB (1710 kDa) [29, 37–39].

Various additional carbon sources are used in order to improve the parameters of polymer biosynthesis. It has been shown that additional carbon sources not only influence the molecular weight of the synthesized polymers, but also result in the synthesis of new copolymers with modified physicochemical and biomedical properties [29–31, 40–46].

Using this method, we demonstrated the possibility of biosynthesizing the PHB4MV copolymer, a novel one for the strain-producer *A. chroococcum* 7B, by adding 4MVA as an additional carbon source and a precursor of the 3H4MV monomer in the copolymer chain to the culture medium. The incorporation of 3H4MV residues into the synthesized PHB4MV polymer was also confirmed by ^{1}H NMR spectroscopy data. In the ^{1}H NMR spectrum, the 4-methyl group (f) and -CH-group (g) of the 3H4MV monomer are represented by signals at 0.90 and 1.91 ppm, respectively (*Fig. 2*), whereas the PHB homopolymer and PHBV copolymer have no signals in this range. We assume that, similarly to PHBV, the obtained copolymer is a multiblock copolymer and its synthesis proceeds as follows: 4MVA → 4-methylvaleryl-CoA → 3-keto-4-methylvaleryl-CoA → *D*-3-hydroxy-4-methylvaleryl-CoA → 3H4MV in the composition of PHB4MV; i.e. similarly to PHBV biosynthesis: VA → valeryl-CoA → 3 ketovaleryl-CoA → *D*-3-hydroxyvaleryl-CoA → 3HV as part of PHVB [29, 37–39] (*Fig. 1*).

The maximum incorporation of 3H4MV monomers into the synthesized PHB4MV polymer is 0.6 mol% for the case when 4MVA is added to the culture medium in a concentration of 20 mM as an additional carbon source; at other concentrations of the precursor carboxylic acid, the incorporation of monomers was much lower. Nevertheless, synthesis of this copolymer is confirmed.

PhbC-encoded PHB synthase is a polymerase of short-chain carboxylic acids, such as 3-hydroxybutyrate and 3-hydroxyvalerate. This polymerase is unable to utilize medium- and long-chain 3-hydroxycarboxylic acids, namely those longer than 3-hydroxyvaleric acid (5C 3-hydroxycarboxylic acid), to synthesize PHAs: i.e., this enzyme cannot incorporate 3-hydroxyhexanoic acid and 3-hydroxyheptanoic acid into the growing PHA chain [22, 23]. Nevertheless, we used HxA as an additive, because as a 4MVA isomer it can serve as a control because it is known that the presence of HxA does not lead to the synthesis of the PHB copolymer by *A. chroococcum* cells. The effect of HxA in itself on the biosynthesis process had to be controlled, though. Our data confirm the restriction on the length of the monomers used by PHB-synthase, which appears to be associated with the strict specificity of this enzyme with respect to the substrates used for polymer synthesis. Incorporation of 3-hydroxy-4-methylvalerate residues only confirms this restriction, because in spite of the fact that 3-hydroxy-4-methylvalerate is a residue of 6C 3-hydroxycarboxylic acid, its side chain is branched and, therefore, the length of the side chain is not increased. However, a linear molecule, 3-hydroxyhexanoic acid (6C linear 3-hydroxycarboxylic acid), cannot be incorporated into the growing polyester chain by the enzyme, for the same reasons.

Interestingly, the addition of VA and 4MVA to the culture medium causes a slight decrease in the molecular weight of the synthesized polymer that can be explained by an inhibitory effect of carboxylic acids on PHA biosynthesis (*Tab. 1*). However, the addition of 4MVA to the culture medium immediately, rather than after 12 hours, results not only in a considerable decrease in the molecular weight of the polymer, but also the PHB4MV copolymer is hardly produced at all. A similar effect was observed in the case of initial addition of VA to the culture medium, which resulted in the synthesis of a PHBV copolymer with a much lower content of 3HV monomers. Reduction of the molecular weight is observed even in the case of addition of HxA to the culture medium, although the corresponding copolymer is not synthesized. This may also be due to the inhibitory action of carboxylic acids on PHB-synthase, which leads to a decrease in the incorporation of the molecular precursor into a growing copolymer chain in the early stages of polymer biosynthesis, even though in theory it must, in contrast, lead to the synthesis of copolymers with a higher content of 3HV and 3H4MV.

The effect of carboxylic acids on polymers biosynthesis is confirmed by the results of the study of *A. chroococcum* 7B culture growth. The results obtained indicate that the addition of carboxylic acids to the medium results in a marked inhibition of cell growth, reduced polymer content, and, consequently, polymer production, and the degree of the inhibitory effect on

cell growth depends on the nature of the chemical additive [29]. For example, despite the fact that the use of HxA as an additional carbon source does not lead to a copolymer synthesis, HxA significantly inhibits cell growth and the production of the polymer (*Tab. 1*).

Despite a slight decrease in PHB4MV biosynthesis parameters, the high productivity (biomass yield, 3.4 g/l; copolymer content, 76.7%) of the strain-producer and high molecular weight of the copolymer (1.3×10^6) should be noted. Biosynthesis of PHB4MV has previously been demonstrated using different producers: *R. eutropha*, *Burkholderia* sp, *Chromobacterium* sp. However, the polymer content in the cells of the producer-strains rarely exceeded 50% and the biotechnological process required highly specific technical conditions that may significantly restrict the use of these techniques for the production of new polymers for biomedical applications. The biocompatibility of the synthesized copolymers was not tested, probably due to the challenges posed by the developed techniques [24–27]. Therefore, it appears particularly important to use a highly productive and hardy strains-producer such as *A. chroococcum* 7B to obtain novel copolymers.

The addition of carboxylic acids to the culture medium also causes changes in the morphology of bacterial cells (*Fig. 3*). *A. chroococcum* is characterized by a high tendency toward cell pleomorphism, and this effect can be attributed to it. For example, if valeric acid was added in low concentrations (5 mM) the morphology would remain almost unchanged, but the addition of VA in relatively high concentrations (20 mM) resulted in a marked change in cell morphology: coccoid cells were transformed into bacillar forms (*Fig. 3B*). The addition of 20 mM HxA resulted in the appearance of filamentous cells, even though coccoid and bacillary forms were also present (*Fig. 3B*). This effect of carboxylic acids on the morphology of bacterial cells is similar to the well-known effect of various stress-inducing agents (acids, alkalis, peptone) on a cell's shape [47, 48].

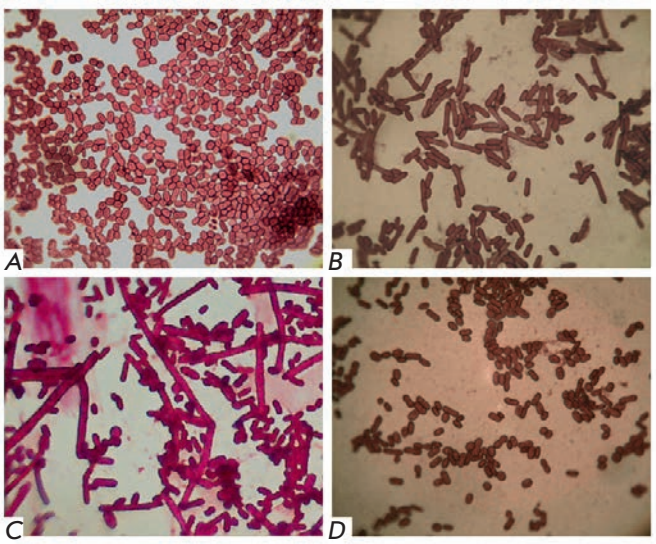

Fig. 3. The effect of adding carboxylic acids to the culture medium on the morphology of strain-producer *A. chroococcum* cells (light microscopy, ×900). A – S + 5 mM VA (added after 12 hours), after 72 hours of culturing; B – S + 20 mM VA (added t 0 h) after 72 h of culturing; C – S + 20 mM HxA (added after 12 hours) after 72 hours of culturing; D – S + 20 mM 4MVA (added after 12 hours), after 72 hours of culturing

Study of the physico-chemical properties of the polymers

The study of the physico-chemical properties of the polymers synthesized by strains of *A. chroococcum* 7B revealed a significant difference between the thermo-physical and hydrophilic properties of PHB copolymers, PHBV1 (2.5 mol% 3HV), PHBV2 (7.8 mol% 3HV) and PHB4MV, as well as PHB homopolymer, despite the low molar content of 3H4MV and 3HV in the PHBV1 and PHB4MV copolymers, respectively (*Tab. 2*).

Fig. 4 shows the DSC thermograms of the PHBV and PHB4MV copolymers compared to PHB. The thermogram of polymers melting contains the expressed melting peaks of semi-crystalline polymers and their crystallization peaks. The melting peaks of the PBHV and PHB4MV copolymers compared to the PHB homopolymer are characterized by:

– a slight change in the melting peak, indicating the absence of a significant change in the melting point of the copolymers;

– a shift of the PHB4MV crystallization peak to higher temperatures, indicating an increase in the crystallization temperature of the copolymer; and

– a decrease in the area of the melting peak, indicating a decrease in the melting enthalpy and accordingly crystallinity of the copolymers.

Calculation of the thermo-physical parameters obtained from the analysis of DSC thermograms data is shown in *Table 2*. As can be seen both the PHBV and PHB4MV copolymers have a much lower degree of crystallinity than PHB (21.9 and 25.1%, respectively), and the new PHB4MV copolymer has an even larger drop in the degree of crystallinity than the PHBV1 copolymer, even though the molar content of 3H4MV in PHB4MV is only 0.6 compared to 2.5% of 3HV in PHBV. However, PHB4MV has a degree of crystallinity comparable to that of the PHBV2 copolymer, in which the molar content 3HV is 7.8%. Partially, this drop in the crystallinity of the copolymers may be due to a lower molecular weight (by more than 300 kDa in comparison

Table 2. Physicochemical properties of the PHB copolymers obtained in *A. chroococcum* 7B cells.

Polymer	Chemical composition			Therophysical properties			Hydrophility
	3HV content, mol. %	Molecular mass, kDa	M_w/M_n	Melting point (zero and peak) (T_m^0/ T_m^{peak}, °C)	Crystallization point (peak) (T_c^{peak}, °C)	Crystallinity (X_c), %	Contact angle, °
PHB	0	1710	1.7	166.8/176.9	62.2	86.6*/74.7**	70.1 ± 2.6
PHBV1	2.5	1290	1.9	166.0/174.8	60.3	56.4/52.8	70.7 ± 2.2
PHBV2	7.8	1020	1.8	161.2/169.0	66.3	47.5/45.2	76.4 ± 2.3*
PHB4MV	0.6	1300	2.0	169.9/177.3	75.1	58.0/49.6	75.1 ± 1.1*

* Calculated for the first heating cycle.
** Calculated for the second heating cycle.
Note. All columns except the last one contain mean data calculated for three measurements; in the last column "contact angle" – * $p < 0.05$ when compared to PHB group, $n = 10$.

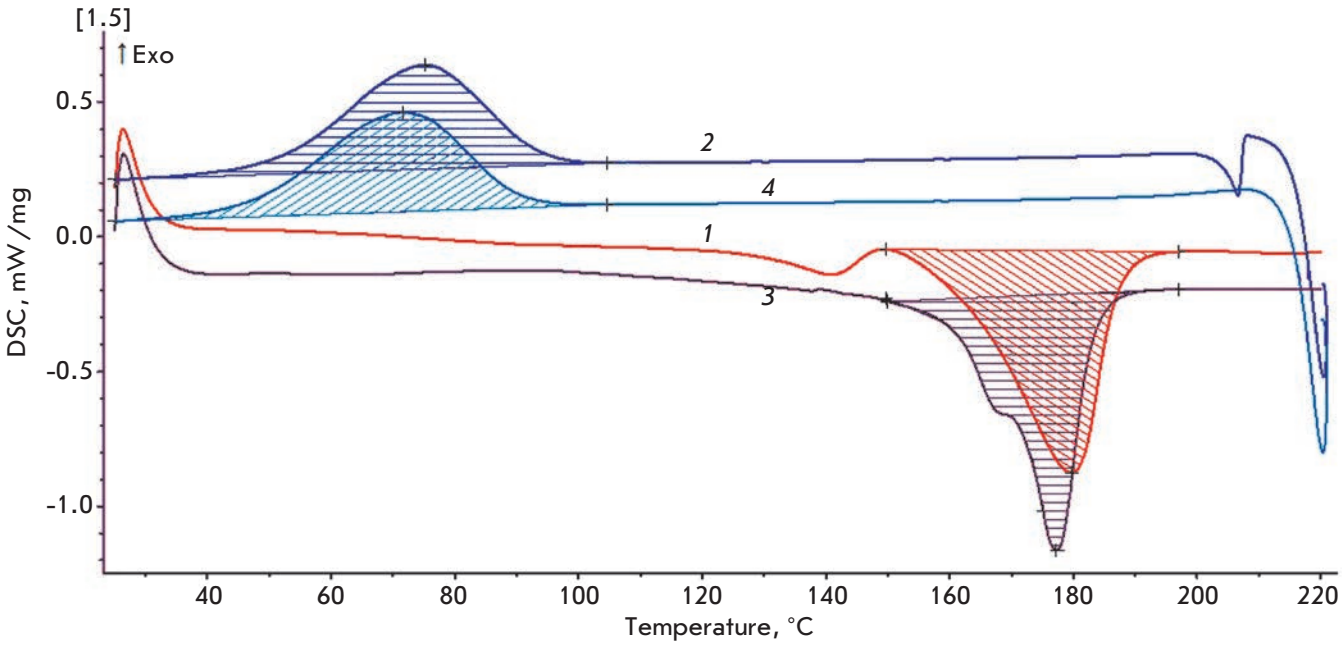

Fig. 4. DSC thermograms of PHB4MV obtained by biosynthesis by *A. chroococcum* 7B: 1 – curve of the first heating cycle; 2 – curve of the first cooling cycle; 3 – curve of the second heating cycle; 4 – curve of the second cooling cycle; areas of the melting and crystallization peaks are shaded, respectively

with PHB). The crystallinity indicators (calculated from the first and second cycles of heating of the polymer samples, see *Table 2*) are in agreement with the published data [49]. A decrease in the molecular weight of the polymers has been shown to lead to a quite significant drop in the degree of crystallinity (10% or more if M_w is reduced two-fold) [49]. However, the main role in the drop in the degree of crystallinity is played by the monomers (3HV and 3H4MV) in the copolymers with a side group longer than that of 3HB. This confirms the data that introduction of 3HV monomers into a PHB polymer chain results in a copolymer with altered physico-chemical properties: a lower melting point, lower crystallinity, higher plasticity, and lower durability and higher biodegradation rate [22, 32], and that the crystallinity of the PHBV copolymer decreases

significantly with the increase in the molar content of the 3HV monomers in its chain [32]. However, in the case of PHB4MV we observe a much more pronounced effect: in its physico-chemical properties the PHB4MV copolymer with only a 0.6% molar content of 3H4MV resembles a PHVB copolymer with a molar content of 2.5 to 7.8%. Something similar is observed in the analysis of the polymers' hydrophilicity. While the contact angles (as an indicator of the hydrophilicity of polymer surfaces) of the PHB homopolymer and PHBV1 copolymer do not differ, the value for the PHBV2 and PHB4MV copolymers was considerably higher and the contact angle of PHB4MV was only slightly lower than that of PHBV2. We have previously shown that the contact angle of the PHBV copolymer increases with an increase in the molar content of 3HV monomers, and that the hydrophilicity of a polymer film is reduced due to an increased concentration of hydrophobic groups on its surface [50]. Thus, based on the data of the analysis of the hydrophilic properties of the polymers, the PHB4MV copolymer containing only 0.6% of 3H4MV corresponds to a PHBV copolymer with a molar content of 2.5 to 7.8%. This may be due to a much more pronounced destabilizing effect of the branched side group (3H4MV residue) on the crystal structure of the polymer compared with the effect of the linear 3HV group in the PHVB copolymer (*Fig. 1*), which explains such a disproportionately large contribution of the low content of 3H4MV to the change in the physico-chemical properties of the polymer.

Investigation of the growth of stromal cells on the polymer films

Studies of the *in vitro* biocompatibility of polymers produced by biosynthesis in *A. chroococcum* 7B cells using a culture of the stromal cells isolated from bone marrow revealed a significant increase in the number of viable BMSCs on the films of three polymers, PHB, PHBV1 (2.5%mol 3HV), and PHB4MV, over 5 days. No statistical differences were observed in the cell proliferation on the films of the different polymers. Therefore, the new PHB4MV copolymer can be used for biomedical research and development, along with its analogues – PHB and PHBV – particularly for the manufacture of matrices used in bone tissue engineering [51, 52].

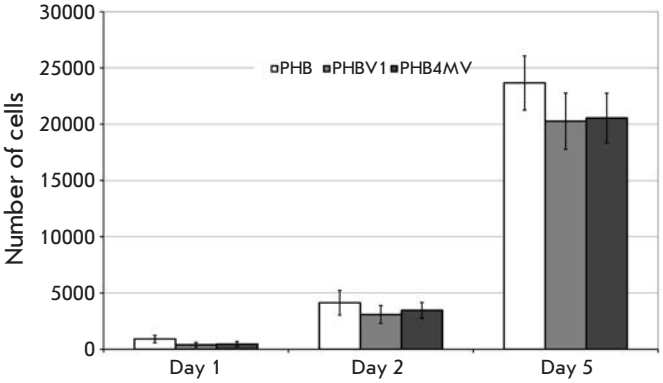

Fig. 5. Changes in the number of viable bone marrow stromal cells of rats cultured on PHB, PHBV1 and PHB4MV polymer films according to the XTT test. * $P < 0.05$ when compared to PHB group, $n = 6$

CONCLUSIONS

We have shown that the addition of 4-methylvaleric acid to a culture medium of the strain-producer *A. chroococcum* 7B leads to the incorporation of the 6C-hydroxycarboxylic acid monomer, 3-hydroxy-4-methylvalerate, into the polymer chain of PHB, and the synthesis of poly(3-hydroxybutyrate-co-3-hydroxy-4-methylvalerate). Despite the low molar content of 3H4MV in the obtained copolymer, the physico-chemical properties of PHB4MV containing only 0.6% of 3H4MV are comparable to those of a PHBV copolymer containing 2.5 to 7.8% of 3HV. The growth of the BMSCs as determined by the XTT test on the PHB4MV copolymer *in vitro* did not differ significantly from their growth on PHB and PHBV, and, therefore, it can be used in biomedical research and development. ●

The authors thank V.O. Popov (Federal Research Centre "Fundamentals of Biotechnology" RAS) for the support. The study used equipment of the shared use centers of the Moscow State University and FRC FOB RAS.

This work was supported by a RFBR ofi_m grant, project No 15-29-04856.

REFERENCES

1. Biomedical polymers / Ed. Jenkins M. Birmingham, UK: University of Birmingham, 2007. 203 p.
2. Shtilman M.I. Polymeric biomaterials. Part 1. Polymer implants. VSP: Leiden, Netherlands, 2003. 294 p.
3. Moisenovich M.M., Pustovalova O., Shackelford J., Vasiljeva T.V., Druzhinina T.V., Kamenchuk Y.A., Guzeev V.V., Sokolova O.S., Bogush V.G., Debabov V.G., et al. // Biomaterials. 2012. V. 33. № 15. P. 3887–3898.
4. Satyam A., Kumar P., Fan X., Gorelov A., Rochev Y., Joshi L., Peinado H., Lyden D., Thomas B., Rodriguez B., et al. // Advanced Materials. 2014. V. 26. № 19. P. 3024–3034.

5. Miroiu F.M., Stefan N., Visan A.I., Nita C., Luculescu C.R., Rasoga O., Socol M., Zgura I., Cristescu R., Craciun D., et al. // Appl. Surface Sci. 2015. V. 355. P. 1123–1131.
6. Baradaran-Rafii A., Biazar E., Heidari-Keshel S. // ASAIO J. 2015. V. 61. № 5. P. 605–612.
7. Bondar O.V., Saifullina D.V., Shakhmaeva I.I., Mavlyutova I.I., Abdullin T.I. // Acta Naturae. 2012. V. 4. № 1. P. 78–81.
8. Ulasov A.V., Khramtsov Y.V., Trusov G.A., Rosenkranz A.A., Sverdlov E.D., Sobolev A.S. // Mol. Therapy. 2011. V. 19. № 1. P. 103–112.
9. Kolotova E.S., Egorova S.G., Ramonova A.A., Bogorodski S.E., Popov V.K., Agapov I.I., Kirpichnikov M.P. // Acta Naturae. 2012. V. 4. № 1. P. 101–106.
10. Agrawal C.M., Athanasiou K.A. // J. Biomed. Mater. Res. 1997. V. 38. P. 105–114.
11. Stevanovic M., Pavlovic V., Petkovic J., Filipic M., Uskokovic D. // Express Polymer. Lett. 2011. V. 5. № 11. P. 996–1008.
12. Kireev V.V., High molecular weight compounds. Moscow: Vysshaya Schkola, 1992. 512 p.
13. Volova T., Shishatskaya E., Mogilnaya O., Sevastianov V., Efremov S. // Biochem. Engin. J. 2003. V. 16. № 2. P. 125–133.
14. Sevastianov V.I., Perova N.V., Shishatskaya E.I., Kalacheva G.S., Volova T.G. // J. Biomat. Sci. Polymer Ed. 2003. V. 14. № 10. P. 1029–1042.
15. Bonartsev A.P., Bonartseva G.A, Shaitan K.V., Kiprichnikov M.P. // Biomed. Khimiya. 2011. V. 57. № 4. P. 374–391.
16. Singh M., Kumar P., Ray S., Kalia V.C. // Ind. J. Microbiol. 2015. V. 55. № 3. P. 235–249.
17. Shtukenberg A.G., Punin Y.O., Gunn E., Kahr B. // Chem. Rev. 2012. V. 112. № 3. P. 1805–1838.
18. Chardron S., Bruzaud S., Lignot B., Elain A., Sire O. // Polymer Testing. 2010. V. 29. № 8. P. 966–971.
19. Bonartsev A.P., Boskhomodgiev A.P., Iordanskii A.L., Bonartseva G.A., Rebrov A.V., Makhina T.K., Myshkina V.L., Yakovlev S.A., Filatova E.A., Ivanov E.A., et al. // Mol. Crystals Liquid Crystals. 2012. V. 556. № 1. P. 288–300.
20. Engelberg I., Kohn J. // Biomater. 1991. V. 12. P. 292–304.
21. Prudskova T.N., Kirillovich V.I., Zakovryashina N.A., Erimilina N.I., Andreeva T.I., Bonartseva G.A., Bonartsev A.P., Iordanskii A.L., Makhina T.K., Myshkina V.L., Popov V.O. // RF Patent for invention № 2333962. 17.10.2006.
22. Pearce R.P., Marchessault R.H. // Macromol. 1994. V. 27. P. 3869–3874.
23. Pettinari M.J., Vazquez G.J., Silberschmidt D., Rehm B., Steinbüchel A., Mendez B.S. // Appl. Environ. Microbiol. 2001. V. 67. № 11. P. 5331–5334.
24. Lau N.S., Tsuge T., Sudesh K. // Appl. Microbiol. Biotechnol. 2011. V. 89. № 5. P. 1599–1609.
25. Saika A., Watanabe Y., Sudesh K., Tsuge T. // J. Biosci. Bioeng. 2014. V. 117. № 6. P. 670–675.
26. Ling S.C., Tsuge T., Sudesh K. // J. Appl. Microbiol. 2011. V. 111. № 3. P. 559–571.
27. Tanadchangsaeng N., Tsuge T., Abe H. // Biomacromolecules. 2010. V. 11. № 6. P. 1615–1622.
28. Myshkina V.L., Nikolaeva D.A, Makhina T.K., Bonartsev A.P., Bonartseva G.A. // Prikladnaya biokhimiya i mikrobiologiya. 2008. V. 44. № 5. P. 533–538.
29. Myshkina V.L., Ivanov E.A., Nikolaeva D.A., Makhina T.K., Bonartsev A.P., Filatova E.V., Ruzhitskii A.O., Bonartseva G.A. // Prikladnaya biokhimiya i mikrobiologiya. 2010. V. 46. № 3. P. 1–8.
30. Bonartsev A.P., Yakovlev S.G., Zharkova I.I., Boskhomdzhiev A.P., Bagrov D.V., Myshkina V.L., Makhina T.K., Kharitonova E.P., Samsonova O.V., Voinova V.V., et al. // BMC Biochem. 2013. V. 14. P. 12.
31. Bonartsev A.P., Yakovlev S.G., Boskhomdzhiev A.P., Zharkova I.I., Bagrov D.V., Myshkina V.L., Mahina T.K., Charitonova E.P., Samsonova O.V., Zernov A.L., et al. // PLoS One. 2013. V. 8. № 2. e57200.
32. Savenkova L., Gercberga Z., Bibers I., Kalnin M. // Proc. Biochem. 2000. V. 36. № 5. P. 445–450.
33. Zheng Z., Bei F.F., Tian H.L., Chen G.Q. // Biomaterials. 2005. V. 26. № 17. P. 3537–3548.
34. Barham P.J., Keller A., Otun E.L., Holmes P.A. // J. Materials Sci. 1984. V. 19. № 9. P. 2781–2794.
35. Maniatopoulos C., Sodek J., Melcher A.H. // Cell Tissue Res. 1998. V. 254. № 2. P. 317–330.
36. Sutherland M.W., Learmonth B.A. // Free Rad. Res. 1997. V. 27. № 3. P. 283–289.
37. Senior P.J., Dawes E.A. // Biochem. J. 1973. V. 134. P. 225–238.
38. Madison L.L., Huisman G.W. // Microbiol. Mol. Biol. Rev. 1999. V. 63. № 1. P. 21–53.
39. Ren Q., Sierro N., Kellerhals M., Kessler B., Witholt B. // Appl. Environ. Microbiol. 2000. V. 66. № 4. P. 1311–1320.
40. Elsayed N.S., Aboshanab K.M., Aboulwafa M.M., Hassouna N.A. // African J. Microbiol. Res. 2013. V. 7. № 43. P. 5025–5035.
41. Pramanik N., Mukherjee K., Nandy A., Mukherjee S., Kundu P.P. // J. Appl. Polym. Sci. 2014. V. 131. № 22. 41080.
42. Xin J., Zhang Y., Dong J., Song H., Xia C.G. // African J. Biotechnol. 2011. V. 10. № 36. P. 7078–7087.
43. Karthikeyan O.P., Chidambarampadmavathy K., Nadarajan S., Lee P.K., Heimann K. // Chemosphere. 2015. V. 141. P. 235–242.
44. Zhu C., Chiu S., Nakas J.P., Nomura C.T. // J. Appl. Polym. Sci. 2013. V. 130. № 1. P. 1–13.
45. Pena C., Castillo T., Garcia A., Millán M., Segura D. // Microbial Biotechnol. 2014. V. 7. № 4. P. 278–293.
46. Pena C., Lopez S., Garcia A., Espín G., Romo-Uribe A., Segura D. // Ann. Microbiol. 2014. V. 64. № 1. P. 39–47.
47. Eisenstark A., McMahon K.J., Eisenstark R. // J. Bacteriol. 1950. V. 59. № 1. P. 75–81.
48. Vela G.R., Rosenthal R.S. // J. Bacteriol. 1972. V. 111. № 1. P. 260–266.
49. Dominguez-Diaz M., Meneses-Acosta A., Romo-Uribe A., Pena C., Segura D., Espin G. // European Polymer J. 2015. V. 63. P. 101–112.
50. Choi G.G., Kim H.W., Rhee Y.H. // J. Microbiol. 2004. V. 42. № 4. P. 346–352.
51. Andreeva N.V., Bonartsev A.P., Zharkova I.I., Makhina T.K., Myshkina V.L., Kharitonova E.P., Voinova V.V., Bonartseva G.A., Shaitan K.V., Belyavskii A.V. // Bull. Exp. Biol. Med. 2015. V. 159. № 4. P. 567–571.
52. Bonartsev A.P., Zharkova I.I., Yakovlev S.G., Myshkina V.L., Makhina T.K., Zernov A.L., Kudryashova K.S., Feofanov A.V., Akulina E.A., Ivanova E.V., et al. // J. Biomaterials Tissue Engin. 2016. V. 6. № 1. P. 42–52.

Cleavage of Human Embryos: Options and Diversity

Yu. K. Doronin[1]*, I. V. Senechkin[2], L. V. Hilkevich[2], M. A. Kurcer[2]
[1]Lomonosov Moscow State University, Faculty of Biology, Leninskie Gory, 1, bldg. 12, Moscow, 119991, Russia
[2]Perinatal Medical Center, Department of Infertility Treatment and IVF, Sevastopolskiy prosp., 24, bldg.1, Moscow, 117209, Russia
*E-mail: ljh_rjycn@mail.ru
Received September 08, 2015; in final form, April 25, 2016

ABSTRACT **In order to estimate the diversity of embryo cleavage relatives to embryo progress (blastocyst formation), time-lapse imaging data of preimplantation human embryo development were used. This retrospective study is focused on the topographic features and time parameters of the cleavages, with particular emphasis on the lengths of cleavage cycles and the genealogy of blastomeres in 2- to 8-cell human embryos. We have found that all 4-cell human embryos have four developmental variants that are based on the sequence of appearance and orientation of cleavage planes during embryo cleavage from 2 to 4 blastomeres. Each variant of cleavage shows a strong correlation with further developmental dynamics of the embryos (different cleavage cycle characteristics as well as lengths of blastomere cycles). An analysis of the sequence of human blastomere divisions allowed us to postulate that the effects of zygotic determinants are eliminated as a result of cleavage, and that, thereafter, blastomeres acquire the ability of own syntheses, regulation, polarization, formation of functional contacts, and, finally, of specific differentiation. This data on the early development of human embryos obtained using noninvasive methods complements and extend our understanding of the embryogenesis of eutherian mammals and may be applied in the practice of reproductive technologies.**
KEYWORDS **human embryos, time-lapse analysis, cleavage, blastomere genealogy**

INTRODUCTION

In the past few decades, with the rapid development and commercialization of reproductive technologies, preimplantation human embryos have become the focus of close attention. Ethical norms and legal constraints have put limitations on all but non-invasive methods in the study of conceptus; i.e. only microscopic observations. As a result of comprehensive phenomenological research, a system for the assessment of the morphology and rate of development of early human embryos *in vitro* was developed which allows one to predict the appearance of implantation-competent (high-quality) blastocysts with a higher or lesser degree of certainty [1, 2]. The introduction of incubators equipped with a continuous video recording device into the practice of reproductive medicine has significantly expanded the possibilities of diagnosis and prognosis of embryo quality [3–5]. Currently, a large body of factual data has been accumulated in the archives of centers of human reproductive biology a thorough analysis of which can not only improve the prognostic capabilities of the morphokinetic approach to the identification of promising embryos, but also deepen our understanding of the early development of placental mammals.

The first (meridional) cleavage furrow of the polarized zygote of placental mammals begins at the animal pole (in the immediate vicinity of the polar body) and extends from the animal to the vegetal pole [6–10]. Cleavage furrows of the blastomeres of 2-cell embryos are orthogonal to the first cleavage furrow and distributed in planes approximately coinciding with the equatorial and meridional planes of the zygote. Thus, there are four possible variants of cleavage of 2-cell embryo blastomeres: the two blastomeres divide either in the equatorial (E) or meridional (M) direction (variants EE or MM) or the first division is meridional and the second is equatorial (variant ME) and vice versa (variant EM).

The listed combinations of second divisions of the cleavage have been described in mouse embryos, with the variants for 4-cell embryos being different in phenotype. In ME and EM divisions, blastomeres form a tetrahedral structure (i.e. they are projected onto the corners of an imaginary tetrahedron). As a result of EE or MM divisions, blastomeres are distributed in the form of a plate or rosette [11, 12]. According to canonical descriptions, a human 4-cell embryo, unlike mouse 4-cell embryos, is formed as a result of successive me-

ridional and equatorial divisions of 2-cell embryo blastomeres and, thereafter, assumes a tetrahedral form [6, 10, 13]. At the same time, the existence of substantive differences, including those in the ways of 4-cell embryo formation, at such early (phylogenetically ancient) basic stages of the embryogenesis of laboratory mammals and humans seems improbable.

The appearance of variants of 4-cell embryos as a result of second divisions of the cleavage seems to be a significant event in early ontogenesis. The differences in ooplasmic segregation are associated with the differences in the dynamic pattern of subsequent embryo development [14, 15], which, on the contrary, would normally result in the formation of a homogenous final structure: i.e. a blastocyst. In other words, this phenomenon should be assumed as one of the reasons for the diversity in subsequent development and, thereafter, the earliest manifestation of the regulatory ability of mammalian embryos.

Based on the assumptions presented above, the purpose of this study is (1) to conduct a detailed analysis of the topographic features of the second division of the cleavage of cultured human embryos; and (2) to analyze the variations in the time parameters of subsequent stages of embryo cleavage that are different in the variants of the second cleavage. Comparison of the genealogy of blastomeres with the sequence of their divisions allowed us to assume the role of cleavage as predetermining the normal course of the events accompanying embryo compaction and cavitation.

EXPERIMENTAL

The material used in the study was time-lapse video recordings of 101 human embryos (microscope Primo Vision incorporated into a Thermo thermostat; video capture every 15 min) obtained under the standard culturing protocol from 20 anonymous patients aged 27 to 44 years (average 34.7 years). The orientation of the first three cleavage divisions in relation to the animal-vegetal axis of the zygote and successive moments of the division of the zygote and each blastomere until the 16-cell stage of development were determined by viewing images of time-lapse recording of individual embryos. The genealogy of blastomeres was traced in parallel. Based on these registrations, 4-cell embryos were classified in accordance with the division variants of the second cycle of cleavage and the durations of the zygotic period (from fertilization to zygote division) and the cleavage cycles were estimated: i.e. the difference in the onset time of the third and first divisions of blastomeres (the second cycle of cleavage), the seventh and third divisions (the third cycle of cleavage), and the 15th and seventh divisions (the fourth cycle of cleavage). The duration of the periods not accompanied by cell division (difference in the onset time of the second and first, fourth and third, eighth and seventh divisions), and the periods of cell divisions (difference in the time of the third and second, seventh and fourth, 15th and eighth divisions) of the second, third, and fourth cleavage cycles were also calculated (see *Fig. 2*). These measurements allowed us to calculate the duration of the cycles of individual blastomeres as the difference between the division moments of corresponding mother and daughter blastomeres. Based on these data, one can reconstruct and compare the genealogy of blastomeres before the 16-cell stage using the duration of blastomere cycles as their marker. The results of the measurement were analyzed and compared using non-parametric methods of variation statistics on the Stadia (A.P. Kulaichev, Lomonosov Moscow State University) and Statistica v6 (StatSoft) software. At the end of the standard cultivation period, the stages of embryo development were diagnosed in accordance with the established classification [16, 17].

Various developmental anomalies were noted by the first divisions of the cleavage of 33 embryos: excessive fragmentation, extremely short or long cell cycles (dozens of minutes or two days and more, and even complete absence of cytokinesis during the entire observation period), fusion of blastomeres right after division, and giant intracellular vacuoles and extracellular cavities in 4 to 8-cell embryos. These embryos were excluded from consideration. However, in some cases, measurable parameters of their first cycles were compared with the corresponding parameters in embryos that developed in the absence of organic disorders.

RESULTS AND DISCUSSION

Relationship between dividing blastomeres

EE, MM, ME, and EM variants of blastomere divisions were detected in 10.3, 19.1, 27.9 and 42.6 % of all cases where 2-cell embryos had developed without structural abnormalities (N = 68). In ME or EM cases, two pairs of sister cells were oriented almost mutually perpendicular to each other due to the orthogonality of division planes for 2-cell embryo blastomeres, while a 4-cell embryo adopted a configuration close to a tetrahedron. Eventually, the geometric correctness of such a tetrahedron is improved due to the slow movements of sister pairs of blastomeres (*Fig. 1*). As a result of EE or MM divisions, a sort of plate or rosette of blastomeres is formed. In these cases, the sister pairs of blastomeres are shifted into a mutually perpendicular orientation. As a result, the plate or rosette also adopts a tetrahedron form (*Fig. 1*). Thus, the form of human 4-cell embryos becomes homogeneous regardless of the orientation of previous cleavage furrows. The displacement of

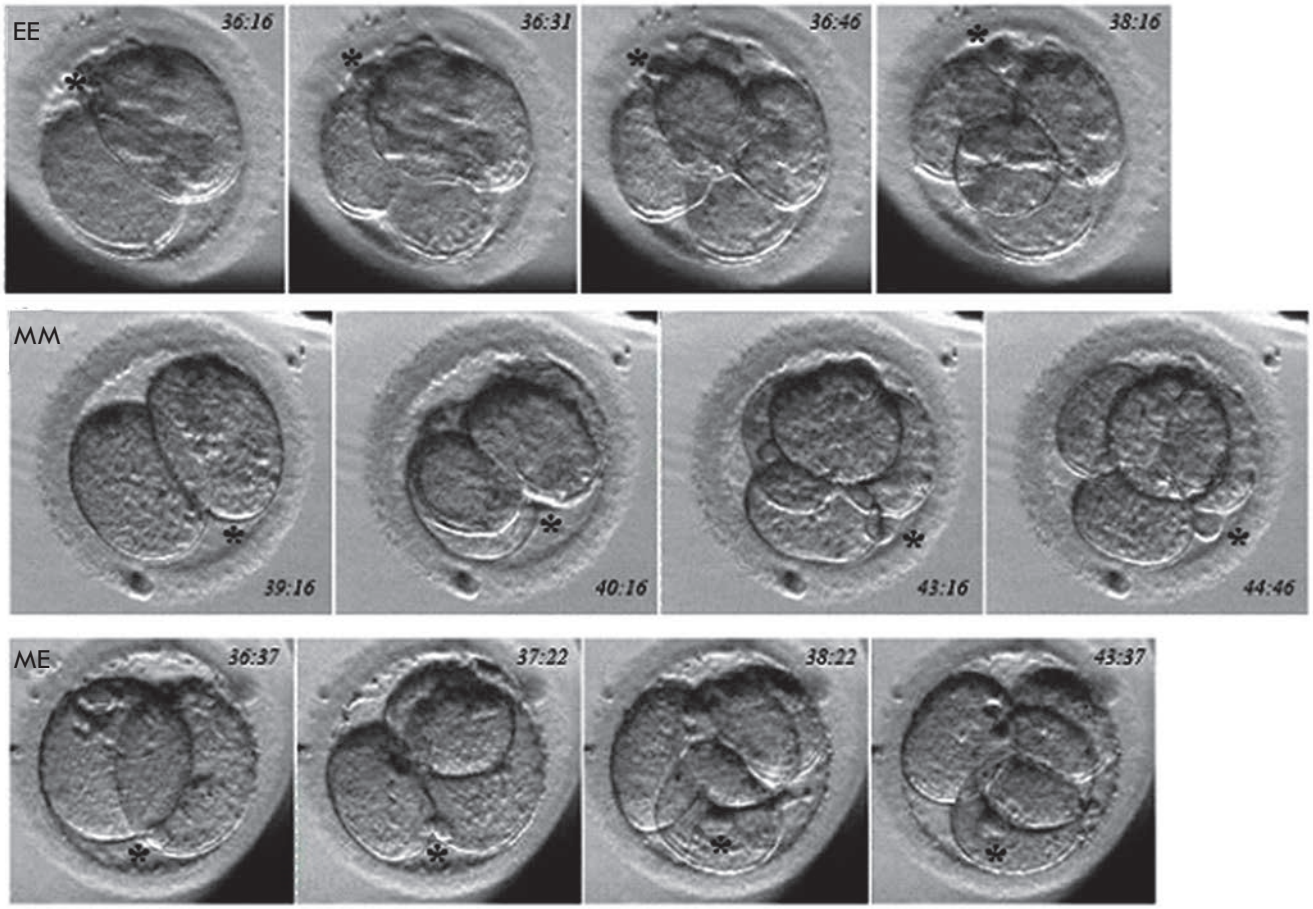

Fig 1. Examples of sequential equatorial (EE), meridional (MM), and meridional followed by equatorial (ME) blastomere divisions and final configuration of a 4-cell embryo in relation to 4-cell embryo formation. Equatorial followed by meridional (EM) cleavage type (not shown) is different from ME cleavage type only in the order of division. The time after intracellular sperm injection (h:m) is indicated on the figure. Asterisk depicts the position of the second polar body

cell pairs is most probably associated with the optimization of the form of 4-cell embryos as a result of the alignment of the mechanical stresses that take place in the limited volume of an embryo after blastomere divisions. Association of sister blastomeres is probably due to the long-term persistence of cytoplasmic bridges [8, 11, 18]. Long-term contact between sister blastomeres promotes the appearance of cell clusters—a compact arrangement of the descendants of 2-, 4- and 8-cell embryo blastomeres. We noticed the formation of such clusters upon reconstruction of blastomere genealogy.

The frequencies of appearance of EE, MM, ME, and EM variants in embryos with structural defects (30.3, 15.2, 24.2 and 30.3 %, respectively; N = 33) do not differ from the frequencies for embryos that developed without structural abnormalities ($\chi^2 = 6.471$, $P = 0.091$) but do not correspond to the distribution typical for the latter ($\chi^2 = 15.130$, $P = 0.002$). This is due to the fact that the proportions of MM, ME, and EM variants of the second cleavage in the two groups of embryos are identical (χ^2 values for the corresponding alternative comparisons are 0.17, 0.09, 0.65; $P = 0.682$, 0.763 and 0.419, respectively). The division frequency in abnormal embryos has a clear tendency to outreach (almost three-fold) the frequency in normal embryos ($\chi^2 = 4.30$, $P = 0.038$; Yates' correction $P = 0.072$). Probably, it should be assumed that EE embryos are to a greater extent prone to organic disturbances in development than embryos with other variants of second divisions of the cleavage. The same tendency was noted in mouse EE embryos [19].

Cleavage cycles and trajectories

Variants of blastomere divisions in the second cleavage cycle are essential for further development. A smoothed wave-like time trajectory of development

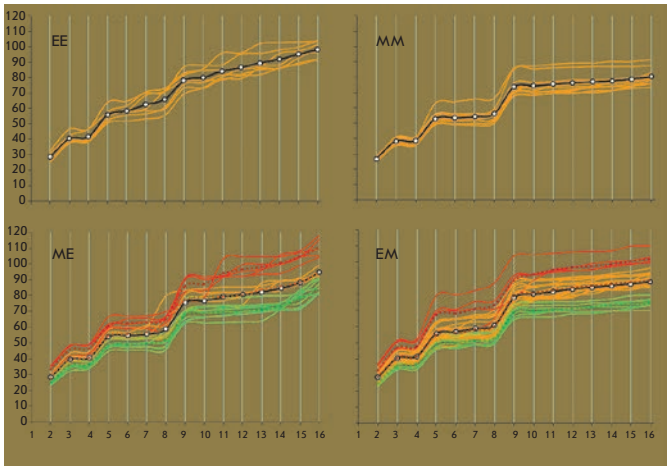

Fig 2. Embryo cleavage trajectories for EE, MM, ME, and EM cleavage type embryos. The green, red, and yellow lines indicate embryos with high, low, and medium cleavage intensities, respectively. Dashed lines indicate average embryo cleavage trajectories for each significantly different cleavage intensity group. Solid lines with markers depict average trajectories for each embryo variant. Horizontal axes stand for the number of blastomeres. Vertical axes indicate the time after intracellular sperm injection (h)

is typical for EE embryos, while MM, ME, and EM embryos are characterized by a pronounced step-like trajectory (*Fig. 2*). Average time trajectories (see *Fig. 2*) differ from each other (paired Wilcoxon test; significance of the differences (*P*) between EE and MM, EE and EM, MM and ME, MM and EM variants equals 0.001; significance of the differences between the EE and EM variants is 0.002; and 0.023 between ME and EM variants).

Differences in the duration of cleavage cycles become apparent in the third cleavage cycle and increase in the 4th cycle. EE embryos have the longest cycles, while MM embryos have the shortest cycles, with EM and ME embryos occupying an intermediate position. Lengthening of the overall cycles of cleavage is mainly due to the extension of cell division periods. Therefore, the division frequency is maximal for MM and minimal for EE embryos (*Tab. 1*). MM embryos reach the 16-cell stage after 80.5 ± 4.85 hours (mean ± standard deviation); EM embryos – after 87.7 ± 9.47 h; and ME and EM embryos – after 94.8 ± 11.29 and 98.1 ± 5.05 h, respectively (the differences of the mean values are statistically significant except for the differences for the EE and ME groups ($P = 0.197$); Van der Waerden test).

Table 1. Time parameters of the cleavage cycles (mean value and standard deviation, h) of embryos with different variants of successive divisions of 2-cell embryo blastomeres

		EE	MM	ME	EM
Number and prospective stages of embryo development		B5(2), B4(1), B3(1), B1(3)	B5(7), B4(3), B3(2), B1(1)	B5(3), B4(5), B3(2), B2(2), B1(5), M(2)	B5(8), B4(6), B3(5), B2(4), B1(5), M(1)
Zygotic period		28.6 ± 2.70[1]	26.7 ± 1.44[1]	28.2 ± 3.96	28.5 ± 3.61
Overall cycle duration	cycle 2	13.1 ± 2.52	12.1 ± 1.05	12.4 ± 1.22	12.8 ± 1.85
	cycle 3	24.4 ± 5.72[2,3,4]	17.4 ± 3.33[2]	18.1 ± 5.58[3]	19.4 ± 4.96[4]
	cycle 4	32.1 ± 8.67[5,6]	24.3 ± 3.06[5,7,8]	36.0 ± 8.12[7,9]	26.9 ± 4.57[6,8,9]
Period without divisions	cycle 2	11.9 ± 1.33	11. 6 ± 1.12	11.5 ± 1.16	11.9 ± 1.48
	cycle 3	14.3 ± 2.81	14.1 ± 2.78	13.2 ± 1.88	14.3 ± 3.72
	cycle 4	12.1 ± 3.36[10,11]	17.5 ± 4.05[10]	16.8 ± 7.04	17.3 ± 4.67[11]
Period of blastomere divisions	cycle 2	1.1 ± 1.60	0.5 ± 0.31[12,13]	0.9 ± 0.55[12]	1.0 ± 0.89[13]
	cycle 3	10.0 ± 4.57[14,15,16]	3.3 ± 2.08[14,17]	4.9 ± 5.07[15]	5.1 ± 2.99[16,17]
	cycle 4	20.0 ± 6.87[18,19]	6.8 ± 2.47[18,20]	19.2 ± 5.93[20,21]	9.6 ± 5.29[19,21]
Mean time between successive cell divisions**	cycle 2	0.6 ± 0.80	0.2 ± 0.15	0.4 ± 0.28	0.5 ± 0.45
	cycle 3	2.5 ± 1.14	0.8 ± 0.52	1.2 ± 1.27	1.3 ± 0.75
	cycle 4	2.5 ± 0.86	0.9 ± 0.31	2.4 ± 0.74	1.2 ± 0.66

Note. The same superscript numbers indicate statistically significant differences in the mean values (Van der Waerden test, $P < 0.05$). *B – blastocyst stage; M – morula stage; figures indicate gradation of embryos at the blastocyst stage; parentheses indicate the number of embryos that have reached each specific stage.

**Mean values differ from each other in the same way as the average values of the duration of blastomere division periods.

Table 2. Time parameters of cleavage cycles (mean value and standard deviation, h) of ME and EM embryos with different terms of development (groups 1, 2 and 3)

		ME			EM		
		Group 1	Group 2	Group 3	Group 1	Group 2	Group 3
Number and prospective stages of embryo development		B5(2), B4(4), B3(1), B1(1)	B2(2), B1(2), M(1)	B5(1), B4(1), B3(1), B1(2), M(1)	B5(5), B4(2)	B1(4), M(1)	B5(3), B4(4), B3(5), B2(4), B1(1)
Zygotic period		25.5 ± 2.01[1,2]	33.3 ± 3.29[1,3]	27.7 ± 2.01[2,3]	25.1±2.19[1,2]	32.9 ± 3.60[1,3]	28.7 ± 2.53[2,3]
Overall cycle duration	cycle 2	11.3 ± 0.62[4,5]	13.3 ± 0.94[4]	13.1 ± 0.87[5]	11.7±1.25[4]	15.0 ± 0.63[4,5]	12.7 ± 1.81[5]
	cycle 3	15.3 ± 3.28[8]	18.4 ± 1.21	21.7 ± 8.22[8]	16.3±1.94[8]	25.7 ± 6.08[8,9]	18.8 ± 3.94[9]
	cycle 4	33.0 ± 3.68[11]	45.5 ± 6.49[11,12]	32.1 ± 7.91[12]	21.9 ± 3.11[13,14]	28.5 ± 4.50[13]	28.5 ± 3.62[14]
Period without divisions	cycle 2	10.5 ± 0.97[6,7]	12.4 ± 0.51[6]	12.2 ± 0.64[7]	10.8 ± 0.41[6]	14.2 ± 0.56[6,7]	11.6 ± 1.21[7]
	cycle 3	11.9 ± 0.87[9,10]	14.6 ± 2.51[9]	13.9 ± 1.08[10]	12.3 ± 1.49[10]	19.6 ± 4.99[10,11]	13.6 ± 2.47[11]
	cycle 4	15.6 ±4.29	21.3 ± 9.22	14.8 ± 7.57	15.6 ± 1.74	15.1 ± 6.65	18.6 ± 4.65
Period of blastomere divisions	cycle 2	0.8 ± 0.60	0.9 ± 0.57	0.93 ± 0.56	0.9 ± 1.01	0.76 ± 0.25	1.08 ± 0.98
	cycle 3	3.4 ± 2.89	3.9 ± 2.18	7.75 ± 7.92	4.0 ± 1.41[12]	6.08 ± 2.16[12]	5.21 ± 3.59
	cycle 4	17.5 ± 2.81	24.2 ± 9.63	17.3 ± 2.66	6.2 ± 2.98[15]	13.4 ± 6.00[15]	9.95 ± 5.19

Notations are the same as in table 1.

Table 3. Terms and comparison of blastomere cycles in embryos with different variants of the second division of the cleavage

Blastomeres	Mean values ± standard deviation			
	EE (N = 7)	MM (N = 13)	ME(N = 19)	EM (N = 29)
1	11.9 ± 1.29[a]	11.6 ±1.13[a]	11.7 ± 1.09[a]	11.9 ± 1.46[a]
2	13.1 ± 2.51[a]	12.0 ± 1.09[a]	12.5 ± 1.21[a]	12.9 ± 1.83[a]
1:1	17.6 ± 6.20[b]	14.9 ± 2.76[b,c]	14.6 ± 2.16[b,c]	15.5 ± 4.01[b,c,d]
1:2	21.1 ± 6.15[1,6,b]	16.6 ± 3.20[6,b]	15.5 ± 2.58[1,9,b,d]	18.2 ± 5.34[9,b,e]
2:1	17.7 ± 2.86[2,7,c]	15.0 ± 3.46[7,d]	14.2 ± 2.44[2,10,d,e]	16.3 ± 3.60[10,c,e,f]
2:2	24.4 ± 9.30[3,4,8,c]	16.2 ± 3.47[5,8,c,d]	17.9 ± 5.66[3,c,e]	18.6 ± 4.33[4,5,d,f]
1:1:1	23.6 ± 5.00[d,e,f]	21.8 ± 3.64[15,e,f]	25.3 ± 6.93[f,g]	24.4 ± 5.15[15,g,h,k,l]
1:1:2	29.7 ± 10.71[d]	23.8 ± 3.99[12,16,e,g,h,k]	32.4 ± 9.71[12,f,h,k,l]	28.0 ± 5.89[16,g,m,n,p,q]
1:2:1	22.4 ± 5.36[g]	21.5 ± 4.13[g,l,m,n]	23.0 ± 6.87[h,m,n,p]	24.3 ± 5.32[m,r,s]
1:2:2	32.2 ± 12.50[20,e,g]	22.7 ± 3.67[17,20,l]	28.1 ± 9.74[m]	27.1 ± 5.55[17,h,r,t,u]
2:1:1	25.4 ± 9.17[h]	21.4 ± 3.8[13,18,h,p]	26.0 ± 7.88[13,k,q]	24.5 ± 4.43[18,n,t,v,x]
2:1:2	33.8 ± 11.38[21,22,f,h,k]	24.3 ± 3.67[19,21,f,m,p,q]	30.3 ± 10.76[g,n,q,r]	27.6 ± 4.78[19,22,k,s,v,y,z]
2:2:1	20.2 ± 3.77[k,l]	21.2 ± 3.26[k,q,r]	22.8 ± 6.30[l,r,s]	21.7 ± 5.94[l,p,u,x,y]
2:2:2	26.5 ± 10.22[l]	23.8 ± 3.33[14,n,r]	28.7 ± 6.34[14,p,s]	25.7 ± 5.01[q,z]

Note. The same superscript letters indicate statistically significant differences ($P < 0.05$, paired Wilcoxon test) in the duration of blastomere cycles in the embryos of each group (value differences are presented in columns). The same superscript numbers indicate statistically significant differences ($P < 0.05$, Van der Waerden test) of the duration of corresponding cycles in embryos of different groups (value differences are presented in lines).

The diversity of development trajectories is notably higher among ME and EM embryos than among EE and MM embryos (see *Fig. 2*; compare the corresponding standard deviations presented in *Table 1*). ME and EM embryos can be subdivided into three groups according to the similarity of trajectories. Average trajectories of development for both ME and EM embryos from these groups differ significantly ($P = 0.0007$ for all comparison variants, paired Wilcoxon test). Embryos of the second group are characterized by a longer duration of the

Table 4. The terms of blastomere cycles (mean values, standard deviation, h) and their comparison for ME and EM embryos with different developmental terms (groups 1, 2 and 3)

Blastomeres	ME			EM		
	Group 1 (N = 8)	Group 2 (N = 5)	Group 3 (N = 6)	Group 1 (N = 7)	Group 2 (N = 5)	Group 3 (N = 17)
1	11.0 ± 1.21[1,2,a]	12.4 ±0.51[1,a]	12.2 ± 0.59[2,a]	10.9 ±0.46[1,a]	14.2 ± 0.59[1,2,a]	11.7 ± 1.15[2,a]
2	11.7 ± 1.11[3,4,a]	13.3 ± 0.94[3,a]	13.1 ± 0.85[4,a]	11.9 ± 1.33[3,a]	15.0 ± 0.66[3,4,a]	12.7 ± 1.80[4,a]
1:1	13.1 ± 2.10[5,8,b]	16.5 ± 1.77[5]	15.1 ± 0,81[8,b]	13.2 ± 1.90[5,9,b,c]	21.0 ± 6.44[5,10,b]	14.9 ± 2.06b[9,10,b,c]
1:2	13.8 ± 2.43[6,9,b,c]	17.5 ± 2.47[6]	16.1 ± 1.25[9,b]	15.2 ± 2.14[6,b]	25.6 ± 6.95[6,11,b]	17.3 ± 3.76[11,b]
2:1	12.4 ± 0.92[7,10,c,d]	15.5 ± 2.79[7]	15.5 ± 2.24[10,c]	14.2 ± 1.40[7,d]	20.9 ± 4.43[7,12,c]	15.8 ± 2.85[12,d]
2:2	14.9 ± 3.13[13,11,d]	18.2 ± 1.53	21.7 ± 8.24[11,c]	15.8 ± 2.06[8,c,d]	23.0 ± 4.89[8,13,c]	18.4 ± 3.96[13,c,d]
1:1:1	20.0 ± 4.06[12,17,e,f,g]	31.9 ± 5.95[12b,c,d]	26.9 ± 5.45[17,d]	20.4 ± 1.83[14,21,e]	24.3 ± 5.07[d,e]	26.0 ± 5.40[14,21e,f]
1:1:2	27.3 ± 6.78[13,e,h,k]	42.9 ± 9.15[13,20,b,e,f]	30.5 ± 7.15[20,d,e,f]	23.1 ± 3.07[15,22,e,f,g]	31.1 ± 6.18[15,d,f]	29.2 ± 5.72e[22,g,h]
1:2:1	20.1 ± 2.98[h,l]	27.2 ± 11.5[e,g,h]	23.5 ± 4.37[e,g]	19.9 ± 2.79[16,23,h,k]	25.1 ± 3.37[16,g]	25.9 ± 5.69[23,g,k,l]
1:2:2	25.8 ± 7.43[f,l,m]	32.9 ± 14.7[f,g]	27.1 ± 7.63[g]	21.5 ± 3.16[17,24,h,l]	28.3 ± 4.68[17,g]	29.0 ± 5.14f[24,e,k,m,n,p]
2:1:1	19.9 ± 2.62[14,18,k,n,p,q]	34.9 ± 7.18[14,21,k]	26.7 ± 5.70[18,21,h,k]	20.6 ± 3.19[18,25,f,m]	26.8 ± 5.97[18,h,k]	25.4 ± 3.54[25,m,q]
2:1:2	21.9 ± 3.56[15,19,n,r]	42.9 ± 9.99[15,22,c,h,k,l]	30.9 ± 6.89[19,22,h,l]	22.4 ± 2.98[19,26,k,m,n]	28.8 ± 6.31[19,h,l]	29.4 ± 3.34[26,f,l,q,r,s]
2:2:1	23.2 ± 5.00[p,s]	27.8 ± 5.17[23,d,f,l,m]	18.2 ± 6.02[23,f,k,l,m]	19.0 ± 2.20[27,g,l,n,p]	19.4 ± 10.43[f,k,l,m]	23.6 ± 4.89[27,h,n,r,t]
2:2:2	27.3 ± 5.30[16,g,m,q,r,s]	34.8 ± 4.67[16,24,m]	25.7 ± 6.02[24,m]	21.2 ± 2.92[20,28,p]	28.0 ± 6.86e[20,e,m]	26.8 ± 4.18[28,p,s,t]

Notations are the same as in table 3.

cycle. Durations of the cleavage cycles for embryos of the third group can be comparable or exceed the ones for the first group embryos, and in some cases, for the second group embryos (see details in *Tab. 2*).

ME embryos of the first, second, and third groups reach the 16-cell stage of development after 85.1 ± 4.28 (mean ± standard deviation), 110.5 ± 6.10, and 94.6 ± 2.57 h; EM embryos – after 74.9 ± 3.10, 102.1 ± 5.20, and 88.8 ± 3.05 h, respectively. The differences in these values are statistically significant (Van der Waerden test, $P = 0.001$, 0.024 and 0.001). At the same time, the average trajectories of the development of ME and EM embryos of the first, second, and third groups do not differ (paired Wilcoxon test; $P = 0.256$, 0.158, and 0.112, respectively).

ME and EM embryos of different groups had reached different stages of development by the end of the registration period (*Tab. 2*). The first groups included embryos that had formed mature blastocysts (grades 4 and 5). The second groups included slowly developing embryos that had reached the stage of morula or blastocyst that had initiated cavitation. The third groups were diverse since their embryos had a whole spectrum of blastocysts by the end of registration, with blastocysts of grades 2 and 3 being the most presented (*Tab. 2*). Comparison of alternative distributions (number of embryos that had reached grades 5 and 4 with the number of earlier embryos at the end of the registration period) showed a clear prevalence of both ME and EM embryos in group 1 and, thus, the prevalence of embryos with delayed development in group 2 (two-sided Fisher's exact test, $P = 0.021$ and 0.001). The same comparison of groups 1 and 3 demonstrated a significant difference in alternative distributions for EM embryos ($P = 0.019$) and similarity among ME embryos ($P = 0.277$).

The period of development for MM embryos to the 16-cell stage occupies an intermediate position between corresponding values for ME and EM embryos of the first groups, and is significantly shorter than the first value (Van der Waerden test, $P = 0.017$) but longer than the second value ($P = 0.001$). The average cleavage trajectory for MM embryos is different from the trajectory for ME and EM embryos of the first groups (paired Wilcoxon test, $P = 0.001$ and 0.000, respectively). Alternative distribution (normally developed embryos compared to embryos with delayed development) in the MM group does not differ from similar distributions in the first groups of ME and EM embryos (Fisher's exact test, $P = 0.590$ and 0.148) but differs from the distribution in the second groups ($P = 0.015$ for both comparisons).

Averaged parameters of cleavage (and thus the trajectories of development during the cleavage period) for ME and EM embryos of the first groups, as well as for MM embryos (i.e. the parameters of rapidly cleaving embryos in total), are in good agreement with prognostic criteria for successfully developing embryos (see *Tab. 1* and *2*).

Blastomere genealogy and cycles

The duration of blastomere cycles in 4- and 8-cell embryos with different variants of the second cleavage

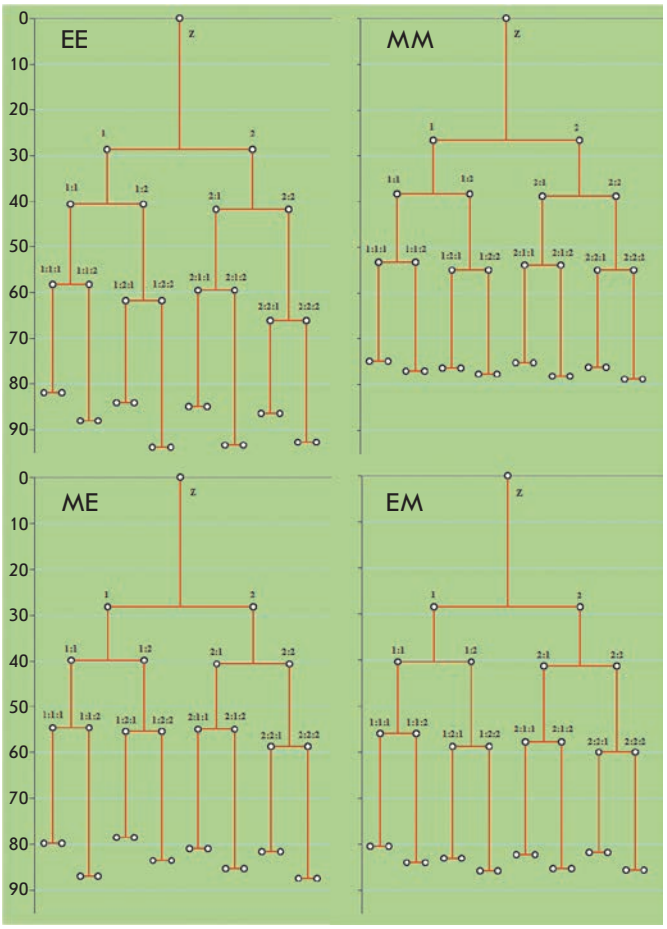

Fig 3. Blastomere genealogy in EE, MM, ME and EM embryos. The numbers at bifurcation points show the order of blastomere appearance (same for every genealogy schemes). The lowest number stands for the shortest cycle length. Vertical axes indicate the time after intracellular sperm injection (h). Z – zygote

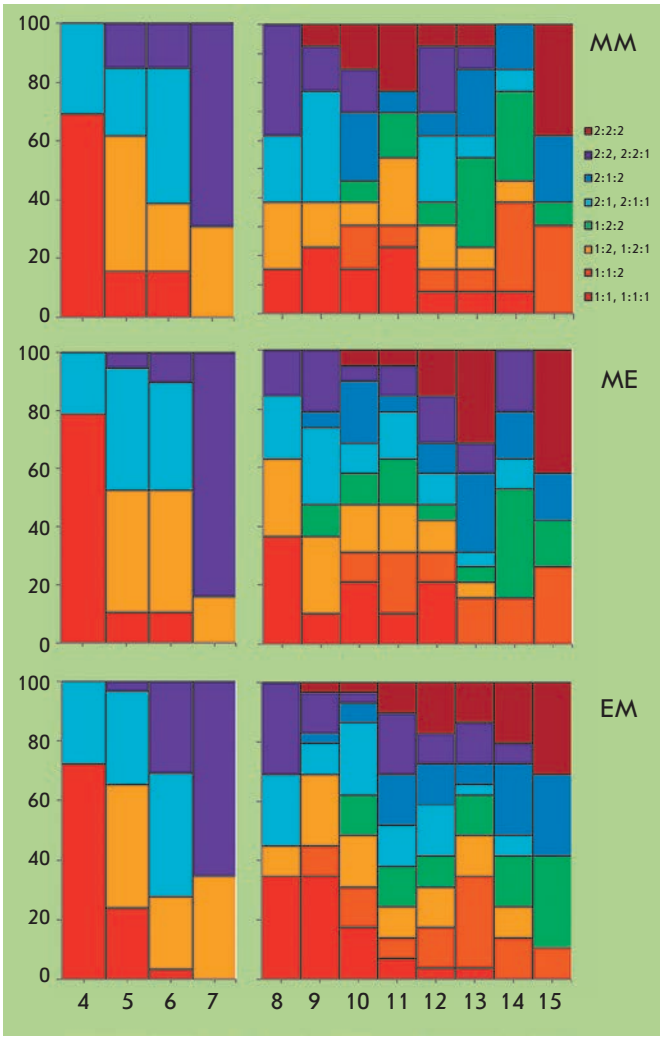

Fig. 4. Distribution of blastomere cleavage periods for 4-cell (left diagrams) and 8-cell (right diagrams) aggregates of MM, ME, and EM embryos. Horizontal axes depict the order of successive cellular divisions. Columns of various colors represent the division frequencies of each blastomere in relation to total cell divisions (in %, vertical axes) at a set moment of sequential division. The color code of blastomeres of different origins is presented in the legend in the upper right corner of the diagram

are different in general (Kruskal-Wallis test, $P < 0.000$ in both cases). The shortest cycles are typical for MM embryos; the longest – for EE embryos. ME and EM embryos, the cycles of which for corresponding blastomeres (especially at the 8-cell stage) are sufficiently similar to each other, have an intermediate position (see *Tab. 3*). The blastomere cycles of the first groups of ME and EM embryos are shorter than the corresponding cycles for embryos of the second and third groups (cycle duration values and their statistical comparisons are presented in *Tab. 4*).

Due to the genealogical hierarchy, the division period of any blastomere is composed of a period of dividing blastomere cycle and the periods of the cycles of blastomeres preceding it. Inequality of the cycles of sister blastomeres (*Fig. 3*) is the event that structures blastomere division periods in each cleavage cycle and the trajectories of the whole cleavage.

Substitution of the time parameters of the cleavage trajectory with the sequence (order) of blastomere divisions (that mediate the terms of a blastomere lineage existence, see *Fig. 3*) allows one to identify the diversity of the cycles of individual blastomeres within various embryos. The distributions connecting the division frequencies of blastomeres of similar origin with the sequence of their division in the third and fourth cycles

of cleavage trajectories are significantly different from the corresponding equality probabilities for both 4-cell EE, MM, ME, and EM embryos (χ^2: 20.0, 40.3, 84.0, and 93.1, respectively; threshold χ^2 value ($P < 0.05$) equals 16.09) and 8-cell MM, ME, and EM embryos (χ^2: 79.4, 98.9 and 133.8, respectively, threshold χ^2 value equals 66.3). The distribution for 8-cell EE embryos does not differ from the equiprobable distribution ($\chi^2 = 56.0$, $P > 0.250$), which is due to the small sample size of such embryos.

In 4-cell ME embryos, blastomere 1 : 1 divides before the others in 78.9 % of cases ($\chi^2 = 31.7$, $P < 0.000$), while the same value for blastomere 2 : 2 is 84.2 % ($\chi^2 = 40.6$, $P < 0.000$). Blastomeres 1 : 1 : 1, 2 : 2 : 2, and 1 : 2 : 2 are significantly more likely to divide in the eighth, 15th, and 14th row (36.8, 42.1 and 36.8 %; $\chi^2 = 12.6$, 26.1 and 15.1; P <0.050, <0.001 and 0.050, respectively). Blastomeres 1 : 1 and 2 : 2 in 72.4 and 65.5 % of EM embryos are the fourth and seventh to divide ($\chi^2 = 40.6$ and 34.6, $P < 0.000$); blastomere 1 : 1 : 1 is the eighth and ninth to divide (in 34.5 % of cases, $\chi^2 = 36.9$ and 22.0, $P < 0.000$ and < 0.005), blastomeres 1 : 1 : 2 and 2 : 2 : 2 are the 14th and 15th (in 31.0 and 34.5 %, $\chi^2 = 35.8$, P <0.000) (see *fig. 4*). In MM embryos, the first and the last to divide are blastomeres 1 : 1 and 2 : 2 (69.2 %, $\chi^2 = 16.8$, P <0.025) and blastomeres 2 : 2 : 1 and 2 : 2 : 2 (in 38.5 % cases, $\chi^2 = 15.9$ and 18.4, P <0.050 and <0.025, respectively).

Thus, blastomeres, despite the similarity of origin, significantly differ in their division sequence (i.e. periods of the existence of blastomere lineages until the moment of their division), appear and increase in number during the third and fourth cycles of cleavage in the embryo. The two blastomeres are the first and last to successively divide in the vast majority of 4-cell embryos, while the division sequences of the two other blastomeres vary. In 8-cell embryos, the probability of early or late successive divisions of blastomeres is reduced. However, the number of blastomeres increases; the division moment for them varies among different embryos. If such a tendency is preserved in the fifth and sixth cleavage cycles, the division sequence for all blastomeres, 16- and 32-cell, will become stochastic. Since the embryos, some of them earlier and some of them later, had reached the final stage of development (blastocysts), it can be assumed that the discussed phenomenon is one of the manifestations of the regulatory aspect of blastomeres and embryos in general, which increases during cleavage. An increase in the regulatory aspect, by definition, involves an expansion of the spectrum of potential differentiation pathways. Therefore, one can expect the expansion of potential abilities to differentiate in blastomeres of 8-cell and, particularly, 16- and 32-cell embryos.

It is traditionally believed that oocytes and zygotes are totipotent. However, according to cytologic criteria, oocytes and zygotes inheriting the structure of oocyte are highly specialized cells. In addition to their characteristic morphology and specific syntheses, zygote specialization is manifested in polarization with uneven volumetric distribution (as well as in the length of the cortical layer) of cellular organelles and the complex of specific regulatory macromolecules [18–20 et al.]. We suggest that blastomeres acquire the ability of self-synthesis and regulation, polarization, and formation of functional contacts and, finally, of specific differentiation only after the elimination of the specific characteristics of zygote organization and release from the influence of zygotic determinants [21–23]. At the molecular genetic level, the events that release blastomeres from "zygote dictatorship" during the period of the first cleavage divisions are poorly studied and are most likely associated with cell cycle regulation [24, 25].

CONCLUSION

In placental mammals, unlike in lower vertebrates, polarization (pre-mapping) of zygote is sufficiently labile, which determines the diversity of time parameters in the early development and, in the case of imperfection or insufficiency of this pre-mapping, a rather high level of early development anomalies. As a result of the realization of all possible combinations of meridional and equatorial furrows, four variants of 4-cell embryos are formed during the cleavage of 2-cell human embryos (as well as mouse embryos and, probably, other types of placental mammals). The blastomeres of embryos that belong to different variants include significantly different parts of zygotes, thus acquiring different "doses" of determinants. Segregation of zygotic cytoplasm and determinants continues during further cleavage divisions. This, in turn, is reflected in the significant diversity in time parameters (blastomere cycles, cleavage cycles and cleavage trajectory in general) in the next cleavage rounds of each variant of 4-cell embryos. The diversity associated with the degree of "perfection" of zygote organization interferes with the diversity provided by way of its segregation, which is manifested in cleavage trajectories. An example of this is the development trajectories for ME and EM embryos with significantly different cleavage rates (the first, second, and third groups). According to preliminary estimates, the formation frequencies of implantation-competent blastocysts tracing to each of the variants of 4-cell embryos are different. Thus, the variant of a 4-cell embryo formation should be taken into account during early prognosis of the prospectivity of each individual embryo.

Substitution of time parameters by ordinal characteristics (i.e. the sequences of blastomere divisions in

the cleavage trajectory or, in other words, mediated terms of the existence of blastomeres lineages) allows one to reveal another form of diversity associated with the characteristics of the cleavage process itself – the diversity in the moment of entry into the next cleavage cycle for blastomeres of similar origin within various embryos. We suggest that this phenomenon may be explained by the gradual decrease in the effects of determinants as a reflection for consecutive elimination of the specific organization of zygote in its fragments (i.e. blastomeres). A dedifferentiation of blastomeres achieved in this way precedes and, possibly, enables their own expression, regulation, and, finally, their own differentiation. Greater or lesser success in blastomeres' dedifferentiation defines a time shift (longer or shorter, respectively) for the events of asymmetric divisions and compaction, which in turn may influence the ratio of inner cell mass to mural trophectoderm in blastocysts. ●

REFERENCES

1. Human preimplantation embryo selection. Reproductive medicine and assisted reproductive techniques. // Eds. K. Elder, J. Cohen. Informa Helthcare, 2007. 379 p.
2. Van den Bergh M., Ebner T., Elder K. Atlas of oocytes, zygotes and embryos in reproductive medicine. NY: Cambridge University Press, 2012. 237 p.
3. Pribenszky C., Losonczi E., Molnar M., Lang Z., Matyas S., Rajczy K., Molnar K., Kovacs P., Nagy P. Conceicao J. et al. // Reprod. BioMed. Online. 2010. V. 20. P. 371–379.
4. Kirkegaard K., Agerholm I.E., Ingerslev H.J. // Hum. Reprod. 2012. V. 27. № 5. P. 1277–1285.
5. Herrero J., Meseguer M. // Fertil. Steril. 2013. V. 99. P. 1030–1034.
6. Gulyas B.J. // J. Exp. Zool. 1975. V. 193. P. 235–248.
7. Graham C.F., Deussen Z.A. // J. Embryol. exp. Morph. 1978. V. 48. P. 53–72.
8. Gardner R.L. // Development. 1997. V.124. P. 289–301.
9. Cooke S., Tyler J.P.P., Driscoll G.L. // Hum. Reprod. 2003. V. 18. P. 2397–2405.
10. Edwards R.G., Hansis C. // Reprod. BioMed. Online. 2005. V. 11. № 2. P. 206–218.
11. Gardner R.L. // Hum. Reprod. 2002. V. 17. № 12. P. 3178–3189.
12. Piotrowska-Nitsche K., Zernicka-Goetz M. // Mech. Dev. 2005. V. 122. P. 487–500.
13. Edwards R.G. // Reprod. BioMed. Online. 2003. V. 6. № 1. P. 97–113
14. Edwards R.G., Beard H.K. // Mol. Hum. Reprod. 1997. V. 3. № 10. P. 863–905.
15. Zernicka-Goetz M., Morris S.A., Bruce A.W. // Nat. Rev. Genet. 2009. V. 10, P. 467–477.
16. Gardner D.K., Schoolcraft W.B. // Towards reproductive certainty: Fertility and genetics beyond 1999. / Eds. R. Jansen, D. Mortimer. Carnforth: Parthenon Publishing, 1999. P. 378–388.
17. Gardner D.K., Stevens J., Sheehan C.B., Schoolcraft W.B. // Human preimplantation embryo selection: Reproductive medicine & assisted reproductive techniques series / Eds. K. Elder, J. Cohen. Informa Healthcare, Informa UK Ltd, 2007. P. 79–87.
18. Goodall H., Johnson M.H. // J. Embryol. exp. Morph. 1984. V. 79. P. 53–76
19. Bischoff M., Parfitt D.-E., Zernicka-Goetz M. // Development. 2008. V. 135. P. 953–962.
20. Kloc M., Ghobrial R.M., Borsuk E., Kubiak J.Z. // Mouse development – from oocyte to stem cells / Ed. J.Z. Kubiak. Berlin, Haidelberg: Springer-Verlag, 2012. P. 23–44.
21. Marikawa Y., Alarcón V.B. // Mol. Reprod. Dev. 2009. V. 76. № 11. P. 1019–1032.
22. Zhang P., Zucchelli M., Bruce S., Hambiliki F., Stavreus-Evers A., Levkov L., Skottman H., Kerkelä E., Kere J., Hovatta O. // PLoS ONE. 2009. V. 4. № 11. e7844.
23. Cockburn K., Rossant J. // J. Clin. Invest. 2010. V. 120. № 4. P. 995–1003.
24. Kiessling A.A., Bletsa R., Desmarais B., Mara C., Kallianidis K., Loutradis D. // J. Assist. Reprod. Genet. 2010. V. 27. № 6. P. 265–76.
25. Duronio R.J. // Genes Develop. 2012. V. 26. P. 746–750.

ZAD-Domain Is Essential for Nuclear Localization of Insulator Proteins in Drosophila melanogaster

N.A. Zolotarev, O.G. Maksimenko, P.G. Georgiev, A.N. Bonchuk*
Institute of Gene Biology, Russian Academy of Sciences, Vavilova str. 34/5, Moscow, 119334, Russia
*E-mail: errinaceus@rambler.ru
Received December 10, 2015; in final form, March 14, 2016

ABSTRACT **Many arthropod zinc-finger transcription factors contain a N-terminal domain called ZAD (Zinc-finger Associated Domain), which consists of four cysteines coordinating a single zinc ion. Dimerization ability has been shown for several ZAD-domains. The functional role of this domain is poorly understood. In this paper, we demonstrate that a point mutation within the ZAD-domain of the Zw5 insulator protein disrupts its nuclear localization without affecting its dimerization ability. The importance of the ZAD-domain for nuclear localization has also been shown for the Pita and Grauzone proteins. Therefore, one of the ZAD-domain functions is control of the nuclear localization of transcription factors.**
KEYWORDS **insulators, chromatin, transcription factors**
ABBREVIATIONS **ZAD, Zinc-finger Associated Domain; IPTG, Isopropyl-β-D-thiogalactopyranoside; PMSF, phenylmethylsulfonylfluoride**

INTRODUCTION

Proteins with a "zinc fingers" DNA-binding domain of C2H2-type are the largest class of transcription factors in higher eukaryotes [1]. The C2H2-domains usually form clusters, some of which are responsible for highly specific binding to DNA. A subclass of C2H2-type "zinc fingers" transcription factors was found in arthropods: its representatives contain a specific domain at the N-terminus, called ZAD (Zinc-finger Associated Domain), which contains four cysteines coordinating a single zinc ion [2, 3]. *Drosophila melanogaster* cells contain over 90 transcription factors (*Fig. 1*) with C2H2- and ZAD-domains [3]. The genomes of other arthropods may encode from four (*Daphnia pulex*) to 120 (anopheles mosquito) factors of this class. Determination of the crystal structure of the ZAD-domain from the Grauzone (Grau) factor revealed that it is a dimer (*Fig. 2A*) [4]. In addition, it has been demonstrated *in vitro* that the ZAD-domains of the Serendipity-δ and Weckle proteins also form dimers [5, 6]. To date, this family of transcription factors remains almost unexplored, with functional roles established only for a few of them [7–9]. Three transcription factors with ZAD-domains (Pita, ZIPIC and Zw5) can be classified as insulator proteins (*Fig. 2B*) [10, 11]. Insulators are regulatory elements that block interaction between an enhancer and a promoter only if they are located between them [12, 13]. Recently, it has been shown that insulators may be involved in establishing distal interactions and the organization of chromosome architecture [14, 15]. The Zw5 protein was found in the SCS insulator, located on the boundary of a heat shock 70 gene cluster [10]. Pita and ZIPIC proteins were initially identified as partners of the insulator CP190 protein, which is believed to play the key role in the formation of chromatin architecture [11]. All insulator proteins bind to specific nucleotide sequences, 9–15 bp in length, whose multiplication creates an effective insulator [10, 11, 16]. A genome-wide analysis showed that Zw5, Pita, and ZIPIC preferentially bind to gene promoters [11]. It is assumed that the ZAD-domain may be involved in the organization of distal interactions between the remote binding sites of one insulator protein [15].

In the present study, we investigated a point mutation in the ZAD-domain of the Zw5 protein, which leads to a lethal phenotype. It has been shown that this mutation disrupts nuclear localization of the Zw5 protein. The ZAD-domains of the other two proteins, Pita and Grau, are also essential for nuclear localization of these proteins. Therefore, one of the functions of the ZAD-domain is the regulation of the nuclear localization of transcription factors.

MATERIALS AND METHODS

Expression and purification of the proteins

The DNA encoding ZAD-domains of the Zw5 protein (wild-type and R14G mutant) of *Drosophila* was cloned into the pET32a(+) plasmid in a frame with six histidine residues and Thioredoxin. The plasmids were used to transform competent cells of the *Escherichia coli* strain BL21(DE3). Protein expression was induced with 1 mM IPTG. 0.2 mM $ZnCl_2$ was added prior to the induction, and the culture was incubated overnight at 18 ˚C on a shaker. The bacterial cells were destroyed by sonication in 50 mM HEPES-KOH buffer (pH 7.6), containing 500 mM NaCl, 20 mM imidazole, 5 mM β-mercaptoethanol, and 1 mM PMSF supplemented with 1:500 Proteinase inhibitor cocktail VII (Calbiochem). The proteins were isolated from the bacterial cell lysate by affinity chromatography on Co-IDA-Sepharose. The elution was performed using 50 mM HEPES-KOH buffer (pH 7.6), containing 500 mM NaCl, 250 mM imidazole, 5 mM β-mercaptoethanol.

Chemical cross-linking of the proteins

Following the isolation, the proteins were dialyzed against PBS buffer. Glutaraldehyde was added to the preparations to a final concentration of 0.01 or 0.1%, and they were incubated at room temperature for 10–15 min. The reaction was quenched by adding glycine to a concentration of 50 mM and incubated at room temperature for 15 min. The products of the cross-linking reaction were visualized by electrophoresis in polyacrylamide gel, followed by silver staining.

Image staining of the S2 cells of *D. melanogaster*

cDNAs encoding either full-length wild-type proteins or mutant ones were cloned into a plasmid in frame with 3×FLAG-peptide for transient expression under the control of the actin 5C gene promoter. The cells were transfected according to the standard procedure using the Cellfectin reagent (Invitrogen). The staining was performed on the third day after the transfection.

1 ml of the suspension of S2 cells was applied to a cover glass of a 35-mm Petri dish. It was incubated overnight at 24 ˚C to precipitate the cells on the glass. The medium with non- adhered cells was removed.

All solutions were applied to the wall of the dish, so as not to wash off the cells from the glass. The incubation was performed at room temperature on a shaker at low speed.

The glass was washed with 1 ml of phosphate-buffered saline (PBS, 2 × 5 min). The cells were fixed with 1 ml of the fixation solution (2% formaldehyde, 50 mM $MgCl_2$ in PBS) for 20 min. They were washed with 1 ml of PBS (3 × 5 min). To increase the permeability of the cell membranes, the cells were treated with 1% Triton X-100 in PBS for 10 min. The cells were washed with PBS (1 ml, 3 × 5 min). They were incubated in a blocking solution (1% bovine serum albumin (BSA), 0.05% Tween-20 in PBS, 2 × 30 min) and incubated with 1 ml of the blocking solution with primary antibodies (1:30 anti-lamin (from the collection of the University of Iowa), 1:300 anti-FLAG (Sigma)). Then they were washed with the solution of 0.25% BSA, 0.05% Tween-20 in PBS (3 × 15 min), incubated with 1 ml of the blocking solution with secondary antibodies conjugated with a fluorophore (Invitrogen) and TO-PRO-3 Iodide for 1 h. They were washed with the solution of 0.25% BSA, 0.05% Tween-20 in PBS (3 × 15 min), and washed with 1 ml of PBS for 5 min. The glass was then washed with water, and the excess water was removed. A Vectashield medium was added for fixing on the cover glass. The edges of the cover glass were, coated with varnish.

RESULTS

Lethal mutation in the ZAD-domain of Zw5 protein does not affect its ability to dimerize

The dwg (*deformed wings*) gene that encodes the Zw5 protein is expressed primarily during embryogenesis. There are many mutations described for the *dwg* gene that produce a lethal phenotype, suggesting that Zw5 plays an important role in embryonic development. One of well-characterized mutations, dwg^8 or $zw5^{62jl}$, leads to substitution of arginine for glycine at position 14 (R14G) of the ZAD-domain [10]. This recessive mutation is lethal at the larval stage. To prove that the $zw5^{62jl}$ mutation is the one responsible for the lethal phenotype, a construct was obtained in which the *dwg* gene was under the control of the *hsp83* gene promoter. *White* gene that determines eye pigmentation was used as the reporter gene to identify the transformants. Four transgenic lines with a single insertion of the construct were obtained as a result of the transformation into *Drosophila* embryos. All transgenes complemented the lethal phenotype of the $zw5^{62jl}$ mutation, confirming the role of this mutation in the manifestation of the lethal phenotype.

Therefore, a point mutation in the ZAD-domain leads to a complete functional inactivation of Zw5. Based on this data, it can be concluded that the presence of R14 in the ZAD-domain is essential. The alignment of the ZAD-domain sequences from different proteins demonstrated that most ZAD-domains contain an arginine residue at position 14 (*Fig. 1*). Out of 93 transcription factors with a ZAD-domain in the *Drosophila* genome, 81 have arginine at position 14 (R14). In five proteins, arginine is replaced with leucine; in three, with phenylalanine; in two, with cysteine; and

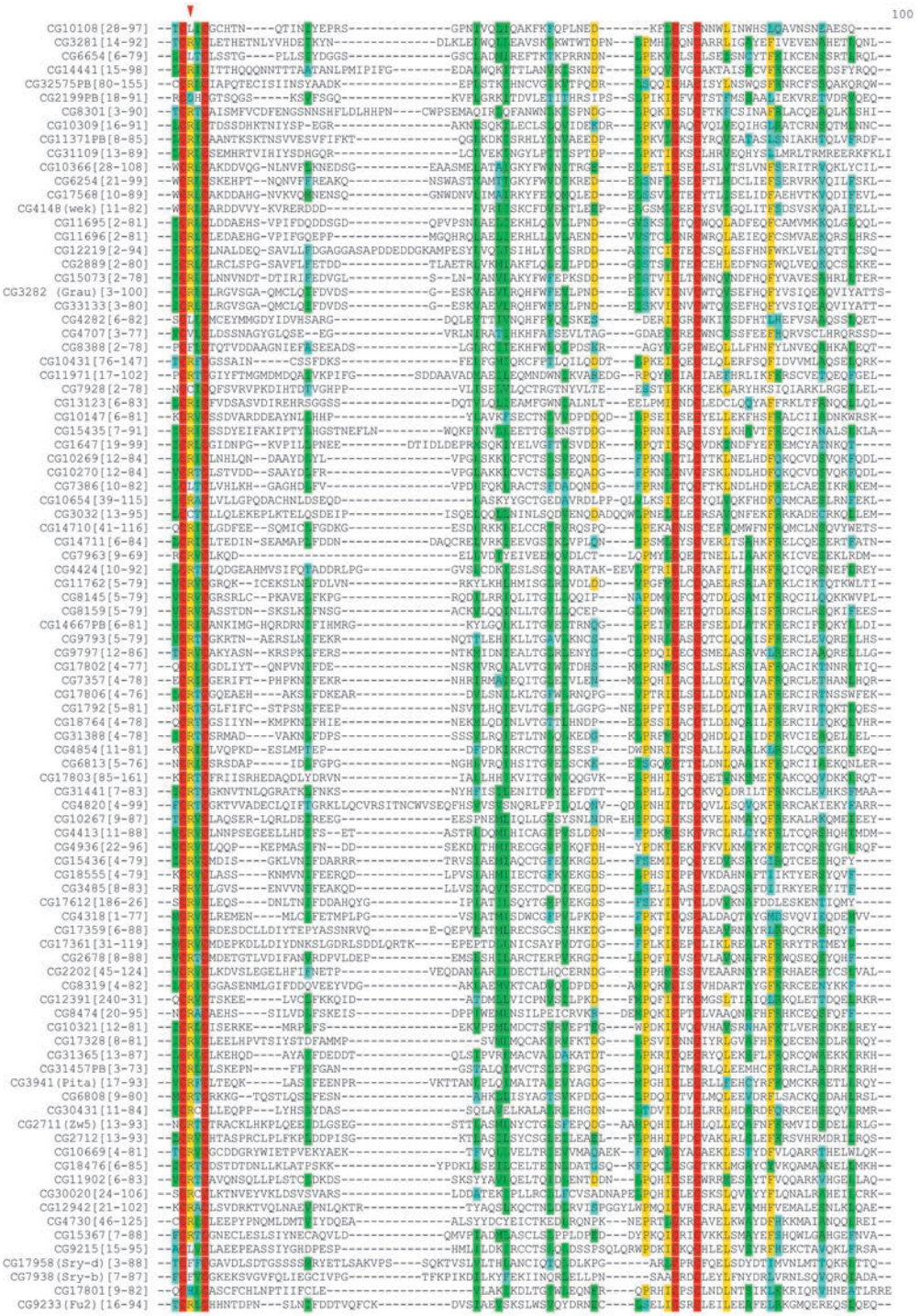

Fig. 1. Multiple sequence alignment of *Drosophila* ZAD-domain amino-acid sequences. Red arrow indicates the position of conserved arginine.

in one, with aspartate and histidine. Previously, it has been suggested that R14 participates in the ZAD-domain dimerization [4], since it (R5 in Grau protein) is involved in the formation of hydrogen bonds with Q74 (*Fig. 2A*), although these residues are only a small part of an extended dimerization interface between two ZAD-domains. In order to test this hypothesis, cDNAs encoding the ZAD^{wt} and ZAD^{R14G} domains fused to Thioredoxin were cloned into a pET32a(+) vector and expressed in *E. coli* cells. It was found that the mutant ZAD-domain is expressed in much lower quantities than the wild-type domain. This may indicate a lesser stability and disruption of the proper conformation of the mutant ZAD-domain expressed in bacteria.

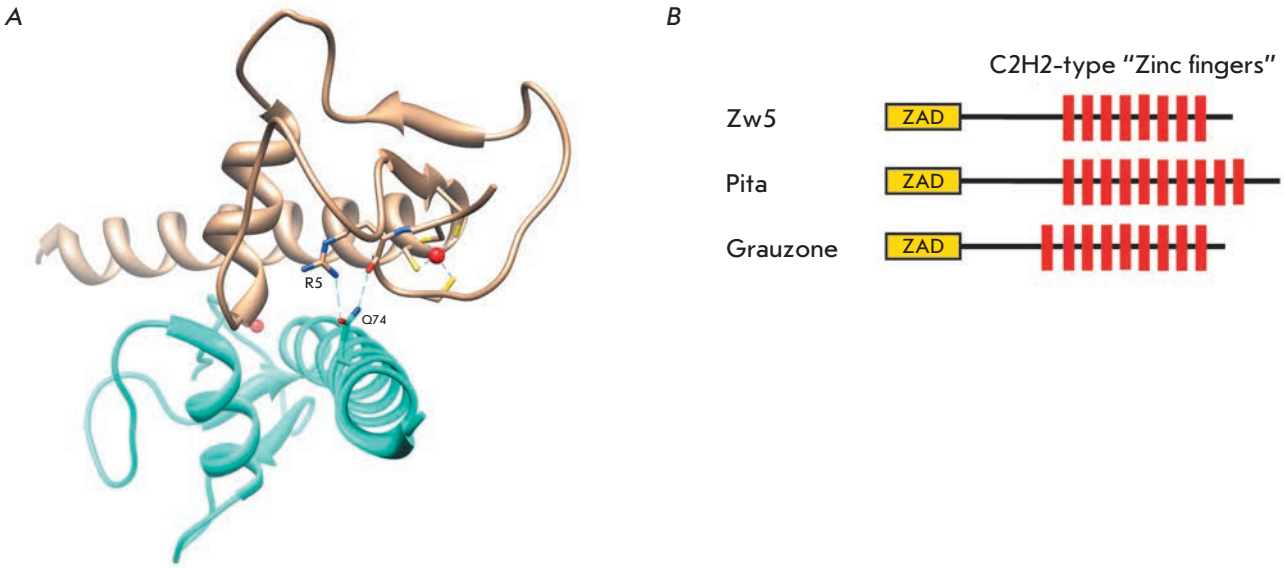

Fig. 2. A – Crystal structure of ZAD-domain dimer from Grau protein (1PZW in PDB). Hydrogen bonds between R5 (residue homological to R14 of Zeste-white 5 protein) and Q74 are shown; also shown are four cysteines coordinating the zinc-ion. B – Domain structure of the Zeste-white 5, Pita, and Grauzone proteins.

To compare the dimerization of the normal and mutant ZAD-domains, we cross-linked the ZAD-domains using glutaraldehyde. As can be seen from *Fig. 3*, at a concentration of 10 μM both ZAD-domains form dimers with a similar efficiency. Therefore, the R14G mutation does not affect the ability of the Zw5 ZAD-domain to dimerize *in vitro*, but we cannot exclude the possibility of reduced stability of the dimer at low protein concentrations in the cell.

ZAD-domains are essential for nuclear localization of the proteins in Drosophila S2 cells

It was found that the mutant ZAD-domain retains its ability to dimerize; therefore, the next task was to study the distribution of the normal and mutant Zw5 proteins in *Drosophila* S2 cells. For this purpose, we had created expression vectors in which the genes encoding the normal and mutant Zw5 proteins fused to 3×FLAG epitope were under the control of the actin promoter. These vectors were used to transfect S2 cells, and the protein distribution was determined using antibodies to 3×FLAG epitope and lamin, and TO-PRO-3 Iodide dye, which stains DNA (*Fig. 4*). The Zw5-3×FLAG protein is localized mainly in the nucleus. Surprisingly, the $Zw5^{R14G}$-3×FLAG protein was found almost exclusively in the cytoplasm. Thus, the point mutation disrupts nuclear localization of the Zw5 protein, which explains the lethal effect of the $zw5^{62j1}$ allele. According to the data of the NucPred service [17], the Zw5 protein does not contain nuclear localization signals.

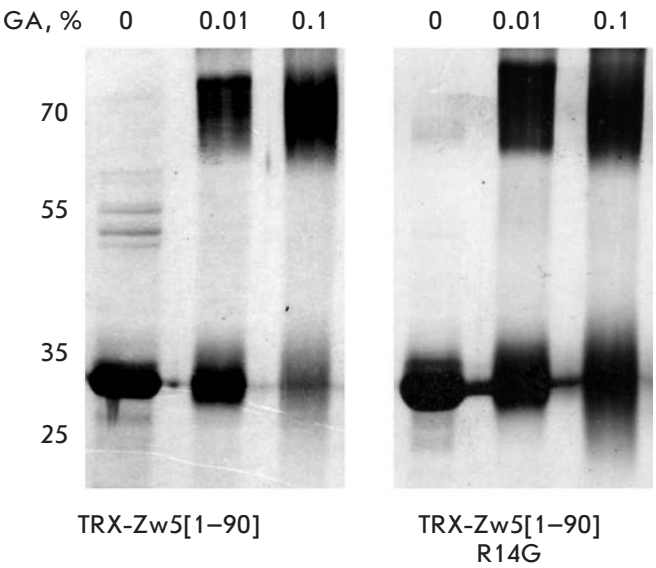

Fig. 3. Results of chemical cross-linking with glutaraldehyde (GA) of the wild-type Zw5 ZAD-domain and the domain with R14G mutation, fused with Thioredoxine (TRX). Protein concentration is 10 μM.

To elucidate the role of the ZAD-domain in the nuclear localization of the proteins, we examined two other well studied proteins with the ZAD-domain: Pita and Grau [4, 8, 11]. These proteins have the same structure, similar to that of Zw5: the ZAD-domain is located at the N-terminus and a group of C2H2 type "zinc-

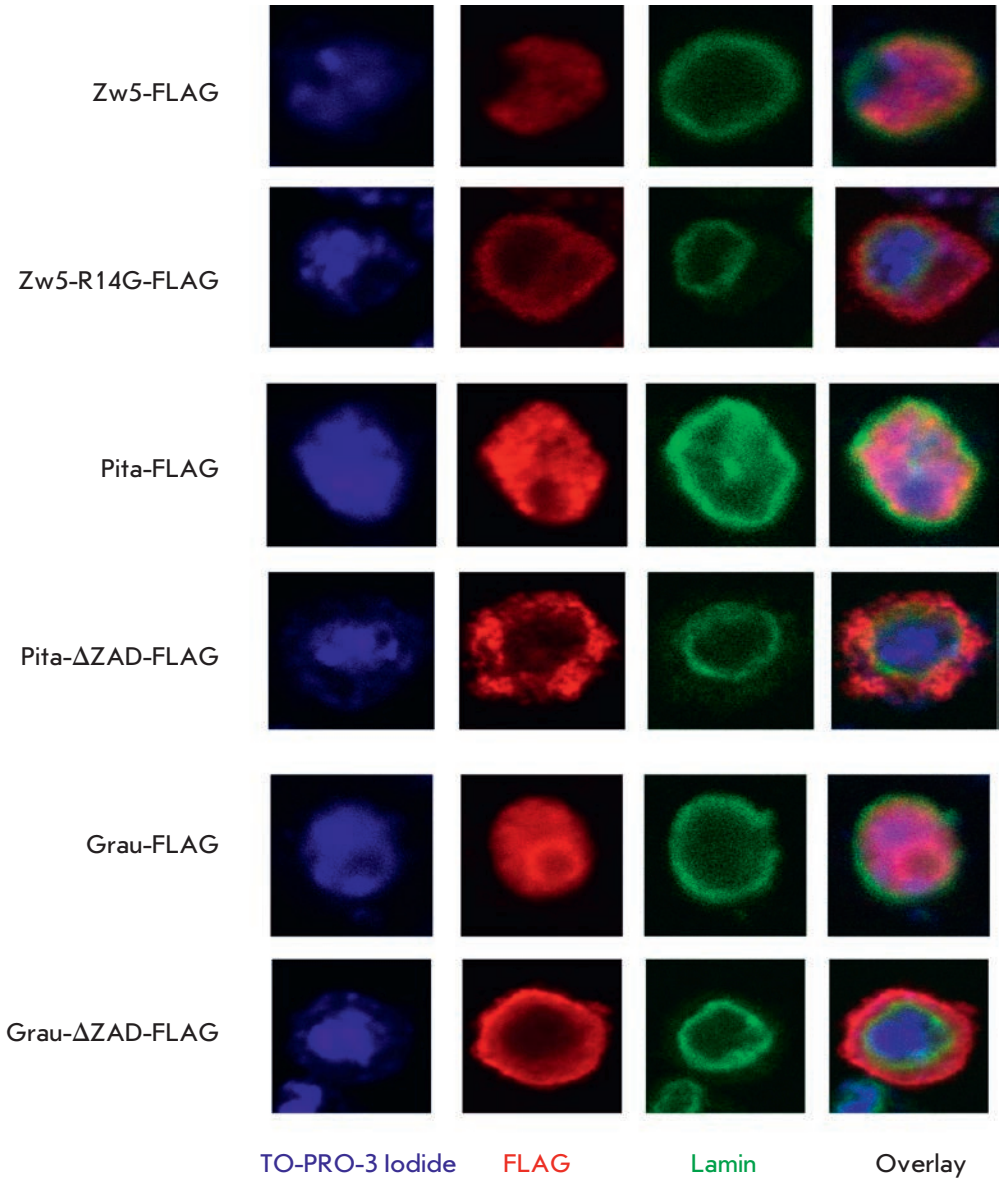

Fig. 4. Immunocytochemical staining of S2-cells expressing proteins with a disrupted ZAD-domain and wild-type proteins fused with the 3xFLAG-peptide.

finger" domains forming a cluster at the C-terminus (*Fig. 2B*). It has been shown that "zinc finger" domains may define the nuclear localization of the proteins [18, 19]. According to the data of the NucPred software [17], Pita has no nuclear localization signals (NLS) and Grauzone has NLS in its central part (170–190 amino acids). The PredictProtein service [20] predicts nuclear localization for all three proteins with a low degree of significance for Zw5 and Pita and with a high degree for Grauzone.

cDNAs, encoding the Grau and Pita proteins with and without the ZAD-domain, were fused with 3×FLAG epitope and incorporated into an expression vector under the control of the actin promoter (Act5C). The resulting constructs were used to transfect S2 cells, and the distribution of the protein in the cells was studied using antibodies to 3×FLAG epitope and lamin (*Fig. 4*). The Pita-3×FLAG and Grau-3×FLAG proteins were located predominantly in the nucleus. Staining of the endogenous Grau, Zw5, and Pita proteins (data not shown) revealed their uniform nuclear-cytoplasmic distribution. Deletion of the ZAD-domain led to localization of the FLAG-antibodies predominantly in the cytoplasm, which can be attributed to a loss of the ability to enter the cell nucleus by proteins without a ZAD-domain (*Fig. 4*).

DISCUSSION

Our results suggest that point substitution of arginine for glycine at position 14 (R14G) of the ZAD-domain

disrupts the nuclear localization of the Zw5 protein. R14 in the ZAD-domain of Zw5 corresponds to the fifth amino acid residue of the ZAD-domain of the Grau protein. According to its crystal structure, the side chain of this residue is exposed at the surface and is capable of forming a hydrogen bond with Q74 [4]. Based on these data, the authors [4] suggested that arginine-5 is involved in the dimerization of the Grau ZAD-domain. However, according to our results, arginine-14 in the ZAD-domain of Zw5 is not essential for protein dimerization. It is possible that the structure of different ZAD-domains can vary significantly, which explains the preferable homodimerizaiton of ZAD-domains (unpublished data).

The putative localization of arginine-14 on the surface of the ZAD-domain may explain the role of this residue in the interaction with the proteins involved in nuclear import. The ZAD-domains of the Pita and Grau proteins have sequence similarity with each other and with the ZAD-domain of Zw5 of less than 58%. However, these ZAD-domains are also required for nuclear localization of the respective proteins.

Interestingly, bioinformatic approaches predicted nuclear localization signals in the central part of Grau and an absence of such signals in the Pita and Zw5 proteins. However, the Pita protein is present in cells as two isoforms which differ by the presence of the first 60 amino acids of the ZAD-domain [according to Flybase]. According to experimental data, subcellular localization of transcription factors with a ZAD-domain is the subject of a complex regulation. For example, it has previously been demonstrated that the nuclear-cytoplasmic localization of the Weckle protein changes during development [6]. The ZAD-containing Trade Embargo protein, which binds to chromatin, is evenly distributed between the nucleus and the cytoplasm [21].

CONCLUSION

Our results show that nucleocytoplasmic distribution of ZAD-containing transcription factors appears to have regulatory importance and that the ZAD-domains are essential for this process. ●

This work was supported by the Russian Science Foundation (Project № 14-24-00166).

REFERENCES

1. Razin S.V., Borunova V.V., Maksimenko O.G., Kantidze O.L. // Biochemistry(Moscow). 2012. V. 77. P. 277-288. (In Russian).
2. Chung H.R., Schafer U., Jackle H., Bohm S. // EMBO Rep. 2002. V. 3. P. 1158–1162.
3. Chung H.R., Lohr U., Jackle H. // Mol. Biol. Evol. 2007. V. 24. P. 1934–1943.
4. Jauch R., Bourenkov G.P., Chung H.R., Urlaub H., Reidt U., Jackle H., Wahl M.C. // Structure. 2003. V. 11. P. 1393–1402.
5. Payre F., Buono P., Vanzo N., Vincent A. // Mol. Cell Biol. 1997. V. 17. P. 3137–3145.
6. Chen L.Y., Wang J.C., Hyvert Y., Lin H.P., Perrimon N., Imler J.L., Hsu J.C. // Curr. Biol. 2006. V. 16. P. 1183–1193.
7. Li J., Gilmour D.S. // EMBO J. 2013. V. 32. P. 1829–1841.
8. Page A.R., Kovacs A., Deak P., Torok T., Kiss I., Dario P., Bastos C., Batista P., Gomes R., Ohkura H., et al. // EMBO J. 2005. V. 24. P. 4304–4315.
9. Gibert J.M., Marcellini S., David J.R., Schlotterer C., Simpson P. // Dev. Biol. 2005. V. 288. P. 194–205.
10. Gaszner M., Vazquez J., Schedl P. // Genes Dev. 1999. V. 13. P. 2098–2107.
11. Maksimenko O., Bartkuhn M., Stakhov V., Herold M., Zolotarev N., Jox T., Buxa M. K., Kirsch R., Bonchuk A., Fedotova A., et al. // Genome Res. 2015. V. 25. P. 89–99.
12. Kyrchanova O., Georgiev P. // FEBS Lett. 2014. V. 588. P. 8–14.
13. Matzat L.H., Lei E.P. // Biochim. Biophys. Acta. 2014. V. 1839. P. 203–214.
14. Maksimenko O., Georgiev P. // Front. Genet. 2014. V. 5. P. 28.
15. Sexton T., Cavalli G. // Cell. 2015. V. 160. P. 1049–1059.
16. Kyrchanova O., Chetverina D., Maksimenko O., Kullyev A., Georgiev P. // Nucleic Acids Res. 2008. V. 36. P. 7019–7028.
17. Brameier M., Krings A., MacCallum R.M. // Bioinformatics. 2007. V. 23. P. 1159–1160.
18. Ito T., Azumano M., Uwatoko C., Itoh K., Kuwahara J. // Biochem. Biophys. Res. Commun. 2009. V. 380. P. 28–32.
19. Bruening W., Moffett P., Chia S., Heinrich G., Pelletier J. // FEBS Lett. 1996. V. 393. P. 41–47.
20. Rost B., Yachdav G., Liu J. // Nucleic Acids Res. 2004. V. 32. P. W321–326.
21. Lake C.M., Nielsen R.J., Hawley R.S. // PLoS Genet. 2011. V. 7. P. e1002005.

Whole-Genome DNA Methylation Analysis of Peripheral Blood Mononuclear Cells in Multiple Sclerosis Patients with Different Disease Courses

O.G. Kulakova[1,2]*, M.R. Kabilov[3], L.V. Danilova[4,5], E.V. Popova[1], O.A. Baturina[3], E.Y. Tsareva[1,2], N.M. Baulina[1,2], I.S. Kiselev[1,2], A.N. Boyko[1], A.V. Favorov[4,5], O.O. Favorova[1,2], V.V. Vlassov[3]

[1]Pirogov Russian National Research Medical University, Ostrovityanova str. 1, Moscow, 117997, Russia

[2]Institute of Experimental Cardiology, Russian Cardiology Scientific and Production Center, 3th Cherepkovskaya str. 15A, Moscow, 121552, Russia

[3]Institute of Chemical Biology and Fundamental Medicine, Siberian Branch of the Russian Academy of Sciences, Lavrentiev Avenue 8, Novosibirsk, 630090, Russia

[4]Vavilov Institute of General Genetics, Russian Academy of Sciences, Gubkina str. 1, Moscow, 119991, Russia

[5]Johns Hopkins School of Medicine, Baltimore, MD 21205, USA

*E-mail: olga.koulakova@gmail.com

Received February 2, 2016; in final form, April 25, 2016

ABSTRACT **Multiple sclerosis (MS) is a severe neurodegenerative disease of polygenic etiology affecting the central nervous system. In addition to genetic factors, epigenetic mechanisms, primarily DNA methylation, which regulate gene expression, play an important role in MS development and progression. In this study, we have performed the first whole-genome DNA methylation profiling of peripheral blood mononuclear cells in relapsing-remitting MS (RRMS) and primary-progressive MS (PPMS) patients and compared them to those of healthy individuals in order to identify the differentially methylated CpG-sites (DMSs) associated with these common clinical disease courses. In addition, we have performed a pairwise comparison of DNA methylation profiles in RRMS and PPMS patients. All three pairwise comparisons showed significant differences in methylation profiles. Hierarchical clustering of the identified DMS methylation levels and principal component analysis for data visualization demonstrated a clearly defined aggregation of DNA samples of the compared groups into separate clusters. Compared with the control, more DMSs were identified in PPMS patients than in RRMS patients (67 and 30, respectively). More than half of DMSs are located in genes, exceeding the expected number for random distribution of DMSs between probes. RRMS patients mostly have hypomethylated DMSs, while in PPMS patients DMSs are mostly hypermethylated. CpG-islands and CpG-shores contain 60% of DMSs, identified by pairwise comparison of RRMS and control groups, and 79% of those identified by pairwise comparison of PPMS and control groups. Pairwise comparison of patients with two clinical MS courses revealed 51 DMSs, 82% of which are hypermethylated in PPMS. Overall, it was demonstrated that there are more changes in the DNA methylation profiles in PPMS than in RRMS. The data confirm the role of DNA methylation in MS development. We have shown, for the first time, that DNA methylation as an epigenetic mechanism is involved in the formation of two distinct clinical courses of MS: namely, RRMS and PPMS.**

KEYWORDS **epigenetics, DNA methylation, multiple sclerosis, peripheral blood mononuclear cells.**

ABBREVIATIONS **DMS, differentially methylated CpG-sites; CNS, central nervous system; EDSS, expanded disability status scale; HLA, human leukocyte antigen; MS, multiple sclerosis; PBMC, peripheral blood mononuclear cells; PPMS, primary-progressive multiple sclerosis; RRMS, relapse-remitting multiple sclerosis.**

INTRODUCTION

Multiple sclerosis (MS) is a severe neurodegenerative disease of the central nervous system (CNS) characterized by a complex combination of pathogenetic processes in which the most important role belongs to a chronic autoimmune inflammation directed against the components of the myelin sheath of neurons and resulting in demyelination, loss of oligodendrocytes, de-

struction of axons, gliosis, and neurodegeneration. The etiology of MS remains unclear. Recent whole-genome studies have clearly demonstrated that the observed mode of MS inheritance, typical for polygenic diseases, is indeed defined by the joint contribution of many independently acting or interacting polymorphic genes [1–3]. However, if one excludes the genes of the major histocompatibility complex (HLA) from consideration, each of the remaining MS risk alleles, taken separately, is associated with a relatively small effect: odds ratios for individual single nucleotide polymorphisms (SNPs) are, with few exceptions, in the range of 1.1–1.3 [4]. The joint contribution of all the genetic variants identified in whole-genome studies explains less than 27% of heritability [5]; a problem known as "missing heritability." These observations, as well as the low level of MS concordance in monozygotic twins [6], the effect of some environmental factors [7] and a higher prevalence of MS among women [8], led to an assumption that, in addition to genetic factors, epigenetic mechanisms may play an important role in MS development and progression.

Epigenetic modifications are various functional changes in the genome that affect the expression of genes in different cells or tissues, but are not associated with changes in the DNA sequence. DNA methylation is one of the best studied epigenetic mechanisms, and its most common form involves the addition of a methyl group to the C5 position of a cytosine ring in CpG-dinucleotides. This process modulates the expression of nearby genes. Although global DNA methylation is a relatively stable epigenetic modification, which is passed onto daughter cells during the mitosis, various environmental factors can cause dynamic changes in the epigenome during a lifetime. Recent results indicate that epigenetic modifications may play an important role in shaping the risk of autoimmune and neurodegenerative diseases, particularly MS [9, 10].

A comparative analysis of gene-specific methylation in MS patients and healthy donors revealed hypomethylation of the promoter region of the *PAD2* gene encoding type II peptidyl arginine deiminase in the white matter of the brain [11] and in peripheral blood mononuclear cells (PBMCs) [12]. Also, the *SHP-1* gene encoding protein tyrosine phosphatase was identified as hypermethylated in PBMCs of MS patients [13]. Several comparative whole-genome studies of DNA methylation profiles in MS patients and healthy individuals have been conducted in the past five years. The methylome was analyzed in both the blood cells (PBMC, CD4+, CD8+ T-lymphocytes) [6, 14–16] and the white matter of the brain [17]. Even though all studies were conducted on small sets of samples, it was found that HLA class II genes and some other immune system genes whose association with the disease had been demonstrated previously were differentially methylated in CD4+ T-lymphocytes [15] and differentially methylated genes associated with survival of oligodendrocytes were identified in the white matter of the brain [16].

MS is characterized by pronounced clinical heterogeneity [8]. The cited papers focused on patients with the most common form of MS, relapsing-remitting MS (RRMS), which is characterized by alternating periods of exacerbation and remission. Approximately 10–15% of patients are suffering from primary progressive MS (PPMS) that manifests as a continuous increase in the neurological deficit from the onset of the disease. The course of PPMS is much more severe than that of RRMS; signs of brain atrophy can be clearly defined already in the early stages of PPMS. To date, there is no specific treatment for PPMS patients and all currently known immunomodulatory drugs and corticosteroids that are used to treat RRMS are ineffective in this case.

In this paper we have conducted the first genome-wide analysis of the DNA methylation profile in PBMCs of patients with RRMS and PPRS in comparison with a control group of healthy individuals in order to identify differentially methylated CpG-sites (DMSs) associated with the development of the two major clinical disease courses, and compared the profiles of DNA methylation in patients with RRMS and PPMS.

MATERIALS AND METHODS

Characteristics of MS patients and controls

The study included 14 patients with RRMS (9 women and 5 men) and 8 patients with PPRS (6 women and 2 men), aged 29 to 58 years. The diagnosis was established according to the latest version of the McDonald criteria from 2010 [18]. The average score on the EDSS disability scale was 2.32 ± 0.823 for RRMS patients and 4.29 ± 0.39 for PPMS patients. The patients included in the study had never received any immunomodulatory drugs. The control group included 6 women and 2 men, aged 28 to 50 years, without acute or chronic neurological diseases. They all lived in the Moscow region; both of their parents were ethnic Russians (according to the survey). All participants provided written informed consent for genetic research.

DNA isolation and whole-genome analysis of methylation

Samples of the peripheral blood from MS patients (8 ml) were collected in tubes containing EDTA (Vacuette® EDTA Tubes, Greiner Bio-One). The peripheral blood mononuclear cells (PBMC) were isolated by centrifugation on a Ficoll-Hypaque gradient. The genom-

ic DNA was isolated using the DNA Midi Kit (Qiagen, Santa Clara, CA, USA) according to the manufacturer's procedure. Bisulfite conversion of the genomic DNA was performed using the EZ DNA Methylation-Gold Kit (Zymo Research). The level of DNA methylation was analyzed using a iScan scanner (Illumina) and Infinium HumanMethylation450 BeadChip [19] at the SB RAS Genomics Core Facility (ICBFM SB RAS).

Bioinformatic analysis

Primary data processing and normalization were performed using specially developed scripts written in R programming language [20].

The assessment of the methylation level for each CpG-site in the sample was performed by calculating a beta-value that is a ratio of the intensity of the methylated signal to the total intensity of the probe (sum of intensities of methylated and unmethylated signals). Beta-values ranged from 0 (unmethylated probe) to 1 (fully methylated probe). The *methylumi* package was used to calculate beta-values for each probe in each sample [21].

The probes containing a single nucleotide polymorphism within 10 bp of the interrogated CpG-site and probes, which overlapped with repeat DNA elements within 15 bp of the interrogated CpG-site, were excluded from the subsequent analysis. The probes with a detection *p*-value greater than 0.05 in more than 5% of the samples and probes located on the X and Y chromosomes were also excluded. As a result, a total of 384,138 CpG-sites out of the initial 485,000 were analyzed.

A CpG-site is considered to be differentially methylated if the difference between the methylation levels in two groups fulfills two conditions: the absolute mean difference of beta-values between groups >0.1, and the corresponding *p*- value <0.01. The localization of an individual CpG-site in a CpG-island was determined using UCSC annotation, version hg19; the CpG-shore was located 2 kbp distant from CpG-islands; and the CpG-shelf, – 2 kbp away from the CpG-shore [19]. The *P*-value was estimated using the empirical Bayes modified *t*-test, as implemented in the *limma* package in R [22]. The small sample size precluded performance of adjustment for the number of hypotheses (probes).

Visualization of DMS signals using the principal component analysis (PCA) and heatmap analysis were performed using R standard methods and customized routines [22].

RESULTS

In order to examine the potential involvement of the epigenetic DNA methylation mechanism in the development of different MS clinical courses, we had carried out a whole-genome profiling of the DNA methylation sites in PBMC from representative groups of patients with RRMS and PPMS and healthy donors (controls) and performed the following pairwise comparisons: RRMS patients vs. the controls, PPMS patients vs. the controls, and RRMS patients vs. PPMS patients.

Heatmaps of the DMSs identified in these three types of pairwise comparisons are shown in *Fig. 1A–B*. A total of 136 DMSs were identified for one or more pairwise comparison. Comparative analysis of DNA methylation for all three pairwise comparisons revealed significant differences in the methylation profiles. Hierarchical clustering by the methylation level of 136 identified DMSs revealed a clearly defined aggregation of DNA samples from patients of each of the groups under study into separate clusters. A visual comparison of the intensity of DMSs signals (ratio of blue and yellow) indicates a higher level of DNA methylation in PPMS patients compared to the controls and RRMS patients.

The data for these DMSs were visualized using the principal component analysis (*Fig. 2)*. As follows from the figure, the samples included in the study are well discriminated in a three-dimensional space of the first three principal components into three groups and these groups correspond to three phenotypes: RRMS, PPMS, and absence of these diseases.

The characteristics of the identified DMSs are presented in *Table 1*. A comparison of RRMS patients with healthy donors (controls) revealed differences in the methylation levels of 30 DMSs; for PPMS patients vs. the controls there were 67 DMSs, and the comparison of the two clinical courses of MS revealed 51 DMSs. In the case of RRMS, most of the probes were hypomethylated compared with the controls (only 43% of 30 DMS were hypermethylated). In contrast, PPMS patients had a higher number of hypermethylated probes compared with both the controls (86% of the probes were hypermethylated) and RRMS patients (82% of the probes were hypermethylated).

More than half of the DMSs are located in the genes: 18 out of 30 for RRMS vs controls, 38 out of 67 for PPMS vs controls, and 35 out of 51 for PPMS vs RRMS (*Table 1*). Since in the HumanMethylation450 platform the probes that are located in genes account for approximately a third of all probes [19], there is a clear excess of the number of expected intragenic DMSs for a random distribution of DMSs across the probes. Some genes contain several DMSs; therefore, the number of genes with DMSs is lower: 17, 25, and 22, respectively. The lists of genes containing DMSs (protein encoding, which are in the majority, and non-protein encoding genes) are also presented in *Table 1*. When RRMS is compared with the control, 53% of the genes in the first group contain DMSs with a higher methylation level;

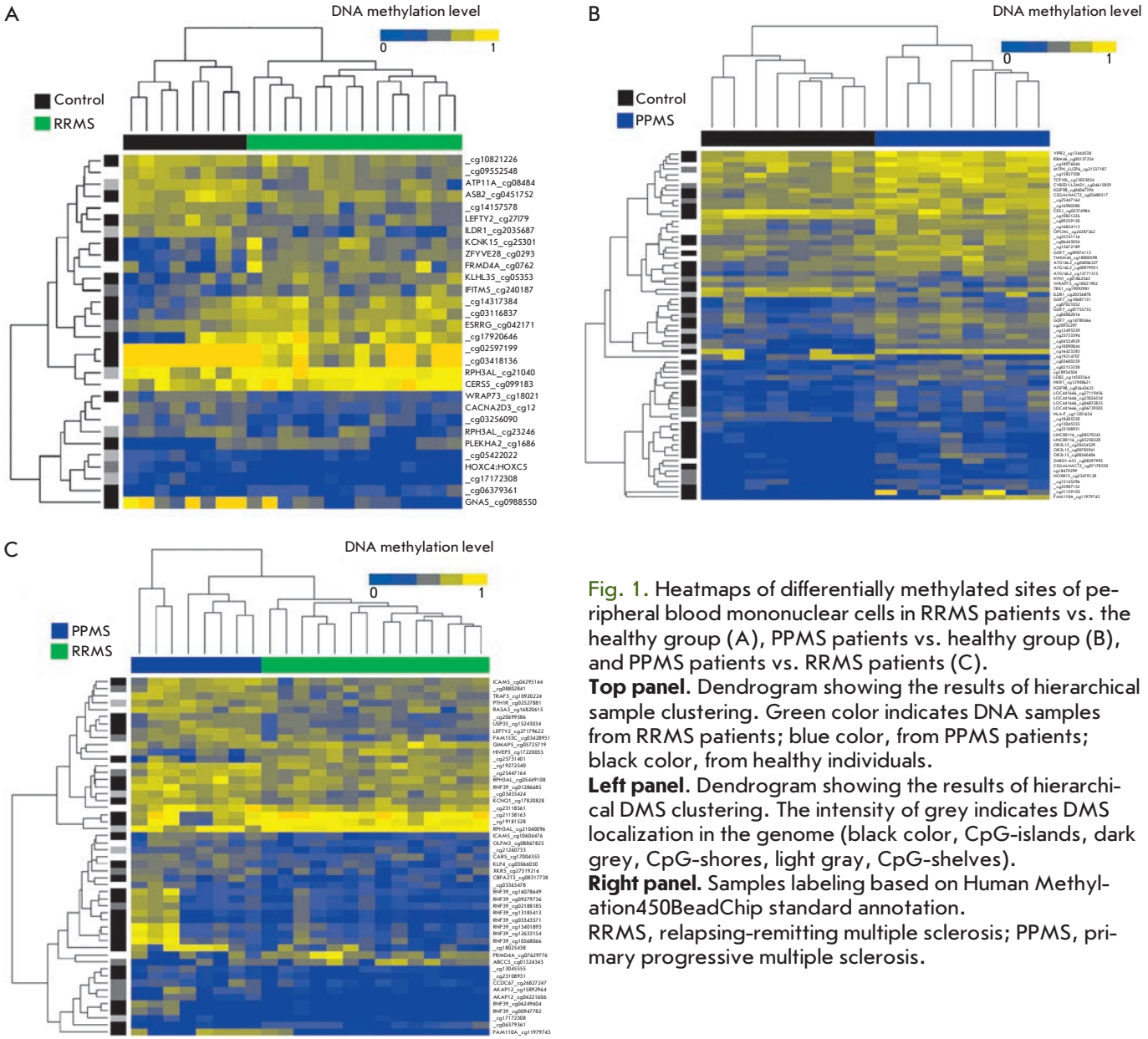

Fig. 1. Heatmaps of differentially methylated sites of peripheral blood mononuclear cells in RRMS patients vs. the healthy group (A), PPMS patients vs. healthy group (B), and PPMS patients vs. RRMS patients (C).
Top panel. Dendrogram showing the results of hierarchical sample clustering. Green color indicates DNA samples from RRMS patients; blue color, from PPMS patients; black color, from healthy individuals.
Left panel. Dendrogram showing the results of hierarchical DMS clustering. The intensity of grey indicates DMS localization in the genome (black color, CpG-islands, dark grey, CpG-shores, light gray, CpG-shelves).
Right panel. Samples labeling based on Human Methylation450BeadChip standard annotation.
RRMS, relapsing-remitting multiple sclerosis; PPMS, primary progressive multiple sclerosis.

these values for the PPMS vs the control and PPMS vs RRMS are 76% and 86%, respectively. The *RPH3AL* gene has two DMSs, one of which is characterized by a higher and the other by a lower methylation level for RRMS vs. control and PPMS vs. RRMS comparisons.

According to the criteria adopted in the study, a CpG-site is considered to be a DMS if there is a 10% difference in the average methylation levels between two groups (i.e. absolute mean difference of beta-values between the groups must be >0.1). Some DMSs are characterized by a significantly higher difference in the methylation level. The absolute mean difference of beta-values for RRMS patients vs. healthy individuals exceeded 20% for five DMSs. Three of these DMSs are located in the genes: the average methylation level of CpG loci cg07629776 (*FRMD4A*) and cg16866567 (*PLEKHA2*) in RRMS patients was 21.5 and 25.1% higher; and of cg09885502 (*GNAS*), 43.5% lower, respectively, compared with the controls. The comparison of PPMS patients with healthy individuals revealed that 6 out of 67 DMSs have an absolute mean difference of beta-values of more than 20%. The highest difference in the methylation level, namely, an increase by 41% was observed for cg11979743 (*FAM110A*), and it was the only one of the six DMSs that was located in a gene. A direct comparison of PPMS and RRMS

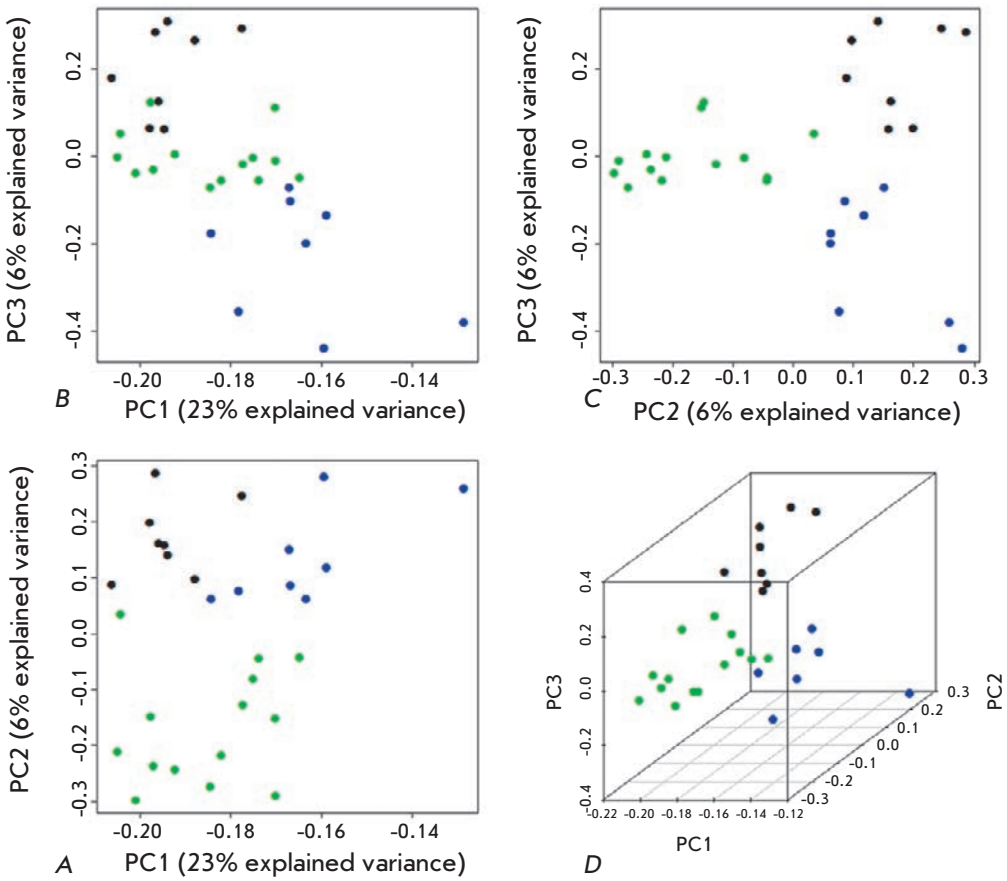

Fig. 2. 2D (*A*–*C*) and 3D (*D*) samples clustering based on a principal component analysis (PCA) of differentially methylated sites (DMSs). The green dots indicate RRMS samples; blue dots PPMS samples; and black dots, healthy controls. The axes: the principal components PC1, PC2, and PC3; the proportion of explained variance of the data is indicated in brackets for each principal component.

identified 7 DMSs whose methylation level differed by more than 20% (20.1 to 31.9%). Of these, 5 DMSs were located in three genes: the average methylation level of cg11979743 (*FAM110A*) was 31.9% higher; and of cg01324343 (*ABCC5*), 21.8% lower in the group of PPMS patients compared with RRMS patients. The third gene, *RNF39*, contained 11 DMSs, and the average methylation level of three of them (cg13401893, cg12633154, cg10568066) was 20.1–21.0% higher in PPMS patients.

Analysis of DMS localization showed that more than half of the DMSs are located in CpG-islands and CpG-shores (*Table 2*; see also *Fig. 1*). This distribution roughly corresponds to the proportion of such probes among all probes of the platform [19]. Comparison of RRMS patients with the controls indicates that 50% of DMSs are located in CpG-islands and 10% in the nearby regions, whereas for PPMS patients the proportion increases to 63 and 16%, respectively, and for PPMS vs. RRMS patients, to 53 and 18% (*Table 2*). Therefore, DNA methylation in PPMS affects more functionally important regions of the genome.

The data taken together form a coherent picture: PPMS differs from RRMS in a higher number of changes in DNA methylation patterns. Indeed, PPMS is characterized by a higher number of DMSs in the genome and its (known) coding part and significantly more than half of the DMSs in both the genome and the genes are hypermethylated. In addition, a higher number of DMSs is localized in CpG-islands and CpG-shores in PPMS compared with the controls (79%), whereas in RRMS their share is only 60%.

DISCUSSION

In order to examine when epigenetic mechanisms are involved in the development of clinically different courses of MS, we performed the first whole-genome analysis of DNA methylation in PBMC of patients with two clinical courses of MS, RRMS, and PPMS, and compared their methylation profiles with healthy donors and with each other. Significant differences in DNA methylation profiles were identified: a pairwise comparison of these three groups (14 RRMS patients, 8 PPMS patients, and 8 individuals in the control group)

Table 1. Characteristics of the differentially methylated sites (DMSs) identified in a comparative analysis of DNA methylation of PBMCs from patients with different clinical courses of MS and healthy individuals (controls)

Compared groups	RRMS vs control	PPMS vs control	PPMS vs RRMS
Number of DMSs	30	67	51
Of them, DMSs with a higher methylation level in the first of the two compared groups	13 (43%)	58 (86%)	42 (82%)
Number of DMSs located in the genes	18	38	35
Number of genes containing DMSs	17	25	22
Of them, genes containing DMSs with higher methylation levels in the first of the two compared groups	9 (53%)	19 (76%)	19 (86%)
Protein encoding genes containing DMSs (number of DMSs in the gene)#	*ASB2* *ATP11A* *CACNA2D3* *CERS5* *ESRRG* *FRMD4A* *GNAS* *HOXC4-HOXC6* *IFITM5* *ILDR1* *KCNK15* *KLHL35* *LEFTY2* *PLEKHA2* *RPH3AL (2)** *WRAP73* *ZFYVE28*	*ATG16L2 (3)* *CES1* *CSGALNACT2 (2)* *CYB5D1;LSMD1* *FAM110A* *GDF7 (4)* *HKR1* *HLA-F* *HOXB13* *IGSF9B (2)* *ILDR1* *LDB2* *MTPN;LUZP6* *NTN1* *OPCML* *OR2L13 (3)* *RBM46* *TBX1* *TCP10L* *TMEM44* *VIPR2* *WRAP73*	*ABCC5* *AKAP12 (2)* *CARS* *CBFA2T3* *CCDC67* *FAM110A* *FRMD4A* *GIMAP5* *HIVEP3* *ICAM5 (2)* *KCNQ1* *KLF4* *LEFTY2* *OLFM3* *PTH1R* *RASA3* *RNF39 (11)* *RPH3AL(2)** *TRAF3* *USP35* *XKR5*
Non-protein encoding genes containing DMSs (number of DMSs in the gene)#	-	*LINC00116 (2)* *ZNRD1-AS1* *LOC441666 (4)*	*FAM153C*

Note. Genes with DMSs with higher methylation levels in the first of the two compared groups are shown in bold.
* Two DMSs were identified in the *RPH3AL* gene: one with a higher methylation level, the other, with a lower one.
# Indicates the number of DMSs located in each gene, if more than one

Table 2. Localization of differentially methylated sites (DMSs) identified in a comparative analysis of DNA methylation of PBMCs from patients with different clinical courses of MS and healthy individuals (controls), regarding the CpG-islands of the human genome

DMS localization	Number of DMS for different comparisons between the groups		
	RRMS vs control	PPMS vs control	PPMS vs RRMS
Any (total DMSs)	30 (100%)	67 (100%)	51 (100%)
In CpG-island	15 (50%)	42 (63%)	27 (53%)
In CpG-shore	3 (10%)	11 (16%)	9 (18%)
In CpG-shelf	6 (20%)	2 (3%)	5 (10%)
In open sea	6 (20%)	12 (18%)	10 (19%)

Note. Localization of individual CpG-sites in the CpG-island was determined using the UCSC-annotation, version hg19; CpG-shore is located up to 2 kbp from the CpG-island; CpG-shelf – up to 2 kbp from the CpG-shore; areas not related to the above three categories are designated as "Open sea."

revealed 136 DMSs with a mean difference in beta-values >0.1 and p-values of <0.01 according to the Student t-test. Three-dimensional visualization of these DMSs using the principal component analysis showed that the DNA samples of the patients from each of the groups under study aggregate into a single cluster, indicating a steady involvement of a differential spectrum of DNA methylation into the development of different clinical courses of MS.

The analysis of the DMS spectrum shows that patients with PPMS, which is a more aggressive clinical course of MS than RRMS, differ from RRMS patients in a higher number of changes in the DNA methylation spectrum in comparison with healthy individuals. Moreover, the number of DMSs with a higher level of DNA methylation is higher in PPMS patients than in the control group and in RRMS patients. At the same time, comparison of RRMS patients with the control group reveals hypomethylation of more than half of the DMSs. The only comparison of our results with published data we can perform is for RRMS patients. A significant DNA hypermethylation in CD8+ T-lymphocytes has been previously identified in patients with RRMS [14], while no changes in the overall level of DNA methylation [14] or a slight decrease were observed [15] in CD4+ T lymphocytes and whole blood.

The analysis of the localization of differentially methylated sites in MS showed that more than half of them are located in either CpG-islands or in the flanking regions (up to 2 kbp distant from a CpG-island, the so-called CpG-shore) (see *Table 2*), which indicates a high probability of the functional importance of the observed DNA methylation, which is known to inhibit the expression of some genes.

We used the GeneCards database of human genes [23], US National Center for Biotechnology Information (NCBI) Gene project [24], and a number of other sources to identify the functions of these genes. Comparison of RRMS patients and healthy individuals reveals differences in the methylation of genes that encode the proteins involved in the development of the immune response (*ASB2*, *LEFTY2*, *PLEKHA2*), the metabolism of lipids (*ILDR1*, *CERS5*), vesicular transport (*RPH3AL*, *ZFYVE28*) and ion channels functioning (*ATP11A*, *CACNA2D3*, *KCNK15*), as well as in the regulation of the expression of many genes (*ESRRG*, *HOXC4-HOXC6*). Among them the *ESRRG* gene encoding estrogen-like receptor gamma deserves special attention. This orphan receptor belongs to the family of nuclear receptors, and through direct binding to the promoter acts as an activator of the transcription for several genes, including the gene encoding the main DNA methyltransferase of mammalian somatic cells, DNA methyltransferase 1 (*DNMT1*) [25], and, thereby, controls the level of DNA methylation in the cell.

Our data on the genes that are differentially methylated in PBMC of RRMS patients compared to healthy individuals do not agree with other studies [6, 14–17]. This is not surprising, since to date a comparative analysis of DNA methylation in RRMS patients and healthy individuals has been performed only in cells of the whole blood, CD4+, CD8+ T lymphocytes [6, 14–16], and in the tissues of the white matter of the brain [17]. There was no agreement between the results obtained for different cell and tissue types, either. The discrepancy between the results may be due not only to the use of different populations of cells, but also to different criteria adopted for the definitions of DMS.

The analysis of the functions of the genes that are differentially methylated in PPMS patients compared with healthy individuals showed that among them there is a group of genes whose products are to some extent involved in the development and differentiation of the nervous system (*GDF7*, *MTPN*, *VIPR2*, *NTN1*, *TBX1*), the functioning of opioid receptors (*OPCML*), and metabolism of various xenobiotics, including cocaine and heroin (*CES1*). Methylation of genes with similar functions was not identified in a pairwise comparison of RRMS patients and healthy individuals. In PPMS, differential methylation also affected the genes involved in the development of the immune response (*HLA-F*, *MTPN*, *VIPR2*), regulating the expression of many genes (*HKR1*, *HOXB13*, *LDB2*, *TCP10L*, *TBX1*), as well as processes of autophagy (*ATG16L2*), hemostasis (*FAM110A*), and the functioning of the extracellular matrix (*CSGALNACT2*).

Among the differentially methylated genes in RRMS and PPMS patients in comparison with controls only two matching genes, *ILDR1* and *WRAP73(WDR8)*, were identified; both of these genes were hypomethylated in patients. The exact functional significance of their products has not been fully elucidated yet, but ILDR1 receptor activity is at least partially associated with lipid metabolism [26], while the WRAP73 protein comprising conservative WD-repeats can form multimeric complexes with other proteins participating in mitosis, signal transduction in the cell [27], and in the formation of cilia [28].

Our work is the first one to identify the genes whose methylation levels are distinguished in patients with the two main clinical courses of MS. The products of these genes are involved in the development and functioning of immune system cells (*HIVEP3*, *GIMAP5*, *TRAF3*), the regulation of the expression of many genes (*AKAP12*, *RASA3*, *CBFA2T3*), degradation processes (*USP35*), and the functioning of the endocrine system (*PTH1R*). Two genes are of particular interest. The first

one, *ICAM5*, encodes a dendrite-specific adhesion molecule of the immunoglobulin superfamily, which is involved in the interaction of nerve cells with each other and with the cells of the immune system in CNS [29]. The other one is *RNF39*. Of the 35 DMSs identified by comparing DNA samples from PPMS and RRMS patients and located in the genes, 11 were located in the *RNF39* gene and had a higher level of DNA methylation in PPMS. For three of these DMSs, the difference in the methylation level exceeded 20%. The *RNF39* gene is located in the HLA class I gene region. *RNF39* function is not yet clear; however, the association of the polymorphisms of this gene with MS [30] and some other autoimmune diseases [31] has been demonstrated previously. Hypermethylation of the gene in CD4+ T lymphocytes was also found in patients with systemic lupus erythematosus [32].

Our results of a whole-genome analysis of the DNA methylation profiles in PBMCs of MS patients indicate that DNA methylation, one of the main mechanisms of transmission of epigenetic information in mammals, plays a role in the development of MS. It has been demonstrated for the first time that epigenetic DNA methylation is involved in the formation of clinically distinct forms of MS, RRMS, and PPMS, and, in the case of PPMS, methylation, apparently, leads to inhibition of the expression of a higher number of genes. ●

This work was supported by grants from Russian Foundation for Basic Research № 13-04-40279-H (LD, AF), 13-04-40280-H (MK, OB, VV) and 13-04-40281-H (EP, NB, AB) within the framework of an integrated project 13-00-40277-K and by Russian Scientific Foundation grant № 14-14-00605 (OK, ET, IK).

REFERENCES

1. Gourraud P.A., Harbo H.F., Hauser S.L., Baranzini S.E. // Immunol. Rev, 2012. V. 248. P. 87–103.
2. Favorova O.O., Kulakova O.G. and Boyko A.N. // Genetika, 2010. V. 46. P. 302–313.
3. Lvovs D., Favorova O.O. and Favorov A.V. // Acta Naturae 2012. V. 3. P. 62–75.
4. Bashinskaya V.V., Kulakova O.G., Boyko A.N., Favorov A.V., Favorova O.O. // Hum. Genet, 2015. V. 134. P. 1143–1162.
5. Lill C.M. // Front. Neurol. 2014. V. 5. P. 130.
6. Baranzini S.E., Mudge J., van Velkinburgh J.C., Khankhanian P., Khrebtukova I., Miller N.A., Zhang L., Farmer A.D., Bell C.J., Kim R.W., et al. // Nature. 2010. V. 464. P. 1351–1356.
7. O'Gorman C., Lucas R., Taylor B. // Int. J. Mol. Sci. 2012. V. 13. P. 11718–11752.
8. Boyko A.N., Favorova O.O., Kulakova O.G., Gusev E.I. // Multiple sclerosis. / Edited by Gusev E.I., Zavalishin I.A., Boyko A.N. M. 2011. P. 7–42.
9. Landgrave-Gomez J., Mercado-Gomez O., Guevara-Guzman R. // Front. Cell Neurosci. 2015. V. 9. P. 58.
10. Meda F., Folci M., Baccarelli A., Selmi C. // Cell Mol. Immunol. 2011. V. 8. P. 226–236.
11. Mastronardi F.G., Noor A., Wood D.D., Paton T., Moscarello M.A. // J. Neurosci. Res. 2007. V. 85. P. 2006–2016.
12. Calabrese R., Zampieri M., Mechelli R., Annibali V., Guastafierro T., Ciccarone F., Coarelli G., Umeton R., Salvetti M., Caiafa P. // Mult. Scler. 2012. V. 18. P. 299–304.
13. Kumagai C., Kalman B., Middleton F.A., Vyshkina T., Massa P.T. // J. Neuroimmunol. 2012. V. 246. P. 51–57.
14. Bos S.D., Page C.M., Andreassen B.K., Elboudwarej E., Gustavsen M.W., Briggs F., Quach H., Leikfoss I.S., Bjolgerud A., Berge T., et al. // PLoS One. 2015. V. 10. P. e0117403.
15. Graves M., Benton M., Lea R., Boyle M., Tajouri L., Macartney-Coxson D., Scott R., Lechner-Scott J. // Mult. Scler. 2013. V. 20. P. 1033–1041.
16. Maltby V.E., Graves M.C., Lea R.A., Benton M.C., Sanders K.A., Tajouri L., Scott R.J., Lechner-Scott J. // Clin. Epigenetics. 2015. V. 7. P. 118.
17. Huynh J.L., Garg P., Thin T.H., Yoo S., Dutta R., Trapp B.D., Haroutunian V., Zhu J., Donovan M.J., Sharp A.J., et al. // Nat. Neurosci. 2014. V. 17. P. 121–130.
18. Polman C.H., Reingold S.C., Banwell B., Clanet M., Cohen J.A., Filippi M., Fujihara K., Havrdova E., Hutchinson M., Kappos L., et al. // Ann. Neurol. 2011. V. 69. P. 292–302.
19. Bibikova M., Barnes B., Tsan C., Ho V., Klotzle B., Le J.M., Delano D., Zhang L., Schroth G.P., Gunderson K.L., et al. // Genomics. 2011. V. 98. P. 288–295.
20. http://www.R-project.org
21. https://www.bioconductor.org/packages/release/bioc/html/methylumi.html
22. Smyth G.K. // Bioinformatics and Computational Biology Solutions using R and Bioconductor / Ed. R. Gentleman V.C., etc. New York: Springer, 2005. P. 397–420.
23. http://www.genecards.org
24. http://www.ncbi.nlm.nih.gov/gene
25. Zhang Y., Wang L. // FEBS Lett. 2011. V. 585. P. 1269–1275.
26. Chandra R., Wang Y., Shahid R.A., Vigna S.R., Freedman N.J., Liddle R.A. // J. Clin. Invest. 2013. V. 123. P. 3343–3352.
27. Shen K.F., Osmani S.A. // Mol. Biol. Cell. 2013. V. 24. P. 3842–3856.
28. Kurtulmus B., Wang W., Ruppert T., Neuner A., Cerikan B., Viol L., Sanchez R.D., Gruss O.J., Pereira G. // J. Cell Sci. 2015. V. 129. P. 621–636.
29. Tian L., Rauvala H., Gahmberg C.G. // Trends Immunol. 2009. V. 30. P. 91–99.
30. Cree B.A., Rioux J.D., McCauley J.L., Gourraud P.A., Goyette P., McElroy J., De Jager P., Santaniello A., Vyse T.J., Gregersen P.K., et al. // PLoS One 2010. V. 5. P. e11296.
31. Kurata R., Nakaoka H., Tajima A., Hosomichi K., Shiina T., Meguro A., Mizuki N., Ohono S., Inoue I., Inoko H. // Biochem. Biophys. Res. Commun. 2010. V. 401. P. 533–537.
32. Renauer P., Coit P., Jeffries M.A., Merrill J.T., McCune W.J., Maksimowicz-McKinnon K., Sawalha A.H. // Lupus Sci. Med. 2015. V. 2. P. e000101.

The Effect of Dopamine Secreted by the Brain into the Systemic Circulation on Prolactin Synthesis by the Pituitary gland in Ontogenesis

Yu.O. Nikishina[1], A.Ya. Sapronova[1*], M.V. Ugrumov[1,2]
[1]Koltsov Institute of Developmental Biology RAS, 26 Vavilov str., Moscow, 119334, Russia
[2]National Research University "Higher School of Economics", 20 Myasnitskaya str., Moscow, 101000, Russia
[*]E-mail: anna_sapronova@mail.ru; mugrumov@mail.ru
Received December 09, 2015; in final form, April 14, 2016

ABSTRACT **This research was aimed at studying the brain's endocrine function in ontogenesis. It has been previously shown in our laboratory that the brain serves as the source of dopamine in the systemic circulation of rats prior to the formation of the blood-brain barrier. This paper provides direct evidence that dopamine secreted by the brain directly into the systemic circulation in this period of ontogenesis has an inhibitory effect on prolactin secretion by pituitary cells. These results provide the basis for a fundamentally new understanding of the brain's role in the neuroendocrine regulation of the development and function of peripheral target organs and, particularly in this study, the pituitary gland.**
KEYWORDS **dopamine, prolactin, brain, pituitary gland, blood-brain barrier, ontogenesis**
ABBREVIATIONS **HPLC – high-performance liquid chromatography; BBB – blood-brain barrier; 6-OHDA – 6-hydroxydopamine; DA – dopamine; AAAD – aromatic *L*-amino acid decarboxylase; PRL – prolactin; TH – tyrosine hydroxylase; *L*-DOPA – *L*-dihydroxyphenylalanine**

INTRODUCTION

In adult animals, the brain, and particularly the hypothalamus, is the central part of the neuroendocrine system responsible for the regulation of the most important functions and maintenance of a constant internal environment for the body. Of particular interest is the formation and function of the neuroendocrine regulatory system in ontogenesis, since hypothalamic neurohormones and hormones of the endocrine glands regulate not only the functional activity of target organs, but their development during the development of an organism, as well. In the latter case, the action of these signaling molecules is of irreversible (imprinting-like, morphogenetic) nature [1–3]. According to the concept established by the end of the 1980s, the brain is not involved in neuroendocrine regulation of peripheral organs until its full maturity; i.e., the formation of interneuron synaptic connections and blood-brain barrier (BBB). It is only after the final differentiation of neurons and establishment of synaptic neurotransmission that it takes control over the pituitary gland and all the other endocrine glands through it [4, 5].

In recent years, our understanding of the brain's role in neuroendocrine regulation in ontogenesis has undergone significant changes. After an analysis of published data and the results of our own research in our laboratory, we noticed that neurons begin to synthesize and secrete signaling molecules long before the formation of interneuron synaptic connections and BBB [6–8]. This observation allowed us to put forth the hypothesis that, prior to BBB formation, the brain functions as an endocrine organ releasing physiologically active substances into the systemic circulation and, thus, affecting the development and function of peripheral organs and target cells [8].

The two pillars of this hypothesis are that

1) The brain is the source of signaling molecules in the systemic circulation from the moment of neuron formation to the final formation of synaptic connections and BBB closure and

2) Signaling molecules secreted by the brain into the systemic circulation during that period of ontogenesis can have a direct para-adenohypophyseal endocrine effect on peripheral target organs.

The first leg of the hypothesis was confirmed by the studies performed in our laboratory. Direct evidence that during the early postnatal period prior to BBB formation the brain serves as the source of dopamine

in the systemic circulation, was demonstrated in the model of specific reversible inhibition of the synthesis of catecholamines in the brain of neonatal animals [9].

When testing the validity of the second part of the hypothesis, with *in vitro* and *ex vivo* experiments in our laboratory, the obtained data showed that dopamine has an inhibitory effect on prolactin production by pituitary cells at the concentration at which it is present in the systemic circulation [10].

In adult animals, neuroendocrine regulation is carried out mainly through the hypothalamic-hypophyseal portal circulation system. In the absence of BBB during the perinatal period of ontogenesis in rats, the regulation can technically be carried out both through portal and systemic circulation. So far, however, no data has been obtained on the contribution of each of the pathways to the neuroendocrine regulation of the function and development of peripheral organs. The answer to this question is of fundamental importance not only for the confirmation of the endocrine function of the brain, but also for understanding the development and function of the neuroendocrine regulation system in ontogenesis.

In this regard, the purpose of our research was to study the effect of dopamine secreted by the brain into the systemic circulation on the synthesis of prolactin by the pituitary gland in ontogenesis. Using 6-hydroxydopamine neurotoxin in the model of a chronic specific shutdown of dopamine synthesis in the brain of neonatal rats, we tried to assess

1) the morphological and functional state of dopaminergic neurons of the tuberoinfundibular system of the brain;

2) the endocrine effect of brain-produced dopamine present in the systemic circulation on the synthesis and release of prolactin by pituitary cells.

EXPERIMENTAL SECTION

Animals, experiments

We used 90 Wistar male rats in the second day of postnatal development (P2). In order to obtain a model of chronic specific inhibition of DA synthesis in the brain, 100 μg of 6-hydroxydopamine (6-OHDA, Sigma, USA) was stereotaxically injected into the lateral ventricles of the brains of the rats, while control animals were injected with 0.9% NaCl [11]. In order to effect selective destruction of dopaminergic neurons and preserve noradrenergic neurons, 25 mg/kg of desmethylimipramine (DMI), an inhibitor of noradrenaline and 6-OHDA reuptake into noradrenergic neurons, was injected subcutaneously 30 min prior to the administration of 6-OHDA. 72 h after 6-OHDA injection brain sections were isolated in anesthetized rats (chloral hydrate, 400 mg/kg, Sigma, USA) as shown in *Fig. 1*. Samples were

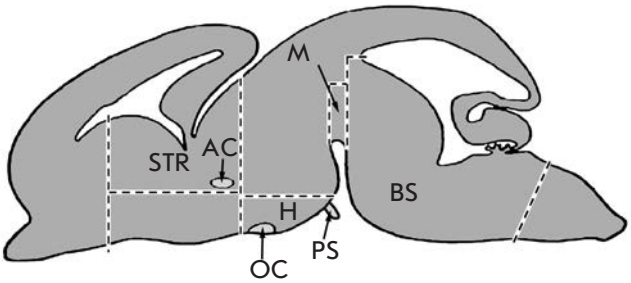

Fig. 1. Scheme of brain structures isolation after the administration of neurotoxin. STR – striatum, AC – anterior commissure, H – mediobasal hypothalamus, PS – pituitary stalk, M –midbrain, BS – brain stem, OC – optic chiasm

frozen in liquid nitrogen and stored at −70°C prior to high-performance liquid chromatography with electrochemical detection (HPLC-ED).

To determine tyrosine hydroxylase (TH) activity, all the animals (experimental and control) were intraperitoneally injected with the aromatic *L*-amino acid decarboxylase (AAAD) inhibitor: 3-hydroxybenzyl hydrazine (NSD-1015, Sigma, USA) at a concentration of 100 mg/kg of body weight 72 hours after stereotactic injection of 6-OHDA and 30 minutes prior to obtaining the samples [12]. Next, mediobasal hypothalamus and the rest of the brain were isolated under anesthesia. TH activity in the collected samples was assessed by accumulation of *L*-dihydroxyphenylalanine (*L*-DOPA) measured by HPLC-ED.

The number of mono- and bienzymatic neurons in the arcuate nucleus of the rats was assessed by immunohistochemistry. For this purpose, transcardial perfusion was carried out first with 0.02 M phosphate-buffered saline (PBS, pH 7.2–7.4) for 10–15 minutes and then with 4% pre-cooled (to +4°C) paraformaldehyde in 0.2 M phosphate buffer (pH 7.3) for 15 min. Then, the brain was isolated and postfixation with 4% paraformaldehyde was performed at +4°C for 12 h. After that, the brain was washed in 0.02 M PBS (3 times for 15 min each), incubated in 20% sucrose at +4 °C for 24 hours and frozen in hexane at −40°C. Prior to the immunohistochemical analysis, the samples were stored at −70°C.

Blood collected from the heart of anesthetized animals was centrifuged (7,000 rpm, 20 min, +4°C), and then the prolactin (PRL) level in the blood plasma was measured by ELISA.

When determining PRL in pituitary tissue, the hormone was first extracted with 0.05 M carbonate-bicarbonate buffer [10].

The PRL mRNA content was measured in the anterior part of the pituitary gland isolated after stereotactic injections. Each sample contained material obtained

from three rats. Prior to RNA isolation, the samples were stored at −70°C.

High-performance liquid chromatography

The content of catecholamines and metabolites in brain tissue was determined by reverse phase HPLC with electrochemical detection [11].

Immunohistochemistry

TH and AAAD were detected in 20-μm sections of mediobasal hypothalamus prepared on a cryostat and mounted onto the glass. Sections were sequentially incubated with (a) 3% bovine serum albumin (Sigma, USA) and 0.3% Triton X-100 (Sigma, USA) in 0.02 M PBS for 30 min at +20°C; (b) 1% sodium lauryl sulfate (SDS, Sigma, USA) in 0.02 M PBS for 3 min at +20°C; (c) sheep polyclonal antibodies to TH (1 : 700) (Chemicon, USA) and rabbit polyclonal antibodies to AAAD (1 : 300) (Abcam, USA) in 0.02 M PBS containing 1% bovine serum albumin and 0.1% Triton X-100 at +20°C for 24 hours; (d) FITC-conjugated donkey antibodies to sheep gamma globulins (1 : 40) (FITC antisheep, Sigma, USA) and Cy3-conjugated goat antibodies to rabbit gamma globulins (1 : 500) (CY3 antirabbit, Sigma, USA) in 0.02 M PBS at +20°C for 2 hours. After each incubation, except for the last one, the sections were washed in 0.02 M PBS for 15 min. After the final incubation, the sections were washed in 0.02 M PBS for 1 h and then embedded into the hydrophilic medium Mowiol (Calbiochem, Germany).

Slices of hypothalamus after double labeling to TH and AAAD were examined using a fluorescence microscope Zeiss Observer Z1 equipped with filters for FITC (for TH) and Cy3 (for AAAD) using the AxioVision 4.8 software.

ELISA

The PRL content in the tissue of the anterior part of the pituitary gland and plasma samples was determined by ELISA using commercial kits SPIbio-Rat Prolactin EIA Kit (Bertin Pharma, France).

Real-time PCR

Total RNA was isolated using TRI Reagent (Sigma, USA) according to the manufacturer's protocol. In order to remove contaminants of genomic DNA, the isolated RNA was treated with DNase (Fermentas, USA). RNA was reprecipitated in 4 M LiCl, and RNA concentration was measured using a Nanodrop 8000 spectrophotometer (Thermo Scientific, USA). cDNA was synthesized using reverse transcriptase M-MLV and hexameric oligonucleotides (Fermentas, USA).

Real-time PCR was performed in an automated thermocycler 7500 Real-Time PCR System (Applied Biosystems, USA) using a qPCRmix-HS SYBR+ROX mixture (Fermentas, USA) and specific oligonucleotides ("Lytech", Russia). Sense sequence: 5'-ATAGATGATTGGGAGGGGAAGAG-3'; antisense sequence: 5'-CATCATCAGCAGGAGGAGTGTC-3'. The values obtained for each sample were normalized to the expression of the household gene *GAPDH*. The *GAPDH* gene expression level was determined using primers: sense – 5'-CTGACATGCCGCCTGGAGAAA-3'; antisense – 5'-TGGAAGAATGGGAGTTGCTGTTGA-3'.

Relative gene expression was calculated by the ΔΔCt method taking into account PCR efficiency. PCR efficiency was determined by the construction of standard curves [13].

Statistical analysis

Analysis of statistical data was performed using the integrated GraphPad Prism Version 6.0 software for Windows (GraphPad Software, USA). Data are shown as mean ± SEM (M ± m). The statistical significance of the results was determined using the parametric Student's *t*-test (*t*-test) and nonparametric Mann-Whitney U-test (U-test).

RESULTS

Concentration of dopamine in various brain regions

Seventy-two hours after 6-OHDA administration, the striatal DA concentration decreased by 92%, and by 40% and 44% in the midbrain and brain stem, respectively. At the same time, the concentration of DA in the hypothalamus did not change compared to the control (*Fig. 2*).

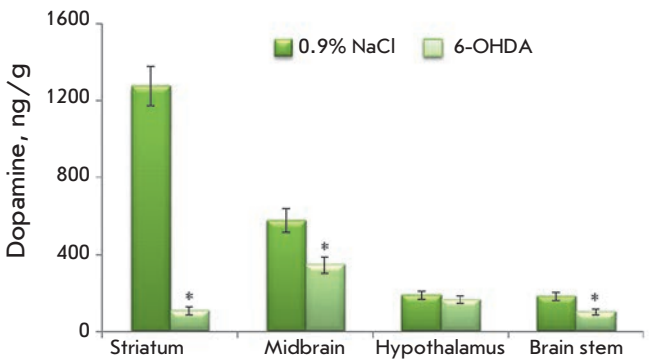

Fig. 2. Concentration of dopamine in various brain regions 72 hours after stereotactic injection of 100 μg of 6-OHDA into the lateral ventricles of the brain following subcutaneous administration of 25 mg/kg DMI; control was injected with 25 mg/kg DMI and 0.9% NaCl. * – Statistically significant differences between the control and the experiment

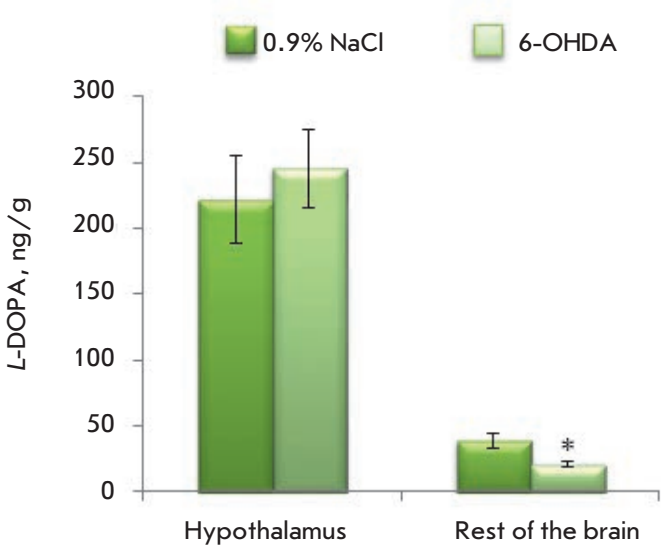

Fig. 3. Tyrosine hydroxylase activity assessed by the accumulation of dihydroxyphenylalanine (*L*-DOPA) 30 minutes after the injection of 3-hydroxybenzylhydrazine (NSD-1015) in the hypothalamus and the rest of the brain on the model of chronic inhibition of dopamine synthesis in the brain with 6-OHDA. * – Statistically significant differences between the control and the experiment

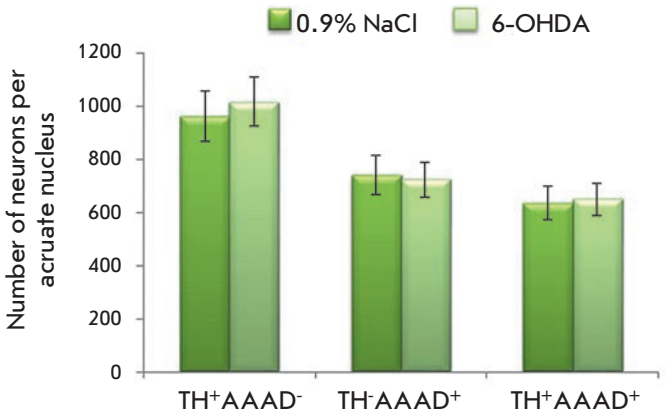

Fig. 4. Number of monoenzymatic TH^+AAAD^-, monoenzymatic TH^- $AADC^+$, and bienzymatic TH^+AAAD^+ neurons in the arcuate nucleus 72 hours after the administration of 100 mg of 6-OHDA into the lateral ventricles of the brain following systemic administration of 25 mg/kg DMI; the control was injected with 25 mg/kg DMI and 0.9% NaCl

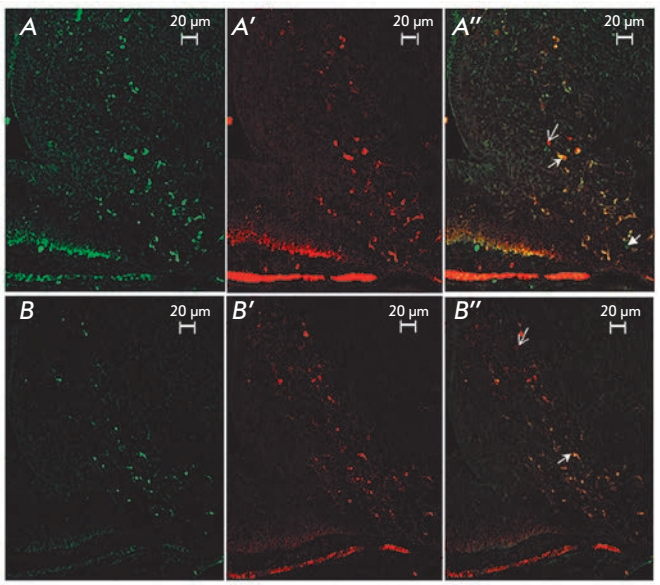

Fig. 5. Fluorescence microscopy. Images of tyrosine hydroxylase positive (*A*, *B*), aromatic amino acids decarboxylase positive (*A′*, *B′*), and tyrosine hydroxylase and aromatic amino acids decarboxylase positive (*A″*, *B″*) neurons in the arcuate nucleus in the control (*A*, *A′*, *A″*) and after stereotactic injection of 6-OHDA (*B*, *B′*, *B″*). Arrows indicate neurons of different phenotypes

TH activity in various brain regions

TH activity was evaluated by the accumulation of *L*-DOPA after the administration of the AAAD inhibitor NSD-1015. When modeling the deficiency of DA synthesis in the brain of neonatal rats, the *L*-DOPA concentration in the hypothalamus did not change compared to the control, while a statistically significant reduction was observed in the rest of the brain (*Fig. 3*).

Number of mono- and bienzymatic neurons in the arcuate nucleus

Seventy-two hours after 6-OHDA administration into the lateral ventricles of the rats, the number of monoenzymatic TH^+AAAD^-, monoenzymatic TH^-AAAD^+, and bienzymatic TH^+AAAD^+ neurons in the arcuate nucleus had not change compared to the control (*Fig. 4, 5*).

Prolactin in pituitary gland and blood plasma

Seventy-two hours after the introduction of 100 μg of 6-OHDA into the lateral ventricles of the rats, the prolactin concentration increased in a statistically significant manner by 70% and 48% in the blood plasma and pituitary gland, respectively. At the same time, the prolactin mRNA content in the pituitary gland increased 2.5-fold (*Fig. 6*).

DISCUSSION

In adult animals, DA transferred from the hypothalamus to the pituitary gland regulates the function of peripheral targets only through the portal circulation sys-

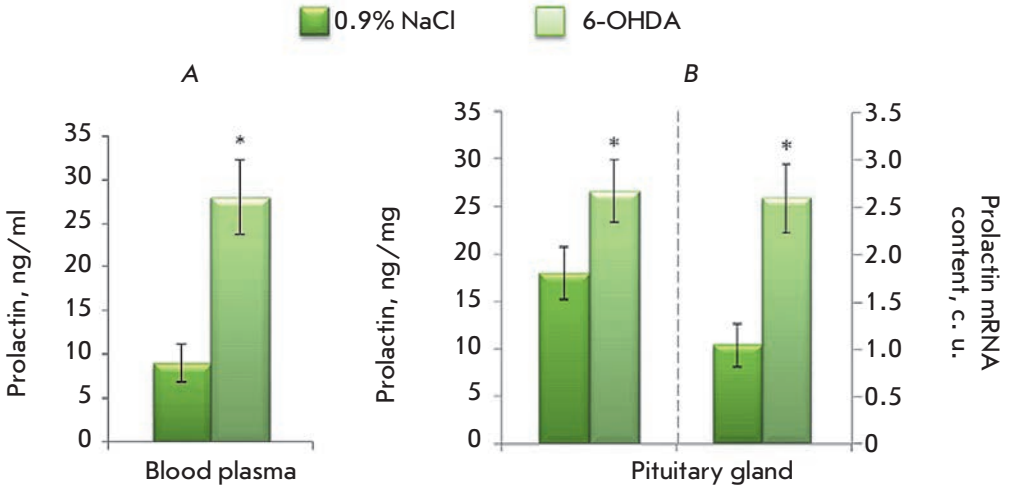

Fig. 6. Concentration of prolactin in the blood plasma (*A*) and concentration of prolactin and prolactin mRNA content in the pituitary gland (*B*) 72 hours after the administration of 100 μg of 6-OHDA into the lateral ventricles of the brain following systemic administration of 25 mg/kg DMI; the control was injected with 25 mg/kg DMI and 0.9% NaCl. * – Statistically significant differences between the control and the experiment

tem, whereas, according to our hypothesis, DA, in the absence of BBB in neonatal animals, can be also transferred from all populations of neurons directly into the systemic circulation. We have earlier shown in *in vitro* experiments that dopamine, at the concentration at which it is present in the peripheral blood of neonatal rats, inhibits prolactin secretion by the pituitary gland [10, 14]. However, pituitary cells are under the constant tonic influence of DA under *in vivo* conditions, while in *in vitro* conditions, the pituitary cells are contained in a medium without DA for a long period of time, which, according to some scientists, can fundamentally change cell physiology [15]. Moreover, this approach does not allow one to say for certain whether the regulation is carried out through the systemic circulation or not, since the concentration of DA in peripheral and portal blood at this stage of ontogenesis can be comparable.

Analysis of the published data allows us to suggest that this problem can be solved by inhibiting DA synthesis in the brain using 6-OHDA-specific neurotoxin of CAergic neurons, which enters the cell via specific transporters of DA and norepinephrine and inhibits the process of oxidative phosphorylation [16].

Due to the fact that the expression level of the membrane transporter of dopamine in mediobasal hypothalamus neurons is rather low and that uptake mechanisms in neonatal animals are undeveloped [17, 18], we hypothesized that the use of 6-OHDA in the modeling of DA deficiency in the brain of neonatal rats would allow us to divide the above-described pathways of regulation of the functional activity of pituitary cells. In this regard, we have developed a model of specific inhibition of dopamine synthesis in the brain of newborn rats. In this model, the dopamine level in the brain fell by 54%, while the decrease was even more dramatic in the blood plasma (70%) [11]. On the basis of the available data, one cannot draw an unambiguous conclusion that the effects that are seen in this model are provided only by DA transferred from the brain into the systemic circulation. In order to assess whether the neurotoxin affects DA-producing mediobasal hypothalamic neurons, we first identified the content of DA and its metabolites in this region after 6-OHDA administration. It has been shown that, in our model, the DA level in mediobasal hypothalamus does not change compared to the control, while it is statistically significantly reduced in the striatum, midbrain, and brain stem. These data can be regarded as an integral indicator that the secretory activity of the hypothalamus does not change under the effect of the toxin.

DA is synthesized from amino acid tyrosine by two enzymes: TH and AAAD. For this reaction chain, the rate-limiting step is the synthesis of *L*-DOPA from tyrosine under the action of TH [19]. Therefore, we evaluated TH activity by determining the accumulation of *L*-DOPA in the mediobasal hypothalamus after the inhibition of the second enzyme of DA – AAAD synthesis as a direct indicator of DA synthesis in our model. It was found that the *L*-DOPA level did not change in this region compared to the control; i.e., TH activity did not change under the action of neurotoxin. At the same time, the concentration of *L*-DOPA in the rest of the brain was reduced 2-fold compared to the control.

The rate of brain neuron degradation under the influence of 6-OHDA was evaluated mainly by immunolabeling for TH. However, it is known that in addition to true DAergic neurons expressing both enzymes of DA synthesis, there are also neurons containing only one of the enzymes [20–22]. It has been previously shown in our laboratory that the number of monoenzymatic neurons in the arcuate nucleus of rats during the perinatal period is much higher than the number of bienzymatic

neurons. Thus, the number of monoenzymatic neurons in this region at E21 is 99%, while the number of bienzymatic neurons is only 1%. At the P9 stage, bienzymatic neurons constitute 38% [23]. Furthermore, it was shown that monoenzymatic neurons are able to carry out a cooperative synthesis of DA [24, 25]. In addition to this, in the case of functional insufficiency of the hypothalamic tuberoinfundibular system caused by the introduction of 6-OHDA into the brain of adult animals, the number of both TH- and AAAD-containing monoenzymatic neurons increases [26]. Apparently, such a reaction is a manifestation of compensatory processes. In this regard, we evaluated the number of neurons in the arcuate nucleus by double immunolabeling for TH and AAAD in the DA deficiency model. It turned out that the amount of bienzymatic, monoenzymatic TH-containing and monoenzymatic AAAD-containing neurons did not change compared to the control.

Thus, we have obtained evidence that specific inhibition of DA synthesis in the brain with the 6-OHDA neurotoxin does not change the morphological and functional state of the mediobasal hypothalamus. This implies that, if changes in PRL synthesis are detected in this model, they are due to the influence of DA, exclusively, via the systemic circulation.

In the next series of experiments, we evaluated the effect of DA secreted by the brain into the systemic circulation on the synthesis of prolactin by the pituitary gland. It has been previously shown in our laboratory that the inhibitory effect of DA on the secretion of prolactin is first detected at the E21 stage [27]; i.e., this mechanism should be sufficiently mature in the analyzed period. It was found that the PRL concentration increased by 70% upon a decrease in DA in the plasma of 73%. This indicator characterizes the level of PRL secretion by pituitary cells. Such a significant increase in PRL concentration in the plasma in response to the decrease in DA concentration implies that dopamine secreted by the brain into the systemic circulation has an inhibitory effect on the secretion of PRL by pituitary cells. Moreover, the concentration of PRL in the pituitary gland increases by 48%. Apparently, DA entering the pituitary gland through the systemic circulation does not only inhibit PRL secretion, but also affects its synthesis. In order to confirm the effect of DA on PRL synthesis in our model, we evaluated the level of PRL mRNA. It was found that the level of PRL mRNA expression in the pituitary gland of animals deficient in DA is 2.5-fold higher than that in the control.

CONCLUSION

Thus, we were able to show that DA secreted by the brain into the systemic circulation has an inhibitory effect on the synthesis and secretion of PRL by the pituitary cells in the early postnatal period prior to BBB formation. According to our hypothesis on the endocrine function of the brain before BBB formation in the early postnatal period, there are two pathways of dopamine regulation of PRL secretion by the pituitary gland: through DAergic neurons of the hypothalamus via the portal circulation system and through other populations of DAergic neurons via the systemic circulation. It can be assumed that during the period of ontogenesis that we studied, the regulation of the pituitary cell function through systemic circulation significantly contributes to the regulation of PRL secretion. ●

This work was supported by the Russian Science Foundation (grant № 14-15-01122).

REFERENCES

1. Gorski R.A., Lakoski J.M., Perez-Polo J.R., Rassin D.K., Gustavson C.R., Watson C.S. Neural control of reproductive function. New York: Alan R. Liss Inc., 1988. P. 33–44.
2. Lauder J.M. // Trends Neurosci. 1993. V. 16. № 6. P. 233–240.
3. Ugrumov M.V. // Int. J. Dev. Biol. 1997. V. 41. P. 809–816.
4. Fuse Y. // Reprod. Fertil. Dev. 1996. V. 8. № 1. P. 1–21.
5. O'shaughnessy P., Baker P., Sohnius U., Haavisto A. // Endocrinology. 1998. V. 139. № 3. P. 1141–1146.
6. Borisova N.A., Sapronova A.Y., Proshlyakova E.V., Ugrumov M.V. // Neuroscience. 1991. V. 43. № 1. P. 223–229.
7. Ugrumov M.V., Popov A.P., Vladimirov S.V., Kasmambetova S., Novodjilova A.P., Tramu G. // Neuroscience. 1994. V. 58. P. 161–165.
8. Ugrumov M.V. // Neurochem. Res. 2010. V. 35. № 6. P. 837–850.
9. Saifetyarova, Yu.Yu., Degtyaryova E.A., Sapronova A.Ya., Ugrumov M.V. // Neurochemical Journal. 2011. V.28. №3. P. 192–199.
10. Saifetyarova, Yu.Yu., Sapronova A.Ya., Ugrumov M.V. // Doklady Biological Sciences. 2012. V. 443. № 6. P. 1–4.
11. Zubova Yu.O., Saifetyarova Yu.Yu., Sapronova A.Ya., Ugrumov M.V. // Doklady Biochemistry and Biophysics. 2014. V. 454. № 4. P. 481–484.
12. Carlsson A., Lindqvist M. // J. Neural Transmission. 1973. V. 34. № 2. P. 79–91.
13. Bookout A.L., Cummins C.L., Mangelsdorf D.J., Pesola J.M., Kramer M.F. // Curr. Protocols Mol. Biol. 2006. P. 15.8.1–15.8.28.
14. Bondarenko N.S., Zubova Yu.O., Sapronova A.Ya., Volina E.V., Ugrumov M.V. // Bulletin of Experimental Biology and Medicine. 2015. V.159. №3. P. 268–273.
15. Ben-Jonathan N., Hnasko R. // Endocrine Rev. 2001. V. 22. № 6. P. 724–763.
16. Blum D., Torch S., Lambeng N., Nissou M.F., Benabid A.L., Sadoul R., Verna J.M. // Progress Neurobiol. 2001. V. 65. № 2. P. 135–172.
17. Yokoyama C., Okamura H., Ibata Y. // Brain Res. Bull.

1993. V. 30. № 5. P. 551–559.
18. Elsworth J.D., Roth R.H. // Exp. Neurol. 1997. V. 144. № 1. P. 4–9.
19. Nagatsu T., Sawada M. // Cell. Mol. Neurobiol. 2006. V. 26. № 4–6. P. 779–800.
20. Meister B., Hökfelt T., Steinbusch H.W., Skagerberg G., Lindvall O., Geffard M., Cuello A.C., Goldstein M. // J. Chem. Neuroanat. 1987. V. 1. № 1. P. 59–64.
21. Okamura H., Kitahama K., Nagatsu I., Geffard M. // Neurosci. Lett. 1988. V. 95. № 1. P. 347–353.
22. Ugrumov M.V. // Adv. Pharmacol. 2013. V. 68. P. 37–91.
23. Ershov P.V., Ugrumov M.V., Calas A., Makarenko I.G., Krieger M., Thibault J. // J. Chem. Neuroanat. 2002. V. 24. № 2. P. 95–107.
24. Ugrumov M.V., Melnikova V.I., Lavrentyeva A.V., Kudrin V.S., Rayevsky K.S. // Neuroscience. 2004. V. 124. № 3. P. 629–635.
25. Ugrumov M., Taxi J., Pronina T., Kurina A., Sorokin A., Sapronova A., Calas A. // Neuroscience. 2014. V. 277. P. 45–54.
26. Ershov P.V., Ugrumov M.V., Calas A., Krieger M., Thibault J. // J. Chem. Neuroanat. 2005. V. 30. № 1. P. 27–33.
27. Melnikova V.I., Orosco M., Rouch C., Calas A., Nicolaidis S., Proshlyakova E.V., Sapronova A.Y., Ugrumov M.V. // Eur. J. Endocrinol. 1998. V. 139. № 3. P. 337–342.

Identification of New Structural Fragments for the Design of Lactate Dehydrogenase A Inhibitors

D.K. Nilov[1]*, A.V. Kulikov[2], E.A. Prokhorova[3], V.K. Švedas[1,3]
[1]Belozersky Institute of Physicochemical Biology, Lomonosov Moscow State University, Lenin Hills 1, bldg. 40, Moscow, 119991, Russia
[2]Faculty of Fundamental Medicine, Lomonosov Moscow State University, Lomonosov prospect 31-5, Moscow, 119192, Russia
[3]Faculty of Bioengineering and Bioinformatics, Lomonosov Moscow State University, Lenin Hills 1, bldg. 73, Moscow, 119991, Russia
*E-mail: nilov@belozersky.msu.ru
Received January 20, 2016; in final form, April 5, 2016

ABSTRACT **Human lactate dehydrogenase A plays an important role in the glucose metabolism of tumor cells and constitutes an attractive target for chemotherapy. Molecular fragments able to bind in the active site of this enzyme and form hydrogen bonds with the Arg168 guanidinium group, as well as additional interactions with the loop 96–111 in the closed conformation, have been identified by virtual screening of sulfonates and experimental testing of their inhibitory effect. The sulfo group can occupy a similar position as the carboxyl group of the substrate and its structural analogs, whereas the benzothiazole group attached via a linker can be located in the coenzyme (NADH) binding site. Thus, the value of merging individual structural elements of the inhibitor by a linker was demonstrated and ways of further structural modification for the design of more effective inhibitors of lactate dehydrogenase A were established.**
KEYWORDS **Lactate dehydrogenase, inhibitor, sulfo group, sulfonates, molecular modeling, docking.**
ABBREVIATIONS **LDH – lactate dehydrogenase, LDH-A – lactate dehydrogenase isoform A.**

INTRODUCTION

Lactate dehydrogenase (LDH) catalyzes the conversion of the glycolysis product pyruvate to lactate, accompanied by the oxidation of NADH to NAD^+ (Fig. 1). In a healthy human organism, LDH isoform A (LDH-A) is found primarily in skeletal muscles; isoform B – in heart muscle; and C – in testes [1, 2]. In many tumor cells, activation of pyruvate conversion by LDH and reduced pyruvate oxidation in the mitochondria is observed. This alteration of metabolism is known as the Warburg effect [3, 4]. One of the reasons for the elevated glycolysis is an increased expression of LDH-A [5, 6]. This enzyme is an attractive oncological target as it plays an important role in the viability and proliferation of tumor cells [7–9]. Therefore, a search for selective inhibitors of human LDH-A and investigation of their effects at the cellular level are of particular interest.

Several classes of LDH-A inhibitors are described in the literature [10, 11], and most of them contain a carboxyl group. Oxamate (the structural analog of the substrate) and its numerous derivatives can serve as an example [12, 13]. Hydrogen bonds of the carboxyl group with a conserved Arg168 residue are crucial for the binding of pyruvate and oxamate [14, 15]. Residues of the mobile loop 96–111 [16] also participate in the binding of the substrate, coenzyme and inhibitors, among which the role of Arg105 should be emphasized (it stabilizes the transition state in the course of substrate conversion). The crystal structures of human LDH-A complexes, where the loop 96–111 is either in the closed or open conformation depending on the structure of the inhibitor, have been determined [17–19]. In the development of LDH-A inhibitors, an attempt has been made to find compounds able to interact with both the substrate and coenzyme binding sites [20, 21]. A promising way to solve this problem may be a search for molecule fragments – small molecules capable of forming specific interactions with selected protein regions. Being subsequently connected by a suitable linker, these fragments may serve as a basis for new and more effective inhibitors of the enzyme. The analysis

of published data on the binding of the substrate, as well as oxamic and malonic acid derivatives, points to the importance of electrostatic interactions with the Arg168 guanidinium group in the active site of LDH-A. Given this fact, the goal was set to explore the possibility of using a negatively charged sulfo group in the design of the structure of new inhibitors.

Sulfo-substituted derivatives of naphthalene 2 and 3 (*Fig. 1*) were referred to in work devoted to the search for inhibitors of LDH from the parasitic microorganism *Plasmodium falciparum* that causes malaria. However, they were found to exert only a weak inhibitory effect [22]. The crystal structure of LDH from *P. falciparum* in a complex with **2** (PDB ID 1u4s) revealed that the sulfo group of the inhibitor interacts with Arg171 (it corresponds to Arg168 in the human LDH-A). The authors assumed that inhibitor **2** binds in a similar manner to the apo form and the LDH-coenzyme complex without competing with NADH. It should be noted that there are significant differences in the arrangement of the active site in human and parasite LDHs, mainly associated with the position of the coenzyme and mobile active site loop, which is 5 residues shorter in the human LDH [23]. This suggests that sulfonate-based structural fragments of human LDH-A inhibitors should differ from compounds **2** and **3**. In our previous work, we constructed models of human LDH-A for searching for inhibitors competing with the substrate and coenzyme, and also determined the structural criteria for the selection of potential inhibitors [24]. The developed approach was used for the screening of molecular fragments with a sulfo group which might be additive components in the design of more effective inhibitors of LDH-A.

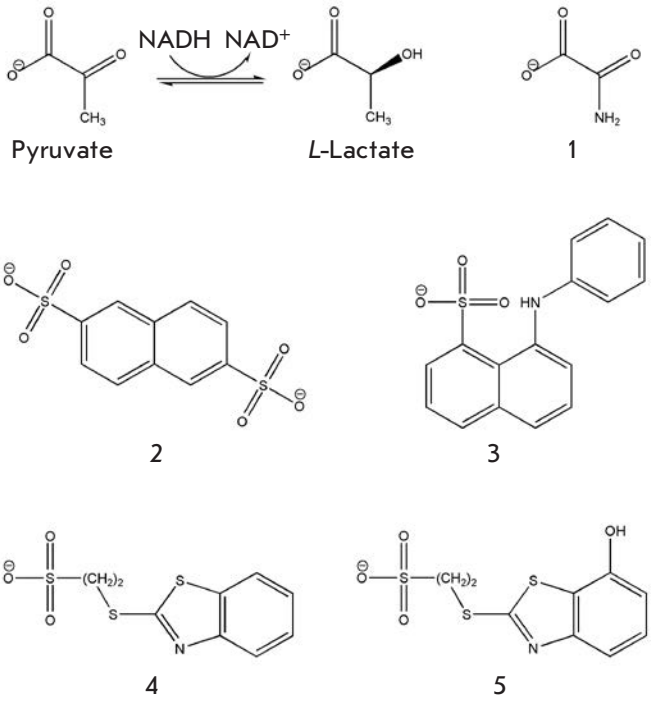

Fig. 1. Chemical structures of human LDH-A substrates and inhibitors (**1**-**5**). **1** – oxamate, **2** – naphthalene-2,6-disulfonate, **3** – 8-(phenylamino)naphthalene-1-sulfonate, **4** – 2-(benzothiazol-2-ylsulfanyl)-ethanesulfonate, **5** – 2-(7-hydroxybenzothiazol-2-ylsulfanyl)-ethanesulfonate.

EXPERIMENTAL SECTION

Virtual screening for LDH-**A** inhibitors was performed among low-molecular-weight compounds from the Vitas-M library [25]. Using the ACD/Spectrus DB 14.0 software [26], compounds containing a sulfo group and conforming to the rule of three [27, 28] were retrieved from the library. This rule defines the ranges of physicochemical parameters associated with molecule fragments (molecular weight < 300, log $P \leq 3$, hydrogen bond donors ≤ 3, hydrogen bond acceptors ≤ 3, and rotatable bonds ≤ 3). Molecular docking of compounds from the obtained focused library was performed using Lead Finder 1.1.15 in the "extra precision" mode [29, 30] and the models of human LDH-A (with and without the bound molecule of NADH) constructed in our previous work [24]. At the first step of the selection of inhibitors, some compounds were eliminated when the distance between the sulfur of the sulfo group and the guanidinium carbon of Arg168 at their binding with LDH-A exceeded 5.5 Å. The remaining compounds that fitted the criteria of the structural filtration were tested for their ability to form hydrogen bonds and hydrophobic contacts with residues of the loop 96–111 [24]. Visualization and analysis of the structures were performed using VMD 1.9.2 [31].

Experimental measurement of enzyme activity was conducted using LDH from rabbit muscle (Sigma-Aldrich). Potassium phosphate buffer 0.1 M, pH 7.0 was used for the preparation of the solutions and performance of the measurements. An enzyme solution containing 1% (g/ml) bovine serum albumin (BSA) was prepared immediately prior to the measurements. The LDH-A activity was monitored spectrophotometrically at 340 nm using a Shimadzu UV-1800 spectrophotometer by detecting the decrease in the NADH absorbance at the conversion of pyruvate to lactate. The reaction mixture containing the buffer, pyruvate (400 μM), NADH (20 μM), and an inhibitor was placed into the cuvette, thermostated for 5 min at 37°C, and then the reaction was started, adding an aliquot of the enzyme. The initial rate of the enzyme-catalyzed reaction was determined in two independent experiments. The IC_{50} value (concentration of an inhibitor at which the enzyme ac-

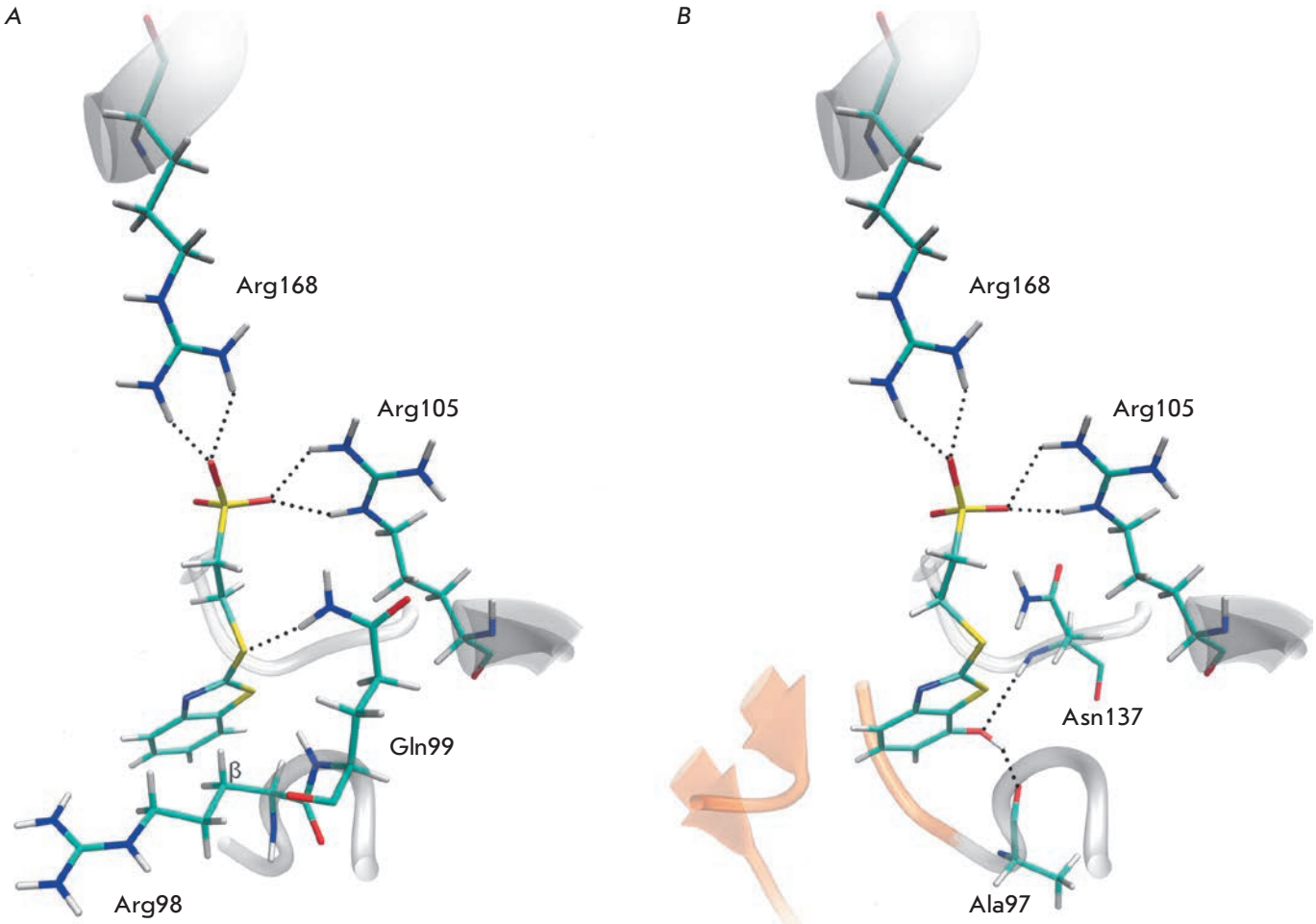

Fig. 2. Positions of inhibitors in the active site of human LDH-A revealed by molecular modeling. A – Binding of compound **4**: hydrogen bonds of a sulfo group with Arg168 are shown, as well as interactions with the active site loop residues Arg98, Gln99, and Arg105. *B* – Binding of compound **5**: additional hydrogen bonds of hydroxyl substituent with Ala97 and Asn137 are shown, interactions with Arg98 and Gln99 are not depicted. A region occupied by the adenine moiety of the coenzyme is colored orange.

tivity is reduced by 50%) was determined by varying the concentration of an inhibitor from 0 to 8 mM.

RESULTS AND DISCUSSION

Crystallographic studies revealed that sulfo-substituted derivative **2** is capable of binding only to the open conformation of LDH from *P. falciparum* in which the active site loop is disordered. Obviously, the structural fragments containing a sulfo group and capable of binding to the enzyme in the closed conformation, i.e. when effective interaction with the loop 96–111 is expected, should substantially differ from compounds **2** and **3**. To identify new fragments, a set of sulfonic acids and their salts (71 compounds) was selected from a library of low-molecular-weight compounds. Compounds were docked into the active site of the previously developed models of human LDH-A, and then their ability to mediate a significant electrostatic interaction with the Arg168 residue, as well as additional interactions with the loop 96–111 in the closed conformation, was analyzed. The most promising inhibitor, compound **4**, capable of efficient binding with the apo form of LDH-A ($\Delta G^{calc} = -9.9$ kcal/mol), was chosen as a result of screening.

The inhibitory properties of compound **4** were experimentally tested against LDH from rabbit muscle, whose active site has high structural similarity with that of human LDH-A [32]. The IC_{50} value was determined to be 1.2 mM. Interestingly, inhibitor 4 binds in a similar manner to the earlier investigated oxamate derivative STK381370 ($\Delta G^{calc} = -7.9$ kcal/mol, IC_{50} 5 mM) [24], forming additional interactions with the

loop 96–111. However, the interaction of 4 is more efficient. The results indicate that the earlier developed model of the closed enzyme conformation adequately simulates the binding of compounds of various classes.

Localization of the structural fragment with the charged sulfo group in the substrate binding site leads to the stabilization of the inhibitor's position due to the formation of hydrogen bonds with guanidinium groups of Arg168 and Arg105 (*Fig. 2A*). A very important issue in the design of LDH-A inhibitors is the way of connecting individual elements in the structure. So, for example, interaction of compound **4** with both the substrate binding site and that of NADH's nicotinamide nucleotide is possible owing to the flexibility of a linker between the sulfo and benzothiazole groups. The thioether linker forms a hydrogen bond with the side chain of Gln99, while the benzothiazole group, located in the site of the first ribose residue of the coenzyme, forms a favorable hydrophobic contact with the C^{β}-atom of the Arg98 side chain. It should be noted that the abovementioned interactions with the residues Arg98, Gln99, and Arg105 important for the stabilization of the active site loop take place when the closed conformation is formed. There are also additional interactions at the sulfonate binding: formation typical for oxamate hydrogen bonds between the sulfo group, Asn137, and Thr247, hydrophobic contacts of the linker with Ile241 and benzothiazole group with Val30, hydrogen bond of a ring's heteroatom with the Asn137 carboxamide (not shown in the figure).

Among the sulfo derivatives examined in the course of screening, there were structures without a flexible linker (including naphthalene derivatives), with a linker elongated by one methylene unit, and with benzene, pyrrole, and pyridine replacing benzothiazole in compound **4**. All of them were characterized by a lower binding energy and were incapable of forming interactions sufficient for the stabilization of the loop 96-111 in the closed conformation. This indicates that scaffold **4** is optimal for binding in the active site and may serve as a basic structure for further modifications. For example, the introduction of the hydroxyl group at position 7 allows this substituent to occupy the site responsible for binding of the 3'-OH group of the first ribose residue of NADH and to form hydrogen bonds with the Ala97 and Asn137 backbones (compound **5**, *Fig. 2B*). The value of the calculated binding energy ($\Delta G^{calc} = -10.9$ kcal/mol) shows that this modification leads to an additional energy gain. Increased efficiency of enzyme inhibition due to the introduction of substituents into the benzothiazole group seems to be a promising perspective for the further merging of structural fragments aimed at achieving additive (and perhaps synergistic) effects in the development of novel LDH-A inhibitors.

CONCLUSIONS

The aim of the present study was to select new molecular fragments for the design of LDH-A inhibitors able to form interactions of a charged acid group with Arg168 and amino acid residues of the active site loop in the substrate binding site, as well as interactions with the coenzyme binding site typical of substrates and previously described inhibitors. As a result of virtual screening and experimental validation of inhibitory properties, new fragments have been identified that comprise a sulfo group, linker, and benzothiazole group. The performed study allowed us to uncover the most important interactions and the amino acid residues that stabilize the position of inhibitors containing a sulfo group (Ala97, Arg98, Gln99, Arg105, Arg168) in the closed enzyme conformation. Thus, the methodology for LDH-A inhibitors search has been tested and ways for further optimizing inhibitor structures have been outlined. ●

This work was supported by RFBR (grant № 14-08-01251).

REFERENCES

1. Kolappan S., Shen D.L., Mosi R., Sun J., McEachern E.J., Vocadlo D.J., Craig L. // Acta Crystallogr. D Biol. Crystallogr. 2015. V. 71. P. 185–195.
2. Everse J., Kaplan N.O. // Adv. Enzymol. Relat. Areas Mol. Biol. 1973. V. 37. P. 61–133.
3. Warburg O. // Science. 1956. V. 124. P. 269–270.
4. Hamanaka R.B., Chandel N.S. // J. Exp. Med. 2012. V. 209. P. 211–215.
5. Goldman R.D., Kaplan N.O., Hall T.C. // Cancer Res. 1964. V. 24. P. 389–399.
6. Koukourakis M.I., Giatromanolaki A., Sivridis E., Bougioukas G., Didilis V., Gatter K.C., Harris A.L. // Br. J. Cancer. 2003. V. 89. P. 877–885.
7. Fantin V.R., St-Pierre J., Leder P. // Cancer Cell. 2006. V. 9. P. 425–434.
8. Le A., Cooper C.R., Gouw A.M., Dinavahi R., Maitra A., Deck L.M., Royer R.E., Vander Jagt D.L., Semenza G.L., Dang C.V. // Proc. Natl. Acad. Sci. U. S. A. 2010. V. 107. P. 2037–2042.
9. Miao P., Sheng S., Sun X., Liu J., Huang G. // IUBMB Life. 2013. V. 65, P. 904–910.
10. Granchi C., Bertini S., Macchia M., Minutolo F. // Curr. Med. Chem. 2010. V. 17. P. 672–697.
11. Granchi C., Paterni I., Rani R., Minutolo F. // Future Med. Chem. 2013. V. 5. P. 1967–1991.
12. Yu Y., Deck J.A., Hunsaker L.A., Deck L.M., Royer R.E., Goldberg E., Vander Jagt D.L. // Biochem. Pharmacol. 2001. V. 62. P. 81–89.

13. Choi S.R., Beeler A.B., Pradhan A., Watkins E.B., Rimoldi J.M., Tekwani B., Avery M.A. // J. Comb. Chem. 2007. V. 9. P. 292–300.
14. Dunn C.R., Wilks H.M., Halsall D.J., Atkinson T., Clarke A.R., Muirhead H., Holbrook J.J. // Philos. Trans. R. Soc. Lond. B Biol. Sci. 1997. V. 332, P. 177–184.
15. Read J.A., Winter V.J., Eszes C.M., Sessions R.B., Brady R.L. // Proteins. 2001. V. 43. P. 175–185.
16. Gerstein M., Chothia C. // J. Mol. Biol. 1991. V. 220, P. 133–149.
17. Ward R.A., Brassington C., Breeze A.L., Caputo A., Critchlow S., Davies G., Goodwin L., Hassall G., Greenwood R., Holdgate G.A., et al. // J. Med. Chem. 2012. V. 55. V. 3285–3306.
18. Dragovich P.S., Fauber B.P., Corson L.B., Ding C.Z., Eigenbrot C., Ge H., Giannetti A.M., Hunsaker T., Labadie S., Liu Y., et al. // Bioorg. Med. Chem. Lett. 2013. V. 23. P. 3186–3194.
19. Fauber B.P., Dragovich P.S., Chen J., Corson L.B., Ding C.Z., Eigenbrot C., Giannetti A.M., Hunsaker T., Labadie S., Liu Y., et al. // Bioorg. Med. Chem. Lett. 2013. V. 23. P. 5533–5539
20. Moorhouse A.D., Spiteri C., Sharma P., Zloh M., Moses J.E. // Chem. Commun. (Camb.). 2011. V. 47. P. 230–232.
21. Kohlmann A., Zech S.G., Li F., Zhou T., Squillace R.M., Commodore L., Greenfield M.T., Lu X., Miller D.P., Huang W.S., et al. // J. Med. Chem. 2013. V. 56. P. 1023–1040.
22. Conners R., Schambach F., Read J., Cameron A., Sessions R.B., Vivas L., Easton A., Croft S.L., Brady R.L. // Mol. Biochem. Parasitol. 2005. V. 142. P. 137–148.
23. Dunn C.R., Banfield M.J., Barker J.J., Higham C.W., Moreton K.M., Turgut-Balik D., Brady R.L., Holbrook J.J. // Nat. Struct. Biol. 1996. V. 3. P. 912–915.
24. Nilov D.K., Prokhorova E.A., Švedas V.K. // Acta Naturae. 2015. V. 7. №2 (25). P. 57–63.
25. ST(K/L) collection. Vitas-M Laboratory, Ltd, http://www.vitasmlab.com. 2012.
26. ACD/Spectrus DB, version 14.01. Advanced Chemistry Development, Inc., http://www.acdlabs.com. 2012.
27. Congreve M., Carr R., Murray C., Jhoti H. // Drug Discov. Today. 2003. V. 8. P. 876–877.
28. Lipinski C.A. // Drug Discov. Today Technol. 2004. V. 1. P. 337–341.
29. Stroganov O.V., Novikov F.N., Stroylov V.S., Kulkov V., Chilov G.G. // J. Chem. Inf. Model. 2008. V. 48. P. 2371–2385.
30. Novikov F.N., Stroylov V.S., Stroganov O.V., Kulkov V., Chilov G.G. // J. Mol. Model. 2009. V. 15. P. 1337–1347.
31 . Humphrey W., Dalke A., Schulten K. // J. Molec. Graphics. 1996. V. 14.1. P. 33–38.
32. Swiderek K., Panczakiewicz A., Bujacz A., Bujacz G., Paneth P. // J. Phys. Chem. B. 2009. V. 113. P. 12782–12789.

Analysis of the Domains of Hepatitis C Virus Core and NS5A Proteins that Activate the Nrf2/ARE Cascade

O. A. Smirnova[1], O. N. Ivanova[1], F. Sh. Mukhtarov[1], V. L. Tunitskaya[1], J. Jansons[2], M. G. Isaguliants[2,3], S. N. Kochetkov[1], A. V. Ivanov[1]*

[1]Engelhardt Institute of Molecular Biology, Russian Academy of Sciences, Vavilov str., 32, Moscow, 119991, Russia

[2]Riga Stradins University, Dzirciema Street, 16, LV-1007, Riga, Latvia

[3]N. F. Gamaleya Research Center of Epidemiology and Microbiology, Ministry of Health of the Russian Federation, Gamaleya str., 18, Moscow, 123098, Russia

*E-mail: aivanov@yandex.ru

Received March 11, 2016; in final form, June 27, 2016

ABSTRACT **The hepatitis C virus (HCV) triggers a chronic disease that is often accompanied by a spectrum of liver pathologies and metabolic alterations. The oxidative stress that occurs in the infected cells is considered as one of the mechanisms of HCV pathogenesis. It is induced by the viral core and NS5A proteins. It is already known that both of these proteins activate the antioxidant defense system controlled by the Nrf2 transcription factor. Here, we show that this activation is mediated by domain 1 of the NS5A protein and two fragments of the core protein. In both cases, this activation is achieved through two mechanisms. One of them is mediated by reactive oxygen species (ROS) and protein kinase C, whereas the other is triggered through ROS-independent activation of casein kinase 2 and phosphoinositide 3-kinase. In the case of the HCV core, the ROS-dependent mechanism was assigned to the 37–191 a.a. fragment, while the ROS-independent mechanism was assigned to the 1–36 a.a. fragment. Such assignment of the mechanisms to different domains is the first evidence of their independence. In addition, our data revealed that intracellular localization of HCV proteins has no impact on the regulation of the antioxidant defense system.**

KEYWORDS **Hepatitis C virus, oxidative stress, regulation, transcription factor, Nrf2**

ABBREVIATIONS **ROS – reactive oxygen species; a.a. – amino acids; HCV – hepatitis C virus, OS – oxidative stress**

INTRODUCTION

The hepatitis C virus (HCV) is a widespread and dangerous pathogen that infects the human liver. In most cases, HCV infection leads to chronic hepatitis, during which there is a high risk of liver fibrosis and cirrhosis, hepatocellular carcinoma, and various metabolic disorders (steatosis, type 2 diabetes mellitus, altered iron metabolism and other pathologies) [1]. Numerous basic and clinical studies have revealed a number of pathogenetic mechanisms related to HCV, including oxidative stress (OS), which plays an important role [2]. OS is a state of a cell characterized by an imbalance between reactive oxygen species (ROS) and the low-molecular-weight compounds (antioxidants) that neutralize them, as well as the enzymes involved in the protection against ROS (referred to as phase II enzymes). The biosynthesis of many enzymes of the antioxidant metabolism and phase II enzymes is controlled by the Nrf2 transcription factor (nuclear factor-erythroid 2-related factor 2), which binds to the common regulatory element ARE (Antioxidant Response Element) in gene promoters [3]. In the absence of stress, the Nrf2 factor is located in the cytoplasm in a complex with its partner protein Keap1. When ROS production is up-regulated, this complex is disrupted either through phosphorylation of the Nrf2 factor by various protein kinases or as a result of Keap1 modification, the free transcription factor is then translocated to the nucleus and transcription with a concomitant activation of the genes encoding antioxidant defense such as heme oxygenase-1 (HO-1) and NAD(P)H:quinone oxidoreductase 1 (Nqo1) [3, 4].

The hepatitis C virus does not only cause OS, but it also activates the transcription factor Nrf2 [2]. In both cases, the viral core and NS5A proteins play the key role [4–7]. Previously, we established that these proteins activate the defense system through two mechanisms, one of which is mediated by ROS and protein kinase C, and the other through ROS-independent activation of factor Nrf2 by casein kinase 2 and phosphoinositide 3-kinase [4]. However, it cannot be ex-

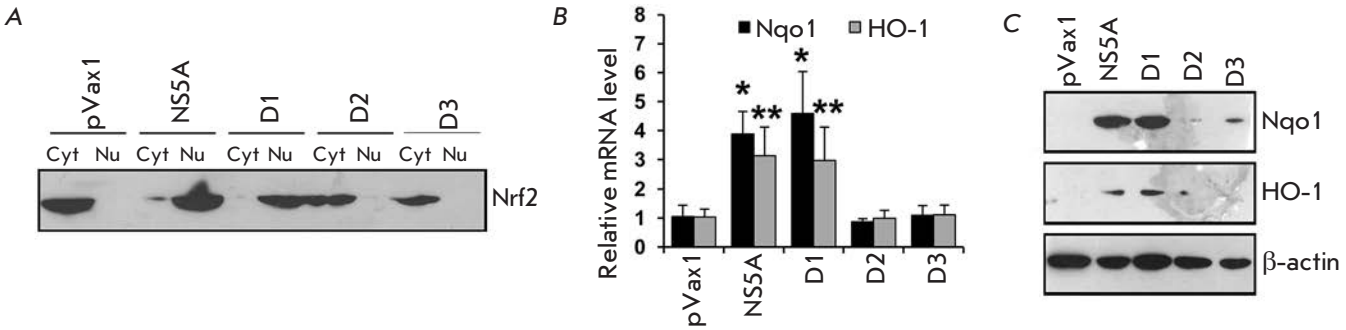

Fig. 1. Activation of the Nrf2/ARE cascade by domain 1 of the NS5A protein results in the translocation of the Nrf2 transcription factor from the cytoplasm into the nucleus (*A*) and induction of human NAD(P)H:quinone oxidoreductase 1 (Nqo1) and heme oxygenase 1 (HO-1) (*B*, *C*). Intracellular localization of factor Nrf2 was determined by separation of cytoplasmic (Cyt) and nuclear (Nu) protein fractions, with subsequent detection of Nrf2 by immunoblotting. Quantification of the Nqo1 and HO-1 expression levels was performed by reverse transcription and real-time PCR (*B*) and immunoblotting (*C*). $*p < 0.01$ and $**p < 0.05$ compared to pVax1.

cluded that both pathways of Nrf2 activation are induced by some common regulator located earlier in the cascade, all the members of which remain unknown. The objective of the current study was to reveal the presence (or absence) of this regulation and identify the structural elements of the core and NS5A proteins involved in the mechanisms of Nrf2/ARE cascade activation.

EXPERIMENTAL SECTION

A human hepatoma Huh7.5 cell line was provided courtesy of C. Rice (Rockefeller University, USA). The plasmid pCMV-core encoding the full-length core protein of HCV genotype 1b (274933RU) has been previously described [4]. Plasmids encoding fragments 1–36, 37–191, and 1–151 a.a. of the core protein were constructed on the basis of the pVax1 vector [8], plasmids encoding the full-length protein NS5A of HCV genotype 1b (AJ238799) and its individual D1 domains (residues 1–249), D2 (250–355 a.a.), and D3 (356–447 a.a.) were based on the pCMV-Tag3B vector [7].

Ro 31-8220, wortmannin, and 5,6-dichloro-1-β-*D*-ribofuranosylbenzimidazole (DRB) (Sigma) were used as inhibitors of the protein kinases.

Culture procedures

Huh7.5 cells were cultured in a DMEM medium supplemented with 10% fetal bovine serum (HyClone, USA), 2 mM glutamine, 50 u/ml penicillin, and 50 μg/ml streptomycin at 37°C in humidified atmosphere of 5% CO_2.

Work with reporter plasmid

Huh7.5 cells were seeded in 24-well plates, transfected with a mixture of reporter plasmid pP-ARE (0.25 μg) [4] and a target-expressing plasmid (0.25 μg) using the Turbofect reagent. After 30 hours, the cells were lysed and luciferase activity was measured as previously described [4].

Reverse transcription and real-time PCR (RT-qPCR)

The Huh7.5 cells were transfected as described above. Forty hours posttransfection, the culture medium was collected, total RNA isolated, and reverse transcription and real-time PCR were performed as previously reported [4].

Western blotting

The Huh7.5 cells were transfected in 6-well plates and lysed 40 h posttransfection. Further manipulations were performed as previously described [4] using mouse monoclonal antibodies against heme oxygenase 1 (ab13248), NAD(P)H:quinone oxidoreductase 1 (ab28947) and β-actin (ab3280) (Abcam, UK) and also secondary antibodies against mouse IgG conjugated with horseradish peroxidase (sc-2005) (Santa-Cruz, USA). For the analysis of the intracellular localization of the Nrf2 factor, the cells were lysed and fractions of cytoplasmic and nuclear proteins were separated using a commercial NE-PER kit (Thermo Scientific). Nrf2 was detected in each fraction by immunoblotting using rabbit polyclonal antibodies against Nrf2 (sc-722) and secondary antibodies against rabbit IgG (sc-2004) (Santa-Cruz).

Statistical analysis

The data were processed using the StatPlus software (AnalystSoft, Canada). The results are presented as a mean ± standard deviation. The statistical significance of the differences was calculated using the paired Student's *t*-test.

RESULTS AND DISCUSSION

Involvement of the fragments of the core and NS5A proteins in the activation of the Nrf2/ARE cascade was analyzed by three methods: quantification of the relative expression levels of the two phase II enzymes (Nqo1, HO-1) by western blotting and RT-qPCR and identification of the intracellular localization of the Nrf2 factor. It has been demonstrated that, among all of the described NS5A protein domains, only domain 1 (1–249 a.a.) can activate the Nrf2 factor; *i.e.*, it causes its translocation from the cytoplasm to the nucleus (*Fig. 1A*) and enhances the expression of Nrf2-dependent genes (*Fig. 1B, C*). It is noteworthy that domain 1, among all of the three domains of the NS5A protein, exhibits a specific three-dimensional structure [9], while domains 2 and 3 are unstructured [10, 11]. Our previous data also indicate that domain 1 possesses prooxidant activity [7]. Furthermore, it has been shown that the ability of the NS5A protein to activate the Nrf2/ARE cascade is associated neither with its post-translational modification (phosphorylation of domains 2 and 3) [12] nor with the ability to disrupt the expression of the interferon β response to HCV infection [1].

In order to study the contribution of various fragments of the core protein (residues 1–191 a.a.) in the activation of the Nrf2/ARE cascade, we used its truncated fragments 1–36 and 37–19 a.a. that previously were shown to trigger ROS production through a variety of mechanisms [8]. Moreover, we used the 1–151 a.a. fragment, which activated all ROS-producing enzymes as the full-length HCV despite being localized not on the endoplasmic reticulum but in the nucleus, as the 1–36 a.a. form does. It was found that all the truncated forms of the HCV core activate the Nrf2 factor (*Fig. 2A*) and induce Nrf2-dependent genes (*Fig. 2B, C*). Thus, there are at least two regions in the core protein that activate the Nrf2/ARE cascade.

Several groups of researchers have reported that the Nrf2/ARE cascade can be activated by various protein kinases, including protein kinase C, casein kinase 2, phosphoinositide 3-kinase, the mitogen-activated protein kinases p38, ERK1/2 and JNK, or regulated by glycogen synthase kinase 3 (GSK3), with the contribution of each kinase being dependent on the cell type and stimulus ([3, 4] and references therein). In order to determine the activation mechanism for each protein fragment, we used antioxidant pyrrolidine dithiocarbamate (PDTC), as well as inhibitors of protein kinase C (Ro 31-8220, Ro), casein kinase 2 (DRB), and phosphoinositide 3-kinase (wortmannin, Wo): *i.e.* the enzymes that are, according to our data, involved in the activation of Nrf2 by the full-length NS5A protein [4]. Using a reporter plasmid pP-ARE encoding luciferase under the control of the minimum ARE-Nqo1 element

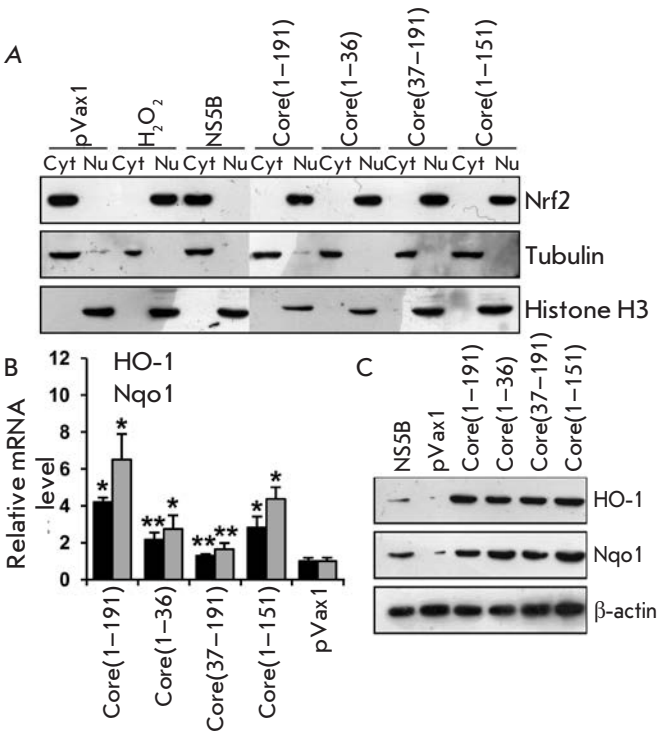

Fig. 2. Fragments 1–36 and 37–191 a.a. of the HCV core protein activate the Nrf2/ARE cascade by triggering the translocation of transcription factor Nrf2 from the cytoplasm into the nucleus (*A*) with subsequent induction of human NAD(P)H:quinone oxidoreductase 1 (Nqo1) and heme oxygenase 1 (HO-1) (*B, C*). Intracellular localization of factor Nrf2 was determined by separation of cytoplasmic (Cyt) and nuclear (Nu) protein fractions, with subsequent detection of Nrf2 by immunoblotting. Quantification of the Nqo1 and HO-1 expression levels was performed by reverse transcription and real-time PCR (*B*) and immunoblotting (*C*). $^{*}p < 0.01$ and $^{**}p < 0.05$ compared to pVax1.

of the human *Nqo1* gene [4], we verified that both the 1–36 and 37–191a.a. fragments of the HCV core activate the transcription of ARE-dependent genes. Treatment with the antioxidant or the protein kinase C inhibitor reduced the level of luciferase expression in the case of the full-length core protein (*Fig. 3A*) and prevented activation in the case of the 37–191 a.a. fragment (*Fig. 3B*). In cells expressing the N-terminal fragment, luciferase expression was blocked only by the inhibitors of casein kinase and phosphoinositide 3-kinase (*Fig. 3B*). Similar results were obtained when studying the action of protein kinase inhibitors on the translocation of the Nrf2 factor (*Fig. 3D*). It is noteworthy that in the case of the full-length core protein, the inhibitors

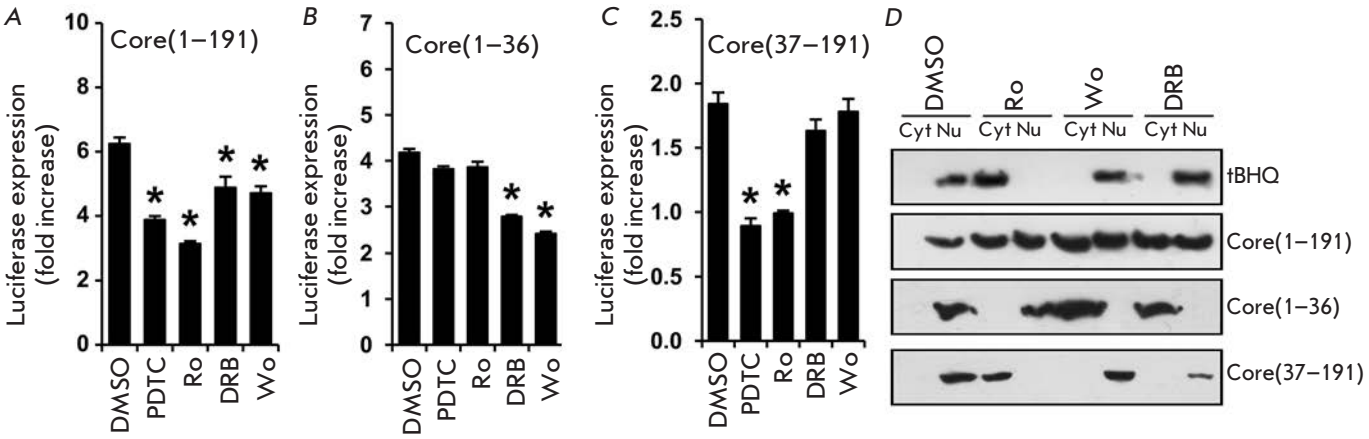

Fig. 3. Fragment 1–36 a.a. of the HCV core protein activates the Nrf2/ARE cascade by the ROS-independent mechanism involving casein kinase 2 and phosphoinositide 3-kinase; the 37–191 a.a. fragment – by the ROS-dependent mechanism involving protein kinase C. The role of protein kinases and reactive oxygen species was estimated by measuring luciferase expression in Huh7 cells co-transfected with the reporter pP-ARE plasmid with constructs encoding the full-length core protein (*A*) or its fragments 1–36 a.a. (*B*) and 37–191 a.a. (*C*) or by an analysis of the intracellular localization of Nrf2 (*D*). The latter was studied by separation of cytoplasmic (Cyt) and nuclear (Nu) protein fractions, with subsequent detection of Nrf2 by immunoblotting. Inhibitors of protein kinases Ro 31-8220 (Ro, protein kinase C inhibitor), DRB (casein kinase 2 inhibitor), or wortmannin (Wo, phosphoinositide 3-kinase inhibitor) in the absence or presence of an antioxidant pyrrolidine dithiocarbamate (PDTC) were added into the culture medium 18 h post-transfection. $^*p < 0.01$.

of all three protein kinases failed to completely prevent Nrf2 translocation to the nucleus and could only inhibit the process by approximately 2-fold, indicating a comparable contribution of the two observed mechanisms in the activation of the cascade.

Our findings showing that the N-terminal domain of the HCV core protein activates Nrf2 through a ROS-independent mechanism involving casein kinase 2 and phosphoinositide 3-kinase, while the fragment 37–191 acts through the ROS-dependent pathway involving protein kinase C, allowed us to confirm the complete independence of these two mechanisms. Moreover, casein kinase 2 and phosphoinositide 3-kinase were activated by the same domain of the HCV core that had been previously shown to interact with various proteins of the host cell, including helicase DDX3, the STAT1 transcription factor and lymphotoxin β receptor ([1, 8] and references therein). In addition, both mechanisms of Nrf2/ARE cascade activation were triggered by different variants of the core protein that are localized in the nucleus (fragments 1–36 and 1–151 a.a.) and on the surface of the endoplasmic reticulum (fragments 37–191 and 1–191 a.a.). Therefore, it is tempting to speculate that activation of the cascade could be achieved during the biosynthesis of the core protein in the endoplasmic reticulum.

CONCLUSIONS

In the current paper we have identified the regions of the HCV core and NS5A proteins that trigger activation of the Nrf2/ARE cascade. In addition, we have shown that the ROS-dependent and ROS-independent mechanisms of this activation are independent. ●

The study of the influence of viral proteins on the Nrf2/ARE cascade was supported by the Russian Science Foundation (grant № 14-14-01021). International collaboration of researchers, including work the construction of the plasmids encoding the core protein and its fragments, was supported by a grant from the Thematic Partnership of the Swedish Institute 09272_2013. Juris Jansons was partially supported by VACTRAIN grant № 692293; Maria Isaguliants – by grant on coordination and support of research BALTINFECT № 316275 of Horizon 2020 programme.

REFERENCES

1. Lemon S.M., Walker C.M., Alter M.J., Yi M.-K. Hepatitis C virus // Fields Virology. Philadelphia: Lippincott, Williams & Wilkins, 2007. P. 1253–1304.
2. Ivanov A.V., Bartosch B., Smirnova O.A., Isaguliants M.G., Kochetkov S.N. // Viruses. 2013. V. 5. № 2. P. 439–469.
3. Zhang M., An C., Gao Y., Leak R.K., Chen J., Zhang F. // Prog. Neurobiol. 2013. V. 100. P. 30–47.

4. Ivanov A.V., Smirnova O.A., Ivanova O.N., Masalova O.V., Kochetkov S.N., Isaguliants M.G. // PLoS One. 2011. V. 6. № 9. P. e24957.
5. Okuda M., Li K., Beard M.R., Showalter L.A., Scholle F., Lemon S.M., Weinman S.A. // Gastroenterology. 2002. V. 122. № 2. P. 366–375.
6. Gong G., Waris G., Tanveer R., Siddiqui A. // Proc. Natl. Acad. Sci. USA. 2001. V. 98. № 17. P. 9599–9604.
7. Smirnova O.A., Ivanova O.N., Bartosch B., Valuev-Elliston V.T., Mukhtarov F., Kochetkov S.N., Ivanov A.V. // Oxid Med. Cell Longev. 2016. V. 2016. P. 8341937.
8. Ivanov A.V., Smirnova O.A., Petrushanko I.Y., Ivanova O.N., Karpenko I.L., Alekseeva E., Sominskaya I., Makarov A.A., Bartosch B., Kochetkov S.N., et al. // Viruses. 2015. V. 7. № 6. P. 2745–2770.
9. Tellinghuisen T.L., Marcotrigiano J., Rice C.M. // Nature. 2005. V. 435. № 7040. P. 374–379.
10. Hanoulle X., Verdegem D., Badillo A., Wieruszeski J.M., Penin F., Lippens G. // Biochem. Biophys. Res. Commun. 2009. V. 381. № 4. P. 634–638.
11. Liang Y., Ye H., Kang C.B., Yoon H.S. // Biochemistry. 2007. V. 46. № 41. P. 11550–11558.
12. Huang Y., Staschke K., De Francesco R., Tan S.L. // Virology. 2007. V. 364. № 1. P. 1–9.

Derivatization of Aminoglycoside Antibiotics with Tris(2,6-dimethoxyphenyl)carbenium Ion

A.P. Topolyan[1], M.A. Belyaeva[1], E.E. Bykov[2], P.V. Coodan[3], E.A. Rogozhin[1,2], D.A. Strizhevskaya[1], O.M. Ivanova[1], A.V. Ustinov[1], I.V. Mikhura[1], I.A. Prokhorenko[1,2], V.A. Korshun[1,2], A.A. Formanovsky[1*]

[1]Shemyakin-Ovchinnikov Institute of Bioorganic Chemistry, Moscow, 117997, Russia

[2]Gause Institute of New Antibiotics, Moscow, 119021, Russia

[3]Research Institute of Nutrition, Moscow, 109240, Russia

[*]E-mail: formanovsky@yandex.ru

Received January 25, 2016; in final form, April 20, 2016

ABSTRACT **Detection of aminoglycoside antibiotics by MS or HPLC is complicated, because a) carbohydrate molecules have low ionization ability in comparison with other organic molecules (particularly in MALDI-MS), and b) the lack of aromatics and/or amide bonds in the molecules makes common HPLC UV-detectors useless. Here, we report on the application of a previously developed method for amine derivatization with tris(2,6-dimethoxyphenyl)carbenium ion to selective modification of aminoglycoside antibiotics. Only amino groups bound to primary carbons get modified. The attached aromatic residue carries a permanent positive charge. This makes it easy to detect aminoglycoside antibiotics by MS-methods and HPLC, both as individual compounds and in mixtures.**

KEYWORDS **aminoglycoside antibiotics, mass-spectrometry, trityl cation, HPLC.**

ABBREVIATIONS **HPLC - High performance liquid chromatography, GC-MS – gas chromatography–mass spectrometry, ELISA – enzyme-linked immunosorbent assay, MALDI-MS – matrix-assisted laser desorption/ionization mass spectrometry, LUMO – lowest unoccupied molecular orbital, CHCA – 1-cyano-4-hydroxycinnamic acid, TLC – thin-layer chromatography, NMR – nuclear magnetic resonance, DMF – dimethylformamide, DMSO – dimethyl sulfoxide.**

INTRODUCTION

Aminoglycosides are a group of bactericidal antibiotics. Aminoglycoside antibiotics display activity mostly against gram-negative aerobes and are most effective against the majority of severe infections (tuberculosis, endocarditis, and septicemia) [1]. The action of these antibiotics does not depend on the reproduction phase of the microorganisms and relies on aminoglycosides' irreversible binding to the 30S subunit proteins of bacterial ribosomes, thus inhibiting protein synthesis in bacteria. However, aminoglycosides are poorly active in anaerobic environments, and that makes them ineffective in tissues with reduced circulation and necrotic tissues. The pH of the medium is another factor that influences the antibacterial activity of aminoglycosides: these antibiotics are less effective in acidic and neutral environments than in weakly alkaline conditions. The high ototoxicity and nephrotoxicity [2, 3] associated with aminoglycoside therapy versus other antibiotics is its major shortcoming. Therefore, constant monitoring of aminoglycoside content both in biological fluids and in foods of animal origin is required. Many laboratory assays have been developed over several decades of therapeutic use of aminoglycosides for the detection of these antibiotics using GC-MS, HPLC (including derivatization), ELISA, capillary electrophoresis etc. Two thorough reviews on this area have recently been published [4, 5]. A number of publications [6–18] highlight the importance of and the need for convenient, simple, and rapid procedures for aminoglycoside detection, since the majority of the available techniques are either laborious and time-consuming or use expensive reagents.

The molecules of aminoglycoside antibiotics typically contain several amino groups (*Fig. 1*). These include amino groups directly bound to the heterocyclic or alicyclic ring and amino groups attached to the primary carbon atom (highlighted in red). Another feature of aminoglycosides is the transparency of their solutions in the UV region due to the lack of aromatics and/or

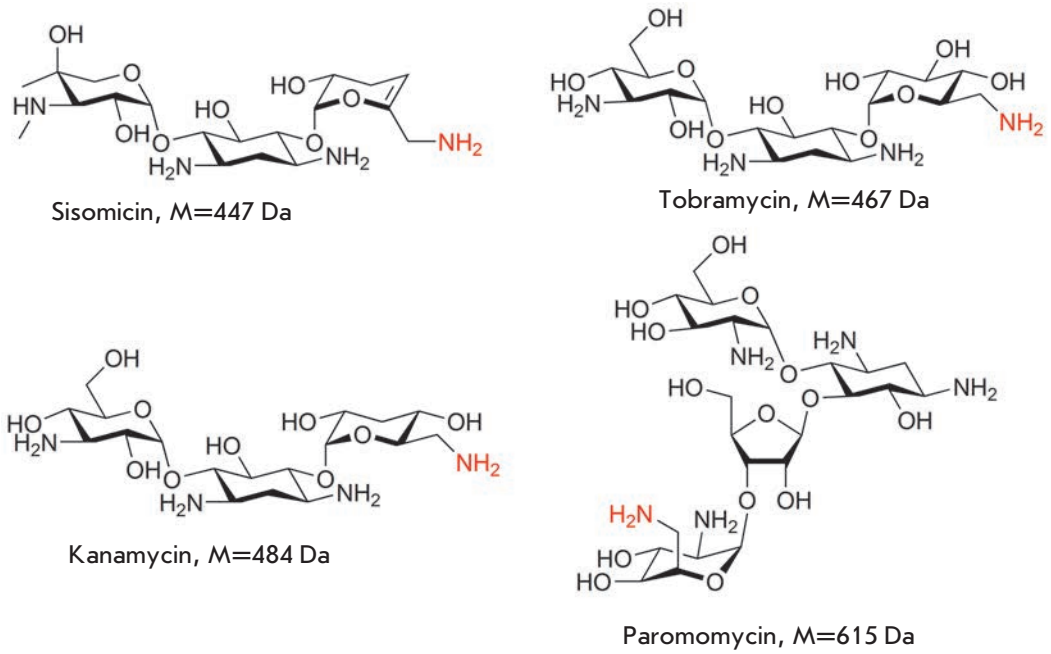

Fig. 1. Examples of structures of aminoglycoside antibiotics

amide bonds. This makes common HPLC techniques with UV-detectors not suitable for their analysis. Abundant hydroxyl groups and amino groups capable of forming hydrogen bonds complicate the release of individual molecules, thus leading to a low aminoglycoside ionization ability in mass spectrometry as compared to, for example, peptides of a similar mass. Moreover, aminoglycoside detection in MALDI mass spectrometry can be complicated by matrix interferences.

Recently, we have developed a mild derivatization method for low molecular amines using the tris(2,6-dimethoxyphenyl)carbenium ion [19]. The resulting derivatives of the 9,10-disubstituted acridinium cation (**Q^+-R**) possess a permanent positive charge (*Fig. 2*). Derivatization also results in an increase in mass of the molecule by a constant value (mass increment is +359 Da) that permits successful detection of amines, including those of the smallest mass, with MALDI mass spectrometry [19]. Meanwhile, the modification of hydrophilic aliphatic molecules with hydrophobic aromatic cation Q^+ may have prospects in terms of reversed-phase HPLC with UV detection.

It was of interest to assess the applicability of the derivatization technique for aminoglycoside detection. In this paper, we present a qualitative mass spectrometry and HPLC detection of aminoglycoside antibiotics derivatized with non-cleavable mass tag.

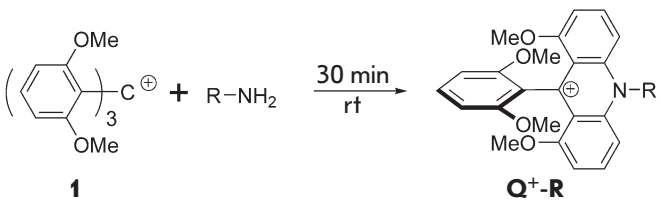

Fig. 2. Common scheme of amines derivatization with tris(2,6-dimethoxyphenyl)carbenium

MATERIALS AND METHODS

Materials

Dimethyl sulfoxide and acetonitrile were from Panreac, and other solvents were from Chimmed and EKOS-1, of chemically pure (cp) grade (hexane, methanol, dichloromethane, ethyl acetate, chloroform, ethanol) and extra-pure grade (toluene, acetone). Dichloromethane was distilled over a calcium hydride, and DMF was distilled over a calcium hydride under vacuum and stored over 3Å molecular sieves. Reagents and sorbents included triethylamine, 1,3-dimethoxybenzene, *n*-butylamine (Sigma-Aldrich-Fluka, USA), aminoglycoside antibiotics kanamycin (OAO Biohimik, Saransk, Russia), sisomicin, tobramycin, paromomycin (Minkhimprom, USSR), TLC silica gel aluminum plates (Kieselgel 60 F_{254}) or aluminum oxide plates, silica gel, and alu-

minum oxide (activity I) for column chromatography (Merck, USA).

Equipment and conditions

1D and 2D (COSY, HMBC, HSQC) NMR spectra were recorded at 500 MHz (^{1}H), 125.7 MHz (^{13}C) using the Bruker AC-500 spectrometer and referenced using the residual proton signals of the solvent, DMSO-d_6 (δ_H 2.50 ppm and δ_C 39.7 ppm) or CD_3CN (δ_H 1.94 ppm for ^{1}H and δ_C 1.32 ppm); chemical shifts are given with respect to $SiMe_4$ (^{1}H and ^{13}C). TLC-plates were visualized under a UV lamp at 254 and 360 nm. Mass-spectra were recorded using a Ultraflex II TOF/TOF time-of-flight mass analyzer (Bruker Daltonics, Germany) equipped with a nitrogen laser (wavelength of 337 nm) operating at 50 Hz in the positive ion mode with reflectron. Modified aminoglycoside antibiotics were analyzed and separated with preparative reversed-phase HPLC in the acetonitrile gradient using the Agilent Technologies 1200 Series system and Synergi polar-RP reversed-phase column (4.5 × 250 mm) under the following conditions: flow rate 0.9 ml/min, 15–50% 80% MeCN + 0.1% TFA for 30 min, 50–70% for 20 min, 70–90% for 10 min, 90% for 5 min, and isocratic elution for 5 min. Absorption was monitored at 285 nm. Conversion of compound (**1**) into compound (**2**) was analyzed using HPLC in the acetonitrile gradient using the Agilent 1100 Series device with multiwave diode array detection. The stationary phase was a Waters Symmetry C_8 reversed-phase column. The following conditions were used: flow rate 1 ml/min, acetonitrile gradient – from 50 to 70% for 20 min, from 70 to 98% for 10 min.

For derivatization and dilution of the analytes and matrix compounds, we used acetonitrile (HPLC-grade, JT Baker), methanol (HPLC-grade, Merck), chloroform (HPLC-grade, Merck), and ultrapure water type I obtained using the system Milli-Q (Millipore). The matrixes included 2,5-dihydroxybenzoic, and sinapic and 1-cyano-4-hydroxycinnamic acids (a solution of 20 mg/ml in acetonitrile with addition of 0.1% trifluoroacetic acid). Sample solution (0.5 µl) in a mixture with the matrix solution (0.5 µl) was loaded onto the target plate spot (MTP 384 massive target gold plate T, Bruker Daltonics, Germany) and air dried.

Tris(2,6-dimethoxyphenyl)carbenium hexafluorophosphate (1) [20–22]

A 2.5 M solution of *n*-butyllithium (30 ml, 76 mmol) was added dropwise to a solution of 1,3-dimethoxybenzene (10.0 g, 72.4 mmol) in 100 ml of tetrahydrofuran with stirring under argon and cooling to –20°C. A solution of diethyl carbonate (2.85 g, 24 mmol) in tetrahydrofuran (10 ml) was slowly added 1 h after and stirred at room temperature for 1 day. The solvent was removed under reduced pressure. Diethyl ether (200 ml), dichloromethane (50 ml), and HPF_6 (30 ml) were added to the residue with stirring. After 3 h, the solvent was removed under decreased pressure, triturated with 300 ml of diethyl ether, and precipitated violet crystals were collected to yield compound **1** (31.0 g, 76%). ^{1}H NMR spectrum (CD_3CN, δ_H, ppm): 3.55 (s, 18H, OCH_3), 6.61 (6d, 6H, *J* 8.54 Hz), 7.63 (3t, 3H, *J* 8.54 Hz). Mass-spectrum (MALDI, m/z, CHCA): 423.15.

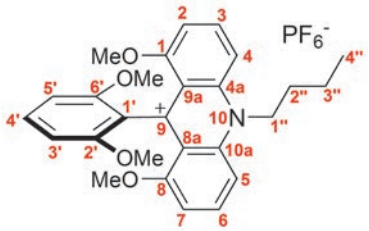

2

1,8-Methoxy-9-(2,6- dimethoxyphenyl)-10-(butyl)acridinium hexafluorophosphate (2)

n-Butylamine (350 µl, 3.52 mmol) was added to a solution of tris(2,6-dimethoxyphenyl)carbenium hexafluorophosphate (**1**) (1.0 g, 1.76 mmol) in acetonitrile (15 ml) with stirring at room temperature under argon. The color of the solution changed from purple to red. After 1 h, the solvent was removed under reduced pressure, the solid precipitate was triturated in diethyl ether, and the resulting red precipitate was filtered off and dried in a desiccator in vacuum to give compound **2** (1.0 g, 98%). ^{1}H NMR spectrum (CD_3CN, δ_H, ppm): 1.15 (t, 3H, *J* 7.3 Hz, H-4''), 1.73–1.80 (m, 2H, H-3''), 2.16–2.22 (m, 2H, H-2''), 3.57 (s, 6H, OCH_3), 3.59 (s, 6H, OCH_3), 5.06–5.09 (m, 2H, H-1''), 6.81 (d, 2H, *J* 8.5 Hz, H-3', H-5'), 7.12 (d 2H, *J* 8.2 Hz, H-2, H-7), 7.45–7.48 (m, 1H, H-4'), 7.93 (d, 2H, *J* 9.2 Hz, H-4, H-5), 8.20–8.24 (m, 2H, H-3, H-6). ^{13}C NMR spectrum (CD_3CN, δ_C, ppm): 12.96 (4''), 19.61 (3''), 29.52 (2''), 52.37 (1''), 55.64 (OCH_3), 56.76 (OCH_3), 103.74 (3', 5'), 106.50 (2, 7), 109.26 (4, 5), 119.67 (1'), 119.89 (9), 129.40 (4'), 139.87 (3, 6), 141.61 (1, 8), 155.79 (2', 6'), 157.18 (8a, 9a), 160.58 (4a, 10a). Mass-spectrum (MALDI, m/z, CHCA): 432.30.

A general procedure for derivatization of amino carbohydrates (aminoglucitol, tobramycin, paromomycin, sisomicin) with tris(2,6-dimethoxyphenyl)carbenium hexafluorophosphate

A relevant amino carbohydrate, 1 eq. in 200 µl of carbonate buffer (pH 9.55), was added to a 0.5 × 10^{-2} M solution of tris(2,6-dimethoxyphenyl)carbenium hexafluorophosphate in acetonitrile (150 µl). The reaction mixture was stirred for 30 min at room temperature. Analysis of the conjugates was carried out directly from the reaction mixture without further purification.

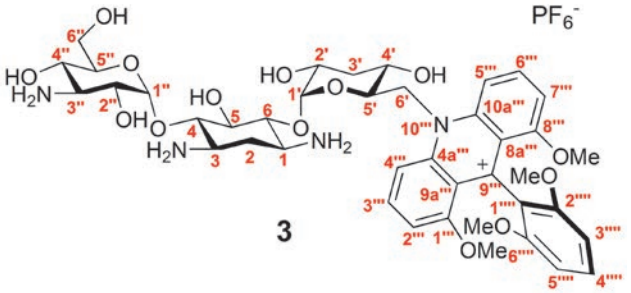

3

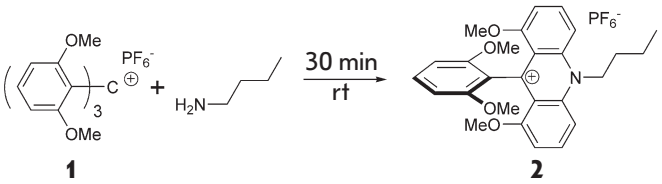

1 2

Fig. 3. Reaction of **1** with *n*-butylamine

1,8-Dimetoxy-9-(2,6-dimethoxyphenyl)-10-(6'-deazakanamycin-6'-il)acridinium hexafluorophosphate (3)

tris(2,6-Dimethoxyphenyl)carbenium hexafluorophosphate (**1**) (2.8 mg, 0.005 mmol) in acetonitrile was added to a solution of kanamycin sulfate (7.8 mg, 0.015 mmol) in 2 ml of buffer solution (pH 9.55). The reaction mixture was kept for 30 min and separated by preparative HPLC. Compound **3** (10.9 mg, 74%) was obtained. ^{1}H NMR spectrum (DMSO-d_6, $\delta_{H,}$ ppm): 1.69–1.72 (m, 1H, H-2), 2.31–2.33 (m, 1H, H-2), 3.17–3.22 (m, 1H, H-3''), 3.36 (m, 1H, H-2'), 3.38 (m, 1H, H-1/H-3), 3.40 (m, 1H, H-4'), 3.45 (m, 1H, H-1/H-3), 3.48 (m, 3H, OCH_3), 3.50 (m, 6H, OCH_3), 3.51 (m, 1H, H-3'), 3.52 (m, 1H, H-6''), 3.53 (m, 1H, H-4''), 3.56 (m, 3H, OCH_3), 3.57 (m, 1H, H4/6), 3.60 (m, 1H, H-6''), 3.66 (m, 1H, H4/6), 3.68 (m, 1H, H-2''), 3.73 (m, 1H, H-5), 3.76 (m, 1H, H-5''), 4.57–4.60 (m, 1H, H-5'), 4.74 (s, 1H, OH), 5.03 (d, *J* 3.7 Hz, 1H, H-1''), 5.26 (s, 1H, OH), 5.32 (m, 1H, H-1'), 5.35 (m, 1H, H-6'), 5.55 (m, 1H, H-6'), 6.49 (m, 1H, OH), 6.79–6.83 (m, 2H, H-3'''', H-5''''), 6.91 (s, 1H, OH), 7.17 (m, 1H, H-2'''), 7.20 (m, 1H, H-7'''), 7.42–7.45 (t, 1H, *J* 8.5 Hz, H-4''''), 8.18 (m, 1H, H-3'''), 8.19 (m, 1H, H-6'''), 8.33–8.35 (m, 1H, H-5'''), 8.45 (m, 1H, H-4'''). ^{13}C NMR spectrum (DMSO-d_6, $\delta_{C,}$ ppm): 27.48 (2), 46.78 (1/3), 49.28 (1/3), 53.34 (6'), 55.32 (3''), 55.87 (OCH_3), 57.06 (OCH_3), 59.49 (6''), 65.28 (4''), 68.39 (2''), 70.49 (5'), 70.94 (5), 70.98 (2'), 72.33 (4'), 72.58 (3'), 73.08 (5''), 80.33 (6/4), 83.46 (4/6), 95.66 (1'), 99.28 (1''), 103.57 (3''''/5''''), 103.79 (3''''/5''''), 106.50 (2'''), 106.75 (7'''), 110.78 (5'''), 111.12 (4'''), 117.60 (1''''), 119.21 (2''''/6''''), 119.30 (2''''/6''''), 129.19 (4''''), 139.08 (3'''), 139.68 (6'''), 142.32 (1'''/8'''), 143.00 (8'''/1'''), 155.65 (9'''), 156.39 (10a'''/4a'''), 158.37 (9a'''/8a'''), 159.63 (8a'''/9a'''), 159.70 (4a'''/10a'''). Mass-spectrum (MALDI, m/z, CHCA): 843.67.

Derivatization procedure of antibiotics mixture

We mixed 10 µl of 0.005 M solutions of every antibiotic (kanamycin, sisomin, tobramycin, and paromomycin) in carbonate buffer (pH 9.55), 100 µl of carbonate buffer (pH 9.55), and 50 µl of a 0.005 M solution of salt **1** in acetonitrile were added. Samples for analysis were taken directly from the reactant mixture.

Experimental evaluation of the pK_{R+} value of compound 2 [21, 22]

A solvent system of H_2O/DMSO/Bu_4NOH with varying proportions of DMSO and water with a constant concentration of tetrabutylammonium hydroxide (Bu_4NOH) was used to assess the pK_{R+} value of compound **2**; its stock solution was added immediately before spectrophotometric measurements. Under strongly basic conditions, the system contains both carbocation R^+ and its respective non-ionic ROH tritanol with maximum absorption at different wavelengths. The obtained absorbance values in the region of the carbocation absorption maximum (λ = 289 nm) were used to calculate the $[R^+]/[ROH]$ ratio. The pK_{R+} value was determined from $\log([R^+]/[ROH])$ using the *H*_ and *C*_ acidity functions, whose values depend on the molar content of DMSO. Taking into account the measurement error, the measured pK_{R+} value was 18.1 ± 0.5.

Quantum chemistry calculations

The structures of the participants of the model transformation mechanism were calculated by the Gaussian-09 [23] software package with a semi-empirical PM3 method with full optimization of the geometric parameters of the molecules of the reactants and products. The subsequent computation of vibrational frequencies according to the standard procedure of the Gaussian-09 package showed that the structures meet the criteria of a stationary point (minima and saddle points at the PES). The calculation results were visualized using the ChemCraft program [24].

RESULTS AND DISCUSSION

The reaction of tris(2,6-dimethoxyphenyl)carbenium hexafluorophosphate with *n*-butylamine was studied in order to determine the optimum conditions for amine functionalization (*Fig. 3*).

The full conversion of the initial substrate **1** into the only product **2** under excess amine was found to be complete in 10 min in acetonitrile at room temperature. Completeness of the conversion is easily monitored by conventional RP-HPLC as compound **2** absorbs in the UV range (*Fig. 4*). The reaction does not require any special conditions.

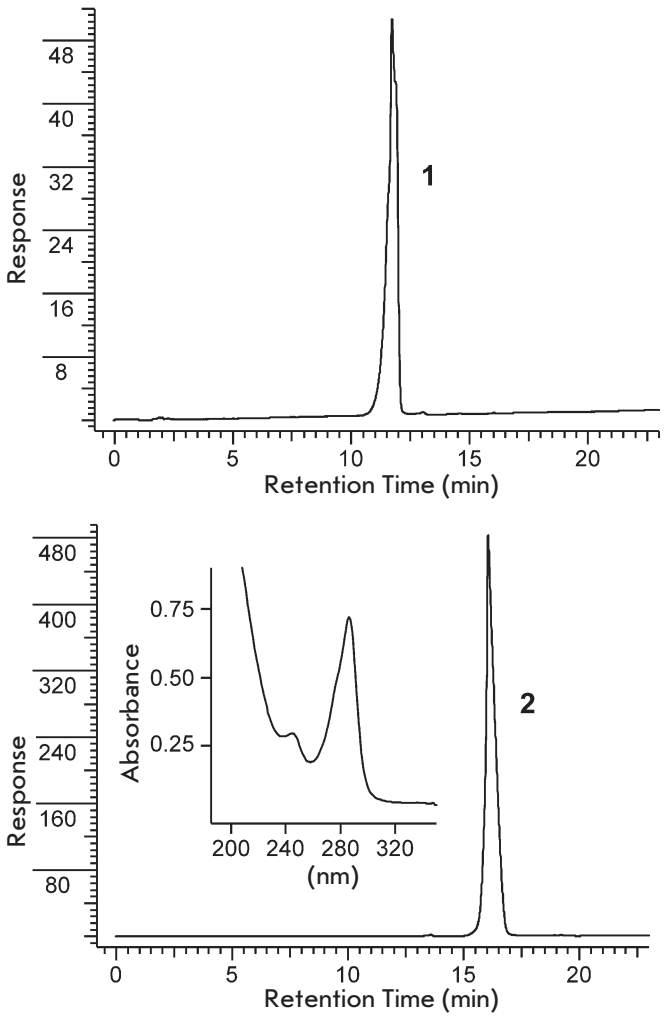

Fig. 4. HPLC profile of initial compound **1** and reactant mixture of **1** with *n*-butylamine. (see Materials and methods section). Inset – absorption specta of **2**

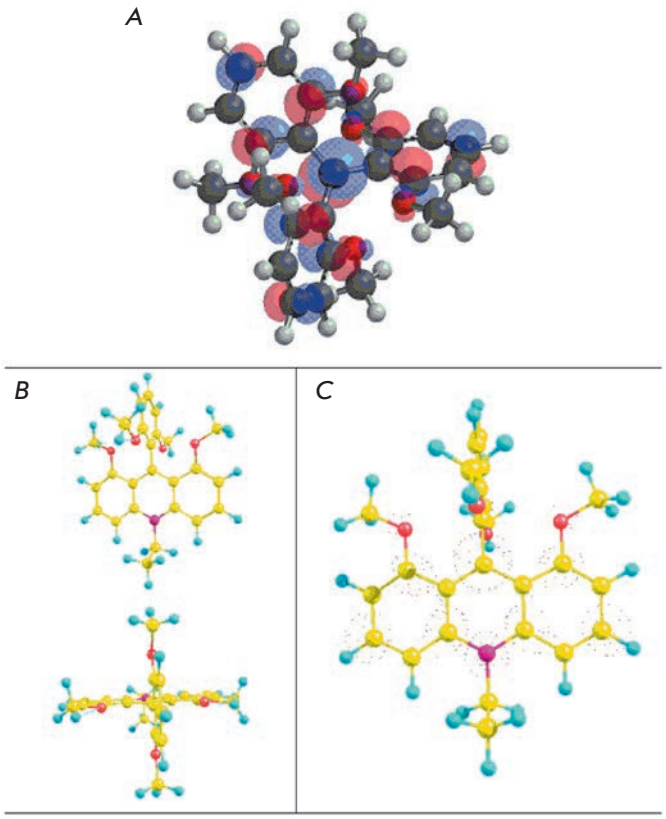

Fig. 5. PM3 method calculated *A* – LUMO configuration of cation **1**; *B* – 3D-stucture of cation **Q$^+$-Et**; *C* – LUMO configuration of cation **Q$^+$-Et.** Carbon atoms – yellow, oxygen atoms – red, nitrogen atoms – pink, hydrogen atoms – turquoise

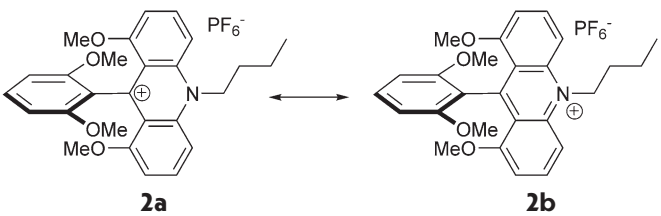

Fig. 6. Resonance structures of compound **2**

The structure of adduct **2** was confirmed by 1D and 2D NMR spectroscopy with complete assignment of signals in the ^{1}H and ^{13}C NMR spectra (see Materials and methods section). The mechanism of compound **2** formation, apparently, involves ipso-attack of the amino group at the ortho-position of a benzene ring followed by elimination of the methoxy group in the form of methanol and repeated nucleophilic substitution on the second ring [21].

In a strongly alkaline medium, the colored cation **2** is able to bind the hydroxide anion to form a colorless tritanol. The pK_{R+} value is a parameter correlating with the stability of the carbocation and corresponding to the pH value at which the concentration of the cationic (colored) form is equal to that of the uncolored form. Based on experimental evaluations, compound **2** has a value of $pK_{R+} \approx 18$, thus indicating the extremely high stability of the cation: the proportion of the cationic form even under mild alkaline conditions is 100%.

Quantum-chemical calculation with a semi-empirical PM3 method shows that cation **1** possesses a propeller-type 3D-structure (*Fig. 5A*). The calculated geometric configuration of cation **2** (with the example of **Q$^+$-Et**) is characterized by a marked positioning of the dimethoxyphenyl group in the plane orthogonal to the acridine fragment and a high degree of symmetry (*Fig. 5B*).

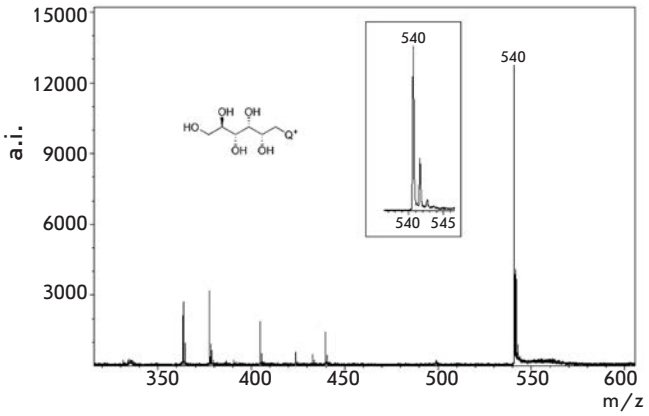

Fig. 7. MALDI specta of conjugate **1** with aminoglucitol (matrix – sinapic acid)

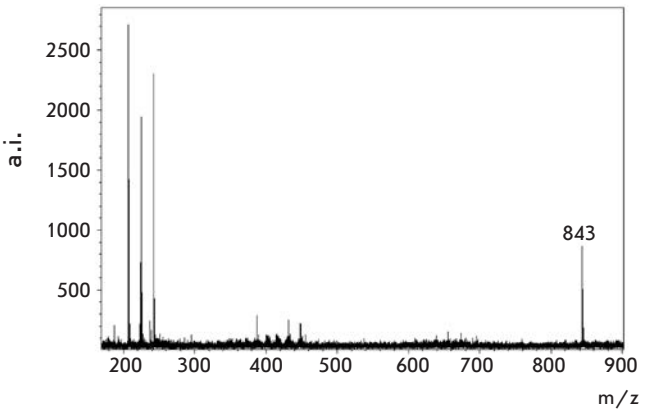

Fig. 9. Peak of conjugate **3** (2×10^{-12} mol of compound per spot) (matrix – sinapic acid) (s/n 47.2)

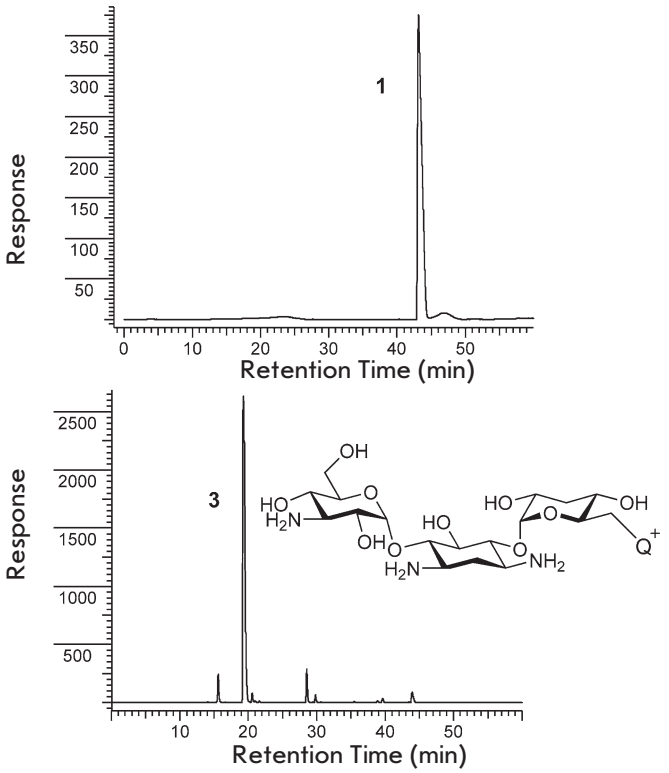

Fig. 8. HPLC profile of compound **1** (top) and conjugate **3** (**1** with kanamycin) (down)

Formal charges were shown to comprise 0.324 at the C-atom and 0.300 at the N-atom of the central ring of the acridine fragment. The calculated LUMO density at the same atoms (*Fig. 5C*) also coincides with this charge distribution. Thus, the positive charge is predominantly localized on the central carbon atom; thus, the resonance structure **2a** better reflects the structure of substances such as **Q^+-R** (*Fig. 6*).

Derivatization of the simplest amino carbohydrate, aminoglucitol, was then studied. Non-derivatized aminoglucitol cannot be detected with MALDI mass spectrometry because of the small molecular weight (181 Da) and poor molecule ionization. TLC monitoring of the original aminoalcohol spot disappearance after subjecting aminoglucitol to an excess amount of the derivatizing agent shows that the reaction is complete within 30 min at room temperature, and the MALDI spectrum demonstrates an explicit signal corresponding to the expected mass of the aminoglucitol conjugate (*Fig. 7*).

We chose the kanamycin, sisomin, paromomycin, and tobramycin antibiotics (*Fig. 1*) to study the aminoglycoside derivatization. Since the most commonly used form of the kanamycin antibiotic is kanamycin sulfate, the sample was dissolved in carbonate buffer (pH 9.55). As in the case of *n*-butylamine, the reaction proceeds with almost complete conversion (*Fig. 8*).

The structure of the aminoglycosides studied differs by the presence of several amino groups, and any of these can be modified. However, the reaction proceeds smoothly and yields one main product (*Fig. 8*), which was separated by preparative RP-HPLC. Analysis of the 2D-NMR spectra of conjugate **3** showed that derivatization occurs selectively on the amino group of the primary carbon atom (see Materials and methods section). Probably, this is due to the higher steric accessibility of this amino group versus the amino groups directly attached to the carbon atoms of six-membered rings and shielded with adjacent hydroxyl groups.

The derivatization product is easy to detect with mass spectrometry: after loading of 2×10^{-12} moles of conjugate **3** per spot, a distinct peak of conjugate **3** with a high

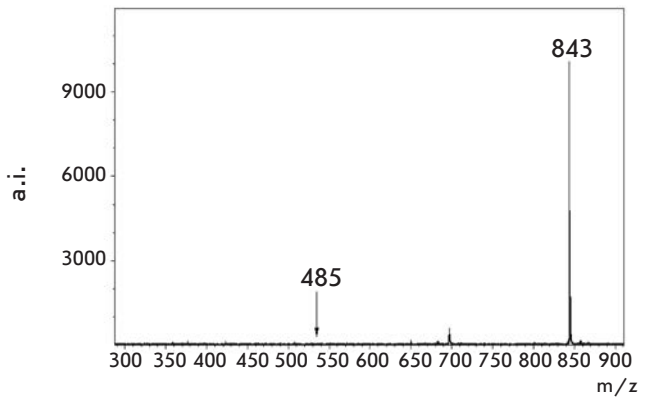

Fig. 10. MALDI specta of equimolar mixture of **3** (m/z 843 (s/n 301.3) and unmodified kanamycin (m/z 485 (s/n 1.8) [M+H$^+$]) (matrix – sinapic acid)

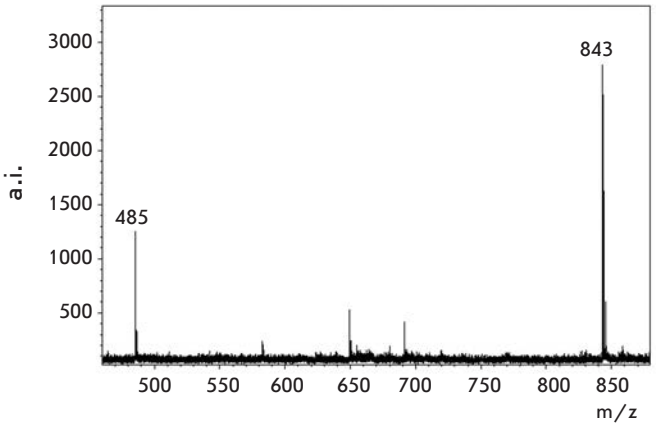

Fig. 11. MALDI specta of mixture kanamycin (m/z 485 (s/n 49.1) [M+H$^+$]) and conjugate **3** (m/z 843 (s/n 89.5)) in ratio 200:1 (0.01M : 0.00005 M) (applied 0.9 μL of every sample) (matrix – CHCA)

signal/noise ratio is observed in the MALDI-MS spectrum (*Fig. 9*). It should be noted that an increase of the conjugate mass by 359 Da shifts the peak to higher values, which eliminates interferences with matrix signals.

With the aim of addressing the effect of derivatization on the detection sensitivity of kanamycin in MALDI-MS, we performed an experiment of simultaneous detection of kanamycin and its derivatization conjugate. *Figure 10* shows the MALDI-MS spectra of an equimolar mixture of conjugate **3** and unmodified kanamycin.

The trityl/acridine derivative peak intensity is so high that it exceeds the unmodified antibiotic peak intensity by at least two orders of magnitude and visually completely dominates. By increasing the ratio of kanamycin/kanamycin-Q$^+$ to 200:1, the signal intensities, becomes similar, but the peak intensity of derivative **3** still exceeds that of the unmodified kanamycin (*Fig. 11*). Thus, Q$^+$derivatization reduces the detection limit of kanamycin in MALDI-MS by several orders of magnitude.

When treating kanamycin with an excess of salt **1**, the product of the reaction remains conjugate **3**: the reactivity of other amino groups is considerably inferior to the activity of the -CH_2NH_2 group. This property was used for simultaneous detection of several aminoglycoside antibiotics by mass spectrometry. A mixture of four antibiotics was treated with an excess amount of salt **1,** and the formed adducts were detected in the MALDI spectrum (*Fig. 12*). Peaks of adducts of kanamycin-Q$^+$ (**3**) (m/z 843, s/n 142.8), sisomicin-Q$^+$ (m/z 806, s/n 166.4), tobramycin-Q$^+$ (m/z 826, s/n 233.2), and paromomycin-Q$^+$ (m/z 974, s/n 56.7) are seen on the spectra.

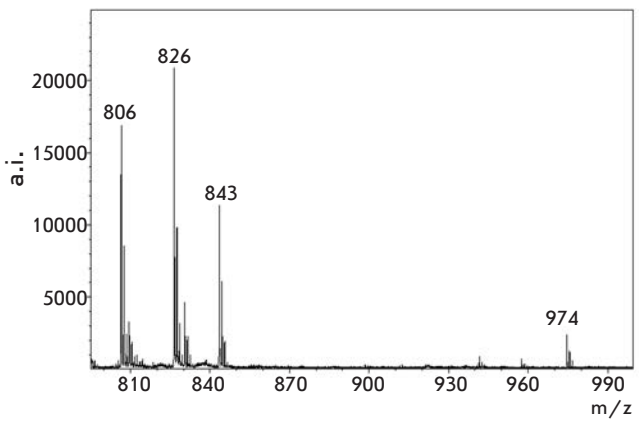

Fig. 12. MALDI specta of mixture of modified antibiotics (matrix – sinapic acid) (see Materials and methods section)

CONCLUISION

The proposed derivatization method of amine carbohydrates makes it possible to detect them with MALDI mass spectrometry and RP-HPLC with UV detection. The modification is shown to occur at the amino group associated with the primary carbon atom. Derivatization enhances the detection sensitivity of aminoglycosides with mass spectrometry by several orders of magnitude. The speed, simplicity, and the availability of reagents are the advantages of the derivatization method. ●

The authors thank N.V. Bovin for providing aminoglucitol and R.S. Borisov for useful discussion.

This work was supported by the Program of the Presidium of RAS "Molecular and cellular biology".

REFERENCES

1. Siegenthaler W.E., Bonetti A., Luthy R. // Am. J. Med. 1986. V. 80. № 6B. P. 2–14.
2. Jackson J., Chen C., Buising K. // Curr. Opin. Infect. Dis. 2013. V. 26. № 6. P. 516–525.
3. Becker B., Cooper M.A. // ACS Chem. Biol. 2013. V. 8. № 1. P. 105–115.
4. Tian Y., Chen G., Guo L., Guo X., Mei X. // Food Anal. Meth. 2015. V. 8. № 7. P. 1842–1857.
5. Farouk F., Azzazy H.M.E., Niessen W.M.A. // Anal. Chim. Acta. 2015. V. 890. P. 21–43.
6. Diez C., Guillarme D., Spörri A.S., Cognard E., Ortelli D., Edder P., Rudaz S. // Anal. Chim. Acta. 2015. V. 882. P. 127–139.
7. Li R., Liu Y., Cheng L., Yang C., Zhang J. // Anal. Chem. 2014. V. 86. № 19. P. 9372–9375.
8. Zengin A., Tamer U., Caykara T. // Anal. Chim. Acta. 2014. V. 817. P. 33–41.
9. Kotova V.Y., Ryzhenkova K.V., Manukhov I.V., Zavilgelsky G.B. // Appl. Biochem. Microbiol. 2014. V. 50. № 1. P. 98–103.
10. Dijkstra J.A., Sturkenboom M.G.G., van Hateren K., Koster R.A., Greijdanus B., Alffenaar J.-W.C. // Bioanalysis. 2014. V. 6. № 16. P. 2125–2133.
11. Li D., He S., Deng Y., Ding G., Ni H., Cao Y. // Bull. Environ. Contam. Toxicol. 2014. V. 93. № 1. P. 47–52.
12. Sharma T.K., Ramanathan R., Weerathunge P., Mohammadtaheri M., Daima H.K., Shukla R., Bansal V. // Chem. Commum. 2014. V. 50. № 100. P. 15856–15859.
13. Bijleveld Y., de Haan T., Toersche J., Jorjani S., van der Lee J., Groenendaal F., Dijk P., van Heijst A., Gavilanes A.W.D., de Jonge R., et al. // J. Chromatogr. B. 2014. V. 951/952. P. 110–118.
14. Korany M.A.-T., Haggag R.S., Ragab M.A., Elmallah O.A. // J. Chrom. Sci. 2014. V. 52. № 8. P. 837–847.
15. Voronezhtseva O.V., Ermolaeva T.N. // Sorbts. Chrom. Prots. 2011, V. 1. № 1. P. 68–76 (in Russian).
16. Levin G.Ya., Sosnina L.N. // Antibiot. Khimioter. 2014. V. 59. № 3/4. P. 10–11 (in Russian).
17. Chen J., Li Z., Ge J., Yang R., Zhang L., Qu L., Wang H., Zhang L. // Talanta. 2015. V. 139. P. 226–232.
18. Wang Y., Ji S., Zhang F., Zhang F., Yang B., Liang X. // J. Chromatogr. A. 2015. V. 1403. P. 32–36.
19. Topolyan A.P., Strizhevskaya D.A., Slyundina M.S., Belyaeva M.A., Ivanova O.M., Korshun V.A., Ustinov A.V., Mikhura I.V., Formanovsky A.A. // Mass-spectrometriya. 2015. V. 12. № 4. P. 253–258 (in Russian).
20. Martin J.C., Smith R.G. // J. Am. Chem. Soc. 1964. V. 86. № 11. P. 2252–2256.
21. Laursen B.W., Krebs F.C. // Chem. Eur. J. 2001. V. 7. № 8. P. 1773–1783.
22. Laursen B.W., Krebs F.C., Nielsen M.F., Bechgaard K., Christensen J.B., Harrit N. // J. Am. Chem. Soc. 1998. V. 120. № 47. P. 12255–12263.
23. Frisch M.J., Trucks G.W., Schlegel H.B., Scuseria G.E., Robb M.A., Cheeseman J.R., Scalmani G., Barone V., Mennucci B., Petersson G.A., et al. // Gaussian, Inc., Wallingford CT, 2009.
24. http://www.chemcraftprog.com/

Minibactenecins ChBac7.Nα and ChBac7.Nβ - Antimicrobial Peptides from Leukocytes of the Goat *Capra hircus*.

O.V. Shamova[1,3], D.S. Orlov[1,3], M.S. Zharkova[1], S.V. Balandin[2], E.V. Yamschikova[1], D. Knappe[4], R. Hoffmann[4], V.N. Kokryakov[1,3], T.V. Ovchinnikova[2*]

[1]Institute of Experimental Medicine, Acad. Pavlov Str. 12, Saint-Petersburg, 197376, Russia

[2]M.M. Shemyakin and Yu.A. Ovchinnikov Institute of Bioorganic Chemistry of the Russian Academy of Sciences, Mikhluho-Maklaya Str. 16/10, Moscow, 117997, Russia

[3]Saint-Petersburg State University, Universitetskaya Emb, 7/9, Saint-Petersburg, 199034, Russia

[4]University of Leipzig, Deutscher Platz 5, D-04103 Leipzig, Germany

*E-mail: ovch@ibch.ru

Received: November 10, 2015; in final form, March 10, 2016

ABSTRACT **Antimicrobial peptides (AMPs) of neutrophils play an important role in the animal and human host defenses. We have isolated two AMPs (average molecular masses of 2895.5 and 2739.3 Da), with potent antimicrobial activity from neutrophils of the domestic goat *(Capra hircus)*. A structural analysis of the obtained peptides revealed that they encompass N-terminal fragments (1–21 and 1–22) of the proline-rich peptide bactenecin 7.5. The primary structure of caprine bactenecin 7.5 had been previously deduced from the nucleotide sequence, but the corresponding protein had not been isolated from leukocytes until now. The obtained caprine AMPs were designated as mini-batenecins (mini-ChBac7.5Nα and mini-ChBac7.5Nβ), analogously to the reported C-terminal fragment of the ovine bactenecin 7.5 named Bac7.5mini [Anderson, Yu, 2003]. Caprine mini-ChBac7.5Nα and mini-ChBac7.5Nβ exhibit significant antimicrobial activity against Gram-negative bacteria, including drug-resistant strains of *Pseudomonas aeruginosa*, *Klebsiella spp.*, *Acinetobacter baumannii* at a range of concentrations of 0.5–4 μM, as well as against some species of Gram-positive bacteria (*Listeria monocytogenes* EGD, *Micrococcus luteus*). The peptides demonstrate lipopolysaccharide-binding activity. Similarly to most proline-rich AMPs, caprine peptides inactivate bacteria without appreciable damage of their membranes. Mini-ChBac7.5Nα and mini-ChBac7.5Nβ have no hemolytic effect on human red blood cells and are nontoxic to various cultured human cells. Therefore, they might be considered as promising templates for the development of novel antibiotic pharmaceuticals. Isolation of highly active fragments of the antimicrobial peptide from goat neutrophils supports the hypothesis that fragmentation of cathelicidin-related AMPs is an important process that results in the generation of potent effector molecules, which are in some cases more active than full-size AMPs. These truncated AMPs may play a crucial role in host defense reactions.**

KEYWORDS **antimicrobial peptides, cathelicidins, mini-bactenecins**

ABBREVIATIONS **AMP – antimicrobial peptide, CEE – continuous elution electrophoresis, CFU – colony forming units, MIC – minimal inhibitory concentration, PBS – phosphate buffered saline, MALDI-TOF MS matrix assisted laser desorbtion/ionization-time of flight mass-spectrometry, MRSA – methicillin resistant Staphylococcus aureus, ONPG – ortho-nitrophenyl β-D-galactopyranoside, PG-1 – protegrin 1, PR-AMP – proline-rich antimicrobial peptide, RP-HPLC – reverse-phase high performance liquid chromatography**

INTRODUCTION

Antimicrobial peptides (AMPs) are cationic molecules contained in leukocytes, barrier epithelial cells, and other cell types, and they are involved in the protection of humans and animals against infectious agents. Along with antimicrobial action, AMPs have other properties, including immunomodulatory activity, which suggest that these compounds can be prototypes for new complex antibiotic drugs. From this perspective, cathelicidin-related AMPs, a large group of peptides widely present in vertebrates, are of particular interest. The peptides of this protein family are generated from precursor proteins by proteolytic cleavage of the N-terminal portion (cathelin-like domain) from the C-terminal region, corresponding to mature AMP. Proteolysis initiates upon activation of neutrophils and barrier epi-

thelial cells during infectious processes. In some cathelicidins, for example human cathelicidin LL-37, mature AMP molecules are also subjected to processing [1], which leads to the formation of fragments with their own specific ranges of biological effects, including antibacterial, antitumor, and other types of activity. A similar proteolytic cleavage of peptides has been also described for ovine bactenecins [2]. It is assumed that the fragmentation of mature AMPs has a biological meaning and that these fragments may play a key role in multiple types of defense response [1, 2].

Among the currently known AMPs, cathelicidins of artiodactyl animas are of special interest due to their high antimicrobial activity and combination of properties, which make these peptides promising for practical application. The peptides isolated from the leukocytes of artiodactyls include the following AMPs: porcine protegrins, PR-39 [3, 4]; bovine bactenecins, BMAP-27 and BMAP-28, dodecapeptide, indolicidin [5–8]; ovine SMAP-29 [9], etc. Some of these peptides have been selected as targets for detailed research aimed at drug design. Interestingly, the neutrophils of some artiodactyls, including goats, contain no defensin-derived AMPs [10], suggesting the crucial role of cathelicidins in the protection of these animals against infections. Thus, the study of the neutrophilic AMPs of artiodactyl animals is important for both a potential discovery of new biologically active molecules, which can serve as templates for new drug design, and for the development of the fundamental concepts of cathelicidin's role in host defense. The present work is aimed at discovering and characterizing new leukocytic AMPs of the domestic goat *Capra hircus*. Previously, we had isolated two peptides, bactenecins ChBac5 and ChBac3.4 [11, 12], from caprine leukocytes. In this paper, other *AMPs* have been studied.

EXPERIMENTAL

Reagents

We used sodium chloride (S9625), tris-(hydroxymethyl) aminomethane (T1503), agarose (Type I, low EEO, A6013) trifluoroacetic (302031) and heptafluorobutyric (52411) acids, o-nitrophenyl-β-galactopyranoside (N1127), MTT (3-(4,5-dimethylthiazol-2-yl)-2,5-diphenyltetrazoliumbromide; M5655), cetyltrimethylammonium bromide (H6269), Sigma, USA; nitrocefin (484400), Calbiochem, USA; acetic acid, ammonium chloride, sodium acetate, Vekton, Russia; fetal calf serum (1.1.8.3.), RPMI-1640 (1.3.4) and DMEM (1.3.5.1.) culture media for cell cultures, Biolot, Russia; Sabouraud culture medium (broth), Research Center of Pharmacotherapy, Russia; Mueller Hinton nutrient broth (M391), HiMedia, India. Chemically synthesized peptides, protegrin 1 provided courtesy of R. Lehrer (University of California, Los Angeles, USA) and bactenecins ChBac5, ChBac5 20-43 and ChBac3.4 provided courtesy of N.I. Kolodkin (State Research Institute of Pure Biochemicals of the Federal Medical and Biological Agency), were used as reference peptides.

Isolation and purification of antimicrobial peptides from leucocytes of the domestic goat

A fraction of white cells enriched with neutrophils was obtained from blood of healthy adult goats (C. hircus). Erythrocyte hemolysis was carried out with an ammonium chloride solution. One liter of whole blood was processed to obtain 2.5 g of leukocytes (wet weight). We used two options of protein extraction. In the first case, the cells were destroyed by homogenization in a 10% acetic acid solution, and the homogenate was suspended with a magnetic stirrer at 4°C for 18–24 h, and then centrifuged at 15,000 *g* for 1 hour. The supernatant was dried and reconstituted in 0.1 M Tris-HCl-buffer, pH 7.5, and incubated at 37°C for 4 hours to digest the cathelicidin precursors. In the second case, the extraction was carried out using a 0.3% cetyltrimethylammonium bromide solution in 0.02 M sodium acetate buffer, pH 4.5. When using this extraction method, we created the conditions for enzymatic reactions as early as during the extraction process. The material resulted from the extraction was ultrafiltered through a YM-10 membrane (NMWCO of 10 kDa) from Amicon (USA) for separation of the low-molecular-weight protein fraction and further concentrated and desalted using ultrafiltration through the YM-1 membrane (NMWCO of 1 kDa). The material containing acid-soluble polypeptides with a molecular weight of less than 10–15,000 Da was placed in a column for electrophoretic separation using preparative continuous elution electrophoresis (CEE) in 12.5% polyacrylamide gel in the acidic buffer system with urea [13], using the Bio-Rad instrument (USA). The fractions with detected antimicrobial activity were collected, and the peptides in these fractions were separated by several consecutive cycles of reverse-phase high-performance liquid chromatography (RP-HPLC) on a Gold System instrument from Beckman (USA) using Vydac C-18 columns (4.6 × 250 mm; sorbent particle size of 5 μm). The purity of the fractions obtained after RP-HPLC was assessed by analytical electrophoresis [14], mass spectrometry, and analytical RP-HPLC. The protein concentration in the purified preparations was determined by the Bradford's method and Wolf's method [15]. The concentration of the solutions of chemically synthesized peptides was calculated on the basis of the weight of the dry peptide powder.

Evaluation of the antimicrobial activity of the peptides

The antimicrobial activity of mini-bactenecins was characterized using two methods: radial diffusion in agarose gel and the broth microdilution method. Microorganism strains were provided courtesy of R. Lehrer (University of California, Los Angeles, USA), A. Tossi (University of Trieste, Italy), E.I. Ermolenko (Institute of Experimental Medicine); members of the Military Medical Academy; G.E. Afinogenov (Vreden Russian Research Institute of Traumatology and Orthopedics, Ministry of Health of the Russian Federation). We used a clinical isolate of *Pseudomonas aeruginosa* resistant to aztreonam, ceftazidime, cefotaxime, a clinical isolate of *Klebsiella spp*. resistant to tetracycline (both strains were obtained from the urine of the patient with cystitis), a clinical isolate of *Acinetobacter baumannii* resistant to meropenem (from an infected wound); a clinical isolate of *Staphylococcus intermedius* (from an infected wound caused by a dog bite) resistant to ciprofloxacin, cefuroxime, clindamycin, erythromycin, rifampin, gentamicin, benzilpenicilin, oxacillin; and a clinical isolate of a yeast-like fungus *Candida parapsilosis* resistant to amphotericin B and clotrimazole (scraping from the nail plate).

The method of radial diffusion in agarose gels. We used the methodology proposed by Lehrer et *al.* [16] and described in detail in [12]. The antibiotic activity of AMPs was quantified by measuring the diameter of the microbial growth inhibition zone around the wells punched in the agarose gel, where the peptides had been applied. The measured values were expressed in units (1 U = 0.1 mm) after subtracting the well diameter (2 mm = 20 U). The minimal inhibitory concentration (MIC) of the AMP was determined by plotting data of the peptides antimicrobial activity vs their concentration using the Sigma Plot 11 software (Systat Software Inc., USA) and calculating the x intercept value of the linear regression plot (peptide concentration in μM), which was taken as the MIC value. Two parallel samples were used in each experiment. The experiments were conducted in triplicate, and the average value of the MIC ± standard deviation was calculated.

The broth microdilution assay. We applied a standard method used in microbiology to test antibiotics, which was slightly modified taking into account the specificity of AMPs [17] according to [12]. The lowest peptide concentration which completely inhibited visible growth of microorganisms in the wells of 96-well plates was taken as MIC. Three parallel samples were tested in each experiment. The results are reported as medians obtained in three to five independent experiments.

Assessment of the effect of peptides on the permeability of the outer and cytoplasmic membranes of *E. coli* ML35p for chromogenic markers

The effect of peptides on the barrier function of membranes of Gram-negative bacteria was studied using the method [18] as revised in [19]. The ML35p strain of *E. coli* is characterized by a lack of lactose permease, constitutive β-galactosidase synthesis in the cytoplasm, and it also contains β-lactamase in the periplasmic space. The state of the outer and cytoplasmic membranes of *E. coli ML35p* cells was assessed based on their permeability to chromogenic markers, nitrocefin, and *o-nitrophenyl-β-D*-galactopyranoside (ONPG), *β*-lactamase and *β*-galactosidase substrates, respectively. Samples were placed in the wells of a 96-well plate according to [12], and the optical density *(OD)* of the solution rising due to the appearance of products of nitrocefin or ONPG hydrolysis was measured at λ = 486 and 420 nm, respectively, using a SpectraMax 250 spectrophotometer (Molecular Devices, USA) at 37°C with regular shaking of the plates for 2 h. The data were processed using the Sigma Plot 11 software.

Estimation of the lipopolysaccharide-binding activity of the peptides

The lipopolysaccharide-binding (lipopolysaccharide-neutralizing) activity of the peptides was studied using the quantitative chromogenic Limulus Amebocyte Lysate test (Lonza Walkersvile, USA). The approaches described by Zhao *et al.* [20] were used to conduct the experiments and analyze the results. The peptides were serially diluted in endotoxin-free acidified water (0.01% acetic acid) and incubated with *E. coli* O111: B4 lipopolysaccharide (LPS) at a final concentration of 0.5 U/ml for 30 min at 37°C in Costar 3596 plates (Corning, USA). We assayed free LPS according to the kit manufacturer's recommendations. The plate was placed in the thermostatic chamber of a SpectraMax 250 spectrophotometer (Molecular Devices, USA) and incubated at 37°C while measuring *OD* of the solution at 405 nm; the difference between the OD values at the beginning of incubation and after 10 min, ΔOD_{405}, was calculated.

The proportion of bound LPS (%) was determined using the formula

$$\% \text{ of bound LPS} = \alpha\,(\text{LPS without peptide}) - \alpha\,(\text{LPS with peptide}) / \alpha(\text{LPS without peptide}),$$

where $\alpha = \Delta OD_{405}$ (peptide (or water) with LPS) - ΔOD_{405} (peptide (or water) without LPS). We constructed the curves representing the relationship between the proportion of bound LPS and the AMP concentration in the incubation medium (Sigma Plot program 11,

Systat Software Inc., USA) and determined EC_{50} (50% effective concentration or peptide concentration corresponding to 50% binding of the LPS).

Analysis of the peptides, hemolytic activity

Red blood cells were isolated from the blood of healthy donors by the standard methods. A red cell pellet was diluted (we assumed that the pellet contained 100% cell suspension) to obtain a 2.8% erythrocyte suspension in phosphate buffered saline (PBS). We placed 27 μl of the erythrocyte suspension and 3 μl of the test peptide (at different concentrations) in PBS or 3 μl of PBS without the peptides (control) to each analyzed sample. The samples (in triplicates) were incubated at 37°C for 30 min, 75 μl of ice cold PBS was added, and then the samples were centrifuged at 5,000 *g* for 4 minutes. Absorbance of the supernatants was measured at λ = 540 nm.

Assessment of the effect of peptides on the viability of cultured cells

The viability of cultured human cells after 20-hour incubation with the peptides was evaluated using the standard MTT assay [21] according to [12]. Cell culturing and separation of neutrophils and mononuclear cells of peripheral blood from healthy donors was carried out using standard methods.

Mass Spectrometry

The molecular masses of the isolated peptides were determined on the MALDI-TOF mass spectrometer Reflect III (Bruker, Germany) equipped with a UV-laser with a wavelength of 336 nm. We used 2,5-dihydroxybenzoic acid (Sigma, Germany) in 20% acetonitrile, 0.1% TFA at a concentration of 10 mg/ml as a matrix. Average molecular masses are shown.

Sequencing

The amino acid sequence was determined using the Procise cLC 491 protein sequencing system (Applied Biosystems, USA). Phenylthiohydantoic derivatives of the amino acid residues were identified on a 120A PTH analyzer (Applied Biosystems, USA).

Synthesis of mini-bactenecins

Mini-ChBac7.5Nα and mini-ChBac7.5Nβ were synthesized using solid phase synthesis and the Fmoc/tBu-strategy on a Syro2000 peptide synthesizer (MultiSynTech GmbH, Germany) [22]. After completion of the synthesis, the peptides were removed using a mixture containing 5% water, 4% of m-cresol, 5% of thioanisole, and 2% of ethanedithiol in TFA at room temperature for 4 hours, cooled and precipitated with diethyl ether. Synthesized peptides were purified on Äkta HPLC (Amersham Bioscience GmbH, Germany) using Jupiter C18 column (20 mm × 250 mm, Phenomenex Inc., USA) with a linear gradient of acetonitrile with 0.1% TFA. The molecular masses of the peptides were confirmed using MALDI-TOF-MS, and purity was confirmed using RP HPLC

Statistical analysis

When determining AMP cytotoxic activity for human cells, the statistical significance of the differences between the experimental and control groups was evaluated according to the Student's *t-test* ($p < 0.05$), $n = 6$ using the Prism 5 software (GraphPad software Inc., USA).

RESULTS

Isolation and purification of new antimicrobial peptides from caprine leukocytes

We isolated the peptides under conditions that enabled the processing of cathelicidin precursors, resulting in the release of mature AMPs. Preparative continuous elution electrophoresis (CEE) was used to separate cationic peptides obtained after the ultrafiltration of caprine leukocyte extracts through the YM-10 membrane. Fractions were analyzed by measuring solution absorbance at 280 nm and evaluating antimicrobial activity by the radial diffusion method *(Fig.* 1A). The fractions 17–24 contained components with the highest electrophoretic mobility toward the cathode, peptides with a molecular weight ranging from 2.8 to 6 kDa, and possessing antimicrobial activity (peak 1). Peaks 2 and 3 comprised the bactenecins ChBac3.4 and ChBac5 *(Fig. 1A)*.

Successive RP-HPLC cycles using various counterions were employed to obtain individual peptides eluting in fractions, corresponding to peak 1. *Figure 1B* shows the results obtained during the first step of chromatographic separation of the peptides contained in the pooled fractions 19–24. Antimicrobial activity was found in the fractions shown by arrows ($24–26^{th}$ minutes) and containing two peptides with average molecular masses of 2895.5 and 2739.3 Da. The peptides were separated by re-chromatography using heptafluorobutyric acid as a counterion *(Fig. 1C)*. We obtained individual peptides (and denominated them mini-bactenecins) eluating from the column in fractions corresponding to the peaks shown by arrows on the chromatogram: peptides with average molecular masses of 2895.5 Da, mini-ChBac7.5Nα, and 2739.3 Da, mini-ChBac7.5Nβ.

The analysis of the primary structure of the isolated AMPs showed that both peptides are N-terminal fragments of caprine bactenecin 7.5. Information about the structure of the latter was previously obtained by gene

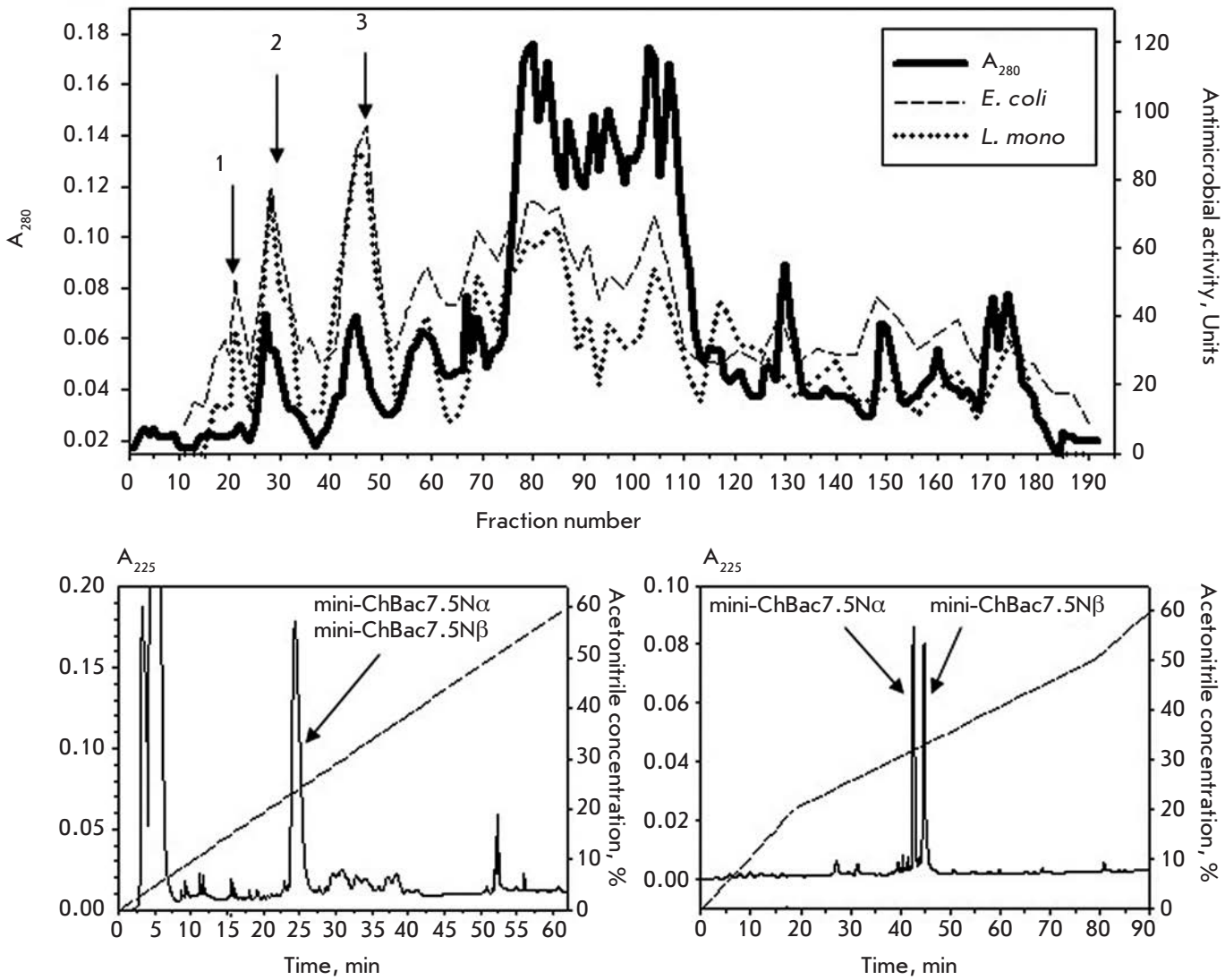

Fig. 1. Purification of antimicrobial peptides from extracts of goat leukocytes. A – Preparative continuous elution electrophoresis (CEE) of YM10 ultrafiltrate of goat leukocyte extract in a polyacrylamide gel (current strength 30 mA, flow rate 36 ml/h, fraction volume 3 ml). Peak 1 – fractions of peptides with a molecular mass of 2.8 – 6 kDa, containing mini-bactenecins; peak 2 – ChBac3.4; peak 3 – ChBac5. CEE fractions were tested for antimicrobial activity against *Listeria monocytogenes* EGD and *E.coli* ML35p in radial diffusion assays (right X axis – antimicrobial activity units). B – RP-HPLC of CEE fractions 19–24, using a linear gradient of acetonitrile (0–60%; 1%/min; 0.1% trifluoroacetic acid) on the Vydac C18-column (0.46 x 25 cm). C – RP-HPLC of fractions 24–26 obtained after RP-HPLC is shown on panel B (acetonotrile gradient: 0–20% during 20 min, 20–50% during 60 min, 50–60% during 10 min, 0.13 % heptafluorobutyric acid). Peaks of peptides with average molecular masses of 2895.5 Da and 2739.3 Da designated as mini-ChBac7.5Nα and mini-ChBac7.5Nβ are shown by arrows.

cloning and represented in the database (Q9XSQ9, (Q9XSQ9_CAPHI) UniProtKB /23], but the corresponding protein has not been isolated from leukocytes *(Fig. 2)*. Isolation of the fragment of ovine bactenecin 7.5 (a peptide structurally similar to caprine bactenecin 7.5) was described: however, this molecule comprised the C-terminal portion of bactenecin 7.5 [2]. Given that this peptide was designated as OaBac7.5mini, we similarly named our peptides mini-ChBac7.5Nα and β. The additional letter N indicates that these are N-terminal fragments (Ch stands for the abbreviation *C. hircus*, domestic goat).

The procedure of isolation and purification was repeated in several series of experiments, resulting in the

mini-ChBac7.5Nα	RRLRPRRPRLPRPRPRPRPRPR
mini-ChBac7.5Nβ	RRLRPRRPRLPRPRPRPRPRP
ChBac7.5	RRLRPRRPRLPRPRPRPRPRPRSLPLPRPQPRRIPRPILLPWRPPRPIPRPQPQPIPRWL
BtBac7	RRIRPRPPRLPRPRPRPLPFPRPGPRPIPRPLPFPRPGPRPIPRPLPFPRPGPRPIPRP
OaBac7.5	RRLRPRRPRLPRPRPRPRPRPRSLPLPRPQPRRIPRPILLPWRPPRPIPRPQPQPIPRWL
OaBac7.5mini	RRIPRPILLPWRPPRPIPRPQPQPIPRWL
ChBac5	RFRPPIRRPPIRPPFNPPFRPPVRPPFRPPFRPPFRPPIGPFP*
ChBac3.4	RFRLPFRRPPIRIHPPPFYPPFRRFL*

Fig. 2. Amino acid sequences of the antimicrobial peptides isolated from goat leukocytes, mini-ChBac7.5Nα and ChBac7.5Nα-β, compared to the previously reported sequences of bactenecins: bovine Bac7 (BtBac7; diverse amino acid residues are underlined) [4], ovine OaBac7.5 [7] and OaBac7.5mini [2], caprine ChBac5 [11] and ChBac3.4 [12]. The structure of the full-size caprine ChBac7.5 is shown. * – amidated C-terminus of the molecule.

same fractions of mini-bactenecins. The abovementioned data were obtained using material where proteins were extracted with 10% acetic acid. Mini-bactenecins were also detected when extracting proteins with a detergent: cetyltrimethylammonium bromide. Protease inhibitors were not used, since mature forms of cathelicidins-derived AMPs could not be obtained in this case.

Thus, new peptides, N-terminal fragments of bactenecin 7.5, were for the first time isolated from goat leukocytes. We have not detected the full-length bactenecin 7.5. Probably, it mostly succumbed to proteolytic cleavage.

Antimicrobial activity of mini-bactenecins

The antimicrobial activity of mini-bactenecins obtained by chemical synthesis was analyzed using two methods: radial diffusion in agarose gel (RD) and the broth microdilution assay *(table)*. When assessing the activity of bactenecins by RD, the peptides were incubated with microorganisms under different conditions: in a medium with low ionic strength (0.01 M sodium phosphate buffer, pH 7.4, without other salts added) and in the same medium but supplemented with 100 mM sodium chloride.

It was reported that the currently known proline-rich AMPs (PR-AMPs) have high antimicrobial activity against Gram-negative bacteria and decreased activity against most Gram-positive bacteria, particularly staphylococci [24]. We have shown that, in a medium with a low ionic strength, mini-bactenecins demonstrate a broad spectrum of antimicrobial activity and high activity against both Gram-negative and Gram-positive bacteria, including staphylococci, and against fungus *C. albicans (Table)*. However, an increase in the medium ionic strength results in reduced AMP activity against both staphylococci and *C. albicans*. In the case of Gram-negative bacteria, the relationship between the activity of mini-bactenecins and the ionic strength of the medium is less pronounced.

The study of the antimicrobial action of the peptides in broth microdilution assay *(Table)* revealed a high activity of mini-bactenecins against Gram-negative bacteria, including strains resistant to some antibiotics used in clinical practice: *P. aeruginosa* (resistant to aztreonam, ceftazidime, cefotaxime), *Klebsiella spp.* (resistant to tetracycline), *A. baumannii* (resistant to meropenem); MIC 2–4 μM. The peptides demonstrated pronounced activity against Gram-positive bacteria *Listeria monocytogenes* and *Micrococcus luteus*, but their antimicrobial activity against staphylococci and fungi from the genus *Candida* was negligible at concentrations ranging from 1 to 64 μM.

The effect of AMPs on the permeability of the outer and cytoplasmic membranes of *E. coli* ML35p for chromogenic markers

One of the most important objectives in studying the functional properties of AMPs is to identify the main target of their antimicrobial action. Bacterial membranes are targets for most AMPs. Peptides cause their rapid and irreversible disintegration. However, some AMPs, including PR-AMPs, mostly alter intracellular processes in bacterial cells and damage their membranes only at concentrations highly exceeding MIC [25]. We studied the effect of mini-bactenecins on the permeability of the outer and cytoplasmic membranes of *E. coli* ML35p. *Fig. 3* shows the kinetics of the action of mini-ChBac7.5Nα at concentrations of 0.6-20 μM on the membranes of *E. coli* ML35p. Caprine bactenecin ChBac3.4 (5 μM, which is 2 times higher than MIC) was used as a reference peptide, and the porcine membrane-active peptide protegrin 1 (PG-1) was used as a positive control. The action of mini-bactenecin results in increased permeability of the bacterial outer membrane to the chromogenic marker almost over

Antimicrobial activity of caprine mini-bactenecins: minimal inhibitory concentrations (MIC, μM) obtained by two methods

	mini-ChBac7.5Nα			mini-ChBac7.5Nβ		
	Radial diffusion assay in agarose gel MIC (μM)*		Broth microdilution assay MIC (μM)**	Radial diffusion assay in agarose gel MIC (μM)*		Broth microdilution assay MIC (μM)**
	without NaCl	100 mM NaCl	Broth***	NaCl	100 mM NaCl	Broth***
E.coli ML35p	0.3 ± 0.1	1.5 ± 0.2	1	0.3 ± 0.1	1.4 ± 0.2	1
E.coli ATCC 25922	0.6 ± 0.1	0.9 ± 0.2	2	0.5 ± 0.2	0.8 ± 0.2	2
E.coli M17	0.5 ± 0.1	0.8 ± 0.1	2	0.5 ± 0.1	0.9 ± 0.2	1
Pseudomonas aeruginosa ATCC 27853	1.1 ± 0.4	3.7 ± 1.2	2	1.0 ± 0.3	3.2 ± 0.8	2
Pseudomonas aeruginosa clinical isolate	ND	ND	2	ND	ND	2
Klebsiella spp. clinical isolate	ND	ND	4	ND	ND	4
Acinetobacter baumannii clinical isolate	ND	ND	2	ND	ND	4
Listeria monocytogenes EGD	0.2 ± 0.1	1.0 ± 0.2	2	0.2 ± 0.1	0.9 ± 0.2	2
Micrococcus luteus CIP A270	ND	ND	1	ND	ND	1
Staphylococcus aureus 710A	0.7 ± 0.2	> 50	> 64	0.6 ± 0.1	> 50	> 64
Staphylococcus aureus ATCC 25923	ND	ND	> 64	ND	ND	> 64
MRSA ATCC 33591	0.7 ± 0.2	> 50	> 64	0.5 ± 0.1	> 50	> 64
Staphylococcus intermedius clin. isolate	ND	ND	> 64	ND	ND	> 64
Candida albicans 820	0.3 ± 0.1	> 50	64	0.3 ± 0.1	> 50	> 64
Candida parapsilosis clinical isolate	ND	ND	> 64	ND	ND	> 64

*data are shown as mean values ± S.D. (n = 6). Radial diffusion assay was performed under the following conditions: low salt (10 mM phosphate buffer, pH 7.4) and high salt (10 mM phosphate buffer + 100 mM NaCl, pH 7.4).
**data are shown as medians derived from 3–5 experiments performed in triplicates.
***Mueller-Hinton broth for bacteria or Sabouraud broth for fungi.
ND – not determined.

the entire investigated concentration range, although in the case of PG-1 (2.5 μM, which is 2 times higher than MIC) this effect is more pronounced. However, the studied peptide from caprine leukocytes has no significant impact on the permeability of the cytoplasmic membrane of *E. coli* to marker molecules. Only at high peptide concentrations (10 and 20 μM), which are significantly higher than MIC (1-2 μM), the results slightly differ from the control values without AMPs. Unlike mini-bactenecin, the effect of ChBac3.4 occurs at a concentration which is only twofold higher than MIC. In the case of the second mini-bactenecin, mini-ChBac7.5Nβ, the results were almost identical for mini-ChBac7.5Nα (data not shown). These findings suggest that bacterial membranes are not the main target of the mini-bactenecins under study, as well as other known PR-AMPs. It is likely that they can bind to the DnaK chaperone, similarly to the bovine Bac7 and ovine OaBac7.5 fragments, and modulate its ATPase activity, disturbing the protein folding process in the cell [25, 26], or interact with the 70S ribosome, impairing the translation process, as shown for apidaecins, oncocins, and the bovine Bac7 fragment 1–35 [27, 28]. Just like the fragment 1–35 of bovine Bac7, which affected the cytoplasmic membrane of *E. coli* ML35p at concentrations several times higher than MIC [24], mini-bactenecins affect the permeability of the inner membrane of this bacterium only at concentrations 10- to 20-fold higher than MIC.

The lipopolysaccharide-binding activity of caprine mini-bactenecins

Binding to lipopolysaccharide (LPS), the component of the outer membrane of Gram-negative bacteria, is one of the essential properties of AMPs, because the capacity of that binding largely determines the subsequent effectiveness of the antimicrobial action of peptides. In the development of pharmaceuticals based on AMPs, special attention is focused not only on antimicrobial properties, but also on the LPS-binding (neutralizing) activity, taking into account the need to obtain a compound which could both contribute to the inactivation of pathogenic microorganisms and prevent or eliminate the consequences of septic shock caused by Gram-negative bacteria, a serious complication of infectious diseases, often with a lethal outcome. Nu-

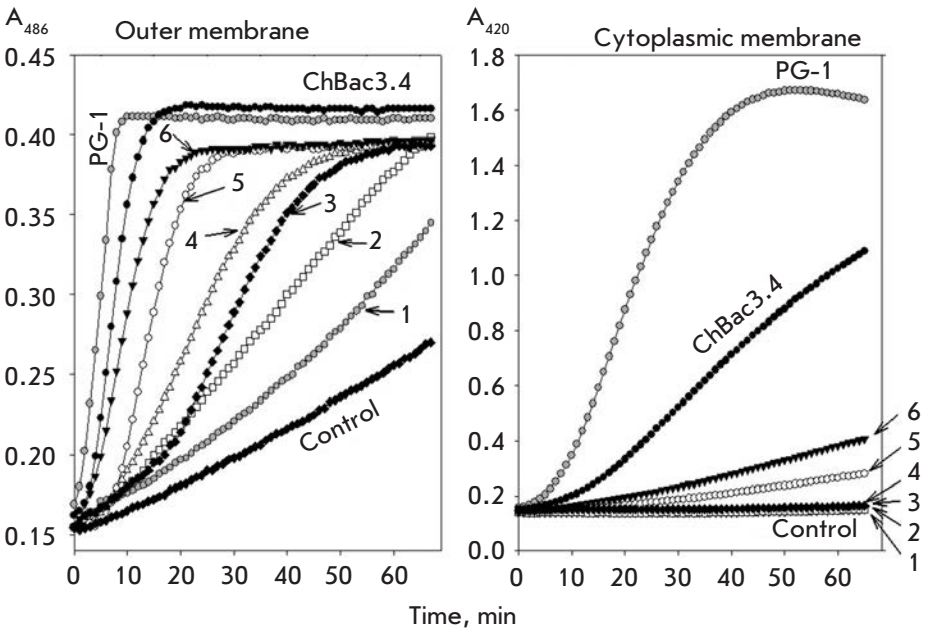

Fig. 3. Kinetics of changes in *Escherichia coli* ML-35p membrane permeability with respect to chromogenic markers resulting from incubation of bacteria with mini-ChBac7.5Nα taken in various concentrations: 1 – 0.6 μM; 2 – 1.2 μM; 3 – 2.5 μM; 4 – 5 μM; 5 – 10 μM; 6 – 20 μM. x-axis – incubation time, min. y-axis – optical density of the solution containing chromogenic markers: nitrocefin hydrolysis product at a wavelength of 486 nm (left panel displaying the outer membrane permeabilization) and ONPG hydrolysis product, o-nitrophenol, at 420 nm (right panel displaying the inner membrane permeabilization). Another caprine bactenecin, ChBac3.4, was used as a reference (at a final concentration of 5 μM, which is 2 x MIC); a membranolytic peptide, porcine protegrin 1 (PG-1), was used as a positive control (2.5 μM).

merous recent publications provide a comprehensive analysis of the relationship between the structural features of the peptides that are used as drug prototypes and their antimicrobial action, selectivity with respect to prokaryotic cells, and LPS-neutralizing properties. It has been shown that the LPS-neutralizing activity of a peptide depends on the hydrophobicity/net positive charge ratio of its molecule [29]. We measured the LPS-binding activity of mini-bactenecins by determining the effective concentration when 50% of LPS (LPS of *E. coli* O111:B4*)* is bound to the peptide [20]. As a reference, we provide the results obtained for other AMPs from goat leukocytes, namely bactenecins ChBac3.4, ChBac5, and the peptide with low antimicrobial activity, the chemically synthesized C-terminal region (residues 20–43) of ChBac5 bactenecin (ChBac5 20-43). Polymyxin B, known as a compound with high affinity to LPSs, was used as a positive control *(Fig. 4)*. Mini-bactenecins are characterized by significantly higher values of this activity compared to ChBac5 20–43, although they are somewhat inferior to the bactenecins ChBas3.4 and ChBac5, which can be explained by the higher net positive charge and lower hydrophobicity of mini-bactenecin molecules compared to ChBas3.4 and ChBac5 *(Fig. 4)*. Mini-ChBac7.5Nα contains 12 arginine residues and only two leucine residues (mini-ChBac7.5Nβ contains 11 arginine residues and 2 leucine residues). Furthermore, mini-bactenecins do not contain aromatic amino acid residues, which (in particular tryptophan residues) are believed to enhance LPS-neutralizing activity [30]. On the contrary, ChBac3.4 and ChBac5 contain a relatively large amount of aromatic amino acid residues, mainly phenylalanine. These data provide valuable information for analyzing the patterns of the various types of biological activity of AMPs and point to the possibility of a development of antibiotic drugs based on mini-bactenecins by designing their analogues containing a larger number of hydrophobic amino acid residues, in particular tryptophan.

The action of mini-bactenecins in mammalian cells

It is known that most PR-AMPs have no pronounced toxicity with respect to mammalian cells [25]. Evaluation of the hemolytic activity of mini-bactenecins toward human erythrocytes shows that, at concentrations of 1–100 μM, both peptides have no pronounced effect on red blood cells. The values of samples containing specified concentrations of the peptides did not differ significantly from those of the control samples containing no AMPs ($p > 0.05$, Student's t-test, $n = 9$).

We assessed the effect of mini-bactenecins at a concentration of 1–30 μM on human cells using the MTT assay. It was found that the peptides have low cytotoxic activity against various types of cultured human cells: namely, erythroleukemia K-562 cells, histiocytic lymphoma U-937 cells, promyelocytic leukemia HL-60, epithelioid lung carcinoma A-549, epidermoid carcinoma A-431, human osteosarcoma MG-63, as well as normal human skin fibroblasts, human embryonic

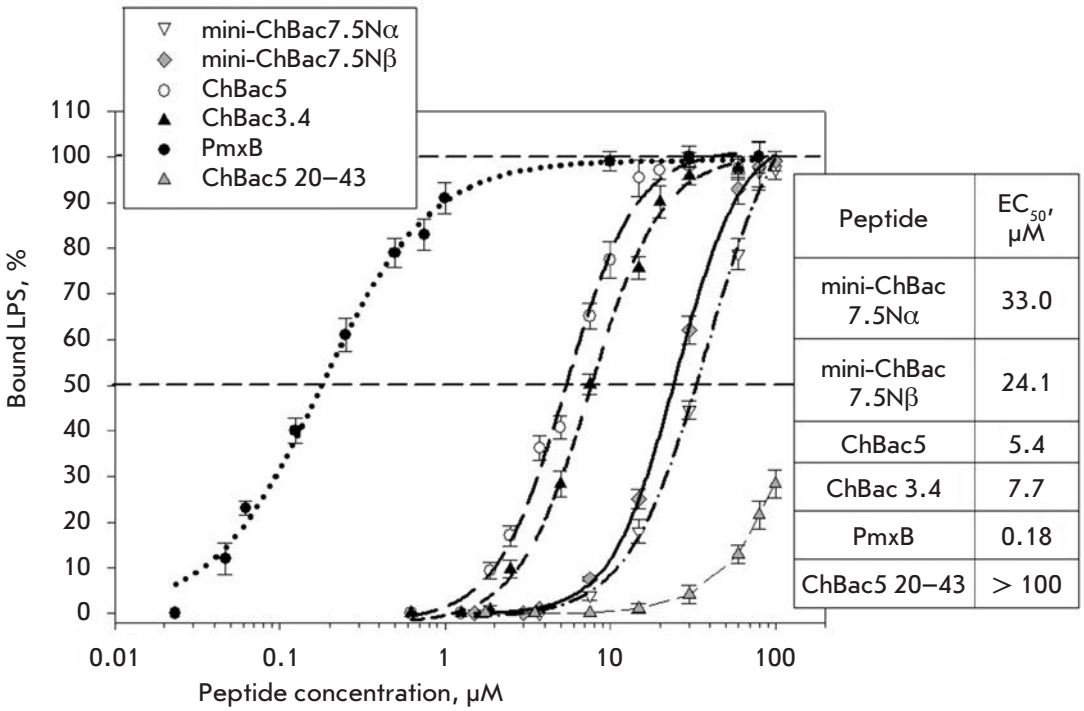

Peptide	EC_{50}, μM
mini-ChBac 7.5Nα	33.0
mini-ChBac 7.5Nβ	24.1
ChBac5	5.4
ChBac 3.4	7.7
PmxB	0.18
ChBac5 20–43	> 100

Fig. 4. Binding of *E.coli* lipopolysaccharide by mini-ChBac7.5Nα and mini-ChBac7.5Nβ as compared with caprine bactenecins ChBac3.4, ChBac5 and its inactive fragment ChBac5 (20-43) in a quantitative chromogenic *Limulus Amebocyte Lysate* Assay. Polymyxin B (PmxB) was used as a positive control. Mean values ± S.D., n=6 are shown. EC_{50} (i.e., peptide concentrations that bound 50% of the LPS) are shown in the inset.

lung fibroblasts MRC-5, and neutrophils and mononuclear cells of human peripheral blood. The cytotoxicity values obtained after 24 h of incubation with peptides were not significantly different from the values calculated for the control samples containing no peptide over the entire range of concentrations: 1–30 μM ($p > 0.05$, Student's t-test, $n = 9$). These data are indicative of the fact that the action of caprine mini-bactenecins is selective with respect to microbial cells, which is consistent with observations showing a low toxicity of N-terminal fragments 1–16, 1–23, 1–35 of bovine Bac7 toward mammalian cells [24].

DISCUSSION

We isolated two antimicrobial peptides, the mini-bactenecins mini-ChBac7.5Nα and mini-ChBac7.5Nβ, from leukocytes of the domestic goat *C. hircus*. They are N-terminal fragments of the ChBac7.5 peptide, which were for the first time obtained from blood cells by us. Several fragments of OaBac11, OaBac5, and OaBac7.5 bactenecins had been previously isolated from ovine leukocytes [2]. The C-terminal fragment (32–60) of OaBac7.5, isolated by Anderson *et al.* [2] and designated as OaBac7.5mini, showed relatively low antibacterial activity [31] compared to the activity of the N-terminal fragments of goat bactenecin 7.5. Caprine mini-bactenecins are structurally similar to the N-terminal part of bovine Bac7 [5] *(Fig. 2)*. An N-terminal region of the bovine Bac7 molecule (at least 16 amino acid residues) [24], whose length approximately corresponds to the peptides isolated by our group, is required for any antimicrobial activity by this bactenecin. The C-terminal fragments of bovine Bac7 had a low antimicrobial activity [24]. The N-terminal sequences of the molecules of caprine and ovine bactenecin 7.5, as well as bovine bactenecin 7, are structurally similar, whereas the C-terminal regions are substantially different. Discovery of the fragments of ovine bactenecins 7.5 [2] and caprine mini-bactenecins suggests that the peptides, formed after the fragmentation of the parent bactenecin molecules, perform the main protective functions: N-terminal derivatives execute an antimicrobial action, while C-terminal fragments may play a different role which remains unclear.

The importance of a fragmentation of mature AMP forms, including regulation of their biological effects in the course of an infectious process, was assumed when studying the proteolytic cleavage of human cathelicidin LL-37. Cleavage of this peptide results in the formation of fragments, some of which have a higher antimicrobial activity than full-length LL-37 [1, 32]. However, it was found that, along with potent antimicrobial effects, the immunomodulatory activity of these peptides is reduced compared to the full-length cathelicidin [32]. The pattern of cathelicidin fragmentation depends on many factors, but mostly on the activity of the proteases involved in its processing and on the activity of their inhibitors [1]. These factors, in turn, depend on the parameters determined by the microenvironment, which can vary during infectious or other pathological pro-

cesses. Therefore, the fragmentation of human cathelicidin may be considered as one of the mechanisms of precise and multifaceted regulation of the functional activity of AMPs. On the other hand, investigation of the biological activity of peptide fragments informs the development of various antibacterials, as well as antitumor peptide pharmaceuticals, LL-37 derivatives, which are regarded as promising templates for new drugs.

Other antimicrobial polypeptides are also subjected to fragmentation. Their cleavage produces truncated forms having a pronounced bactericidal activity. For example, processing of lactoferrin, a component of specific neutrophilic granules, generates the antimicrobial peptide lactoferricin, which is considered as a compound that plays an independent role in the biological defensive functions of neutrophils [33]. Fragments of histones that have antimicrobial activity and are expected to provide a protective effect were isolated from the leukocytes and skin of some fish and amphibians [34, 35].

The enzymes that can perform the corresponding processing of PR-AMPs, in particular caprine bactenecin 7.5, are of great interest. It can be assumed that this process involves several different proteases and that cleavage may consist of several stages. In the case of mini-ChBac7.5Nβ, prolyl endopeptidase (PREP [EC 3.4.21.26]) or prolyl carboxypeptidase (PRCP [EC 3.4.16.2]) could be one of these enzymes. They cleave the peptide bond between the arginine and proline residues (in the ChBac7.5 molecule presumably between the proline 21 and arginine 22 residues). These proteases are present in neutrophilic granulocytes and have been shown to play an important role in inflammatory responses [36]. Further investigation using different types of protease inhibitors will shed light on this issue.

CONCLUSION

Isolation of highly active antimicrobial peptides comprising N-terminal fragments of bactenecin 7.5 (we call them mini-bactenecins: mini-ChBac7.5Nα and mini-ChBac7.5Nβ) from the leukocytes of domestic goat supports the idea that fragmentation of antimicrobial peptides of the innate immune system is an important requirement for the triggering and regulation of protective responses in the course of inflammatory or infectious processes. We have shown that mini-bactenecins exert a potent antimicrobial activity against Gram-negative bacteria, including antibiotic-resistant strains, posses lipopolysaccharide-binding activity, and are non-toxic toward cultured human cells. The obtained data point to the prospectivity of further investigations of the antimicrobial activity of these compounds on a wider spectrum of microorganisms in order to prove the possibility of developing new antibacterial pharmaceuticals on their basis. ●

This work was supported by a grant from the Federal Target Program Research and development on priority directions of the scientific and technological complex of the Russian Federation for 2014–2020 (agreement No 14.604.21.0104). Unique identifier RFMEFI60414X0104.

REFERENCES

1. Yamasaki K., Schauber J., Coda A., Lin H., Dorschner R., Schechter N., Bonnart C., Descargues P., Hovnanian A., Gallo R.L. // FASEB J. 2006. V. 20. № 12. P. 2068–2080.
2. Anderson R., Yu P.L. // Biochem. Biophys. Res. Commun. 2003. V. 312. P. 1139–1146
3. Kokryakov V.N., Harwig S.S., Panyutich E.A., Shevchenko A.A., Aleshina G.M., Shamova O.V., Korneva H.A., Lehrer R.I. // FEBS Lett. 1993. V. 327. P. 231–236.
4. Agerbert B., Lee J.Y., Bergman T., Carlquist M., Boman H.G., Mutt V., Jörnvall H. // Eur. J. Biochem. 1991. V. 202. P. 849–854.
5. Gennaro R., Skerlavaj B., Romeo D. // Infect. Immun. 1989. V. 57. P. 3142–3146.
6. Skerlavaj B., Gennaro R., Bagella L., Merluzzi L., Risso A., Zanetti M. // J. Biol. Chem. 1996. V. 271. P. 28375–28381.
7. Romeo D., Skerlavaj B., Bolognesi M., Gennaro R. // J. Biol. Chem. 1988. V. 263. P. 9573–9575.
8. Selsted M., Novotny M., Morris W., Tang Y., Smith W., Cullor J. // J. Biol. Chem. 1992. V. 267. № 7. P. 4292–4295.
9. Huttner K.M., Lambeth M., Burkin H., Burkin D., Broad T. // Gene. 1998. V. 206. P. 85–91.
10. Zhao C., Nguen T., Liu L., Shamova O., Brogden K.A., Lehrer R.I. // Infect. Immun. 1999. V. 67. № 11. P. 6221–6224.
11. Shamova O., Brogden K.A., Zhao C., Nguen T., Turner J., Kokryakov V., Lehrer R.I. // Infect. Immun. 1999. V. 67. № 8. P. 4106–4111.
12. Shamova O., Orlov D., Stegemann C., Czihal P., Hoffmann R., Brogden K., Kolodkin N., Sakuta G., Tossi A., Sahl H.-G., Kokryakov V., Lehrer R.I. // Int. J. Pept. Res. Therap. 2009. V. 15. № 1. P. 31–42.
13. Harwig S.S., Chen N.P., Park A.S.K., Lehrer R.I. // Anal. Biochem. 1993. V. 208. P. 382–386.
14. Schagger H., von Jagow G. // Anal. Biochem. 1987. V. 166. P. 368–379.
15. Wolf P. // Anal. Biochem. 1983. V. 129. Pt. 1. P. 145–155.
16. Lehrer R.I., Rosenman M., Harwig S.S., Jackson R., Eisenhauer P. // J. Immunol. Meth. 1991. V. 137. № 2. P. 167–173.
17. Tossi A., Scocchi M., Zanetti M., Genaro R., Storici P., Romeo D. In Antibacterial peptide protocols / Ed. Shafer W. Totowa, N.J.: Humana Press Inc., 1998. P. 133–151.
18. Lehrer R.I., Barton A., Ganz T. // J. Immunol. Meth. 1988. V. 108. P. 153–158.
19. Artamonov A.Yu., Shamova O.V., Kokryakov V.N., Orlov D.S. // Vesnik Sankt-Peterburgskogo unuversiteta. Ser. 3. Biology. 2008. №. 2. P. 139–142 [in Russian].
20. Zhao C., Nguyen T., Boo L., Hong T., Espiritu C., Orlov

D., Wang W., Waring A., Lehrer R.I. // Antimicrob. Agents Chemother. 2001. V. 45. № 10. P. 2695–2702.
21. Mosmann T. // J. Immunol. Meth. 1983. V. 65. P. 55–63.
22. Singer D., Lehmann J., Hanisch K., Härtig W., Hoffmann R. // Biochem. Biophys. Res. Commun. 2006. V. 346. P. 819–828.
23. Zhao C., Nguyen T., Brogden K., Lehrer R. // EMBL/GenBank/DDBJ databases. 1999.
24. Gennaro R., Zanetti M., Benincasa M., Podda E., Miani M. // Curr. Pharmaceut. Design. 2002. V. 8. P. 763–778.
25. Scocchi M., Tossi A., Gennaro R. // Cell. Mol. Life Sci. 2011. V. 68. P. 2317–2330.
26. Zahn M., Kieslich B., Berthold N., Knappe D., Hoffmann R., Strater N. // Protein Pept Lett. 2014. V. 21. № 4. P. 407–412.
27. Krizsan A., Volke D., Weinert S., Sträter N., Knappe D., Hoffmann R. // Angew. Chem. Int. Ed. Engl. 2014. V. 53. № 45. P. 12236–12239.
28. Mardirossian M., Grzela R., Giglione C., Meinnel T., Gennaro R., Mergaert P., Scocchi M. // Chem. Biol. 2014. V. 21. № 12. P. 1639–1647.
29. Rosenfeld Y., Lev N., Shai Y. // Biochemistry. 2010. V. 49. P. 853–861.
30. Nan Y., Bang J., Jacob B., Park I., Shin S. // Peptides. 2012. V. 35. № 2. P. 239–247.
31. Anderson R.C., Hancock R.E.W., Yu P. // Antimicrob. Agents Chemother. 2004. V. 48. № 2. P. 673–676.
32. Braff M., Hawkins M., Di Nardo A., Lopez-Garcia B., Howell M., Wong C., Lin K., Streib J., Dorschner R., Leung D., et al. // J. Immunol. 2005. V. 174. P. 4271–4278.
33. Gifford J., Hunter H., Vogel H. // Cell Mol. Life Sci. 2005. V. 62. № 22. P. 2588–2598.
34. Park I.Y., Park C.B., Kim M.S., Kim S.C. // FEBS Lett. 1998. V. 437. P. 258–262.
35. Shamova O.V., Orlov D.S., Balandin S.V., Shramova E.I., Tsvetkova E.V., Panteleev P.V., Leonova Yu.F., Tagaev A.A., Kokryakov V.N., Ovchinnikova T.V. // Acta Naturae. 2014. V. 6. № 4 (23). P. 99–109.
36. Waumans Y., Baerts L., Kehoe K., Lambeir A., De Meester I. // Front. Immunol. 2015. V. 7. № 6. 387. doi: 10.3389/fimmu.2015.00387.

GENERAL RULES

Acta Naturae publishes experimental articles and reviews, as well as articles on topical issues, short reviews, and reports on the subjects of basic and applied life sciences and biotechnology.

The journal is published by the Park Media publishing house in both Russian and English.

The journal *Acta Naturae* is on the list of the leading periodicals of the Higher Attestation Commission of the Russian Ministry of Education and Science. The journal Acta Naturae is indexed in PubMed, Web of Science, Scopus and RCSI databases.

The editors of *Acta Naturae* ask of the authors that they follow certain guidelines listed below. Articles which fail to conform to these guidelines will be rejected without review. The editors will not consider articles whose results have already been published or are being considered by other publications.

The maximum length of a review, together with tables and references, cannot exceed 60,000 characters with spaces (approximately 30 pages, A4 format, 1.5 spacing, Times New Roman font, size 12) and cannot contain more than 16 figures.

Experimental articles should not exceed 30,000 symbols (approximately 15 pages in A4 format, including tables and references). They should contain no more than ten figures.

A short report must include the study's rationale, experimental material, and conclusions. A short report should not exceed 12,000 symbols (8 pages in A4 format including no more than 12 references). It should contain no more than four figures.

The manuscript and the accompanying documents should be sent to the Editorial Board in electronic form:
1) text in Word 2003 for Windows format;
2) the figures in TIFF format;
3) the text of the article and figures in one pdf file;
4) the article's title, the names and initials of the authors, the full name of the organizations, the abstract, keywords, abbreviations, figure captions, and Russian references should be translated to English;
5) the cover letter stating that the submitted manuscript has not been published elsewhere and is not under consideration for publication;
6) the license agreement (the agreement form can be downloaded from the website www.actanaturae.ru).

MANUSCRIPT FORMATTING

The manuscript should be formatted in the following manner:

- Article title. Bold font. The title should not be too long or too short and must be informative. The title should not exceed 100 characters. It should reflect the major result, the essence, and uniqueness of the work, names and initials of the authors.
- The corresponding author, who will also be working with the proofs, should be marked with a footnote *.
- Full name of the scientific organization and its departmental affiliation. If there are two or more scientific organizations involved, they should be linked by digital superscripts with the authors' names. Abstract. The structure of the abstract should be very clear and must reflect the following: it should introduce the reader to the main issue and describe the experimental approach, the possibility of practical use, and the possibility of further research in the field. The average length of an abstract is 20 lines (1,500 characters).
- Keywords (3 – 6). These should include the field of research, methods, experimental subject, and the specifics of the work. List of abbreviations.
- INTRODUCTION
- EXPERIMENTAL PROCEDURES
- RESULTS AND DISCUSSION
- CONCLUSION

  The organizations that funded the work should be listed at the end of this section with grant numbers in parenthesis.
- REFERENCES

  The in-text references should be in brackets, such as [1].

RECOMMENDATIONS ON THE TYPING AND FORMATTING OF THE TEXT

- We recommend the use of Microsoft Word 2003 for Windows text editing software.
- The Times New Roman font should be used. Standard font size is 12.
- The space between the lines is 1.5.
- Using more than one whole space between words is not recommended.
- We do not accept articles with automatic referencing; automatic word hyphenation; or automatic prohibition of hyphenation, listing, automatic indentation, etc.
- We recommend that tables be created using Word software options (Table → Insert Table) or MS Excel. Tables that were created manually (using lots of spaces without boxes) cannot be accepted.
- Initials and last names should always be separated by a whole space; for example, A. A. Ivanov.
- Throughout the text, all dates should appear in the "day.month.year" format, for example 02.05.1991, 26.12.1874, etc.
- There should be no periods after the title of the article, the authors' names, headings and subheadings, figure captions, units (s – second, g – gram, min – minute, h – hour, d – day, deg – degree).
- Periods should be used after footnotes (including those in tables), table comments, abstracts, and abbreviations (mon. – months, y. – years, m. temp. – melting temperature); however, they should not be used in subscripted indexes (T_m – melting temperature; $T_{p.t}$ – temperature of phase transition). One exception is mln – million, which should be used without a period.
- Decimal numbers should always contain a period and not a comma (0.25 and not 0,25).
- The hyphen ("-") is surrounded by two whole spaces, while the "minus," "interval," or "chemical bond" symbols do not require a space.
- The only symbol used for multiplication is "×"; the "×" symbol can only be used if it has a number to its

right. The "·" symbol is used for denoting complex compounds in chemical formulas and also noncovalent complexes (such as DNA·RNA, etc.).
- Formulas must use the letter of the Latin and Greek alphabets.
- Latin genera and species' names should be in italics, while the taxa of higher orders should be in regular font.
- Gene names (except for yeast genes) should be italicized, while names of proteins should be in regular font.
- Names of nucleotides (A, T, G, C, U), amino acids (Arg, Ile, Val, etc.), and phosphonucleotides (ATP, AMP, etc.) should be written with Latin letters in regular font.
- Numeration of bases in nucleic acids and amino acid residues should not be hyphenated (T34, Ala89).
- When choosing units of measurement, SI units are to be used.
- Molecular mass should be in Daltons (Da, KDa, MDa).
- The number of nucleotide pairs should be abbreviated (bp, kbp).
- The number of amino acids should be abbreviated to aa.
- Biochemical terms, such as the names of enzymes, should conform to IUPAC standards.
- The number of term and name abbreviations in the text should be kept to a minimum.
- Repeating the same data in the text, tables, and graphs is not allowed.

GUIDENESS FOR ILLUSTRATIONS

- Figures should be supplied in separate files. Only TIFF is accepted.
- Figures should have a resolution of no less than 300 dpi for color and half-tone images and no less than 500 dpi.
- Files should not have any additional layers.

REVIEW AND PREPARATION OF THE MANUSCRIPT FOR PRINT AND PUBLICATION

Articles are published on a first-come, first-served basis. The members of the editorial board have the right to recommend the expedited publishing of articles which are deemed to be a priority and have received good reviews.

Articles which have been received by the editorial board are assessed by the board members and then sent for external review, if needed. The choice of reviewers is up to the editorial board. The manuscript is sent on to reviewers who are experts in this field of research, and the editorial board makes its decisions based on the reviews of these experts. The article may be accepted as is, sent back for improvements, or rejected.

The editorial board can decide to reject an article if it does not conform to the guidelines set above.

The return of an article to the authors for improvement does not mean that the article has been accepted for publication. After the revised text has been received, a decision is made by the editorial board. The author must return the improved text, together with the responses to all comments. The date of acceptance is the day on which the final version of the article was received by the publisher.

A revised manuscript must be sent back to the publisher a week after the authors have received the comments; if not, the article is considered a resubmission.

E-mail is used at all the stages of communication between the author, editors, publishers, and reviewers, so it is of vital importance that the authors monitor the address that they list in the article and inform the publisher of any changes in due time.

After the layout for the relevant issue of the journal is ready, the publisher sends out PDF files to the authors for a final review.

Changes other than simple corrections in the text, figures, or tables are not allowed at the final review stage. If this is necessary, the issue is resolved by the editorial board.

FORMAT OF REFERENCES

The journal uses a numeric reference system, which means that references are denoted as numbers in the text (in brackets) which refer to the number in the reference list.

For books: the last name and initials of the author, full title of the book, location of publisher, publisher, year in which the work was published, and the volume or issue and the number of pages in the book.

For periodicals: the last name and initials of the author, title of the journal, year in which the work was published, volume, issue, first and last page of the article. Must specify the name of the first 10 authors. Ross M.T., Grafham D.V., Coffey A.J., Scherer S., McLay K., Muzny D., Platzer M., Howell G.R., Burrows C., Bird C.P., et al. // Nature. 2005. V. 434. № 7031. P. 325–337.

References to books which have Russian translations should be accompanied with references to the original material listing the required data.

References to doctoral thesis abstracts must include the last name and initials of the author, the title of the thesis, the location in which the work was performed, and the year of completion.

References to patents must include the last names and initials of the authors, the type of the patent document (the author's rights or patent), the patent number, the name of the country that issued the document, the international invention classification index, and the year of patent issue.

The list of references should be on a separate page. The tables should be on a separate page, and figure captions should also be on a separate page.

The following e-mail addresses can be used to contact the editorial staff: vera.knorre@gmail.com, actanaturae@gmail.com, tel.: (495) 727-38-60, (495) 930-87-07

Science and Technologies in Russia – STRF.RU

40% of scientists agree that the publication of research results helps the enlightenment of the society, leads to the growth of authority of scientific work

34% believe that wide communicating of research results helps to rise the foundation

12% hope that media communications helps them to stand out in public opinion…

…but

17% never speak to journalists*

Open your work to the world!

*According to 2008 STRF.RU poll.

Colours do not play at nanometer scale

But you can colour molecules by their Raman spectra.

Enter code NTEGRA0501AG and get a gift*

Raman mapping by TERS with ultra-high resolution

NTEGRA Spectra

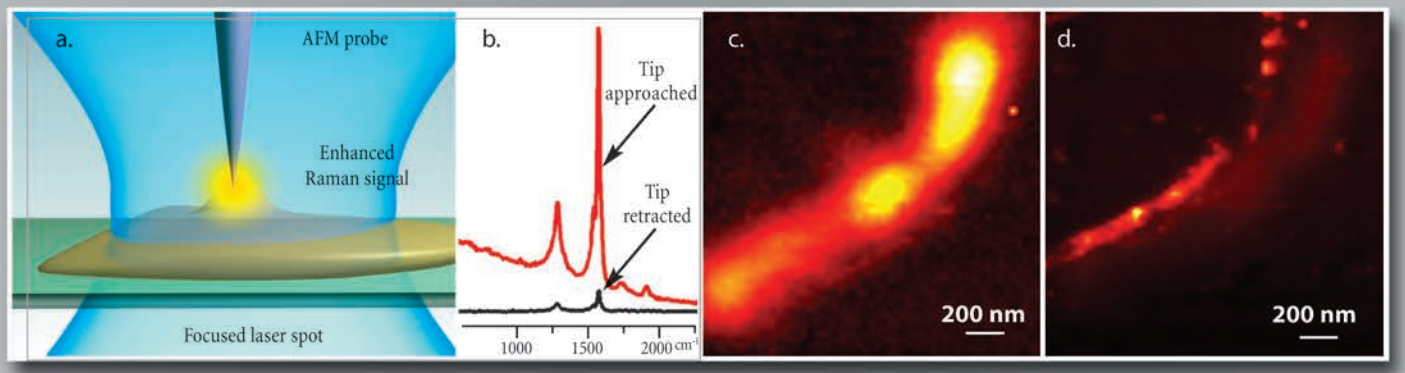

a — a specially prepared AFM probe (metal coated cantilever or etched metal wire) is precisely positioned inside a tightly focused laser spot. b — intensity of carbon nanotube G- and D- Raman bands increases by several orders of magnitude when the special AFM probe is landed and positioned over a small (5 nm height) nanotube bundle - the effect of Tip enhanced Raman scattering (TERS). c — "conventional" confocal Raman image of the nanotube bundle, the observed width of the bundle is ~250 nm (diffraction limit of confocal microscopy, laser wavelength - 633 nm). d — TERS image of the same bundle - now the observed width is ~70 nm.

Note, in this example, TERS provides more than 4-times better spatial resolution as compared to confocal microscopy. Resolution down to 10 nm and less is theoretically possible. Measurements are done with NTEGRA Spectra in Inverted configuration.

Data courtesy of Dr. S. Kharintsev, Dr. J. Loos, Dr. G. Hoffmann, Prof. G. de With, TUE, the Netherlands and Dr. P. Dorozhkin, NT-MDT Co.

*** Enter the Gift code at www.nt-mdt.com and get a present from NT-MDT Co. Attention: limited quantity! Be in time to get your gift!**

NT-MDT
Molecular Devices and Tools for NanoTechnology

NT-MDT Co., building 100, Zelenograd, 124482, Moscow, Russia
tel: +7 (499) 735-0305, +7 (495) 913-5736
fax: +7 (499) 735-6410, +7 (495) 913-5739
e-mail: spm@ntmdt.ru; www.ntmdt.com

NT-MDT Europe BV, High Tech Campus 83 5656 AG Eindhoven ,the Netherlands
tel: +31(0) 88 338 99 99
fax: +31(0) 88 338 99 98
e-mail: info@ntmdt.eu, www.ntmdt.com